Fall 2016

Radiochemical analysis of protactinium speciation: applications in nuclear forensics, nuclear energy, and environmental radiochemistry

Andrew William Knight
University of Iowa

RADIOCHEMICAL ANALYSIS OF PROTACTINIUM SPECIATION: APPLICATIONS IN NUCLEAR FORENSICS, NUCLEAR ENERGY, AND ENVIRONMENTAL RADIOCHEMISTRY

BY

ANDREW WILLIAM KNIGHT

A thesis submitted in partial fulfillment
of the requirements for the Doctor of
Philosophy degree in Chemistry
in the Graduate College of
The University of Iowa

December 2016

Thesis Supervisors: Associate Professor Tori Z. Forbes

Associate Professor Michael K. Schultz

Graduate College
The University of Iowa
Iowa City, Iowa

CERTIFICATE OF APPROVAL

_____

PH.D. THESIS

_____

This is to certify that the Ph.D. thesis of

ANDREW WILLIAM KNIGHT

has been approved by the Examining Committee
for the thesis requirement for the Doctor of Philosophy
degree in Chemistry at the December 2016 graduation.

Thesis Committee: _____
TORI Z. FORBES, Thesis Supervisor

_____
MICHAEL K. SCHULTZ, Thesis Supervisor

_____
DANIEL R. McALISTER

_____
EDWARD G. GILLAN

_____
JOHNA LEDDY

To Paige and Muña, thanks for all the love with open arms and a wagging tail.

Nothing in life is to be feared, it is only to be understood. Now is the time to

Understand more, so that we may fear less

Marie Skłodowska-Curie
As Quoted in Our Precarious Habitat (1973) by Melvin A. Bernarde

Since then it's been a book you read in reverse

So you understand less as the pages turn

"Pink Bullets" by The Shins

ACKNOWLEDGMENTS

First and foremost, I would like to thank my wife, Paige, for all the support and sacrifices made for me to pursue my degree. Also thank you for joining me in all the occasions where we "were not going to talk chemistry" with other chemists. I think by now you at least have honorary degree in Chemistry. I would also like to thank my family for their love and support., and for instilling confidence, curiosity, and perseverance in me.

I would like to thank Drs. Tori Forbes and Michael Schultz for being incredible mentors. Without their mentorship I would not be where I am today. I owe all my accomplishments and opportunities to the both of them. I appreciate the patience and unbelievably helpful insight from Tori, countless times of struggle ended with an enlightened conversation with her. Tori always took the time out of her increasingly busy schedule to aid in research woes and celebrate research successes. Mike was always enthusiastic, exciting and pushed me to always be thinking of the next step. He inspired me with his great optimism and tenacity for research and his curiosity (mostly) led to interesting research questions and new ways to approach a problem. I am an extremely lucky graduate student to have two amazing academic mentors and can only hope to one day reach their caliber of scientist.

I would also like to thank my labmates Eric Eitrheim and Andy Nelson. Not only were you two immensely helpful and supportive you also made getting a PhD very fun and exciting. I greatly enjoyed all the help input and criticism when it came to preparation for presentations, writing papers, and designing future experiments and not to mention the unofficial lab meetings at Joe's Place. It was truly a collaborative environment that greatly strengthens my scientific skills and knowledge as well as my basketball and Frisbee golf skills. I wish the best for you two in the future.

Further, I would like to thank everyone else at the University of Iowa, specifically the Forbes group; Josh de Groot, Ashini Jayasinghe, Madeline Basile, Maurice Payne, Adam Johns, and Madeline Peterson as well as Schultz group; Kyle Kloepping, Mengshi Li, Jess Reedy, Somya Kapoor and Dustin May. Thank you for listening to my project presentations and thank you for sharing your projects with me, I learned an incredible amount from you all. Additional acknowledgments to

Grace Lu, Fu Chen, Sarah Larsen, Michael Sinnwell, Amanda Haes, David Peate, Jeff Dorale, Johna Leddy, Edward Gillan, Garry Buettner, and Amanda Kalen.

Lastly, I would like to extend additional acknowledgments to those from outside the University of Iowa that had a significant impact on my dissertation and development as a scientist. From Savannah River National Laboratory; Jake Venzie, Justin Halverson, and Andrea Bridges, from Idaho National Laboratory; Peter Zalupski, from Argonne National Laboratory; Renato Chiarizia, Lynne Soderholm, Ross Ellis, Boafu Qiao, Geoffroy Ferru, Mark Antonio, Will Rock, Skantha Skanthakumar, and Shanna Estes. Additional thanks to Dan McAlister, Steffan Heppel, Stephane Bourg, Lindsay Shuller-Nickles, and Robert Shannon.

ABSTRACT

Protactinium (Pa) is an actinide with chemical properties that are unique among the actinide elements. While the properties of other actinides are to a large extent understood, much of the chemistry of Pa remains a mystery. This thesis aims to illuminate new understanding of Pa chemistry through behavioral analysis using analytical techniques including liquid-liquid extraction (LL); extraction chromatography (ExC); and spectroscopic studies.

Applications of radioanalytical chemistry and Pa: Through the research presented in this dissertation, we have developed a new way to separate uranium (U), thorium (Th), and Pa from complex environmental samples. The approach has been demonstrated for U-series dating of materials by alpha spectrometry. The method can be applied to geochronology, as well as to nuclear-forensic analysis of uranium-containing materials. In studies presented here, samples from a Paleolithic lake (Lake Bonneville, Utah USA) were analyzed for the radioactivity concentration of ^{230}Th, ^{231}Pa, ^{234}U, ^{235}U, and ^{238}U by isotope dilution alpha spectrometry. Radioactivities were used to estimate of the time period of formation of the deposit from which the samples were collected. Ages were determined by isotopic ratios; *i.e.*, ^{231}Pa/^{235}U (40 ka); and ^{230}Th/^{238}U (39.5 ka) we found to be concordant with radiocarbon-14 dates (37 ka) obtained by collaborators at Brigham Young University. These studies inspired the development of a novel ExC resin to facilitate preparation of highly pure tracer isotope (^{233}Pa) from a neptunium-237 (^{237}Np) source. The material used for this development comprised 1-octanol adsorbed to a semi-porous resin material. The new approach greatly improved the yield and purity of ^{233}Pa used for these chronometric analyses

Developing an understanding of the chemistry of Pa at trace concentrations: The new-improved analytical described above led to the hypothesis that analytical separations approaches could be used to develop a more detailed understanding of Pa chemistry. Toward this goal, experiments were conducted to understand how the extraction of Pa is impacted by solution acidity [H^+], anion concentration [A^-; Cl^-, NO_3^-], and extractant concentration ([2,6-dimethyl-4-heptanol, DIBC]). A full-factorial experimental design was employed to create a model that would allow for predictions in Pa behavior, as well as describe the nature of the observations. This model

generated a multivariate equation that relates the distribution coefficient ($[Pa]_{\text{organic phase}}/[Pa]_{\text{aqueous phase}}$) to each of the parameters ($[H^+]$, $[A^-]$, and [DIBC]). Further studies expanded to other alcohols (ROH) used as extractants (1-octanol, (2,6)-dimthyl-4-heptanol, and 2-ethyl-hexanol); and the results were analyzed using the slope analysis and comparative extraction studies using the model and compared to other actinide elements (Th, U, Np, americium (Am)) by both LL and ExC systems. These experiments revealed unique chemical behavior of Pa with respect to the other actinides. For example, it was found that Pa was the only actinide element to be extracted into the organic phase under acidic conditions (HCl and HNO_3). Slope analysis experiments elucidated the stoichiometric identity of Pa species, with respect to the anion and extractant. Future studies will aim to identify the oxygen stoichiometry and species by X-ray absorption techniques.

Investigations of the organic phase: In the final sections of this thesis, experiments are presented that are intended to determine if aggregation plays a key role in the extraction of Pa in systems containing 1-octanol and 2-ethyl-hexanol. This work is done in the absence of metal ions to control the dynamics of the organic phase; and are analyzed by tensiometry and Karl Fisher titrations with small angle X-ray scattering and molecular dynamic simulations. A key novel finding of these studies in that ROH molecules arrange in nanoscale aggregates that decrease the interfacial tension between the phases and extract a significant amount of water into the aggregates stabilized by a network of H-bonding. These studies lead to the hypothesis for future studies that Pa extraction is likely facilitated by solvation into the organic phase via ROH aggregates.

The sum of the findings and observations of this dissertation provide insight into the chemical nature of Pa: (1) Novel extraction methods to obtain radiochemically pure fractions show that Pa can be efficiently extracted and separated from complex matrices to aid in chronometric analysis for geochronology or nuclear forensics; (2) Statistical modeling to develop a better understanding of the main effects of solvent extraction parameters; (3) Equilibrium analysis to improve our understanding of chemistry of Pa and how it is unique to the actinides; (4) Aggregation analysis to demonstrate a solvent centric understanding of extraction studies, these results lead to

future experiments to investigate how organic phase aggregation can influence solvent extraction selectivity.

PUBLIC ABSTRACT

Protactinium (Pa) is an actinide with chemical properties that appear to diverge from the other actinides. While the other actinides have been extensively studied in the past few decades, Pa remains a mystery. This dissertation aims to highlight the unique chemistry of Pa through strategic extractions and advanced spectroscopic studies.

This thesis identifies new ways to separate U, Th, and Pa from complex environmental samples using extraction chromatographic resins. These methods have demonstrated superior ability for U-series dating of materials by alpha spectrometry, and can be applied to geochronology and nuclear forensic analysis of uranium-containing materials. Additionally, we have produced novel extraction chromatographic resins, consisting of aliphatic alcohols that demonstrate selectivity for Pa, which can be used to aid researchers engaging in Pa and related actinide research.

Chemical equilibrium analyses were performed to elucidate the chemical species allowing for the selective extraction of Pa through an understanding of the chemical equilibrium in solvent extraction systems and how it relates to distribution ratios principles. Lastly, a greater understanding of how the organic phase complex ordering can influence the extraction of Pa, ternary solutions of 1-octanol and 2-ethyl-hexanol were investigated via small angle X-ray scattering at the Advanced Photon Source at Argonne National Laboratory. These experiments demonstrate the formation of aggregates in the organic phase and a significant uptake of water.

These methods provide insight into the chemical nature of Pa. Collectively; these studies aim to understand the chemical differences that make Pa unique among the actinides.

TABLE OF CONTENTS

LIST OF TABLES

LIST OF FIGURES

PREFACE

This dissertation is based upon the work of Andrew Knight at the University of Iowa from 2012-2016. The chapters in this work are original works. Chapters II-V have been published previously, the original citations are as followed:

Chapter II: Knight, A.W., Eitrheim, E. S., Nelson, A. W., Nelson, S., Schultz, M. K. (2014). A Simple Rapid Method to Separation Uranium, Thorium, and Protactinium for U-Series Age Dating of Materials. *Journal of Environmental Radioactivity,* **134**: 66-74.

Chapter III: Knight, A.W., Eitrheim, E. S., Nelson, A. W., Forbes, T. Z., Schultz, M. K. (2016). A Chromatographic Separation of Neptunium and Protactinium using 1-octanol Impregnated onto a Solid Substrate. *Journal of Radioanalytical and Nuclear Chemistry,* **307**(1): 59-67.

Chapter IV: Knight, A.W., Eitrheim, E. S., Nelson, A. W., Schultz, M. K. (2015). A Calculation Model for Liquid-liquid Extraction of Protactinium by 2,6-dimethyl-4-heptanol. *Nukleonika,* **60**(4): 837-845.

Chapter V: Knight, A.W., Eitrheim, E. S., Nelson, A. W., Peterson, M. C., McAlister, D., Forbes, T. Z., Schultz, M. K. (2016). Trace-Level Extraction Behavior of Actinide Elements by Aliphatic Alcohol Extractants in Mineral Acids. Insights into the Trace Solution Chemistry of Protactinium. *Solvent Extraction and Ion Exchange,* **34** (6): 509-521.

CHAPTER I: INTRODUCTION TO RADIOCHEMISTRY AND PROTACTINIUM

1.1. Introduction

The actinides describe known elements of the period table from Z=89 (actinium; $_{89}$Ac) to Z=103 (lawrencium; $_{103}$Lr). As a group, analysis of the physico-chemical properties of these elements can be complicated by relatively low abundances; and because there are no stable isotopes. These attributes present analytical and safety considerations that complicate experimentation.[1] One actinide element whose properties and chemistry has been particularly illusive is protactinium ($_{91}$Pa).[2] Researchers investigating the chemistry of Pa have referred to its chemistry as "puzzling"[3], "peculiar"[4], "mysterious"[5], and even "witchcraft"[5]. The thesis seeks to advance our understanding of Pa chemistry by application of novel analytical chemistry and modeling approaches. These techniques also contribute improvements to Pa radioanalytical chemistry for applications in nuclear forensics; the nuclear fuel cycle; and environmental geochronology, where isotopic Pa quantification is key to understanding.

From $_{89}$Ac to $_{103}$Lr, actinide half lives range from billions of years to sub-seconds, and the only naturally-occurring isotopes belong to the first four actinides ($_{89}$Ac, thorium; $_{90}$Th, $_{91}$Pa, and uranium; $_{92}$U) in the family.[1] Interestingly, the discovery of radioactivity by Henri Becquerel (1896) arose out of analysis of a uranium-mineral and most natural materials contain actinide elements. In addition, actinide elements arising from anthropogenic activities (e.g., nuclear weapons testing; nuclear power industry activities) can be found in significant quantities in natural materials. Examples of common anthropogenic actinide elements found in nature include neptunium ($_{93}$Np), plutonium ($_{94}$Pu), americium ($_{95}$Am), and curium ($_{96}$Cm).[6] Furthermore, the development of nuclear transmutation processes has led to the ability to produce of many of the isotopes of each of the actinide elements that are predicted by nuclear physics. Isotopes of a given actinide share the same chemical properties, but each possesses distinct nuclear and radioactive-decay properties.[6] In this thesis, the known chemical properties of individual actinide elements represent a basis by which to infer new information about Pa chemistry; and the nuclear and decay properties of isotopes of actinides investigated provide the quantification basis that underlies these comparisons and inferences. It is hoped that the findings and observations presented in this thesis can contribute to

improvement in our understanding of Pa for a range applications from environment science,[7-11] to nuclear energy; and nuclear forensics.[6, 12-14]

1.2. Radioactive Decay

Radioactive decay is the process by which an unstable atom emits energy, in the form of radiation, to stabilize the nucleus. The forms of radiation include particles; alpha (α, ${}^{4}_{2}\mathrm{He}$), beta (β^-, ${}^{0}_{-1}\mathrm{e}$), positron (β^+, ${}^{0}_{+1}\mathrm{e}$), and waves; gamma (γ) or X-rays emitted from the nucleus.[6] The emission particle is predictable, because a nuclide will always decay in a way that brings the proton to neutron ratio closer to the valley of stability (**Figure 1**). While each radioactive event occurs randomly, the frequency of decay events occurring is empirically known (with some precision) for most known nuclides. The rate of radioactive decay follows first order kinetics. This frequency term is known as the decay constant (λ, units: reciprocal time) and it is related to the half-life ($t_{1/2}$, units: time) of an isotope, where:

$$t_{1/2} = \frac{\ln(2)}{\lambda} \qquad \text{eq. 1}$$

Likewise, the decay constant is relates the radioactivity of a sample to the number atoms present. Where:

$$A = N\,\lambda \qquad \text{eq. 2.}$$

Where A is the radioactivity in Becquerel (Bq; 1 Bq = 1 decay/second), N is the number of atoms, and λ is the decay constant (sec^{-1}). Furthermore, the radioactivity of a sample can be determined with respect to time in the first order integrated rate equation, where:

$$N = N_0 * e^{-\lambda t} \qquad \text{eq. 3}$$

In which N is the current number of atoms, N_0 is the initial number of atoms, and t is the amount of time elapsed (in the same unit of time as λ). Using these relationships, radiochemists are able to relate the concentration of a sample to the radioactivity within that sample. This ability allows radiochemist to use radiometric detection technique to characterize a sample.

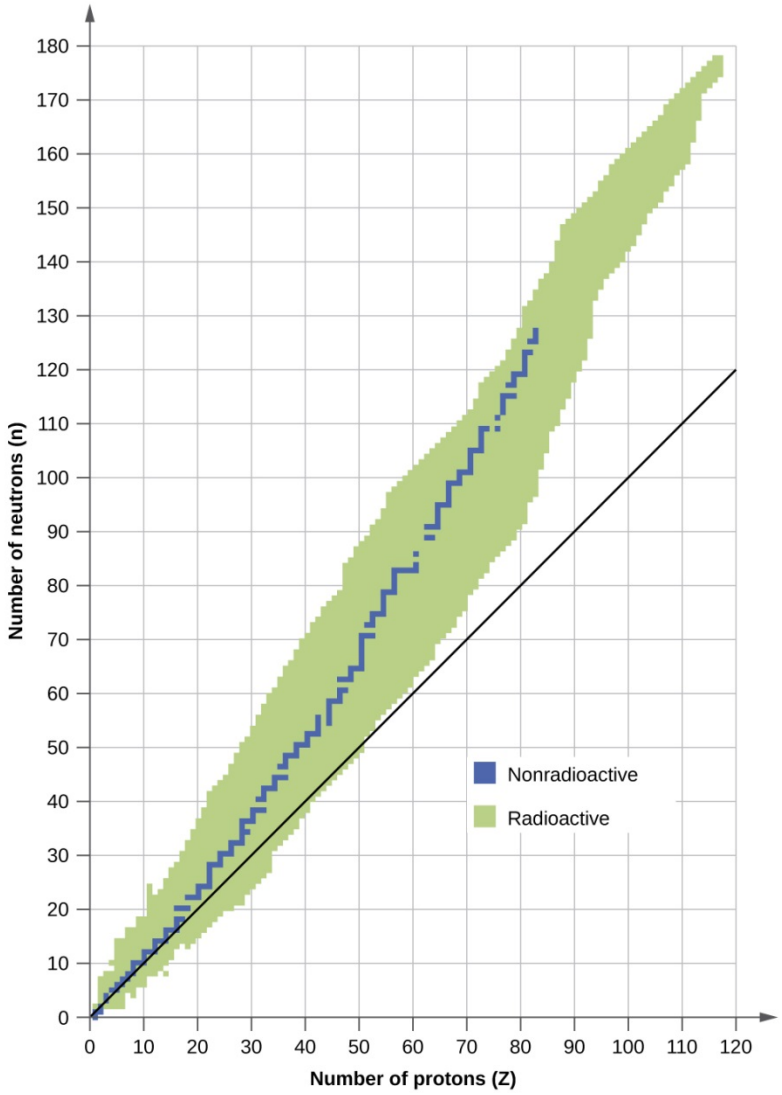

Figure 1. The chart of the nuclides highlighting the valley of stability. Any isotope existing outside of the valley of stability is radioactive.[1]

1.2.1. Sources of Radioactivity

While radioactivity is ubiquitous in the environment and can originate from **primordial**, **anthropogenic**, or **cosmogenic** sources, the actinide elements only originate from two of these sources; primordial decay series and anthropogenic sources.[6] The primordial elements are elements that have existed since the origins of the planet (and perhaps beyond). These elements

have half-lives with a similar order of magnitude or greater than the age of the earth (approx. 4.56 billion years).[15] Naturally, there are three main primordial decay series which provide the natural source for all elements beyond lead ($_{82}$Pb); these series are ^{238}U ($t_{1/2}$ = 4.468x10^{9} years), ^{235}U ($t_{1/2}$ = 7.04x10^{8} years), and ^{232}Th ($t_{1/2}$ = 1.40x10^{10} years), which decay through a series of elements to stable isotopes ^{206}Pb, ^{207}Pb, and ^{208}Pb, respectively (**Figure 2**).[16, 17] Furthermore, additional decay series are hypothesized to have existed because of isotopic anomalies; however the half-life of the parent radionuclide is too short to persist today, specifically ^{237}Np ($t_{1/2}$ = 2.144x10^{6} years) decay series, which results in stable thallium-205 ($_{81}^{205}$Tl). Each of these decay chains consists of a series of decays that result in atomic mass change leading to different, elements, and scenarios where the geochemical behavior of the parent does not match the daughter. This can lead to **radioactive disequilibria** (described further below). The occurrence of disequilibria in naturally-occurring radionuclides can provide isotopic signatures that can be used to determine analytical age, sedimentation rates, and geological origins of materials.[7, 9]

Anthropogenic sources of the actinide elements include nuclear energy and nuclear weapons technologies. The anthropogenic actinides formed as a result of nuclear activities are the transuranic elements, specifically isotopes of Np, Pu, Am, and Cm. While other transuranic elements can form, either their yields are low and/or their half-lives are too short to accumulate from these activities.[6] Furthermore, since resulting anthropogenic parent isotopes are radioactive, they decay through a series of isotopes (natural or anthropogenic) to a stable isotope product. Like natural radioactivity, the occurrences of these decay chains yields disequilibrium among isotopes. These disequilibria provide isotopic signatures that can be used to glean analytical age, process, and geographical information for nuclear forensic analysis. This type of information is currently critical for the development of nuclear forensics, in which legally defensible sample analysis can lead to the determination of source origin, age, and process.

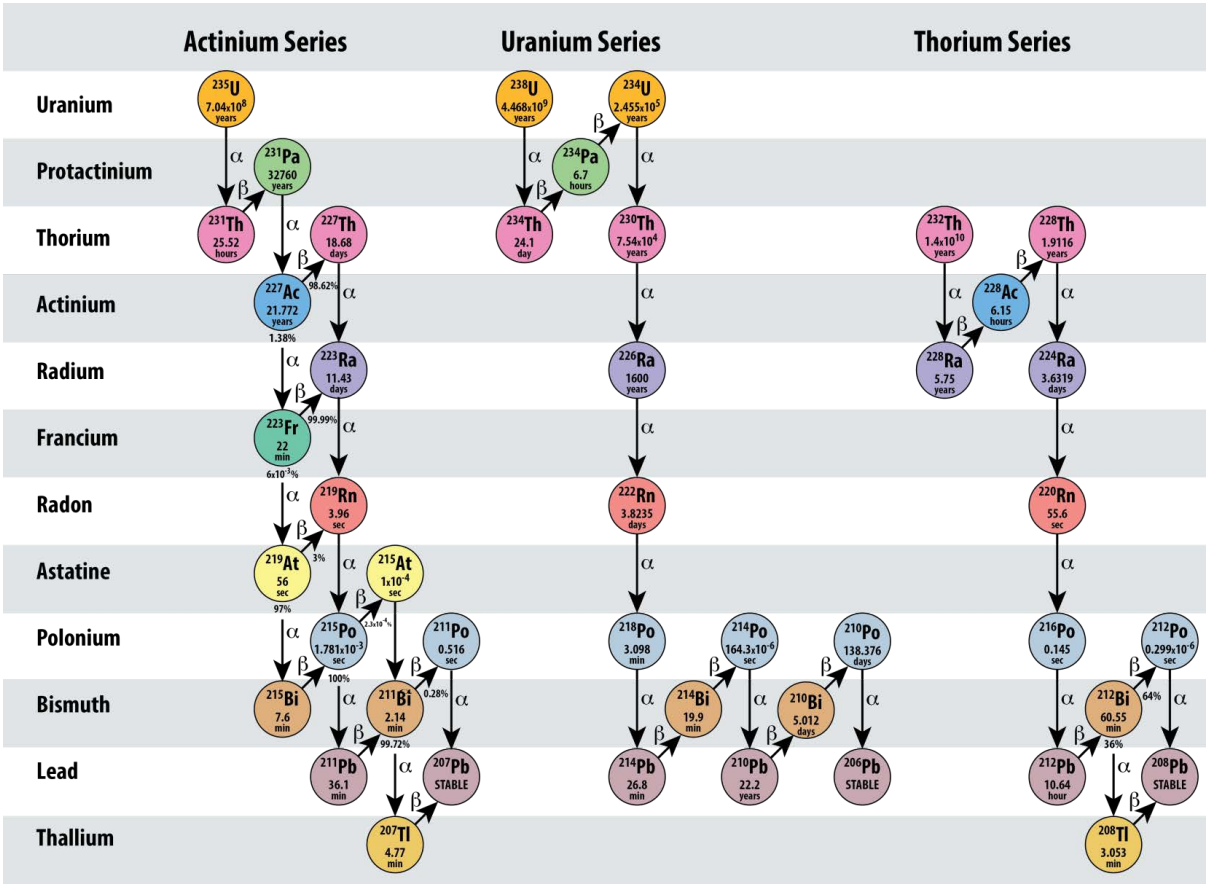

Figure 2. Natural decay chains; actinium series, uranium series, and thorium series.[17]

1.2.2. Radioactive Disequilibria

Radioactive disequilibrium is a phenomenon in which the progenitor and its decay products have not established equilibrium (i.e. secular equilibrium or transient equilibrium). [18] From this process, isotopic signatures can be identified which can provide valuable information regarding origin, age, and processing of natural and special nuclear material. [19] In order for this information to be obtained, there are three primary assumptions that must be made – (*i*) The decay constants of the progenitor and decay products must be known and accurate, (*ii*) The system is closed, in which the only change in levels of radioactivity are due to radioactive decay, and (*iii*) The radioactivity of the decay product is known at t=0. With these assumptions met, the decay product will either decay

or grow into equilibrium with the progenitor radionuclide at a rate related to its own half-life, and will generally be considered to be in equilibrium with the progenitor following 7-10 half-lives.

There are three types of processes used to describe the ingrowth of a decay product; **secular equilibrium, transient equilibrium**, and **no equilibrium** can describe radioactive equilibrium and ingrowth **(Figure 3)**. The type of equilibrium that occurs is dependent on the relationship between the progenitor and decay product half-lives. In general, if the half-life of the progenitor is much larger than the decay product, the ingrowth of the decay product can be described by **secular equilibrium**. And the integrated ingrowth equation is defined as:

$$N_2 = \left(\frac{\lambda_1}{\lambda_2 - \lambda_1}\right) N_1^0\left(e^{-\lambda_1 t} - e^{-\lambda_2 t}\right) + N_2^0\left(e^{-\lambda_2 t}\right) \qquad eq.4$$

Where N_1 and λ_1 refer to the number of atoms and decay constant for the parent isotope and N_2 and λ_2 are the number of atoms and decay constant for the isotope that is formed through decay. This equation can be simplified by the fact that $\lambda_1 << \lambda_2$, then the equation becomes:

$$N_2 = \left(\frac{\lambda_1}{\lambda_2}\right) N_1^0\left(1 - e^{-\lambda_2 t}\right) + N_2^0\left(e^{-\lambda_2 t}\right) \qquad eq.5$$

Over time, N_2 continues to grow in at a rate proportional to its $t_{1/2}$, and will achieve equilibrium following 7-10 half-lives. In this case, the radioactivities of the progenitor and decay product are equal.

When the half-lives of the decay product and progenitor are of similar magnitudes, then they are described by **transient equilibrium**, and also defined **equation 4.** But in this case, since $\lambda_1 << \lambda_2$ is no longer true, over time the atomic ratio does not converge at unity, but at a relationship proportional to their half-lives:

$$N_2 = N_1\left(\frac{\lambda_1}{\lambda_2 - \lambda_1}\right) \qquad eq.6$$

The final case is when the half-life of the progenitor is shorter than that of the decay product. In this case, no equilibrium is established because the radioactivity of the progenitor isotope decreases more rapidly than the decay product can grow in.

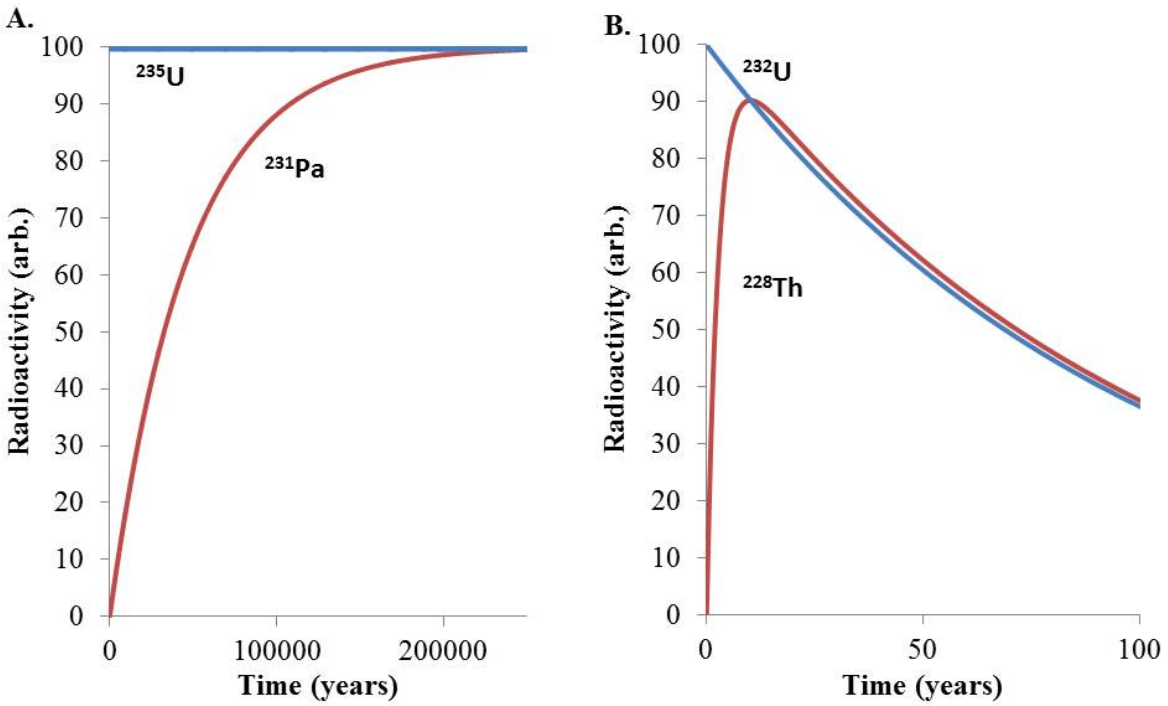

Figure 3. (A). Demonstrates secular equilibrium in the example of the decay of ^{235}U to ^{231}Pa over the course of 250,000 years for the radioactivities to establish unity. (B.) Demonstrates transient equilibrium shown by the example of ^{232}U decaying to ^{228}Th.

1.3. Quantification of Radionuclides

Depending on sample type and application, there are numerous ways to quantify radionuclides in a sample. These methods include but are not limited to isotope dilution, neutron activation, emanation, and direct counting. However, for the actinide elements, isotope dilution methods are the most effective. This is because the concentrations of the actinides are generally low and all isotopes of actinides are radioactive -- and potentially fissile-- thus ruling out neutron activation from many cases. In general, the quantification of radionuclides can be broken down into

6 steps (**Figure 4)**: *(i)* collect and weigh the sample, *(ii)* homogenize the sample and add the tracer isotope, *(iii)* remove non-homogenized impurities, *(iv)* separate and purify elements, *(v)* prepare sources for analysis, and *(vi)* analyze the samples.

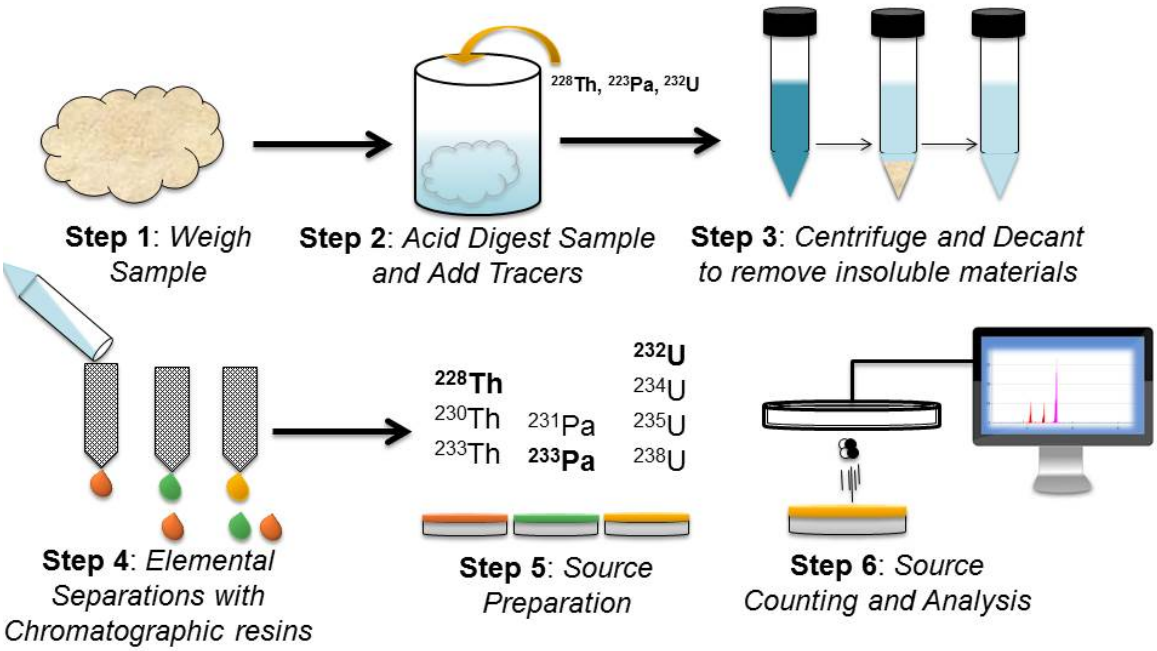

Figure 4. Simple schematic describing the steps involved in quantifying radionuclides from environmental, nuclear, or biological samples.

1.3.1. Sample Collection and Homogenization

The first step in an elemental and isotopic analysis is the sample collection. Sample collection is extremely important, as the sample must be appropriate to address the analytical question as well as be representative of the whole. The samples analyzed in this dissertation were collected by trained scientists and were sent to our lab for analysis, therefore this dissertation will not focus on the sample collection process.

The sample must be carefully weighed and homogenized prior to chemical separation for consistent results. There are many methods to digest simple solid (*i.e.* soils, carbonates) and liquid

(*i.e.* waste water, bioassay) samples; which include fusions (*i.e.* molten NaOH), microwave and thermal digestions, as well as an acid leach methods. For this dissertation, an acid leach method was used to homogenize the samples analyzed, and was typically performed by adding dilute HCl heating to dryness and followed by adding HNO_3/30% H_2O_2. At this point exogenous tracer isotopes are spiked to the acidic sample (**See section 1.3.2 for a description of isotope dilution**). This process is repeated until all soluble components are recovered. Once in a homogenized liquid form (generally acidic to ensure soluble, non-hydrolyzed forms of the actinides), pre-concentration steps may be performed to remove any bulk interferences (*i.e.* calcium). This can be done through precipitation procedures or by group extraction methods. Once the sample is in a relatively clean acidic form, elemental separations can be performed *via* extraction methods. In this dissertation, both conventional solvent extraction (**Section 1.3.3.1**) and extraction chromatography (**Section 1.3.3.2**) are utilized.

1.3.2. Addition of Tracer Isotopes and Isotope Dilution

The most common and precise method to determine isotopic composition in a sample is by isotope dilution. Isotope dilution is an analytical method in which a precisely known amount of an exogenous radioisotope is added to a sample to act as a **tracer** for an analyte isotope. This method is regarded as highly precise and has become a mainstay process for the analysis of environmental and nuclear materials for specific radionuclides. The isotopic tracer allows for the researcher to have a yield assessment quantifying the analyte following chemical processes. Because a **tracer** is chemically identical (some mass deviations can occur for lighter elements but is essentially irrelevant for the actinides), a tracer can be used directly to quantify an analyte using **equation 7:**

$$[analyte]_{sample} = [tracer]_{initial} * \frac{[analyte]_{detected}}{[tracer]_{detected}} \qquad eq. 7.$$

Where $[analyte]_{sample}$ is the true concentration of analyte in a sample, $[tracer]_{initial}$ is the known concentration of the tracer added to the sample, $[analyte]_{detected}$ and $[tracer]_{detected}$ are

experimentally determined concentrations determined by either radiometric detection or mass spectrometry techniques.

For analysis, isotope dilution procedures can be adapted for radiometric detection techniques as well as mass spectrometry techniques. However, it is essential to choose a tracer and analysis method that will allow for the greatest precision on the measurement. For example, in radiometric detection techniques, the uncertainty in a measurement is determined by:

$$counting\ uncertainty = \frac{1}{\sqrt{total\ counts}} \qquad eq.8$$

From **Equation 8**, it is clear that as the number of counts (radioactive events) increases, the uncertainty on the measurement decreases. That means there are two ways to decrease the counting uncertainty, increase count times or increase radioactivity. Because of this principle, radiometric detection techniques are best suited for elements with shorter half-lives (*i.e.* $t_{1/2} < 100$ years). In this case, a small number of exogenous atoms will be added to the sample while still achieving a sufficient total radioactivity to minimize the counting uncertainty.

For elements with longer half-lives, mass spectroscopic detection techniques will achieve more precise analyte concentrations. With a multi-collector inductively coupled plasma mass spectrometer (MC-ICP-MS), atoms are detected based upon isotopic mass are counted simultaneous with a series of detectors. For this detection method it is important to have enough mass (atoms) to achieve highly precise measurements.

Although mass spectrometry is generally considered to be a more precise method for the quantification of the longer-lived actinides, in the investigations in this dissertation, the quantification was performed *via* radiometric techniques. This decision was made based upon accessibility to instrumentation and costs associated with a mass spectroscopy analysis.

1.3.3 Extraction and Separation Methods

Following the sample homogenization, isotopic and elemental extractions and separations can be performed. The sample aliquot, prior to extraction and separation, must exist in an acidic liquid form suitable for the condition required to the extraction and separation protocol. In this dissertation two extraction and separation methods were utilized, **liquid-liquid solvent extraction** and **extraction chromatography**.

1.3.3.1 Liquid-Liquid Solvent Extraction

Solvent extraction is a mainstay for chemical separation processes, and its uses span all disciplines of chemistry. In general, liquid-liquid solvent extraction involves the transfer of an analyte between two immiscible phases. For radiometal purposes, the two phases generally consist of an aqueous, acidic phase in contact with an immiscible oil phase with an extractant molecule. These systems can be adjusted to allow for the appropriate extractions to occur. In the aqueous phase, the acidity as well as the anion identity and concentration can be adjusted. These adjustments will influence the equilibrium speciation of the radiometals in solution. In the organic phase, the identity of the diluent and the concentration and identity of the extractant can be adjusted. These adjustments will influence the separation factor, organic phase capacity, as well as the potential for third phase formation.[20, 21] A simple diagram (**Figure 5)** demonstrates the solvent extraction process.

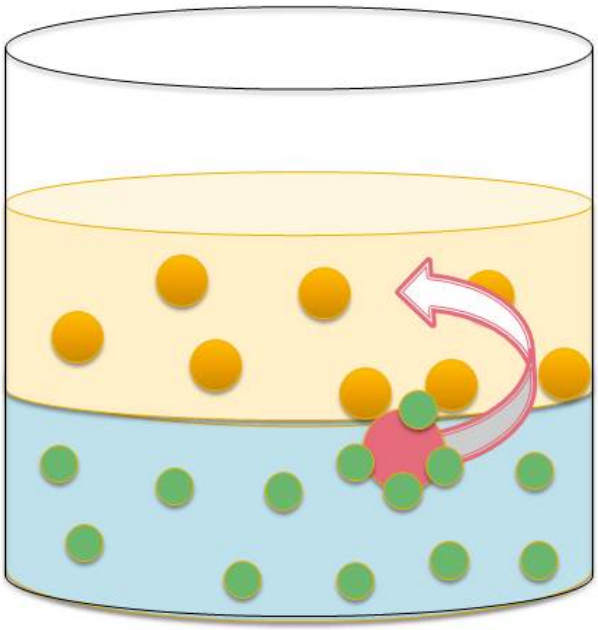

Figure 5. Simple diagram showing the solvent extraction process. A denser aqueous phase contains electrolyte ligands (Cl^-, NO_3^-, ect) and form a complex with the metal. This complex when mixed with an organic phase may result in the extraction of a specific metal species into the less dense organic phase containing the extractant.

For solvent extraction, the aqueous phase is adjusted to allow for **extractions**, **back extractions**, and **separations** to occur. Extraction is the transfer of a metal from the an aqueous phase into an organic phase utilizing an organic phase extractant. Back extraction is the transfer an extracted metal species back into the aqueous phase *via* an aqueous complexant (*i.e.* EDTA) or different acid concentration. And separation is the process of extracting one metal across the phase boundary while an inferring metal remains in the original phase. In general, adjustments are made by increasing or decreasing the acidity of the aqueous phase solution. For nuclear reprocessing purposes, nitric acid (HNO_3) is most commonly used.[22, 23] Having sufficient acidity (in most cases pH < 2) will prevent metals from forming insoluble hydrolyzed species. Hydrolysis can impact extractions by producing less extractable species, leading to precipitation of metal ions, or formation of species that adsorb to surfaces. For investigations into the fundamental chemistry of

radiometal and for radioanalytical methods, additional acid are available to the researcher (since industrial scale operations is not necessary). Additional common acids for extractions and separations are hydrochloric (HCl), perchloric ($HClO_4$), sulfuric (H_2SO_4), hydrofluoric (HF), and phosphoric (H_3PO_4) acids. Generally the latter three are used to extract analytes from organic phases back into the aqueous phase, due to the increased binding constants for actinides and these ligands and also the formation of less extractable species due to changes in: (i) charge or stoichiometry, (ii) size, shape or steric effects, (iii) thermodynamic properties of extracting the complex. In addition to changing the acid concentration, the anion concentration can be independently adjusted using an ionic salt. For example, to increase the [NO_3^-] without changing the solution acidity, researchers may add $NaNO_3$ to the aqueous phase. Further, mixed acid/salt solutions are used as well to create specific environments that will result in extraction or separation (*i.e.* 0.01 M HCl + 2 M NH_4SCN for Am extraction from lanthanides). [24]

The organic phase diluent is commonly an inert hydrocarbon (*i.e.* dodecane),[25] but can also be aromatic (*i.e.* xylenes),[26]or other material chosen for specific properties (*i.e.* phenyl trifluoromethyl sulfone for radiation resistance and stability toward nitric acid) [27]. The extractant molecules vary widely depending on the specific goal of the experiment. The most common extractant used for nuclear processing is tributyl phosphate (TBP).[22, 25, 28, 29] In general, phosphorous containing functional groups (*i.e.* phosphates, phosphonates, phosphine oxides, ect) readily extract higher valent actinide elements from acidic solutions. This is very effective to remove group I and II metals as well as the lanthanide elements from bulk processing streams. However, phosphorus containing functional groups are not as effective at separating the actinide elements from each other compared to some other functional groups. The use of nitrogen containing functional groups (*i.e.* ammonium salts) can provide efficient separations of the actinides. [30, 31]

To assess the extent at which a metal will be extracted into the organic phase of a solvent extraction system, the **distribution ratio** (D) is evaluated. The D values can be defined by **Equation 9**:

$$D = \frac{[analyte]_{organic}}{[analyte]_{aqueous}} \qquad eq.9$$

Where the analyte concentrations are determined at equilibrium. From the D values researchers can identify **separation factors** (SF) between two analytes, which is define by **Equation 10**:

$$SF = \frac{D_1}{D_2} \qquad eq.10$$

Where D_1 and D_2 are the equilibrium distribution ratios of two metals in identical solvent extraction system.

1.3.3.2. Extraction Chromatography

While liquid-liquid solvent extraction is a method that spans many chemical disciplines and has existed for decades, extraction chromatography is relatively new and (mostly) applied for radiochemical separations. Extraction chromatography became widely applied in the early 1990s at Argonne National Laboratory by Dr. Phil Horwitz with Dr. Renato Chiarizia and others for rapid bioassay analysis The innovation was embedding extraction reagents into the macro-structure of an inert solid substrate. These systems now are considered a solid-liquid extraction and therefore generally extraction chromatographic resins are prepared into columns and the extraction process occurs *via* elution. Unlike ion exchange resins where the active component is directly bound to the substrate, the extractants in extraction chromatography remain immobilized on the solid substrate through hydrophobic and Van der Walls interactions. This allows for greater specificity than ion exchange, while simplifying the extraction and separation processes compared to that of solvent extraction methods.

All of the extraction chromatographic resins in this thesis were prepared by Eichrom Technologies, LLC (Lisle, IL); a company that stemmed from the early work at Argonne National Laboratory. Because these materials are purchased (or specifically prepared) by Eichrom Technologies, the extractant weight percentage (w:w%) is fixed at 40% unless otherwise stated. A

cartoon demonstrating the structure of these materials can be seen in **Figure 6**, where the stationary phase is the extractant, the mobile phase is the aqueous solvent, and the inert support is a polymethylacrylate resin bead (25-100 μm).

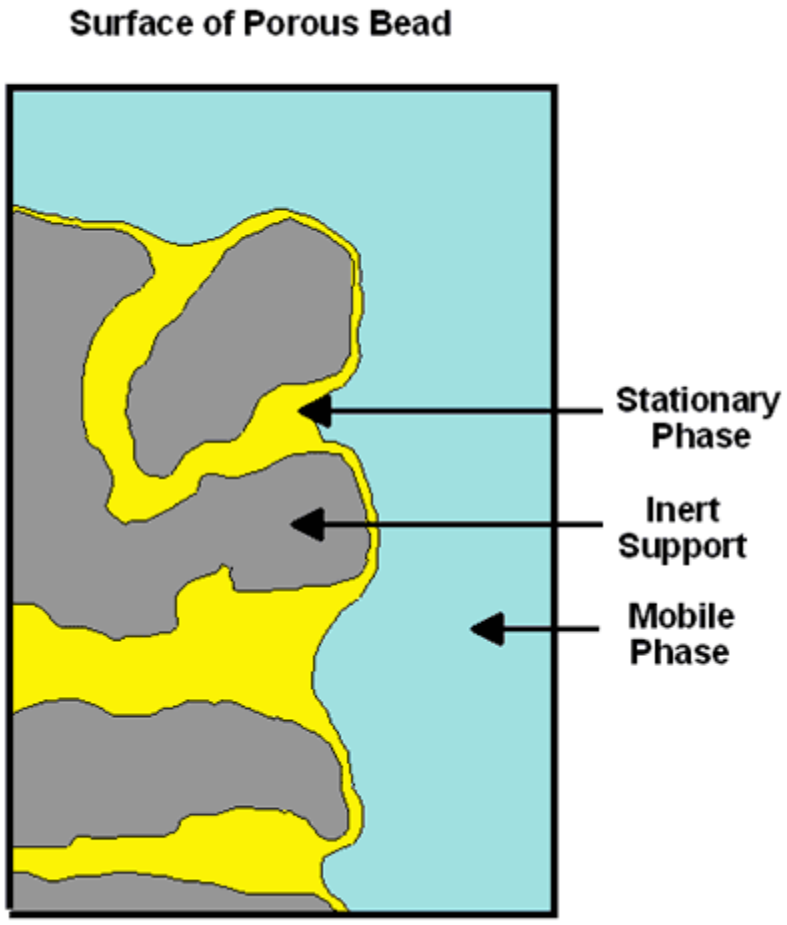

Figure 6. Cartoon demonstrating the structure of extraction chromatographic resins. [32]

Similar to liquid-liquid extraction the aqueous solution, utilized as the mobile phase in extraction chromatography, is prepared strategically to allow for analytes to be retained on the

column and undesired species to be eluted. The aqueous solutions used are similar to those used in solvent extraction, but generally smaller volumes are required.

To assess a metal elution behavior, the **capacity factor** (k') must be determined. The capacity factor is related to the number of **free column volumes** (FCV), or the mobile phase required to achieve the elution peak maximum of a particular analyte metal. To determine the k' for a metal, first the **weight distribution ratio** (D_w) must be determined. The D_w is calculated from **Equation 11**.

$$D_w = D * \frac{V}{m} \qquad eq. 11$$

Where D is the **distribution ratio** determined from **Equation 9**, V is the volume of aqueous phase in L, and m is the mass of the resin in g. From the D_w, the k' value can be calculated with additional parameters regarding the resin physical properties that describe the **stationary phase volume** (v_s) and **mobile phase volume** (v_m). To determine v_s and v_m, the **resin density** (g/cm^3), **bed density** (g/cm^3), and **mass of extractant per gram of resin** (g) must be determined. The mass of extractant per gram of resin is fixed in all cases at 0.4 grams extractant per 1 gram resin. The **bed density** was determined by transferring the dry resin to a tarred graduated cylinder; weighing the resin and dividing by the volume in the cylinder. Then, **resin density** was determined by achieving neutral buoyancy in solutions of known densities (dilute HNO_3). Lastly, the v_m was calculated by subtracting the **resin density** by the **bed density**, and v_s is calculated by multiplying the **bed density** by 0.4 (or the 40% w:w). Finally, the k' value can be calculated by **Equation 12**.

$$k' = \frac{D_w * \rho_{resin} * v_s}{0.4 * v_m} \qquad eq. 12$$

Where ρ_{resin} is the density of the resin. From this equation, batch experiments can be performed and the k' values, demonstrating the adsorption of a metal on to the resin mobile phase, can be calculated. Like liquid-liquid solvent extraction, the SF can be determined from the quotient

of the k' values of two metals using **Equation 10**. Additional factor that impact separations by extraction chromatography include: column dimensions, particle size, temperature, and particle porosity.

1.3.3.3. Other Separation methods

While solvent extraction and extraction chromatography are great techniques for elemental separations, sometimes the sample matrix can greatly complicate (if not completely inhibit) the ability of these methods. In these cases, other non-extraction based separations methods can be employed. These methods include, but are not limited to, **precipitation methods** and **electrochemical methods**. In this thesis only precipitation methods are used as an alternative to extractions. These precipitation methods rely on the differences in the solubility product (k_{sp}) of different metals that will result in a chemical separation. A common group separation method for the actinide elements is a manganese dioxide or iron hydroxide co-precipitation. In these methods, the actinide elements are precipitated while monovalent and divalent cations remain soluble in solution. This method is very effective for samples containing high concentrations of low valent metals.

1.3.4. Source Preparation

Following the elemental separation procedures, the samples matrix must be transformed into an appropriate form for counting procedures. For some techniques (*i.e.* gamma spectrometry, liquid scintillation counting; *see below*), the analysis form can be virtually any matrix (so long as the same geometry is used for energy calibrations and efficiency), but for alpha spectrometry, the source preparation is fundamental to the measurement. This is because alpha particles interact with matter over short distance due to the fact that they have charge and mass, and therefore can be easily attenuated. In an alpha spectroscopic analysis, the detector counts the number of decay events attributed to specific particle energy. Therefore, it is essential to create a source that is thin, evenly distributed, and representative of the sample. The two methods used for source preparation in this thesis are **co-precipitation** and **electrodeposition**.

The co-precipitation source preparation method generally uses a carrier metal to facilitate the participation of the trace actinide.[33] While there are numerous co-precipitation methods, the two used in this thesis are **cerium fluoride** (CeF_3) and **cerium hydroxide** ($Ce(OH)_3$). In general CeF_3 will co-precipitate trivalent and tetravalent actinides, and therefore high valent actinides (*i.e.* UO_2^{2+}) must be chemically reduced, by titanium (III) chloride, in order for the co-participation to occur. While this can complicate U source preparation it can be a beneficial final clean up step for the preparation of Th, Am, and Pu (IV or III) sources. This method is extremely effective; however the source of F^- ion is HF, and can be potentially troublesome and hazardous in the lab. An alternative, and relatively redox independent, is the $Ce(OH)_3$ precipitation, in which the Ce carrier is added and the pH is adjusted to about 8. Both these methods are then filtered *via* vacuum filtration using Resolve Filters. The filters collect the micro-precipitate and that filter is mounted to a metal planchette to be counted by alpha spectrometry.

An alternative to co-precipitation methods is electrodeposition. For electrodeposition procedures, the elution matrix of samples is taken to dryness and re-dissolved in a sodium sulfate (Na_2SO_4)/sodium bisulfate ($NaHSO_4$) buffer and transferred to the electrodeposition apparatus equipped with a stainless steel planchette and platinum electrode.[34] The current is adjusted and the analytes are electrodeposited onto the planchette (~90 mins). The planchettes are subsequently washed prior to counting by alpha spectrometry.

These two methods differ slightly for analysis purposes. Electrodeposition is a more time consuming process and potentially low recoveries; however, the alpha resolution is generally superior to that over co-precipitation methods. In contrast, the co-precipitation methods are rapid and generally result in nearly 100% recovery of the analyte, at the expense of resolution. In this thesis both methods are used.

1.3.5. Radiometric Detection Techniques

Unlike most chemical characterization processes, where samples must be activated (ionization, excitation), radiometric detection techniques rely on the inherent energy emitting from

the atoms themselves. The instrumentation of detection depends on the type of radioactivity emission desired to be detected (α, β^-, or γ). In this dissertation, four different radiometric detection techniques were used, **alpha spectrometry**, **gamma spectrometry**, **liquid scintillation counting**, and **alpha/beta counting**.

Each alpha particle emitted from a nucleus has a specific energy, which has been organized in a database by the Department of Energy's New Brunswick National Laboratory in the Evaluated Nuclear Structure Data File and obtained through the National Nuclear Data Center.[16] Alpha spectrometry utilizes this phenomenon, in which a sample is contained in a vacuum chamber with a detector at a fixed distance with a fixed voltage.[35] When an alpha particle is emitted, because it is charged (charged helium nucleus), it hits the detector and changes the voltage on the surface of the detector.[36] This change in voltage is calibrated (internal standards) to represent a specific energy of a particular alpha particle. Therefore one would expect a specific alpha spectrum of for each particular radioisotope. In a given spectrum, the total number of counts in a region can be directly correlated to the total activity in the sample. Each detector has a known efficiency (number of decay events detected/number of decay events that occurred), and each decay pathway has a specific and known branching ratio. By taking into account these corrections, an alpha spectrum can provide a total radioactivity for a sample and therefore a concentration of a particular radionuclide in a sample.

Gamma spectrometry, like alpha spectrometry, generates a spectrum based upon the number of events detected at a specific energy, which are tabulated in the NNCD. In this dissertation, two types of gamma spectrometer detectors were used, **sodium iodide** (NaI) and **high purity germanium** (HPGe) crystals. Unlike alpha spectrometry, where alpha particles have mass and charge, gamma spectrometry measure massless and neutral gamma rays. Therefore in order for an event to be detected, the gamma rays interact with the crystal and the crystals scintillate provide the detector with a signal proportional to the energy deposited by the gamma particle. Because gamma particles are well shielded by high Z materials (*i.e.* lead, uranium, tungsten), the gamma scintillation detectors are encased in lead to minimize (as much as possible) the

background radiation. It is necessary to correct count rate received by the detector to the true decay rate through the correction of the sample geometry (*i.e.* material, shape, and distance from detector). This correction is required to account for the interaction of gamma rays with the sample that results in scattering or absorption. A correction also accounts for the sample geometry owing to the fact that gamma rays are emitted in 360°.

The final two methods of radiometric detection, **liquid scintillation** (LS) and **gas flow proportional counting**, are non-spectral counting techniques (although LS counting can generate a spectrum, the resolution is not sufficient for most quantitative techniques). These methods simply measure a count rate based upon the number of counts detected over a known amount of time. For LS counting, a sample is dissolved in a scintillating fluid, called liquid scintillation cocktail, when alpha or beta particles are emitted, they excite the scintillating fluid and the subsequent scintillation is recorded by the detector. For LS counting, it can be assumed that alpha particle efficiency is 100%, since every alpha particle has enough energy to excite the scintillation fluid. However, for beta (and even some gamma rays), an efficiency curve must be generated to know the scintillation efficiency at particular beta energies. With gas flow proportional counting, a solid or liquid source is directly placed into a counting chamber, and the detector records decay events over a certain counting time frame.

1.4 Protactinium

1.4.1. Discovery

Dmitri Mendeleev predicted the existence of Pa when he arranged the periodic table, but even though Pa is a naturally occurring element, it was not discovered until the 20th century. From Mendeleev's periodic table, a vacant space existed in group V between elements U and Th, and below tantalum (Ta) and was referred to as "*eka-tantalum*" with a proposed atomic mass of 235.[1] From this point forward, scientist sought to find *eka-tantalum* by searching for an element with chemistry similar to that of tantalum—which greatly prolonged its discovery. In 1900, Sir William Crookes was investigating the radioactivity of U and dissolved uranium nitrate in ether. In doing so,

he managed to extract U into the ether and separate it from its natural short-lived decay products, ^{234}Th and ^{234}Pa. However Crookes was unable to characterize the element and had simply referred to it as Uranium-X (UX).[37]

A decade later in 1913, Kasimir Fajans and Oswald Helmuth Göhring identified that UX was comprised of a mixture of two distinct radioelements.[1] These elements were identified to be UX_1 (^{234}Th; $t_{1/2}$= 24.10 days) and UX_2. While the chemistry of Th was known and allowed for UX_1 to be identified as ^{234}Th, UX_2 was considered to be a new unique element that was short-lived and emitted β^- radiation that fits in the vacant space for *eka-tantalum.* [1, 2] Fajans and Göhring gave this element the name *brevium,* deriving from the Latin word *brevis* for brevity. This isotope, ^{234}Pa, has a ground state and metastable state with half-lives of 6.70 hours and 1.17 mins, respectively. This isotope of Pa exists as a decay product of the most abundant U isotope, ^{238}U, through the β^- decays of short-live intermediate ^{234}Th, and decays to a long lived intermediate ^{234}U ($t_{1/2}$ = 2.455x10^5 years) **(Figure 2)**. A few years later, the longest lived isotope, ^{231}Pa ($t_{1/2}$ = 32,760 years) was discovered independently by Otto Hahn with Lise Meitner in Germany in 1917, and by Frederick Soddy with John Cranston in 1918 in the UK through the processing of pitchblende.[1, 2] As a result of this discovery of ^{231}Pa the origins of Ac were understood, and the name was changed from *brevium* to *protoactinium*. This name as well suited because ^{231}Pa decays by α-emission to ^{227}Ac ($t_{1/2}$ = 21.772 years) in the ^{235}U decay chain **(Figure 2)**. The name was later changed to *protactinium* for pronunciation reasons by the International Union of Pure and Applied Chemistry in 1949. Adding Pa to the existing periodic table, the Mendeleev periodic table was nearly completed – missing technetium and transuranic elements. [1]

Moving forward, scientist attempted to isolate or generate significant quantities of Pa to study the fundamental properties of the element.[1] To isolate of Pa from U-ores researchers continued to use the method developed by Crookes, but more intricate and effective methods were also developed. In 1927, a German scientist named Aristid von Grosse isolated 2 mg of Pa_2O_5 and later in 1934 converted that Pa-oxide to Pa metal through irradiation with 35 keV electrons. In that same year, 5.5 ton of pitchblende residues were processed and nearly 0.5 grams of protactinium

were recovered. From this quantity, researchers identified the molar mass to be 230.6 ± 0.5 grams per mol.[1] The United Kingdom Atomic Authority at the Springfield Refinery performed the largest production of Pa in 1961. The Springfield refinery had accumulated stockpiles of high-grade U-ores and vast amounts of processing waste. This *ethereal sludge*, containing siliceous precipitates, contained nearly 4 ppm Pa, and research sought to separate U and Pa from the waste material.[1, 2] During this campaign, nearly 60 tons of U waste material was processed in a 12-stage process to generate 125 grams of pure protactinium. This source of Pa was the world's only significant supply of Pa (until it was mysteriously buried somewhere in England).

Another, anthropogenic, isotope of Pa was isolated and identified in 1964 by the National Reactor Testing Station in Idaho.[1, 2] This isotope, ^{233}Pa ($t_{1/2}$ = 26.975 days), was formed *via* neutron irradiation of natural ^{232}Th to produce fissile ^{233}U. Another route to the formation of ^{233}Pa was from the decay of ^{237}Np that formed as a transuranic product in nuclear reactors, which can be formed directly from neutron capture reactions or by the decay of ^{241}Am (**Figure 7**). Because of these pathways, and the favorable half-life and gamma emissions, ^{233}Pa is the most common tracer used in isotope dilution methods for the quantification of ^{231}Pa in samples.[1]

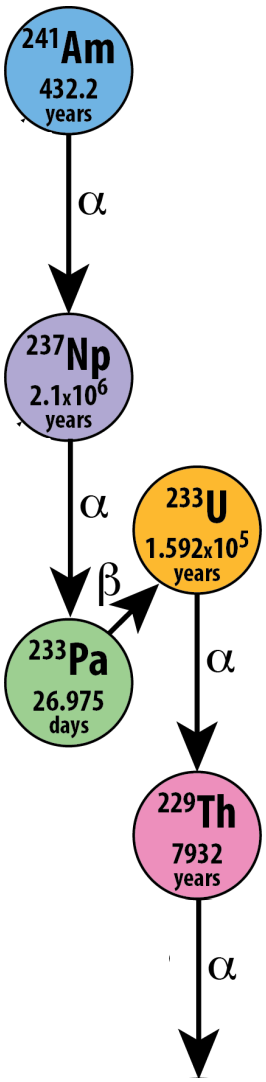

Figure 7. Partial decay scheme of ^{241}Am, showing the production pathway for ^{233}Pa.

Following the large-scale production of Pa, the state of Pa research looked promising driven by the role of Pa in homogeneous Th reactors to form ^{233}U fuels (**Figure 8**) and the contemplated use for the production of ^{232}U.[2] At its peak interest, three international conferences existed dedicated entirely to Pa physical and nuclear properties.[1] However, research interests faded quickly following nuclear disasters (*i.e.* Three Mile Island; 1979 and Chernobyl; 1986), and disinterest in alternative nuclear reactor, resulting in investigations into Pa chemistry to nearly disappear. Today

Pa remains one of the most mysterious and understudied elements on the periodic table. A new wave of interest has opened up legacy vaults of Pa to study its chemistry for fundamental applications to understand the *f*-electrons (Argonne National Laboratory, Chicago IL), its measurement and detection for nuclear forensics applications (Pacific Northwest National Laboratory, Richmond WA; Lawrence Livermore National Laboratory, Livermore CA), and its solvent extraction behavior (National Physical Laboratory, London UK).

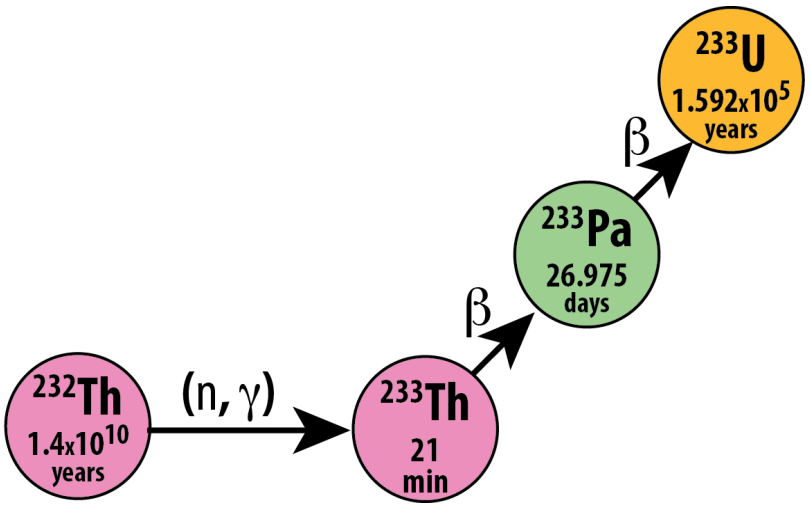

Figure 8. Production pathway for the breeding process of irradiating natural-fertile ^{232}Th with neutrons to form fissile ^{233}U fuels.

1.4.2. Occurrence

There are 29 isotopes of Pa (^{212}Pa-^{239}Pa) that are known to exist, however only three isotopes are relevant to chemists. Those isotopes are, as mentioned previously, ^{231}Pa, ^{233}Pa and ^{234}Pa. Although Pa is naturally occurring, it is an extremely rare element. Terrestrially, only ^{231}Pa has a half-life sufficient enough to accumulate in any mass amount. Since the origin of ^{231}Pa is from the decay of ^{235}U, its terrestrial abundance is linked to U. The average abundance of U in the earth's crust is 2.7 ppm, and the isotopic abundance of ^{235}U is only 0.711% wt:wt.[38] Therefore the abundance of ^{231}Pa is a mere 0.87×10^{-6} ppm. [1]

Beyond the natural terrestrial abundance, Pa isotopes also form in nuclear reactors from a few different pathways. Again, the most significant accumulation is from the decay of ^{235}U, which is enriched in nuclear reactors up to 10%, resulting in the potential accumulation of ^{231}Pa over time. Likewise, ^{233}Pa occurs readily from the decay of ^{237}Np formed in reactors, though the half-life is far too short to accumulate a significant mass,. Additionally, ^{233}Pa can be formed *via* neutron capture of ^{232}Th (and subsequent decay of ^{233}Th). This is a breeding process that can lead to the development of ^{233}U fuels. In this context ^{233}Pa exists as an essential intermediate whose chemistry must be understood.

1.4.3. Current Applications

There are very few applications of Pa. This is largely due to being 1) being intensely radioactive, 2) being extremely rare and 3) having poorly understood chemistry. The primary application of Pa is to age date U-containing materials. There are numerous dating methods available to geologists to date a variety of sample types. Even within U-containing materials, there are three different chronometric ratios, $^{230}Th/^{238}U$, $^{231}Pa/^{235}U$, and Pb-Pb. While Pb-Pb dating is a method most suited for very old samples *(i.e.* method used to date the earth), the other two chronometric ratios can be used for similar times scales, $^{230}Th/^{238}U$ up to 400,000 and $^{231}Pa/^{235}U$ up to 200,000 years. The $^{231}Pa/^{235}U$ chronometer is more sensitive with samples of younger ages. Most notably, $^{231}Pa/^{235}U$ has been used to date a Qafzeh human skull that helped establish the chronology of mankind,[39] as well as Neanderthal bones in Israel, thus confirming that humans and Neanderthal did not exist together in the Lavant. [40] Furthermore, these two isotopic ratios can be used together to determine sedimentation rates or provide extremely precise ages. [41-43]

The $^{231}Pa/^{235}U$ isotopic ratio can be used to date nuclear material for a nuclear forensic analysis. In this case, sample ages are extremely young (<100 years old) and therefore the ingrowth of ^{231}Pa is extremely small. However, since the concentration of ^{235}U is significantly greater than that of natural samples, these samples can be aged dated with great precision. [12, 14] This endeavor is an interest of Department of Homeland Security and the Department of Defense to regulate nuclear

safeguards. In the case of the confiscation of illicit nuclear material, the sample analysis will identify the isotopic signatures required to determine the source origin. In this case, the $^{231}Pa/^{235}U$ isotopic ratio provides invaluable age information that can allow for researchers and investigators to determine when the ^{235}U was enriched.

Another facet of Pa research, as a result of the development of nuclear processes, is developing a greater understanding of the fate and transport of Pa in the environment. As the world continues to burn more nuclear fuel and accumulate more nuclear waste the need for a waste management plan becomes more pressing. Therefore the consideration of a solidified nuclear waste form must evaluate the chemical behavior of the actinide elements (include Pa) in these waste forms.

1.5. Chemistry of Protactinium and the Actinides

The actinide and lanthanide elements are the only (yet discovered) elements in which the valence electron shell is an *f*-electron orbital. While the chemistry of the lanthanide elements remains relatively consistent (*i.e.* trivalent hard cations) across the series, the chemistry of the actinide elements has greater diversity. Investigations into the chemical properties of the actinides (An) have revealed unique chemical bonding characteristics that can be attributed to the population of 5*f*-electron orbitals. [1] These findings observed similarities in chemical bonding characteristics in the actinide series and also highlight unique differences in bonding character attributed to specific electronic configurations and their relationship within the An series.[3, 44] For example, in the early An-series elements (i.e. thorium, Th), the energy of the *5f*-electron orbitals is higher than the *6d* orbitals. This results in bonding interactions that contain more d character—closely resembling the transition metals. Continuing across the actinide series, the *5f* electron orbitals decrease in energy –dropping below the energy of the *6d*-electron orbital, forming the familiar actinyl cations (i.e. $AnO_2^{2+/+}$) observed for uranium (U), neptunium (Np), and plutonium (Pu). [1, 45] Thus, differences in *f* and *d* orbital energies represent a critical link in the observed

differences in the bonding character for individual An in the series. One actinide whose chemistry is distinctly different from all the others in the An series is protactinium (Pa). [44]

Interestingly, Pa exists in a critical location (within the An series); where the 6*d* and 5f electron orbitals cross in energy and are nearly degenerate. Research suggests the 6*d*/5*f* orbital near degeneracy underpins the formation of chemical species and bonding characteristics that are distinctive to Pa.[4] Within this context, the proposed research seeks to develop a detailed understanding of the chemical and electronic properties of Pa. With success in the proposed investigation, we expect to establish an understanding of the interplay between the *d* and *f* orbitals in Pa that will play an important role in explaining the chemical behavior and bonding characteristics of Pa.

The unique electronic structure of Pa influences its physical and chemical properties, thereby challenging the development of efficient separations methodologies for use in nuclear forensics, energy, and radiometric dating. Initial work towards my graduate thesis, has focused on developing novel materials that selectively extract Pa from acidic solutions-- relative to the other An at tracer concentrations of Pa ($<10^{-10}$ M). These investigations have identified two materials in particular (aliphatic alcohols extraction chromatographic resins and mesoporous carbon materials; CMK), which result in remarkably effective and efficient separation of Pa from complex matrices containing other actinides and interfering metals, while maintaining high recovery and purity of Pa.[5] However, because these developments were conducted at Pa concentrations below the detection limits of molecular and atomic spectroscopic instrumentation, we are limited to radiometric detection techniques (i.e. gamma and alpha spectrometry), which do not reveal speciation and bonding information of Pa and the other actinides on the surface of the resin materials. Thus, the speciation of Pa that supports the remarkable separation of Pa from other actinides using these materials remains unknown. Our working hypothesis is that, under our experimental conditions, Pa forms the PaO^{3+} moiety (unique amongst the actinides). And that this distinct species allows a strong interaction with hydroxyl groups on the surface of these novel resins.

1.6. Developments in This Thesis

The ***goal*** of this thesis is to develop a greater understanding of the chemistry of Pa, at trace concentrations, and its applications in the nuclear fuel cycle, nuclear forensics, and the environment. Toward this goal, four ***specific aims*** were established and presented in the following five chapters.

1.6.1. Radiochemical Separations and Quantification of Protactinium Isotopes

Develop new radiochemical methods that facilitate the extraction and isolation of Pa isotopes from complex matrices for isotope dilution methods that offer improvements in recoveries and radiochemical purity. As stated in 1966, in order to eliminate the perceived "witchcraft and mystery" of the chemistry of Pa, "this objective would be facilitated greatly if a convenient radioactive tracer were more easily available to a large number of potential investigators".[46] This aim is achieved through two objectives, 1) the development of a rapid method for the extraction and separation of Th, Pa, and U from complex environmental matrices for age dating applications by isotope dilution alpha spectrometry (**Chapter II**) and 2) the development of a convenient method for the preparation of a ^{233}Pa tracer from a ^{237}Np standard source (**Chapter III**). From these developments we have laid the foundation for ^{231}Pa/^{235}U age dating of materials to become a procedure that is more easily performed in the laboratory with satisfactory recoveries to improve the uncertainties in the measurements. Furthermore using this method, nuclear forensics scientist can determine the age of illicit nuclear material rapidly following confiscation. Likewise, by promoting the use of ^{231}Pa/^{235}U as a chronometric ratio allows for a greater number of investigators to make concordant measurement using ^{230}Th/^{238}U to greatly improve the ages of quaternary age materials.

1.6.2. Development of Calculation Modeling of Solvent Extraction Systems

Advance predictive models for solvent extraction behavior through a full factorial investigation of the main effects of extraction parameter **(Chapter IV).** These studies investigate how the changes to the concentration of (2,6)-dimethyl-4-heptanol, anion, and proton affect the distribution ratio of Pa. The anion effects on the distribution ratio were investigated with both Cl^- and NO_3^- anions from the addition of HCl/NaCl and HNO_3/$NaNO_3$. The resulting model provided an equation in which input concentrations of each parameter would result in a predictive D value, which was demonstrated to strongly agree with the experimental results. From these data, 3-D surface plots were generated with the Design-Ease software that allowed for D values to be predicted at any parameter concentration within the experimental window. This data provide valuable insight into the global effects that small changes can have on extraction systems as well as better predictability. While these studies involved three experimental parameters ([(2,6)-dimethyl-4-heptanol], [A^-, Cl^- or NO_3^-], and [H^+]), future experiments will be expanded to include more parameters fully describe a complex extraction systems, such as the effects of radiolysis, hydrolysis, contact time, metal concentration, and diluent composition.

1.6.3. Equilibrium Analysis of Solvent Extraction and Extraction Chromatographic Systems

Establish dominant solution and solid-state complexes of Pa extracted by aliphatic alcohols in HCl and HNO_3 and determine the thermodynamic parameters that govern the extraction **(Chapter V)**.[47] The availability of significant mass quantities of Pa for advanced spectroscopy analysis is limited to a few location globally (Argonne National Laboratory; USA, National Physical Laboratory; UK), this chapter utilizes an understanding of chemical equilibria and solvent extraction techniques to better our understanding of Pa chemistry and illuminate the differences in the chemistry of Pa with respect to the other actinides. To do so, solvent extraction experiments were performed to determine the dependency of the extractant and anion on the distribution ratio.

This information was then used to approximate the average stoichiometry between the central metal, Pa, and the extractant and anion. In these experiments the extractants used were (1-octanol, 2-ethyl-hexanol, and (2,6)-dimethyl-4-heptanol) in both hydrochloric and nitrate acid forms.

1.6.4. Organic Phase Aggregation and the Influence on Solvent Extraction

Develop a greater understanding of the surfactant like behavior and complex ordering in ternary systems consisting of dodecane-water and an aliphatic alcohol in the formation of aggregates and reverse micelles in the organic phase **(Chapter VI)**. This chapter investigates simple biphasic systems of water and dodecane containing an aliphatic alcohol (1-octanol or 2-ethyl-hexanol) to evaluate the equilibrium ordering of these solutions at a molecular level. In these experiments physical measurements were corroborated with small angle X-ray scattering (SAXS) and molecular dynamic simulations to gain an in-depth understanding of what these solutions look like at equilibrium and what factors influence the occurrence and morphology of aggregates.

CHAPTER II: A SIMPLE-RAPID METHOD TO SEPARATE URANIUM, THORIUM, AND PROTACTINIUM FOR U-SERIES AGE-DATING OF MATERIALS

This chapter was accepted for publication 18 February, 2014, published online 28 March, 2014. This chapter is reprinted with permission. Please refer to Knight, A.W., Eitrheim, E.S., Nelson, A.W**.,** Nelson, S.T., Schultz, M.K. (2014). A Simple Rapid Method to Separate Uranium, Thorium, and Protactinium for U-Series Age-Dating of Materials. *Journal of Environmental Radioactivity*, **134**: 66-74.

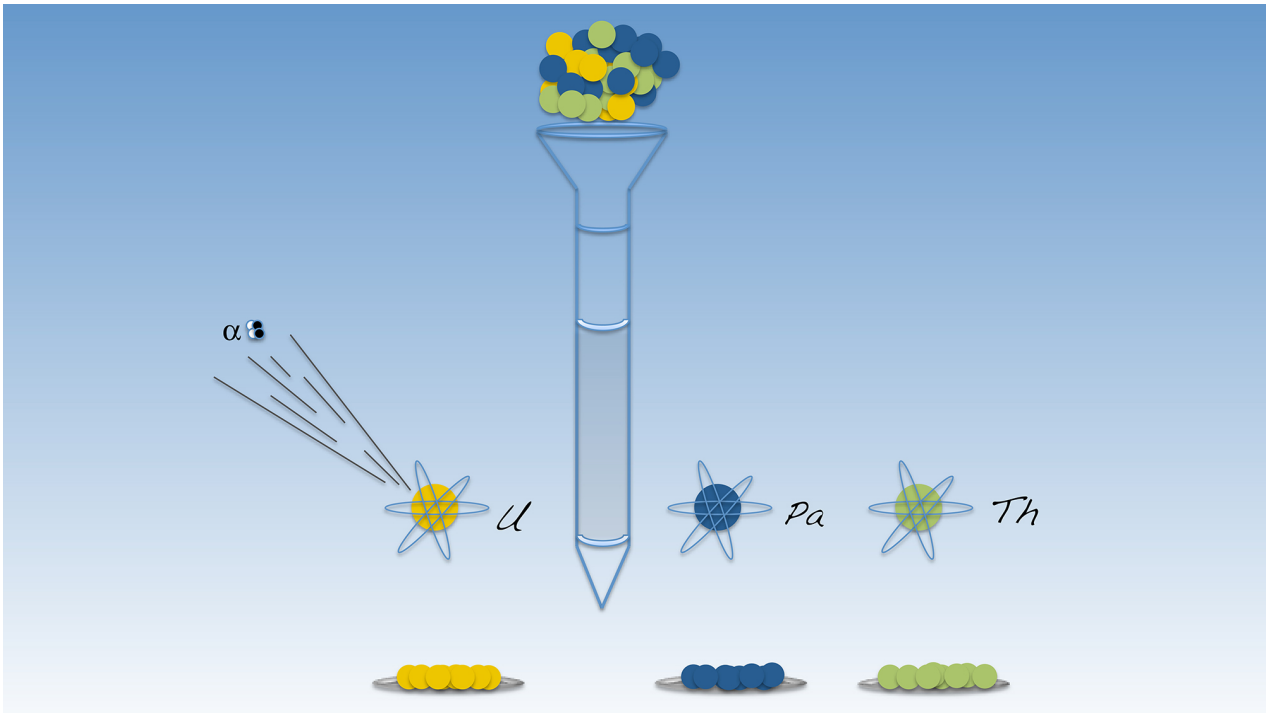

2.1. Abstract

Uranium-series dating techniques require the isolation of radionuclides in high yields and in fractions free of impurities. Within this context, we describe a novel-rapid method for the separation and purification of U, Th, and Pa. The method takes advantage of differences in the chemistry of U, Th, and Pa, utilizing a commercially-available extraction chromatographic resin (TEVA) and standard reagents. The elution behavior of U, Th, and Pa were optimized using liquid scintillation counting techniques and fractional purity was evaluated by alpha-spectrometry. The overall method was further assessed by isotope dilution alpha-spectrometry for the preliminary age determination of an ancient carbonate sample obtained from the Lake Bonneville site in western Utah (United States). Preliminary evaluations of the method produced elemental purity of greater than 99.99% and radiochemical recoveries exceeding 90% for U and Th and 85% for Pa. Excellent purity and yields (76% for U, 96% for Th and 55% for Pa) were also obtained for the analysis of the carbonate samples and the preliminary Pa and Th ages of about 39,000 years before present are consistent with ^{14}C-derived age of the material.

2.2. Introduction

Radiometric age-dating techniques are powerful tools that are used often to understand geological events; describe geochemical processes; and more recently, to develop an understanding of materials for nuclear forensic analysis. Because the nuclear half lives ($t_{1/2}$) of the radionuclides involved are well known, radiometric techniques have the potential to reveal precise information regarding the time (t_0) at which a parent and daughter were separated biogeochemically. For geochronology applications, precise knowledge of $t_{1/2}$ is combined with understanding of distinct differences in the geochemical behavior of radionuclides to establish assumptions that guide the selection of parent/daughter relationships that are relevant to answering the geochemical question at hand. Thus, known radioactive daughter-ingrowth can be used to extrapolate radiometric measurements (performed today) to a time in the past when parent/daughter radionuclide disequilibrium is likely to have occurred. For environmental science applications, this information

can be used to estimate geomorphic growth rates[43] and sedimentation rates; [48] as well as to obtain information about the rates of weathering of geological formations.[49] For nuclear forensic applications, this information represents a powerful tool that can be combined with other forensic evidence to develop a more detailed understanding of the process, time, and location from which the material may have originated.[12, 14]

A mainstay for the last four decades in age-dating materials for various geochronology applications involves the disequilibria and daughter ingrowth of radionuclides in the natural U and Th decay series (^{238}U, ^{235}U, ^{232}Th).[7] With $t_{1/2}$ s ranging from billions of years to microseconds, U-series radionuclide disequilibria enable observers to obtain temporal information for a variety of chronometric uses.[50] Several excellent reviews provide detailed descriptions of the underlying assumptions that form the foundation for various time-dependent phenomena that can be described, and the time frame within which specific parent-daughter relationships can be most effectively employed. For timescales between approximately 10,000 to 375,000 years before present, two of the most commonly used disequilibria employed are ^{230}Th/^{234}U and ^{231}Pa/^{235}U. [7, 9, 50, 51] Because Th and Pa ages can be confirmatory, radioanalytical methods developed for U-series radiochronometry applications have sought to combine the analysis of Th, Pa, and U in a single analytical run. Methods of analytical quantification for these analyses include isotope dilution alpha spectrometry and (more recently) mass spectrometry.[10, 52]

Numerous approaches to radiochemical separations have been established for U-series radiochronometry.[11, 14, 53] Early methods using standard ion-exchange technologies and liquid-liquid extraction were effective, but often suffered from relatively low radiochemical yields in the analysis of more complex matrices. Low radiochemical yields potentially increase the detection limits of the approach, which can be particularly detrimental to Pa dating, due the relatively low natural abundance of Pa in terrestrial samples (<300 fg/g, > 0.03 dpm/g).[11, 41, 54, 55] In addition, relatively large quantities of acid and mixed organic/acid waste prompted the development of improved approaches. While more recent methods have improved radiochemical yields, in general, two or more columns are usually employed, which complicates the process and can result in

relatively large volumes of chemical waste.[41] Within this context, we explored the potential to develop a new method, which might combine improved elemental purity of U, Th, and Pa fractions, with fewer steps, and less waste. In this paper, we describe this new method and present the application of the approach for the isotope dilution alpha-spectrometry analysis and preliminary age determination of an ancient carbonate sample obtained from the Lake Bonneville site in western Utah.[56, 57] The method is relatively rapid; produces only small amounts of chemical waste; utilizes a commercially-available extraction chromatographic resin (TEVA; Eichrom Technologies, Inc.); and employs standard laboratory reagents.

2.3. Materials and methods

2.3.1. General

Radioactivity standards were prepared in Aristar Ultra (Sigma Aldrich) nitric acid (HNO_3, metals grade, certified to parts per trillion metal, PPT, purity), which had been diluted to working concentrations using ultra-pure distilled-deionized water of similar certified metal content (Baseline, Seastar Chemicals, British Columbia, Canada). Tracers were prepared from Standard Reference Materials (SRM's) obtained from the United States (USA) National Institute of Standards and Technology (NIST, Gaithersburg, MD, USA) or from NIST-traceable certified reference materials (CRM's, Eckert Ziegler Radioisotopes, Atlanta, GA USA). Analysis of U consisted of Natural-U (U-NAT, CRM 92564) and ^{232}U standards (CRM 92403), certified to be in secular equilibrium with ^{228}Th, which was used as a tracer for Th analysis. A control standard ^{230}Th (SRM 4342A) was purchased from NIST. Radiochemical yields for Pa analysis were achieved by isotope dilution techniques using ^{233}Pa tracer, prepared by solvent extraction from ^{237}Np (CRM 92566). Tracers were prepared within six months of studies presented here and tracer solutions were stored in double-sealed plastic bottles (certified for low metal content, Seastar Chemicals) and stored at 5°C continuously to minimize potential evaporation effects. Acids and salts used for radiochemical separations included: HNO_3; hydrochloric acid (HCl); hydrofluoric acid (HF); perchloric acid ($HClO_4$); sulfuric acid (H_2SO_4); and ammonium bioxalate [$(NH_4)_2C_2O_4$]) and were ACS reagent grade

purity (Fischer Scientific) or higher. Chemicals used for electrodeposition included: sodium sulfate (Na_2SO_4); sodium bisulfate ($NaHSO_4$); potassium hydroxide (KOH); and ammonium hydroxide (NH_4OH) and were reagent grade (Fisher Scientific). Half-lives and alpha-particle emission energies stated are values originating from the Evaluated Nuclear Structure Data File (ENSDF) and were obtained through United States National Nuclear Data Center (NNDC, Brookhaven National Laboratory, US Department of Energy).[16] Unless otherwise stated explicitly, all uncertainties cited are "standard uncertainties," corresponding to a coverage factor k = 1.[58] Acid dependencies of extraction chromatographic resins were identified from the manufacturer's website and can be found at www.eichrom.com.

2.3.2. Safety Considerations

Solutions containing HF and $HClO_4$ are potentially dangerous and appropriate personal protective equipment should be used when using these acids. Similarly, use of radioactive materials is potentially hazardous and appropriate ALARA principals should be considered prior to conducting experiments using radioactive materials.

2.3.3. Radiotracer Preparation

The isotopic tracers used for this study were $^{232}U/^{228}Th$, and ^{233}Pa. The ^{232}U ($t_{1/2}$ =68.81 years) tracer used is in radioactive equilibrium with daughter ^{228}Th ($t_{1/2}$ = 1.9 years). Control spikes used for method validation were U-NAT and ^{230}Th ($t_{1/2}$ = 7.5 x10^4 years). The U-NAT standard solution contains natural U isotopes; ^{238}U ($t_{1/2}$ = 4.5 x 10^9 years), ^{235}U ($t_{1/2}$ = 7.0 x 10^8 years), and ^{234}U ($t_{1/2}$ = 2.5 x 10^5 years) in natural abundances. Radioactive standard solutions were prepared by serial dilutions, which were performed volumetrically (with gravimetric and radiometric confirmations), with dilutions of 5- and 500-fold performed in 1.0 M Aristar Ultra HNO_3 to obtain final-working secondary-standard solutions. Volumetric dilution factors for standards were confirmed gravimetrically and radiometrically (via liquid scintillation counting (LSC) and alpha-spectrometry) to within 2% for all radiotracers employed, according to our quality control

protocols. Radiotracers and control spikes were added using calibrated volumetric pipet according to our routine procedures.

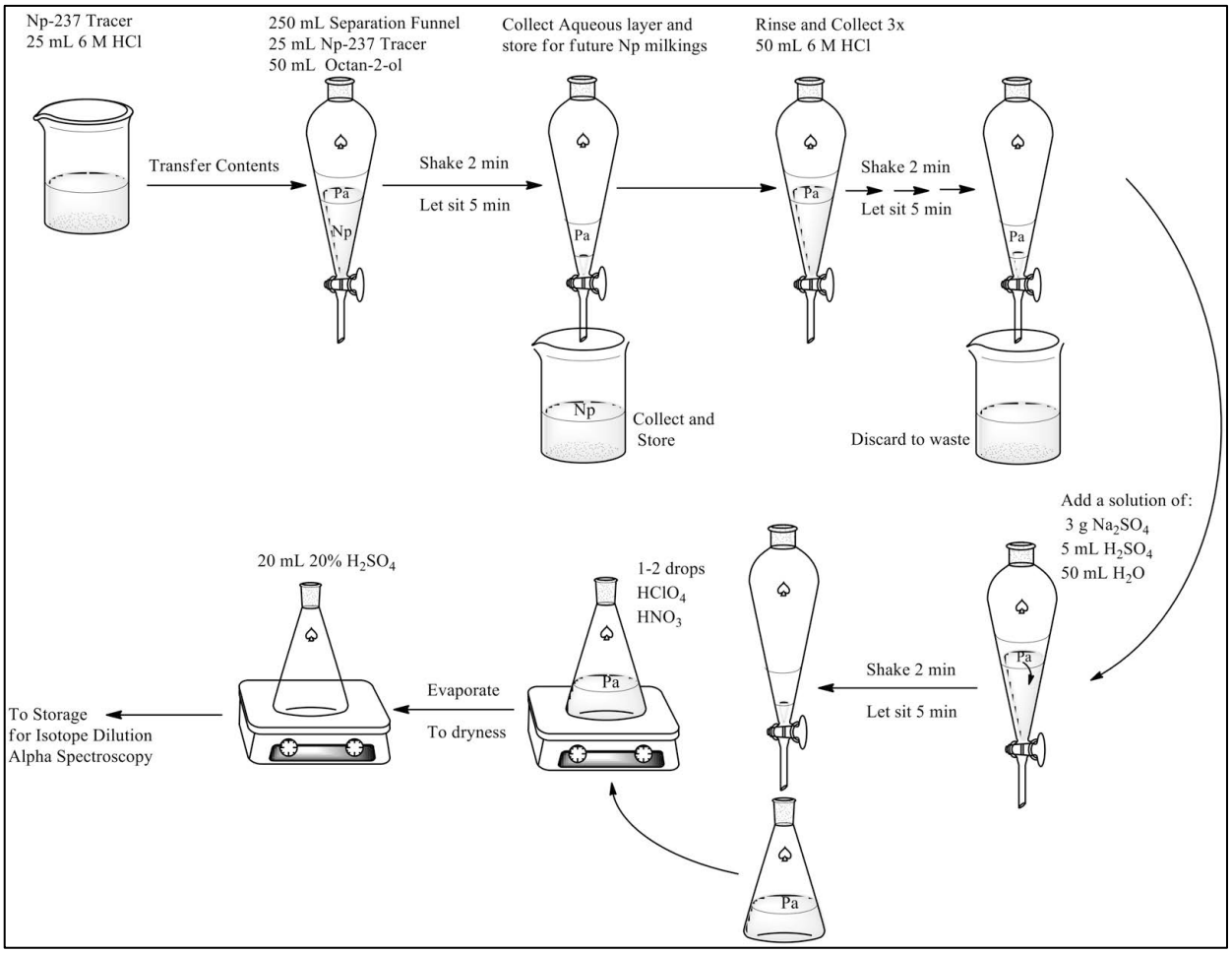

Figure 9. Schematic illustrating the liquid-liquid extraction of ^{233}Pa from ^{237}Np liquid-standard (CRM 92566) for use as a radiometric tracer.

Radiochemical yield determinations for Pa were carried out using an isotopically-pure ^{233}Pa ($t_{1/2}$ = 26.967 days) solution obtained via solvent extraction isolation from ^{237}Np ($t_{1/2}$ = 2.14 x 10^6 years) based on procedures described previously with slight modifications (**Figure 9**). [46, 59, 60] Briefly, the glass ampoule containing the ^{237}Np solution (in 0.5 M HNO_3) was opened and the contents were transferred and stored in a new Seastar Teflon bottle. At the time of preparation, this solution was transferred and taken to dryness in a Teflon beaker and redissolved in a minimum volume of 6 M HCl (Ultrapure, Fluka). This process was repeated three times to ensure that the

solution was fully converted to the chloride form and the ^{237}Np was redissolved in 50 mL 6 M HCl (Ultrapure, Fluka) and transferred to a 250 mL glass-separatory funnel. Extraction of ^{233}Pa was achieved by the addition of 50 mL octan-2-ol (pre-equilibrated in Xylenes). The funnel was shaken vigorously for 1 min and the aqueous and organic layers were allowed to separate (~5 min). The aqueous layer, containing ^{237}Np, was collected and returned to the storage bottle for future ^{233}Pa tracer preparations. The organic fraction, containing ^{233}Pa, was washed with 50 mL of 6 M HCl and shaken for 1 min (to extract residual ^{237}Np) and allowed to separate 5 min. Washings were repeated a total of three times to remove any residual ^{237}Np. Each time, the aqueous-acid layer was discarded. Back-extraction of purified ^{233}Pa into an aqueous solution that would be suitable for tracer additions, was accomplished by adding 50 mL of water containing 3 g Na_2SO_4 in 5 mL concentrated H_2SO_4 to the separatory funnel. Again the contents were shaken for 1 min and allowed to stand for 5 min. The aqueous layer, containing ^{233}Pa, was transferred to a 250-mL Erlenmeyer flask and heated on a hot plate at medium heat. A few drops of concentrated $HClO_4$ and HNO_3 were added to oxidize any residual organic matter. This solution was then taken to dryness, redissolved in 20 mL 20% H_2SO_4, and stored in a 30 mL Teflon bottle (Seastar Chemicals) to minimize adsorption of Pa to the walls during storage.

To confirm the purity of the ^{233}Pa fraction (i.e., absence of ^{237}Np), a sampling (n=3) of electrodeposited sources was analyzed by alpha-spectrometry and beta counting. These sources were also used as standards for yield monitoring (by beta counting) of the Pa radiochemical yields for method evaluation as described previously.[46, 60] To confirm quantitative electrodeposition of Pa to the stainless steel planchettes (for use in yield determinations), the supernatant of the electrodeposited sources were also analyzed for residual ^{233}Pa by High Purity Germanium (HPGe) gamma-spectrometry. No residual ^{233}Pa could be detected in the supernatant solutions, based on examination of the count rate of ^{233}Pa gamma emissions peaks (311.9, 98.4, and 94.6 keV peaks, 24 h count time), with a calculated limit of detection of 0.4 mBq.[58] Further, no ^{237}Np could be detected by alpha-spectrometry (absence of 4.7 MeV peak, 168 h count time, data not shown), thus confirming the purity of the ^{233}Pa standards and quantitative deposition on the surface of the disk.

2.3.4. Chemical Separations

Development of the analytical method presented here was carried out using an extraction chromatographic resin, TEVA, which has been described in detail previously.[61] Briefly, the material consists of Amberchrom CG-71 solid-phase support-resin beads that have been impregnated with a quaternary-mixed-aliphatic-chain (primarily n=8 or n=10) functionalized ammonium salt (n=8, N-methyl-N,N-dioctyloctan-1-ammonium chloride; or n=10, N-methyl-N,N-didecyldecan-1-ammonium chloride; specifically $(C_8H_{17})(CH_3)N^+$ Cl^-, 27%; $(C_{10}H_{21})(CH_3)$ N^+ Cl^-, 47%; $(C_{10}H_{21})_2(C_8H_{17})(CH_3)$ N^+ Cl^-, 27%; $(C_{10}H_{21})(C_8H_{17})_2(CH_3)$ N^+ Cl^-, 2%), commonly known as Aliquat•336. Columns were prepared by slurrying the TEVA resin in water to a concentration of 0.66 g per 5 mL and transferring a vortexed homogenized 5 mL aliquot of the stock slurry to empty columns and allowing the water to drain by gravity flow. Pre-manufactured frits (provided with the empty columns) were inserted on top and beneath the resin and a 25 mL reservoir (AC-120, Eichrom) was attached and the column (**Figure 10**).

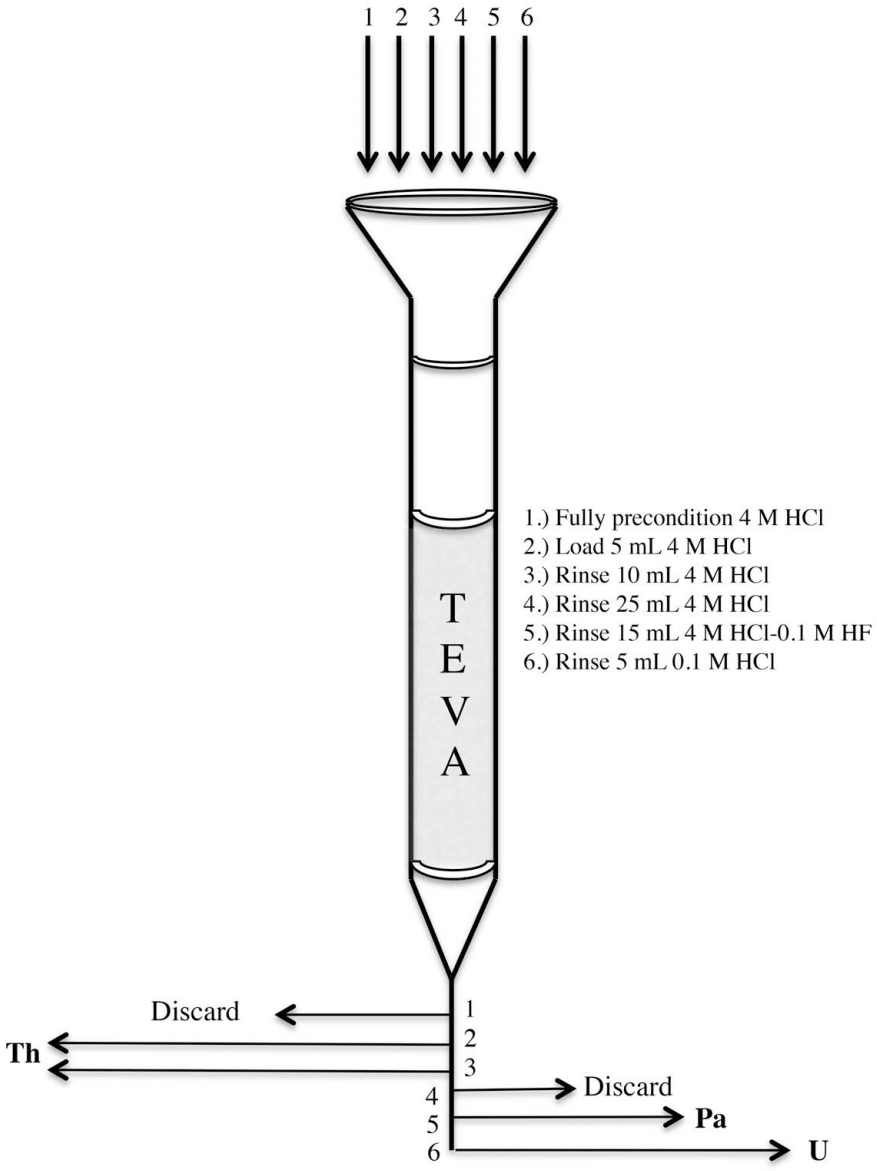

Figure 10. The new column separation protocol using TEVA for separation and purification of Th, Pa, and U.

To arrive at the optimum separation strategy, the elution profiles for Th, Pa, and U were determined by step-wise elution of 1-mL aliquots of eluent solutions directly to 20-mL standard plastic or glass LS vials for direct counting by LSC. To prepare, ~75 Bq $^{232}U/^{228}Th$ and ~180 Bq ^{233}Pa

were taken to dryness and redissolved in 5-15 mL 4 M HCl. These experiments were undertaken to determine the elution peak maximum at test acid concentrations and no attempt was made in these experiments to assess or correct for scintillant quench or background contribution. Unlike alpha emitting radiotracers, ^{232}U and ^{228}Th, that have a LSC counting efficiency near 100%, the LSC counting efficiency for beta-particle emitter ^{233}Pa is less than 100%. Nonetheless, because the signal is proportional to the activity of the samples, the LSC experiments provide the necessary information to determine the elution peak maximum values of Pa. Prior to separations, the TEVA column was preconditioned with 10 mL of 4 M HCl and the sample was loaded on the column in 1 mL aliquots using an autopipet. Each aliquot was collected into a separate LS vial containing 15 mL of LS cocktail (Ecolite™, MP Biomedicals, Solon, OH USA). Once each 1-mL aliquot was collected (**Figure 10**), vials were shaken, dark adapted, and counted by LSC for 30 min each for two cycles using routine counting parameters.

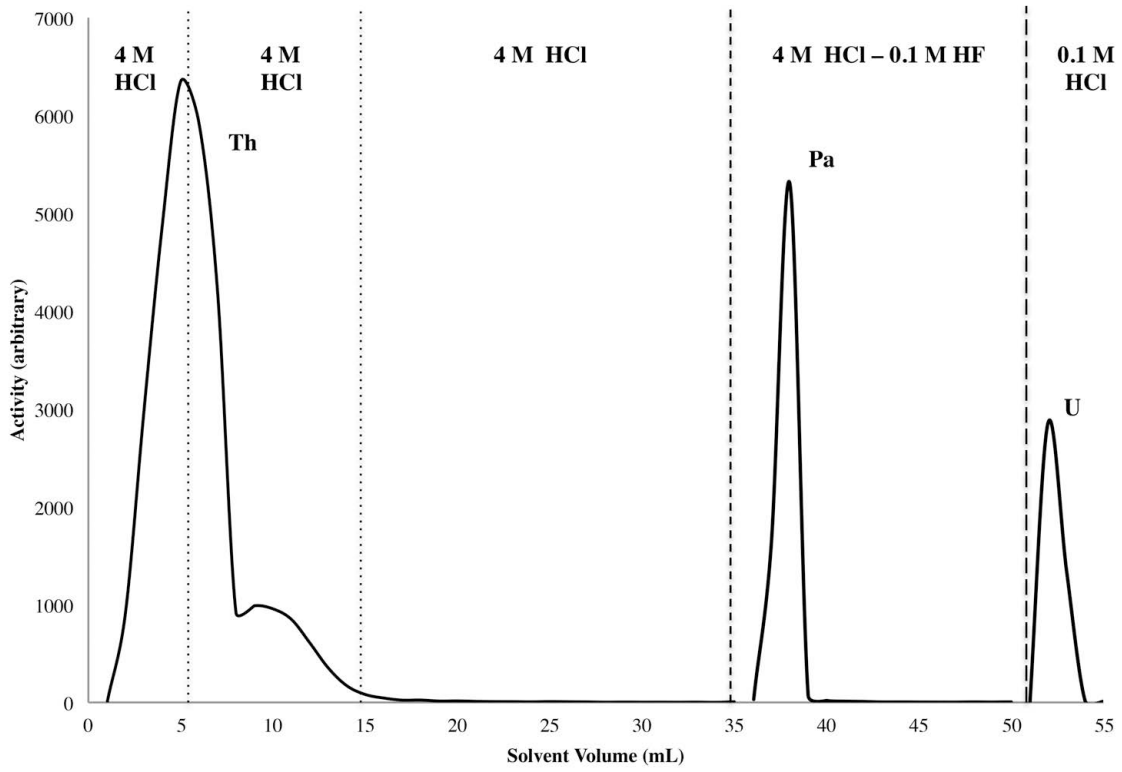

Figure 11. Elution curves that describe the final separation procedure as a function of elution volume. The procedure for the separation of U, Th, and Pa was performed in 1 mL aliquots.

For alpha-spectrometry analysis, TEVA columns were again assembled and preconditioned with 10 mL of 4 M HCl. The sample was loaded in 5 mL of 4 M HCl to the column via transfer pipette directly onto the frit at the top of the column. The eluent of the load solution was collected for Th and the remaining Th was collected in the same beaker with an additional 10 mL rinse with 4 M HCl (**Figure 11**). Another rinse containing 25 mL of 4 M HCl eluted any residual Th prior to the elution of Pa, but was discarded (*i.e.* this discarded fraction contains very little Th). Following the removal of residual Th, Pa was selectively stripped from the column (*i.e.* U is retained) in 15 mL of 4 M HCl-0.1 M HF and this fraction was collected for Pa analysis. Finally, U was eluted from the column with 5 mL of 0.1 M HCl. Once fractions were collected, they were set aside for source preparation and analysis.

2.3.5. Source Preparation

Instrumental methods employed for the studies presented here were carried out by LSC, alpha-spectrometry, and beta counting. Sources analyzed by alpha-spectrometry and beta counting were prepared via electrodeposition according to an approach developed previously,[34] using a model EP-4 electrodeposition module (Phoenix Scientific Sales, Roswell, GA USA). Briefly, following separation and purification the Th, Pa, U, each analyte fraction was slowly taken to dryness. For Th fractions, once the eluent reached a minimal volume (~3 mL), it was necessary to add 1 mL of concentrated HNO_3 and a few drops of 30% H_2O_2 to destroy possible organic resin material that co-eluted from the column bed of the TEVA column. The beaker was then covered with a watch glass and allowed to reflux for 20 min. Our experience indicated that neglecting the oxidation of organic matter step resulted in a visible cake on the Th planchettes that decreased yield and degraded spectral resolution. Once completely dry, all three fractions were redissolved in a buffer containing 5 mL 15% Na_2SO_4, 2.5 mL 5% $NaHSO_4$, and 2 mL of H_2O. The contents were transferred to plastic electrodeposition cells, which had been fitted with a stainless steel planchette (25 mm outer diameter, AF Murphy, Quincy, MA USA), with 3 rinses of 1 mL of H_2O. Once the module was assembled, a platinum electrode was inserted and the current was adjusted to 0.5 A for 5 min, and then kept at constant current (0.75 A) for 90 min. To terminate the deposition, 2 mL of 25% KOH was added (dropwise) with constant current for 1 min, followed by removal of the current and discarding of the solution. A final rinse of the inside wall of the cell was performed with 5% NH_4OH. The planchets were then removed from the cell and rinsed with minimal volumes of NH_4OH, ethanol, and acetone to clean and dry the counting source. Once dry, the sources could be analyzed by alpha spectrometry and beta counting.

2.3.6. Source Counting

Alpha-spectra were collected using vacuum-controlled alpha spectrometers (Alpha Analyst, Canberra, Meridan, CT USA) equipped with 450 mm^2 passivated ion-implanted silicon detectors (PIPS, Canberra), with a source-to-detector distance of approximately 10 mm, which resulted in a

counting efficiency of approximately 20%. Thus, radiochemical yield determinations were obtained by standard calculations using efficiencies determined using standards prepared from NIST SRM 4342A (^{230}Th) in an identical geometry. Prevention of alpha-daughter recoil contamination of alpha-detectors was accomplished by use of thin films, prepared as described previously (using a mixture of iso-amyl acetate and collodion). These thin films have been demonstrated to have no effect on the alpha emission detection efficiency or spectra resolution.[62] Alpha-counting sources were counted for approximately 168 h, with a matched count-time background subtraction of each region of interest (ROI) applied to obtain background corrected integrated count rates. Standard isotope dilution techniques were used to calculate the apparent activity of added controls ^{230}Th and U-NAT radionuclides based on the ratio of control to added ^{232}U and ^{228}Th integrated counts.[56]

Beta counting for ^{233}Pa yield determinations was conducted using a Ludlum model 3030 Alpha Beta Radiation Sample Counter (Ludlum Measurements, Inc., Sweetwater, TX). Each Pa source was counted in triplicate for 10 min, with appropriate matched-count time background subtraction. The count rate was compared to sources of ^{233}Pa with known activity to determine the radiochemical yield. Purity of the ^{233}Pa tracer solution was confirmed by gamma-spectrometry using a P-Type HPGe detector (ORTEC, Oak Ridge, TN USA), which was calibrated for energy and efficiency using a NIST-traceable multi-line gamma-ray source obtained from Eckert Zeigler.

For the determination of elution peak maximum values for radiochemical separations, LS counting was carried out using a Packard (1600 CA Tri-Carb) LS counter using EcoLite LS cocktail in plastic LS vials with a water fraction of approximately 10%. The LS sources were counted so as to achieve at least 1000 total counts for a counting uncertainty of approximately 3% (k = 1).

2.3.7. Method Evaluation

Preliminary evaluation was carried by validation runs in which control standards U-NAT and ^{230}Th were used to simulate the analysis of natural samples. For method evaluation experiments analyzed by alpha-spectrometry, Th, Pa, and U tracers and analytes were added to a Teflon beaker volumetrically (50 mL ^{232}U/^{228}Th, ~0.07 Bq; 50 mL U-NAT, ~0.025 Bq; 100 mL ^{233}Pa,

~18 Bq; and 1 mL ^{230}Th, ~0.07 Bq), and taken to dryness. A nominal 5 mL volume of 4 M HCl was added and the process was repeated three times to convert the matrix to the chloride form for separations. After conversion of the carrier to the chloride form, the tracer and analyte radionuclides were redissolved in the load solution (5-15 mL 4 M HCl) for TEVA separation and purification (**Figure 10**).

To further evaluate the potential of the new method, the approach was applied for the age determination of a natural matrix geological material - an ancient carbonate sample (GC2 1980-2050, Brigham Young University) obtained from the Lake Bonneville site in western Utah.[57] A complete description of the material and its preparation will be described elsewhere. For these further evaluation runs, 0.5 g aliquots (n = 3) of GC2 1980-2050 were added to Teflon beakers and dissolved in minimal 1 M HCl. To this slurry, the radiometric tracers were added (0.07 Bq ^{232}U/^{228}Th, ~18 Bq ^{233}Pa). The slurry was diluted to approximately 10 mL of concentrated HCl, covered with a Teflon watch glass, and refluxed under low heat over night. At the completion of the dissolution step, the remaining sand and other insoluble materials were separated via centrifugation at 3100 rpm for 30 min (IEC MediSpin, Thermo Scientific, Waltham, MA; USA). The pH was kept low to minimize adsorption of Pa and Th to the beaker or particulate matter. Following centrifugation, samples were transferred back to Teflon beakers and taken dry. Once completely dry, samples were redissolved in 2 M HNO_3. This process was repeated four times to ensure the complete conversion from the chloride to the nitrate form. As a precautionary step, the redissolved carbonate samples were centrifuged again for 30 min to remove any colloidal silica that could potentially interfere with the column separation steps. For these natural matrix samples, a pre-concentration step was included by the use of TRU resin (Eichrom Technologies, Lisle, IL) in a procedure previously described by Hull *et al.* previously.[63] Briefly, the sample was loaded to a preconditioned TRU column (1 mL column volume geometry as in TEVA separations) in 10 mL 2 M HNO_3. The column was rinsed with 30 mL of 2 M HNO_3 to remove common ions, followed by group-elution of the actinides with a rinse of 10 mL of 0.1 M ammonium bioxalate. The fraction containing ammonium bioxalate was sublimated to apparent completion in a glass beaker at moderate heat.

Following complete removal of the ammonium bioxalate reagent, the sample matrix was converted to 4 M HCl, and separation of Th, Pa, and U was conducted according to the procedure described above using the TEVA resin (**Figure 10**). Following the TEVA separation, electrodeposited sources were prepared and counted for 168 h in alpha-spectrometry chambers with known efficiencies. The ^{233}Pa yield was determined as described above. Analysis of alpha-spectra allowed for the determination of a preliminarily age of formation for the carbonates using U-series dating techniques (^{230}Th/^{234}U, ^{231}Pa/^{235}U) to be described in detail in future publications.

2.4. Results and Discussion

2.4.1. Results

We have developed a new method for separation and purification of Th, Pa, and U using the commercially-available extraction chromatography resin TEVA. Estimations of the elution peak maximum value for each element under conditions that achieved highly pure fractions were determined by LS techniques. To further evaluate the method, a proof-of-concept isotope dilution alpha spectrometry study was performed using a mixture of tracers (^{228}Th, ^{233}Pa, and ^{232}U) and controls (^{238}U, ^{235}U, ^{234}U, and ^{230}Th) in a simple acid matrix. These experiments were designed to determine the radiochemical recovery, purity, and alpha-spectral resolution that could be achieved using the method. For this proof-of-concept study (n = 3), the mixture of radionuclides was loaded to preconditioned columns in 4 M HCl and elemental fractions were eluted separately. While Th passes directly through the column with the load solution and rinses, Pa and U are initially retained and can then be eluted sequentially from the column in 4 M HCl-0.1 M HF and 0.1 M HCl respectively. To further evaluate the new TEVA method, we performed an analysis of an ancient carbonate sample obtained from a relevant geological formation at the Lake Bonneville site in western Utah. These samples were weighed and acid digested by routine sample preparation techniques and analyzed by isotope dilution alpha-spectrometry.[56, 57, 64]

While analysis of ^{231}Pa/^{235}U and ^{230}Th/^{234}U ratios are considered powerful tools for age dating of materials, improved methods for obtaining elementally-pure fractions of all three

elements in a single analytical run is desirable. Early assessments of available chromatography-based separations technologies led us to investigate extraction chromatographic resin TEVA (Eichrom Technologies), composed of Amberchrom resin beads impregnated with undiluted Aliquat•336. Aliquat•336 has been used previously as the organic layer in liquid-liquid extractions for the separation of actinides from complex environmental matrices and for nuclear fuel cycle applications.[65, 66] For efficient extraction using quaternary-amine-based extractants, radio-metals must be present as anionic species.[66] The anionic complex forms a stable cation-anion pair with the quaternary-amine, achieving extraction from the aqueous phase. For example, at low pH (e.g., 4 M HCl), the predominate species are U(VI) and Pa(V), which are known to form strong anionic chloro-complexes,[5, 67] and are readily extracted into a solution of Aliquat•336,[65, 66] presumably as cation-anion pairs. On the other hand, Th(IV) (the predominant redox state of Th) is weakly associated with Aliquat•336 due to the formation of a relatively weak-neutral $ThCl_4•8H_2O$ complex in HCl. [66, 68, 69] This working hypothesis is supported by a subsequent study, which demonstrated low retention of Th on TEVA resin in all concentrations of HCl.[61] Thus, we hypothesized that U(VI) and Pa(V) could be isolated from Th(IV) by reaction with the Aliquat•336-ligand-based TEVA in a strong acid solution of HCl. Experimentally, we observed little retention of Th on the TEVA column, with an observed elution peak maximum at 5 mL, resulting in radiochemical yields of 90 ± 4%, and no observable radionuclidic impurity (**Figure 12; Figure 13; Table 1**).

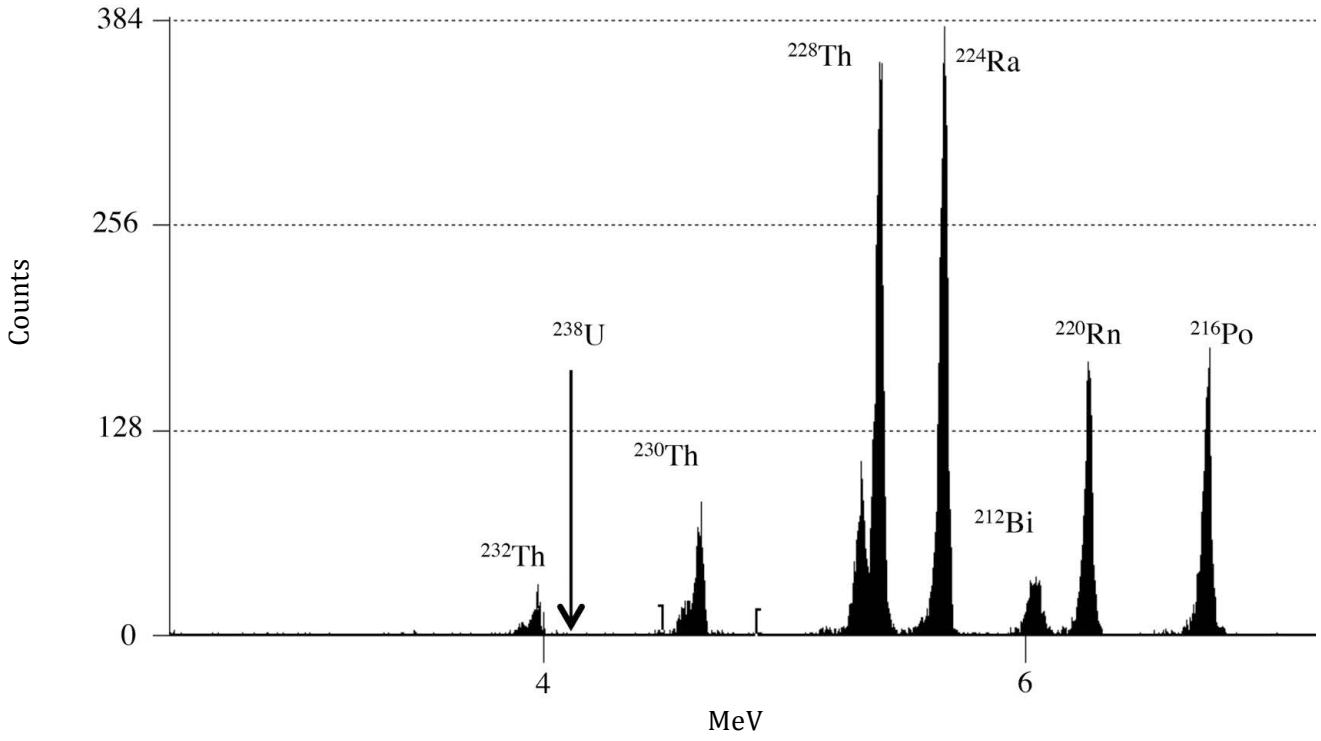

Figure 12. Alpha-spectra of the Th fraction obtained in the analysis of carbonate samples from Lake Bonneville.

Once isolated from Th(IV) (in the organic-extractant phase of the TEVA resin), we further hypothesized that differences in the chemistries of U(VI) and Pa(V) could be exploited to achieve separation and elemental purification. At this step, U(VI) and Pa(V) remain adsorbed to the TEVA column. For the isolation of U(VI) from Pa(V) a stripping agent was necessary because elution curves on TEVA for U(VI) and Pa(V) were very similar in dilute HCl solutions d thus difficult to separate.[61, 70] Potential stripping agents to remove Pa(V) from an organic phase or extraction chromatographic resin has been previously examined. These studies demonstrated that stripping agents such as; HF, $HClO_4$, and Na_2SO_4 are effective in the quantitative elution of Pa(V).[5, 65, 71] For our purpose, the addition of a stripping agent must not only elute the Pa(V), but also it must leave the U(VI) adsorbed to the column. The most promising of these studies indicated that the introduction of a low concentration of HF would result in the formation of strong innersphere-soluble Pa fluoride species (presumably PaF_7^{2+}), which should effectively remove Pa quantitatively.[11, 41, 54, 60] As a starting point, we chose a low concentration of HF (0.1 M) in combination with the same HCl concentration (4 M) as was used to elute Th(IV), which we hypothesized would maintain the adsorption of U(VI). While recent published efforts to develop similar methodologies were unsuccessful in establishing an effective separation step for Pa, these attempts did demonstrate that even very low concentrations of HF were sufficient to abrogate binding of Pa to Aliquot 336-quarternary-amine-based TEVA resin.[5, 11] Thus, we applied a solution of 4 M HCl-0.1 M HF, which we expected would remove Pa(V) while the adsorbed U(VI) species, presumably of the form $R_3CH_3NUO_2Cl_3$, would remain immobilized.[5, 66] Fortuitously, experimental results validated that adding 15 mL of 4 M HCl-0.1 M HF successfully removed Pa(V) from the column with an observed elution peak maximum of approximately 3 mL (**Figure 10**). LSC data shows all of the activity was accounted for in the first 5 mL of the solvent added. Radiochemical recovery of 85 ± 12% was determined by beta counting, and elemental purity in excess of 99.99% was quantified by alpha-spectrometry (**Table 1**).

Interestingly, early experiments showed the presence of observable-residual adsorption of Th(IV) in the alpha-spectrum, which was removed with the Pa fraction. Modifications were made to

fully rinse the TEVA column until LSC data showed the Th(IV) activity dropped to background levels. Notably, a secondary broad elution peak (**Figure 10. 2-2**) characterized the elution of Th(IV) and at least 25 mL of added 4 M HCl rinse was required for complete removal of Th(IV). These results suggest: (1) the potential existence of a low-concentration of contaminant extractant of unknown composition in the resin bed with an affinity for Th(IV); (2) the incomplete conversion of the resin bed to the Cl^- form at the preconditioning step; or potentially (3) that Th adsorbed to the beads or other column materials may contribute to the ultimate shape of the elution profile and create the need for significant rinsing to remove residual Th(IV). Following elution of Pa(V), sequential elution of U(VI) from the column was achieved by elution with 10 mL of 0.1 M HCl as described in Section 2.4 (**Figure 10**).[61] Electrodeposited sources revealed overall process radiochemical yields of 93 ± 3%, with apparent radiochemical purity of 100% confirmed by beta counting, alpha spectrometry, and high-resolution gamma spectrometry (**Table 1, Figure 13**).

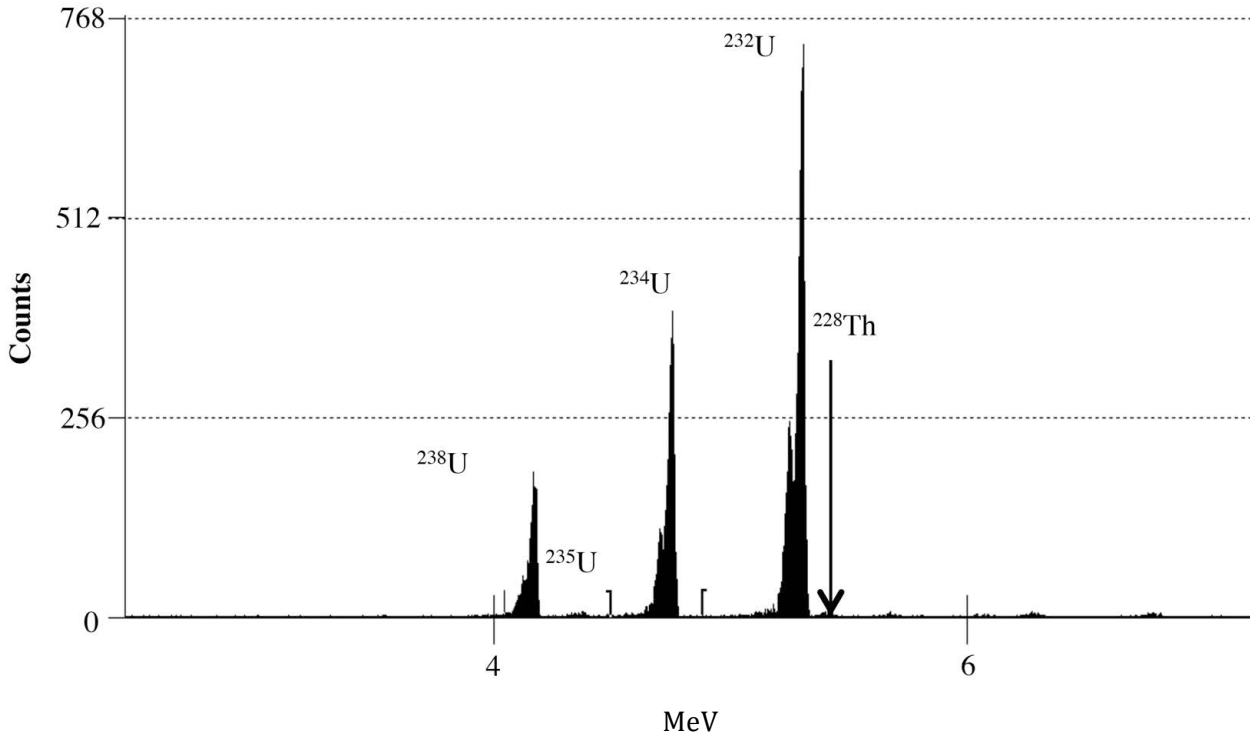

Figure 13. Alpha-spectra of the resulting U fraction obtained by analysis of carbonate samples from Lake Bonneville.

Table 1. Resulting radiochemical yield, spike recovery, observable impurities, and spectral resolution for U, Th and Pa *via* alpha-spectroscopy and beta-counting. The radiochemical yield and spike recovery for U and Th were determined from alpha-spectroscopy.

Element	Radiochemical Yield[1] (%)	Spike Recovery[2] (%)	Impurity[3] (%)	Resolution[4] (keV)
Th	90 ± 4	97 ± 3	ND	31
Pa	85 ± 12	NA	~0.1%	NA
U	93 ± 3	98 ± 1	ND	31

[1] Radiochemical yield was determined from alpha spectroscopy as the average integrated count rate for each isotope divided by the total activity added.

[2]Spike recovery was calculated using isotope dilution α-spectroscopic techniques for the recovery of each control using the isotopic ratio (control/tracer) multiplied by the tracer activity added.

[3]Impurity was calculated from the percentage of activity identified due to any element that would be considered a contaminant.

[4]Resolution was obtained from the full width half max (FWHM) of peaks in the α-spectra as generated by Genie 2000 Software (Canberra)

2.4.2. Control Method Evaluation

We further evaluated the new radiochemical separation approach for purification of Th, Pa, and U by preparing acid solutions with control spikes (^{238}U, ^{235}U, ^{234}U and ^{230}Th) - and analyzing them by isotope dilution alpha-spectrometry using tracers (^{232}U/^{228}Th and ^{233}Pa). We evaluated the method based on critical metrics: achievable radiochemical yield of the tracers; the impurities in each alpha-spectra; and control-spike recovery (**Table 1**).[56] Radiochemical tracer yields were >90% for U and Th for these experiments, while Pa yields were slightly lower (**Table 1**). Spike recoveries for ^{230}Th and U-NAT were calculated to be in excellent agreement with the expected values (**Table 1**). It should be noted that the recoveries determined by alpha-spectrometry were lower than those observed by LS counting, suggesting that some loss of analyte occurs at the electrodeposition step.

Further optimization of source preparation is ongoing in our laboratory and will be presented in a future manuscript. It is also recognized that the activity concentration of our available solutions did not include a test matrix with a sufficiently high concentration of ^{231}Pa to collect sufficient counts for statistical evaluation of a control spike recovery. Rather, our results here are focused on radionuclide purity of the Pa fraction through alpha spectrometry and radiochemical recovery based on beta counting. Future experiments will include testing of matrices with higher concentrations of alpha-emitting ^{231}Pa to enable a statistical evaluation of ^{231}Pa control spike recovery.[58]

The resulting alpha-spectra for Th, Pa, and U from this present study were also analyzed for radiochemical purity. Inspection of the alpha-spectra from the Pa fraction revealed no observable contamination of U for the optimized column separation. Early evaluation of the method pointed to the potential for Th contamination of Pa sources as a possible confounding metric. To mitigate the presence of Th in the Pa fraction, we optimized the method by increasing the rinse volume (4 M HCl; following elution of the Th fraction) to desorb all residual Th from the column prior to the Pa elution. Our results indicate that a total volume of 40 mL of 4 M HCl is required to quantitatively remove residual Th. Based on an examination of counts in the ^{230}Th ROI in the Pa spectra, the increase in rinse volume decreased cross-contamination of ^{230}Th to levels that approach the limit of detection. Thus, in Pa spectra, we observed an upper limit of < 0.1% ^{230}Th added, based on an average net count rate of 2.3×10^{-6} cpm in the ^{230}Th region of interest and a 100 h count time and alpha-detector counting efficiencies of approximately 20%.[58, 72] The Th and U spectra were analyzed for contamination by quantification of counts in the ^{238}U and the ^{230}Th ROI's, respectively. No indication of early elution of U from the TEVA column was observed in Th spectra, nor was the presence of any residual Th observed in U spectra. Expected presence of the decay products of ^{228}Th in the alpha-spectrum could be attributed to ^{232}U-daughter ingrowth (sample count time was 168 h) (**Figure 12**).

2.4.3. Lake Bonneville Carbonate Method Evaluation

As a final proof-of-concept evaluation of the new method for radiochemical separations for U-series age determination of natural materials, we analyzed carbonate samples obtained from the Lake Bonneville site in western Utah (USA). In our first attempt, samples (0.5 g) were digested to dissolve the carbonate material according to established procedures [64] and analyzed by isotope dilution alpha-spectrometry.[56] Using standard Bateman equation-based dating techniques, our preliminary estimate of the formation of the deposit is approximately 39,500 ($^{230}Th/^{234}U$) and 40,000 ($^{231}Pa/^{235}U$) years before present. These ages compare favorably with preliminary ^{14}C ages of roughly 37,000 years (obtained with appropriate corrections). These ages should only be considered nominal, and no statistical conclusions can be made regarding concordance because the estimated detection limit of this separation protocol (TRU/ TEVA) (3 mBq per g sample, counted for 168 h) is greater than the decay rate determined for Pa and the estimation of the detection limit was based on a single count.[58] Future investigations will established a more rigorous understanding of achievable detection limits and focus on techniques to improve the Pa measurement to minimize the uncertainties associated with the age determinations. Although the uncertainties associated with the measurements are large, calculated ages correspond well with the ^{14}C derived ages, radiochemical yields for tracers were less than expected d 62 ± 12%, 24 ± 9% and 37 ± 9% for ^{232}U, ^{228}Th, and ^{233}Pa respectively. Control experiments demonstrated that losses associated with the TRU and TEVA column separations were negligible (see above) and it was determined that losses could be attributed to sample preparation and source preparation steps. Modifications were made to improve the overall yields associated with these steps; including substitution of the electrodeposition source preparation with microprecipitated rare-earth-fluoride based filtered source preparation. It was also found that a digestion procedure in 25 mL of 2 M HNO_3 (1 h), followed by filtration of the sample to remove residual silicate residue (instead of centrifugation), prior to loading onto the TRU column improved the overall radiochemical yields for this carbonate sample. These modifications improved the overall radiochemical yields being 76 ± 11%, 96 ± 10% and 55 ± 12% for tracers ^{232}U, ^{228}Th, and ^{233}Pa respectively (n = 4). Future studies will include a

more comprehensive optimization of the sample preparation and source preparation for these carbonate samples and a complete examination of the age of the material based on both $^{230}Th/^{234}U$ and $^{231}Pa/^{235}U$ disequilibria. Alpha-spectral results of the U content in the carbonate samples reveled isotopic enrichment of ^{234}U relative to parent ^{238}U, which will be further examined also in these future studies.

2.5. Conclusions

Here we described a new simple method for the separation of Th, Pa, and U, using extraction chromatography resin TEVA, that can be applied for age-dating or radioanalytical analysis applications by isotope dilution alpha spectrometry or mass spectral techniques. The separation procedure can be performed in less than 3 h using a standard gravity-flow ion-exchange-type column arrangement and results in less than 50 mL of acid waste. The method provides acceptable to excellent radiochemical yields that are comparable to the other methods, with virtually 100% radiochemical counting source purity. Ongoing studies are underway to examine the potential to improve the overall speed of the approach by vacuum based rapid chromatography approaches and the development of a column chromatography approach to preparation of ^{233}Pa tracer working standards.

2.6. Associated Content

Notes: The authors declare no competing financial interest.

Acknowledgments: The authors extend sincere thanks to Phil Horwitz and Daniel McAlister of Eichrom Technologies, Inc. for guidance in the experimental design, as well as thoughtful review and commentary on the manuscript. We thank Jake Venzie at the Savannah River National Lab (SRNL) for helpful conversations on the separations approach. This material is based upon work supported by the U.S. Department of Homeland Security under Grant Award Number, 2012-DN-130-NF0001-02. The views and conclusions contained in this document are those of the authors and should not be interpreted as necessarily representing the official policies, either expressed or

implied, of the U.S. Department of Homeland Security. Further support was provided by the US Nuclear Regulatory Commission, US NRC-HQ-12-G-38-0041.

CHAPTER III: A CHROMATOGRAPHIC SEPARATION OF NEPTUNIUM AND PROTACTINIUM USING 1-OCTANOL IMPREGNATED ONTO A SOLID PHASE SUPPORT

This chapter was accepted for publication and published online 12 May, 2015. This chapter is reprinted with permission. Please refer to Knight, A. W., Eitrheim, E. S., Nelson, A. W., Forbes, T. Z., Schultz, M. K. (2016). A chromatographic separation of neptunium and protactinium using 1-octanol impregnated onto a solid substrate. *Journal of Radioanalytical and Nuclear Chemistry,* **307**(1): 59-67

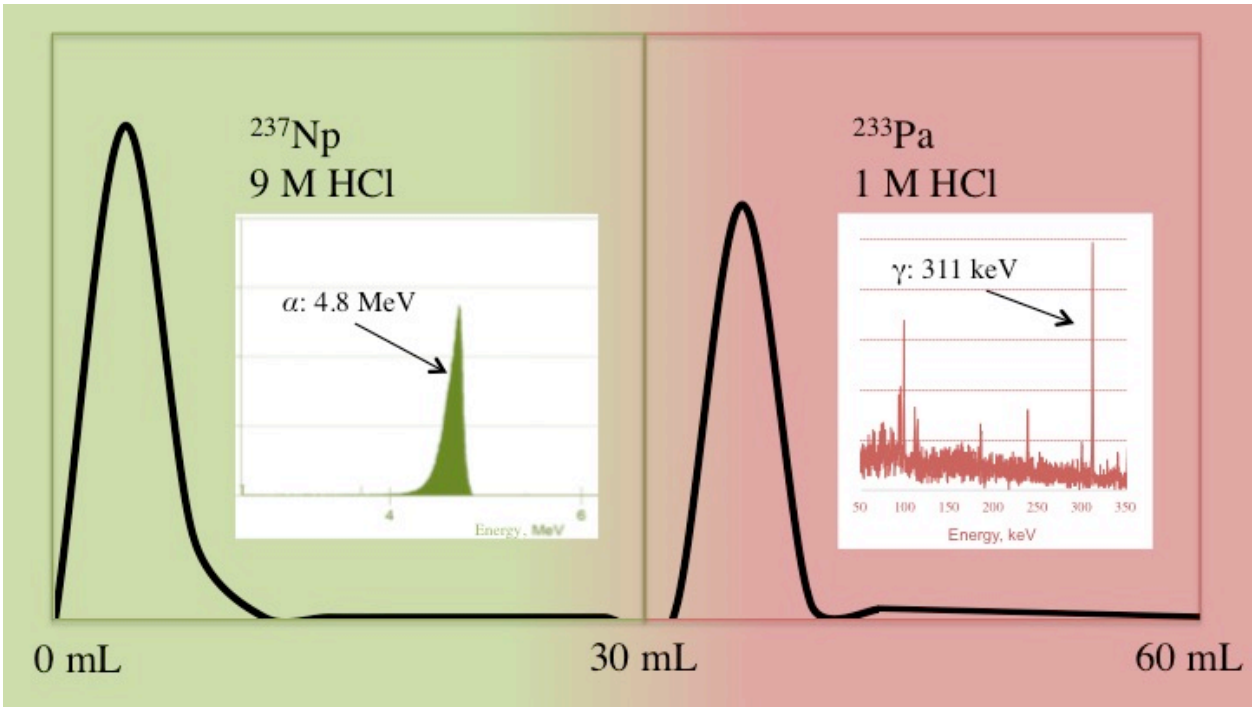

3.1. Abstract

We have developed a new chromatographic method to efficiently separate and isolate neptunium (Np) and protactinium (Pa), based on the selective extraction of protactinium by primary alcohols. The effectiveness of the new technology is demonstrated by efficient separation of ^{233}Pa from parent radionuclide ^{237}Np, using a hydrochloric acid mobile-phase medium. Our new approach reproducibly isolated 233Pa tracer with a yield of 99 ± 1 % (n = 3; radiochemical purity 100 %) and enabled chemical recovery of ^{237}Np parent material of 92 ± 3 % (radiochemical 99 %) for future ^{233}Pa tracer preparations. Compared to previous methods, the new approach reduces radioactive inorganic and organic waste; simplifies the separation process by eliminating cumbersome liquid– liquid extractions; and allows isolation of radiochemically pure fractions in less than 1 h.

3.2. Introduction

Investigations to understand the chemical properties of the rare actinide (An) elements protactinium (Pa; Z = 91; [Rn]5f^{2}6d^{1}7s^2) and neptunium (Np; Z = 93; [Rn]5f^{4}6d^{1}7s^2) over the past few decades have led to a greater understanding of the physico-chemical properties of the 5f-group An. The chemistry and applications of these elements are fascinating and diverse.[1, 37] For example, Pa isotopic signatures and radioactive steady-state relationships can provide important information for geologists;[7, 9, 11, 54] nuclear forensic scientists;[12, 14, 73] and nuclear engineers. [66] However, deficiencies in our understanding of Pa chemistry often complicate radioanalytical methods employed for these investigations.[4, 11, 74]

While many of these complications arise from limited accessibility to appreciable quantities of Pa for spectroscopic studies, expanding investigations into Pa separations and purifications have led to exciting new applications. For example, efficient analysis of Pa-bearing nuclear materials for applications in nuclear forensics and Th-based nuclear fuel development are leading to an increasing need for technologies that enable isolation of radiochemically-pure Pa from complex and (in some cases) high-radiation-field media.[13, 74] Specifically, beta-emitting Pa radionuclide, ^{233}Pa

($t_{1/2}$ = 26.967 days), may be an undesirable contaminant in uranium-233 (^{233}U) nuclear fuels because of its large neutron cross section.[75] Within this same context, nuclear forensic and geochronological analysis of long-lived ^{231}Pa ($t_{1/2}$ = 3.2769 x10^5 years) by isotope dilution techniques generally requires the use of ^{233}Pa as a yield monitor for accurate determinations of ^{231}Pa by alpha spectrometry and mass spectrometry.[10-12] Interestingly, research investigators published the most comprehensive reports on Pa chemistry during the 1950s and 1960s, and anticipated that ''much of mystery and witchcraft [of protactinium chemistry]'' would be eliminated with the advent of appropriate tracer preparation techniques.[5, 46] Ironically, to this day, much of the mystery of Pa remains unresolved, due in part to the need for more effective strategies for the preparation of isotopic tracers.[4] Thus, there is a critical need to develop robust technologies for separating and isolating Pa from materials.

Like Pa, isotopes of Np are of interest for applications in environmental science; nuclear engineering; and as part of isotopic signatures in nuclear materials for forensic applications.[76] While identification of isotopes of Pa occurred in the early part of the twentieth century, it was not until the 1940s that investigators isolated sufficient quantities of Np radionuclides to confirm its predicted-basic electronic and chemical properties.[1] Of the isotopes of Np, alpha emitting radionuclide ^{237}Np ($t_{1/2}$ = 2.149 x10^6 years) is of significant interest because it has been identified as an environmental concern and as a radionuclide that has the potential to assist in nuclear forensic analysis of materials.[73, 77] In environmental science, $^{237}Np(V)$ is highly mobile in subsurface systems and is considered a problematic radionuclide for the long-term storage of high-level wastes produced from nuclear fuel cycle and weapons development. Worries regarding effectiveness of engineered barriers and accidental release have led to research into the mechanism of Np adsorption and transport in biogeochemical systems.[76, 78] While the relatively long half-life of ^{237}Np is one rationale for concern in terms of its fate, transport, and potential for bioaccumulation, the half-life and easily-detected alpha emissions of ^{237}Np also enable its use for studies of fundamental Np properties.[1]

On the other hand, investigations of the chemical properties of Np using ^{237}Np are often complicated by radioactive ingrowth of its immediate radionuclide decay product, ^{233}Pa, and current separations technologies are cumbersome for routine analyses.[79] Due to a relatively short half-life, the observed radioactivity of ^{233}Pa increases rapidly toward secular equilibrium (steady state) with ^{237}Np, which is undesirable for many applications. Conversely, the rapid ingrowth of ^{233}Pa facilitates the use of calibrated ^{237}Np standard solutions for the preparation of ^{233}Pa tracer for isotope dilution analysis of ^{231}Pa in materials, as described above. Consequently, researchers must routinely remove ^{233}Pa from ^{237}Np sources.[10, 46, 63] Unfortunately, current methods to isolate ^{233}Pa from ^{237}Np involve anion-exchange (e.g., AG-MP1,[10] Dowex-1,[5] AG1-X8 [11]) and liquid–liquid extraction (e.g., diisobutylketone,[10] diisobutylcarbinol[5]) techniques that generate substantial liquid (organic and inorganic) wastes—and often employ potentially hazardous hydrofluoric acid (HF).[10, 11, 63] Although HF is an effective complexing agent for Pa, which allows back-extraction into the aqueous phase,[46] excess F- can prevent Pa extraction in subsequent steps.[11] Furthermore, HF poses a serious health hazard and should be avoided when possible.[80]

Within this context, we have developed a new technology and approach for the efficient separation and purification of Pa and Np that will be beneficial for the preparation of ^{233}Pa tracer from ^{237}Np for isotope dilution radioanalytical analysis,[10, 46, 60] and for the removal of ^{233}Pa from ^{237}Np for research investigating fundamental and environmental Np chemistry.[76] In this article, we describe this new and highly efficient separation of Np and Pa, which is based on selective extraction of Pa by 1-octanol in hydrochloric acid (HCl) media. Our new method reproducibly isolated ^{233}Pa tracer with a yield of 99 ± 1 % (n = 3; radiochemical purity 100 %) and enabled chemical recovery of ^{237}Np parent material of 92 ± 3 % (purity [99 %) for future ^{233}Pa tracer preparations). Compared to previous methods, our new approach significantly reduces radioactive inorganic and organic waste; simplifies the separation process by eliminating liquid–liquid extraction required by previous methods; and reduces the time required—yields radiochemically-pure fractions of Pa and Np in less than 1 h. We anticipate this method can be further adapted for numerous applications and desired experimental conditions.

3.3. Experimental

3.3.1. General

Chemical regents for radiochemical separation and source preparation (HCl), ammonium hydroxide (NH_4OH), 35% hydrogen peroxide (H_2O_2), and bromocresol purple were ACS regent grade (Fisher Scientific) or higher. A calibrated source (1000 µg mL^{-1}) of cerium (Ce) (chloride form) was used for micro-precipitation of radionuclide sources (High Purity Standards, Charleston, SC). Radioactivity standards were prepared in Ultra-pure HCl (Fisher Scientific) and diluted with ultra-pure distilled deionized water (Baseline, Seastar Chemicals, British Columbia, Canada), both certified to parts-per-trillion (ppt) trace metals content. Half-lives and alpha-particle/gamma-ray energies are values originating from the Evaluated Nuclear Structure Data File (ENSDF) that were obtained through the United States National Nuclear Data Center (NNDC, Brookhaven National Laboratory, US Department of Energy).[16] All uncertainties are ''standard uncertainties'' corresponding to a coverage factor k = 1,[58] unless explicitly stated otherwise.

3.3.2. Safety Considerations

Use of radioactive materials is potentially hazardous and appropriate ALARA principles should be considered prior to conducting experiments using radioactive materials. Both ^{233}Pa (beta-particle and gamma-ray emissions) and ^{237}Np (alpha-particle and gamma-ray emissions) are radioactive isotopes and should be used only in facilities designed to handle radioactivity.

3.3.3. ^{237}Np and ^{233}Pa Sources

The radiation solution standards of ^{237}Np (Reference Numbers 92566, 96584, 93498) used for this study were purchased from the Eckert and Ziegler Radioisotopes (Atlanta, GA, USA). Standards were used after at least 7 months of the reference date to allow for ingrowth of radioactive decay product ^{233}Pa. The material has been certified to include a minor alpha-emitting impurity (^{238}Pu).[73] To prepare working solutions, the glass ampoule (5 mL in 0.5 M HNO_3) was scored at the neck and broken—and the contents were transferred to a pre-acid-leached beaker (25

mL). The contents were taken dry slowly, and re-dissolved in ultra-pure 6 M HCl (Seastar Chemicals, British Columbia, Canada). This process was repeated four times to an apparent complete matrix conversion to the chloride form; and finally redissolved to provide a working stock solution in 25 mL ultra-pure 6 M HCl (~145 Bq mL^{-1} ^{237}Np and ^{233}Pa). Final solutions were transferred and continuously stored in a metals-grade ultra-pure Seastar (Seastar Chemicals, Canada) Teflon bottle at 5 °C to prevent evaporation.

3.3.4. Resin Preparation

The primary-alcohol extractant 1-octanol was chosen (based upon previous methods) to prepare the ^{233}Pa radiometric tracer.[46, 60] The resin form of 1-octanol used for the experiments was prepared using a procedure developed by Eichrom Technologies, Inc. (Lisle, IL USA).[81] Briefly, 1-octanol (10 g) was dissolved into methanol (100 mL) then mixed with the resin beads (15 g; Amberchrom CG71, 25–50 lm, Rohm and Haas, Philadelphia, PA USA). The mixture was stirred (1 h) in a rotary evaporator, and then the methanol was removed under vacuum at room temperature. The resulting material was 40% (w:w) 1-octanol (verified by thermogravimetric mass analysis). This material is not commercially available, but can be made available on request at no cost by the authors. The material was prepared approximately 1 year prior to these investigations. Qualitatively consistent results have been produced during this time, which reflect the stability of the material stored at room temperature under typical laboratory conditions.

Columns were prepared by a previously described routine procedure.[8] Briefly, a slurry (0.66 g per 5 mL) was homogenized and transferred to an empty 2 mL column (AC-141-AL, Eichrom) allowing the water to drain by gravity flow. The column was secured with pre-manufactured frits (provided with empty columns) and a 25 mL reservoir (AC-120, Eichrom). The column was then preconditioned (10 mL of 9 M HCl) prior to loading of the $^{237}Np/^{233}Pa$ solution (**Figure 14**).

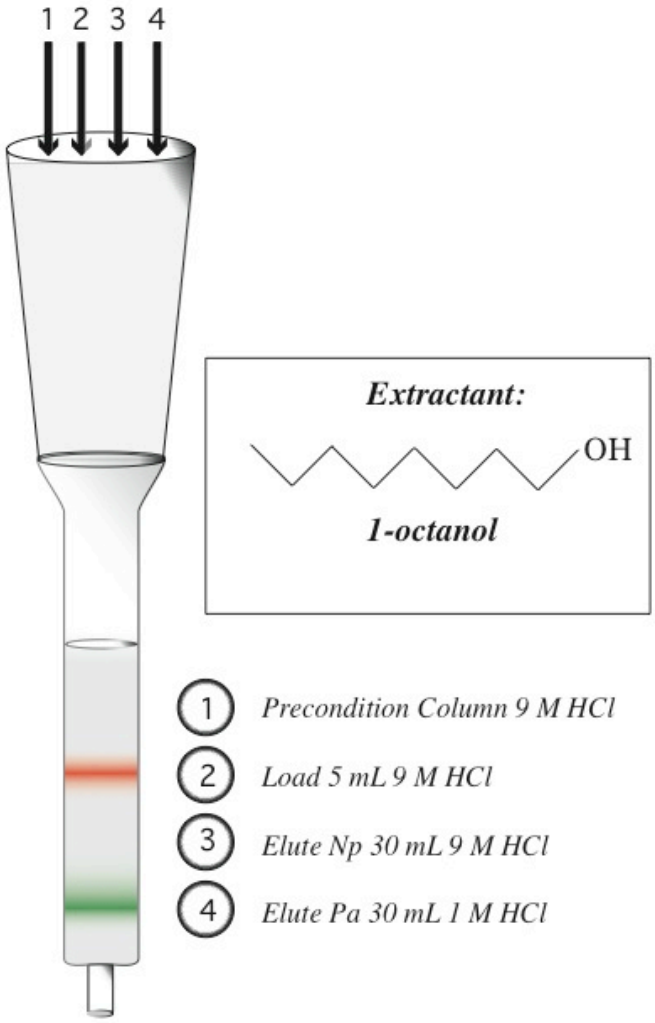

Figure 14. The protocol used to separate Pa and Np using a resin form of 1-octanol. Each fraction was then analyzed separately by gamma and alpha spectroscopy.

3.3.5. Separation Protocol

To separate ^{233}Pa and ^{237}Np, aliquots of the calibrated standard solution (100 µL, n = 3) that contained 14.5 Bq of both ^{237}Np and ^{233}Pa (in secular equilibrium) were transferred to a liquid scintillation (LS) vial (25 mL), diluted to 1 mL with 9 M HCl, and added to the column. The eluent of the load solution was collected for ^{237}Np analysis. Next, the LS vial was rinsed (4 mL, 9 M HCl) and added to the column. The column was then rinsed directly with 30 mL 9 M HCl to wash any

remaining ^{237}Np that was retained on the column. All solvent fronts of 9 M HCl were collected together in an LS vial (50 mL) to be analyzed for ^{237}Np yield and purity. Following the removal of ^{237}Np, ^{233}Pa was eluted by passing 30 mL of 1 M HCl through the column. The eluent was collected in another LS vial (50 mL) to be analyzed for ^{233}Pa yield and purity. Each liquid LS vial was precisely "time-stamped" to the time that the final drop was collected into the LS vial. This timestamp was used as the reference to correct for the radioactive decay of ^{233}Pa activity. An internal standard was prepared containing the same amount of radioactivity from the stock solution (100 µL, 14.5 Bq; ^{237}Np and ^{233}Pa) of the solution standard in an identical geometry with HCl (30 mL) in a LS vial (50 mL).

Table 2. The dominant gamma ray and alpha particle energies of ^{233}Pa and ^{237}Np used to assess the purity and radiochemical recovery of each analyte.

Radionuclide	Gamma Energies, keV (%)	Alpha Particle Energy, MeV (%)
Protactinium-233	311.904 (38.54)	N/A
	300.129 (6.63)	
	340.476 (4.45)	
	86.595 (1.95)	
Neptunium-237	29.374 (14.12)	4.78 (47.64)
	86.47 (12.4)	4.77 (23.2)
	8.22 (9.09)	4.64 (6.43)

3.3.6. Gamma Spectrometry

Immediately following the separation process, the sources were counted by routine procedures using high-purity germanium (HPGe) gamma-ray spectrometry and analyzed using the gamma spectrometry software GammaVision (Ortec, Oak Ridge, TN).[82] The internal standard was counted for 4 h and used to calibrate the energy and effi- ciency of the ^{237}Np and ^{233}Pa peaks (using 86.47 and 311.90 keV respectively) (**Table 2**). A matched count time blank background spectra was collected using an LS vial with 30 mL HCl to account for background spectral corrections. The detection limit was calculated to be 2.4 mBq (0.01 % of the total activity).[58] Each sample was counted for 4 h and "time-stamped" at the acquisition time, which was used to determine the total elapsed time between the end of the separation and the starting of the HPGe analysis. All of the sources were counted within 48 h of separation, to ensure that $(^{233}Pa)_{time}/(^{233}Pa)_{initial} < 95$ %, allowing for negligible effect of the decay constant to the overall uncertainty of the Pa measurement.

3.3.7. Source Preparation and Alpha Spectrometry

To assess the yield and purity of Np and Pa fractions, ^{233}Pa and ^{237}Np alpha-counting sources were prepared by cerium hydroxide micro-precipitation and were analyzed by alpha spectrometry by previously described routine procedures.[8] Briefly, the contents were transferred to a beaker together with Ce carrier (50 µg), H_2O_2 (500 µL), and bromocresol purple pH indicator. Note: $H_2O_2$and 9 M HCl will fade the color, so addition of more bromocresol is acceptable to ensure the final pH range is determined correctly. The pH was then increased with the addition of concentrated NH_4OH to pH ~ 8, where the presence of the indicator resulted in a purple solution. The mixtures were set aside for 10–20 min to allow for the microprecipitate to form. In the meantime, a filtration apparatus was assembled on a vacuum box and lined with 0.1 µm Resolve Filters™ (RF-100-25PP01, Eichrom) that were pre-wetted with 80% ethanol. The samples were then filtered via vacuum filtration and allowed to dry for 30 min with the vacuum pump on. Once dry, the filters were mounted on stainless steel planchettes (31.75 mm outer diameter, AF Murphy,

Quincy, MA, USA). Finally, to prevent contamination of the alpha detectors resulting from daughter recoil, thin films consisting of iso-amyl acetate and collodion were placed directly on the source as we described previously.[62]

All alpha spectra were collected with 450 mm^2 passivated ion-implanted silicon detectors in vacuum controlled-alpha spectrometers (Alpha Analyst, Canberra, Meridan, CT) with a fixed source to detector distance of about 10 mm. Efficiencies are determined for each detector every 6 months using a standard of identical geometry (Eckert and Ziegler; SRS: 91005; ^{238}U, ^{234}U, ^{239}Pu, and ^{241}Am) and range from ~17 to 20 % depending on which detector is used. For each measurement the efficiency of the detector used for an individual measurement is used to determine the radioactivity. Alpha sources of the ^{237}Np sources were counted for about 24 h (>100,000 counts) contributing <0.3 % uncertainty from counting statistics. The ^{233}Pa sources were counted for 100 h to determine presence of trace ^{237}Np. In each ^{233}Pa source, presence of trace ^{237}Np achieved >500 counts attributing to <4.5 % uncertainty from counting statistics. A matched count-time background was obtained and subtracted from the ^{237}Np region of interest (ROI) (**Table 2**).

3.3.8. Liquid Scintillation Counting

To determine the elution peak maximum values for ^{237}Np in 9 M HCl and ^{233}Pa in 9 M HCl and 1 M HCl, samples were counted by LS counting. For LS counting experiments, a Packard 1600 CA Tri-Carb (Perkin Elmer, Waltham, MA) was used with EcoLite LS cocktail in 30 mL glass LS vials with a water fraction of 10%. The samples were counted by routine lab procedure.[8]

3.4. Results and Discussion

3.4.1. General

This paper presents a novel approach to the chemical separation and isolation of radiochemically-pure fractions of Pa and Np that is based on selective extraction of Pa by aliphatic primary alcohols—using a new chromatographic-resin material and 1-octanol as the extractant-functional moiety. We prepared batches of the 1-octanol extraction chromatographic resin via

standard evaporative techniques and evaluated the new approach using a typical gravity-flow column-chromatography arrangement. Excellent separation and radiochemical isolation of ^{233}Pa and recovery of parent ^{237}Np were observed at radioactivity concentrations of ^{233}Pa tracer (14.5 Bq/sample) typical to environmental radiochemistry laboratories employing ^{233}Pa tracer for isotope dilution alpha spectrometry analysis of ^{231}Pa in environmental samples. We anticipate that the method could be modified to accommodate elevated levels of ^{237}Np for other applications.

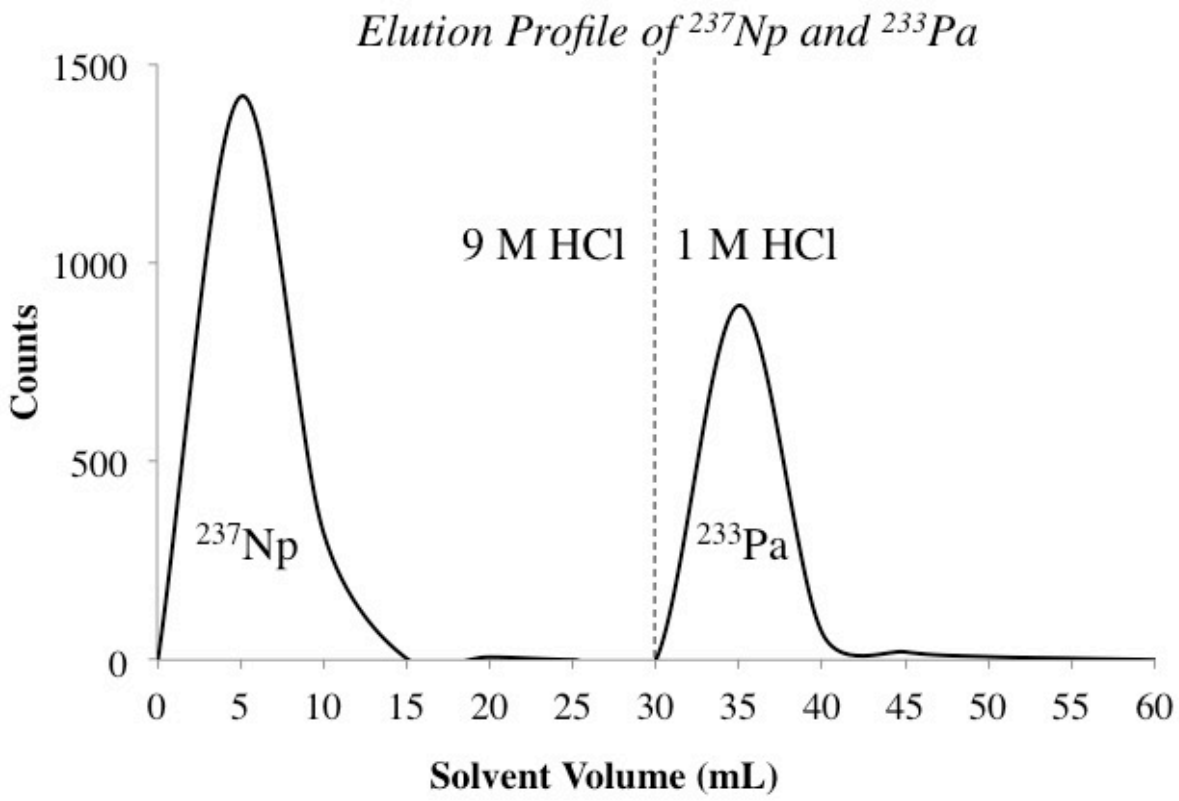

Figure 15. The elution peak profile of showing the elution of ^{237}Np in 9 M HCl on the 1-octanol resin material and the subsequent elution of ^{233}Pa when the acid concentration is diluted to 1 M HCl.

The procedure comprised four basic chromatographic steps (**Figure 14; Figure 15**): (*i*) preconditioning of the solid-phase aliphatic-alcohol-bearing resin with 5 mL of 9 M HCl (discarded to waste); (*ii*) a loading step, in which 5 mL 9 M HCl (1 mL load; 4 mL rinse) containing ^{237}Np/^{233}Pa is passed through the column and collected to recover ^{237}Np parent material, while ^{233}Pa is selectively retained via adsorption to the primary alcohol solid phase; (*iii*) a rinse step (30 mL 9 M HCl to remove remaining ^{237}Np parent material); and (*iv*) elution of radiochemically-pure ^{233}Pa in 30 mL of 1 M HCl. Radioactivity counting sources were prepared by standard alpha spectrometry techniques. Radiochemical purity was evaluated by alpha spectrometry using standard solid-state ion-implanted silicon detectors and HPGe gamma-ray spectrometry. Significant improvements that were observed relative to previous methods include. [10, 12, 46, 60]

3.4.2. Less Waste

Previous separation protocols for the isolation of ^{233}Pa and ^{237}Np generally require a liquid–liquid extraction step that utilizes a 50 mL organic phase separatory-funnel-based step, with up to five subsequent-additional aqueous washes (50 mL each) to complete the purification of extracted ^{233}Pa.[46] Our new approach results in a maximum volume of 60 mL HCl residue and no radioactive liquid organic solvent waste. We anticipate future refinements will lead to further reduction of the total acid volume required.

3.4.3. Improved Safety and Efficiency (Removal of HF and Sulfuric Acid; H_2SO_4)

All previous approaches to ^{237}Np/^{233}Pa separation (to our knowledge) include the use of HF or H_2SO_4 for separation and isolation of ^{233}Pa and ^{237}Np [46, 60]—and prevention of Pa hydrolysis through the separation procedure.[83] The use of these reagents not only adds significantly to potentially hazardous radioactive mixed waste, but also requires additional steps to remove F^- and SO_4^{2-} for subsequent source preparation and radioactivity measurements.[10, 11] Our new approach eliminates the need for F^- and SO_4^{2-}. At the tracer concentrations used for this study, we observed no evidence of irreversible Pa hydrolysis.

3.4.4. Improved Efficiency

Column chromatography as a whole has greatly simplified and reduced the hands-on time for chemical separations, relative to liquid–liquid extractions. While previous liquid– liquid extraction procedures require approximately 5 h of technician-hands-on attention, our new approach with this extraction chromatographic resin containing 1-octanol as the extractant allows separation and isolation of radiochemically-pure fractions of ^{237}Np and ^{233}Pa in less than an hour.

3.4.5. Isolation of Neptunium

The Np fraction was isolated (n = 3) in outstanding purity with excellent recovery for future preparations of ^{233}Pa tracer solution. This fraction is collected in 9 M HCl, which is convenient for future Np storage and can be easily converted to other desired chemical matrices for other applications.[70] While previous studies hypothesized that primary alcohols may represent an adsorption nucleation site for Np(VI), this study finds no evidence of Np retention on the column, resulting in an effective radiochemical separation from Pa(V) in a system containing the primary alcohol, 1-octanol, thus suggesting that Np is maintained in the pentavalent oxidation state. Evaluation by gamma spectrometry demonstrated excellent radiochemical purity with the absence of ^{233}Pa gamma-ray emission peaks (311.9, 300.1, 340.5 keV and X-rays; kα_{Pa} and kβ_{Pa}) (**Figure 16**). Based on these analyses, the radiochemical purity of ^{237}Np was calculated to be 99 ± 2 %, where the uncertainty is primarily attributed to low counts in the ^{233}Pa ROI's with activities at or below the detection limit (~2.4 mBq). Importantly, the radiometric purity of a ^{237}Np source begins to decrease rapidly (~2 % per day) with the ingrowth of ^{233}Pa, daughter of ^{237}Np. From an elemental mass perspective, although the radiometric purity of the ^{237}Np solution decreases due to daughter ingrowth, the atomic (mass) purity will remain essentially 100% ^{237}Np, due to the short half-life of ^{233}Pa. However, routine removal of ^{233}Pa is an important consideration for Np research because it will minimize overall radiation exposure to the researcher by reducing the gross beta activity and removing relatively high-energy ^{233}Pa gamma rays.

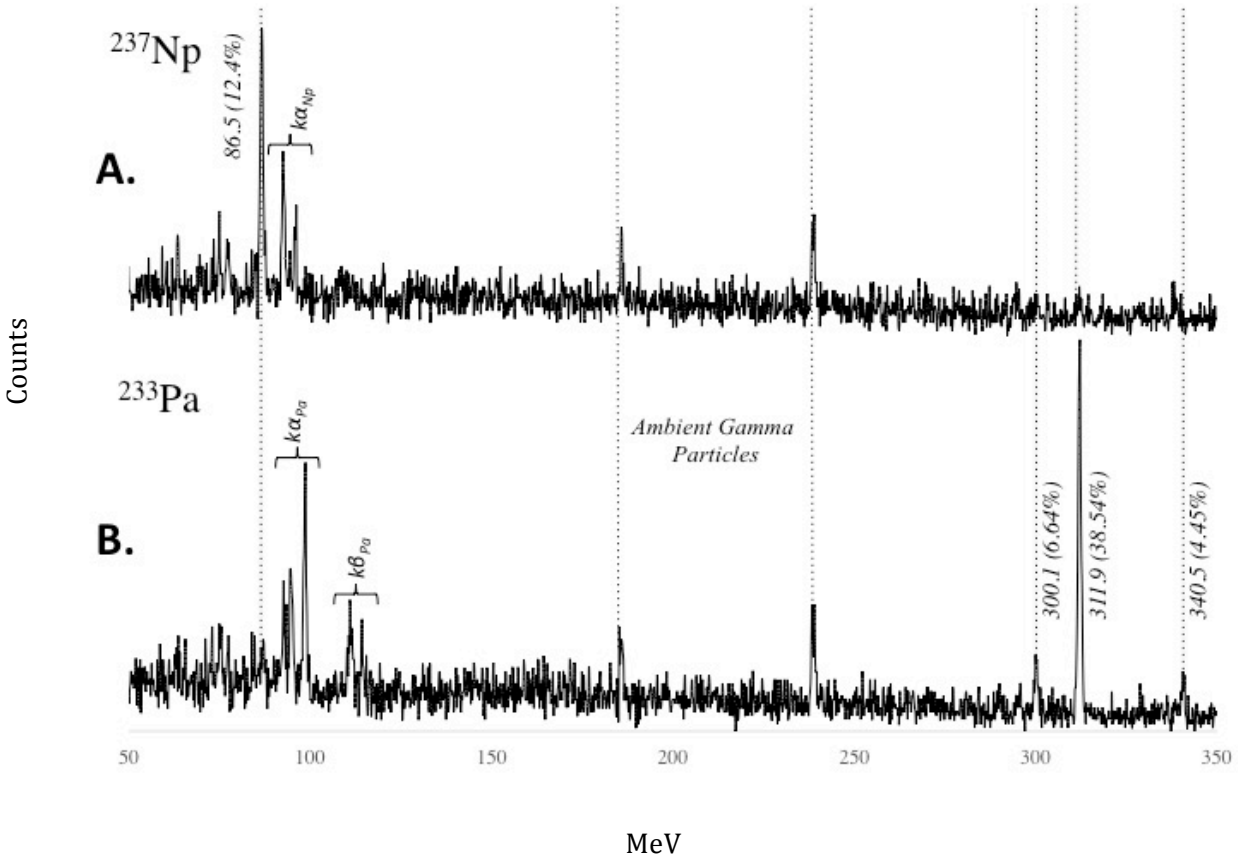

Figure 16. High-purity germanium gamma-ray spectra of the (A) ^{237}Np fraction, (B) and ^{233}Pa fraction analyzed following the separation, to assess the purity of ^{237}Np and the yield of ^{233}Pa. The purity of the ^{237}Np was assessed in the regions 300.1, 311.9, and 340.5 keV and was determined to be 99 ± 2 %. The yield of ^{233}Pa was determined from the 311.9 keV region and was determined to be 99 ± 1 %.

The radiochemical yield of ^{237}Np was determined by alpha spectrometry using cerium hydroxide micro-precipitated sources. We observed that quantitative co-precipitation of Np was ensured through redox control by addition of H_2O_2 due to reduction of the soluble Np(V) to the insoluble Np(IV) form.[84, 85] While in aqueous solution Np(V) is the most stable oxidation state, it will not be incorporated into the cerium hydroxide microprecipitation, so Np(V) must be reduced. Previous research demonstrates that Np(V) can be reduced to Np(IV) with the addition of excess H_2O_2.[1, 86] Thus, excellent radiochemical yields for ^{237}Np (92 % ± 3) were achieved based analysis of

alpha spectra (4.7 MeV peak) (**Figure 17; Tables 2; Table 3**) and losses could be attributed the micro-precipitation step rather than column elution step.

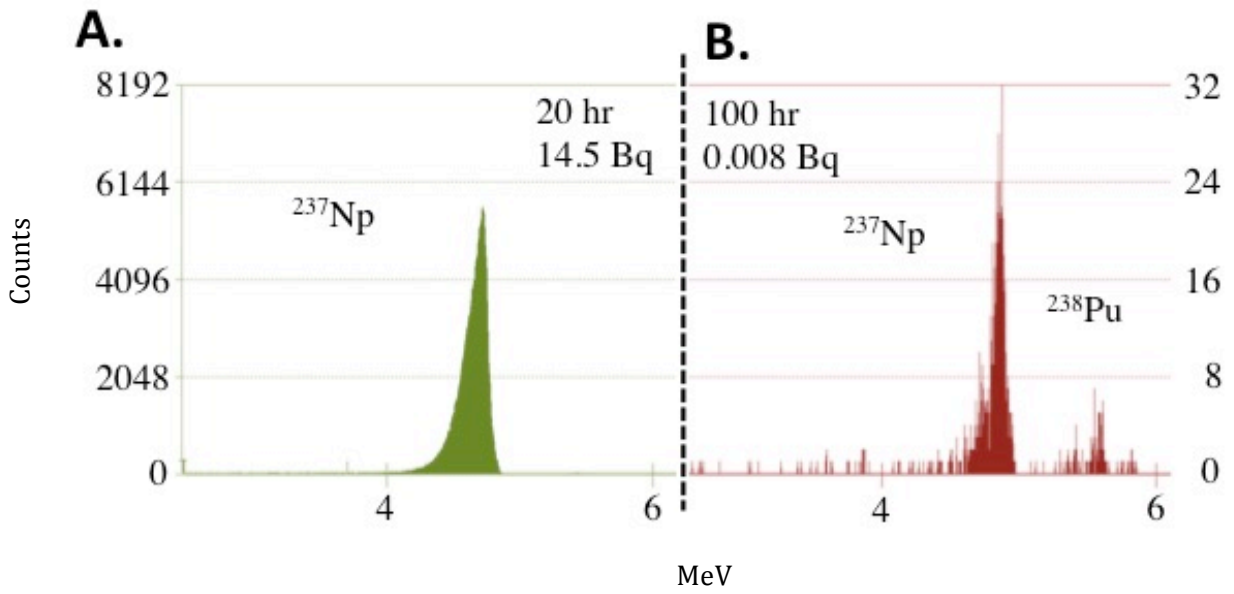

Figure 17. Alpha spectra used to determine the yield of ^{237}Np and purity of ^{233}Pa. (A.) shows the ^{237}Np alpha spectra the radiochemical recovery was 92% ± 3, as seen in the region of interest at 4.78 MeV. (B.) Shows the alpha spectra of the ^{233}Pa. The integrated count rate of ^{237}Np region of interest (4.78 MeV) results in a radiochemical purity of 100% ± 0.2 for ^{233}Pa.

3.4.6. Isolation of Protactinium

Following the isolation of the ^{237}Np parent material in 9 M HCl, in which ^{233}Pa is strongly retained on the column, ^{233}Pa (n = 3) was recovered with near quantitative radiochemical yield by elution with 30 mL of 1 M HCl (**Figure 14**). While the behavior of Pa under these conditions afforded excellent separation from Np, the chemical form of the extraction Pa species into 1-octanol is not well understood.[5] Previous investigations have identified the predominant species of Pa and Np under the conditions of our separations protocol as existing in the pentavalent oxidation state, and it has been generally believed that the behavior of these elements is similar.[3] Although it is well understood that Np(V) in aqueous conditions forms the linear dioxo-neptunyl cation, NpO_2^+,[1, 45] less

is known about the molecular features of the Pa complex in solution. It was hypothesized, and recently demonstrated, that Pa forms a linear mono oxo-protactinyl moiety.[45, 83, 87] The extracted species of Pa, in concentrations of [HCl] > 4 M, are suspected to be $PaCl_7^{3-}$, $PaCl_6^{2-}$, $PaOCl_6^{3-}$, $Pa(OH)OCl_6^{2-}$, $PaOCl_5^{2-}$, but no dominant species has been empirically agreed upon.[1, 83, 88, 89] To quantitatively desorb Pa from the stationary phase, the [HCl] is diluted to 1 M, and the resulting Pa species is likely to be $PaOOH^{2+}$.[1]

In addition to the lack of information regarding the dominate Pa(V) species, the exact mechanism for the extraction is unclear. Previous studies hypothesized that the interactions between Pa and the extractant are mainly electrostatic, as the highly acidic environment forms a protonated alcohol, $[HROH^+]_{1-2}$, and anionic Pa complex.[13] However, electrostatic interactions alone do not sufficiently describe the selectivity to Pa over Np, because Np is also expected to form anionic complexes in 9 M HCl.[1] Future studies in our laboratory seek to identify the specific differences in speciation that allow for the selective extraction of Pa over Np with 1-octanol.

The radiochemical yield for ^{233}Pa was 99 ± 1 %, determined by HPGe gamma spectroscopy based on the gamma emission at 311.9 keV (**Figure 16**). Each fraction was decay corrected based on the time elapsed from Pa elution to start of gamma spectral collection. Radiochemical purity of ^{233}Pa was determined from a 100-h count of a cerium hydroxide micro-precipitated source by alpha spectrometry. Radiochemical purity of the ^{233}Pa sources was determined to be 100 ± 0.2 %. Nearly quantitative isolation from ^{237}Np parent material was achieved, with ~5 mBq (count rate < 0.002 counts/s) of the 14.5 Bq ^{237}Np added (0.03%) to the solution were identified by alpha particle emission on the ^{233}Pa (**Figure 17; Table 3**). While this separation factor approaches the limitations of extraction chromatographic resins, additional steps can be taken to further purify ^{233}Pa if necessary. These include: (*i*) passing the solution through the 1-octanol column additional times until the desired purity is achieved; (*ii*) application of the cerium hydroxide micro-precipitation step without the addition of an oxidizing agent, which would exclude precipitation of ^{237}Np, which does not form a cerium hydroxide micro-precipitation as Np(V); and (3) the use of multiple-

smaller-increment elution volumes to improve the overall removal of Np (i.e. 6 rinses of 5 mL 9 M HCl vs. 1 rinse of 30 mL).

Table 3. The results from the alpha and gamma spectroscopy the recovered fractions of ^{233}Pa and ^{237}Np using 1-octanol resin.

Radionuclide	Radiochemical Yield[1], %	Purity[2], %
Protactinium	99 ± 1	100 ± 0.2
Neptunium	92 ± 3	99 ± 2

[1] Radiochemical yield of Pa was determined by gamma spectrometry, and Np was determined by alpha spectrometry

[2] Radiochemical purity of Pa was determined by alpha spectrometry, and Np was determined by gamma spectrometry

3.5. Conclusions

A novel approach to efficient separation and isolation of Np and Pa into radiochemically-pure fractions, using a new chromatographic resin material has been described. The approach takes advantage of highly-selective adsorption of Pa to primary-aliphatic alcohols in HCl media using a solid-phase chromatography resin-based material with 1-octanol as the extractant. The material can be produced easily in-house (at low cost) and our observations suggest that the material shelf-life exceeds 1 year without apparent degradation (stored at room temperature under typical laboratory conditions). The new approach significantly reduces waste (e.g. acid, organic, radioactive, and mixed) produced during the separation and isolation of ^{233}Pa and ^{237}Np and eliminates the need for HF and H_2SO_4. The method reproducibly (n = 3) isolated ^{233}Pa tracer with a yield of 99 ± 1 % (radiochemical purity 100 %) and enabled chemical recovery of ^{237}Np parent material of 92 ± 3 % (purity > 99 %) for future ^{233}Pa tracer preparations. It is anticipated that the procedure could be adjusted to meet more stringent criteria for purity and yield of Pa and Np.

3.6. Associated Content

Notes: The authors declare no competing financial interest. Interested investigators are invited to inquire with the authors for access to the new resin-based material for further research applications.

Acknowledgements: The authors would like to thank Phil Horwitz, Daniel McAlister, and Eichrom Technologies for the production of the resin form of 1-octanol for these experiments. This material is based upon work supported by the U.S. Department of Homeland Security under Grant Award Number, 2012-DN-130-NF0001-02. The views and conclusions contained in this document are those of the authors and should not be interpreted as representing the official policies, either expressed or implied, of the U.S. Department of Homeland Security.

CHAPTER IV: CALCULATION MODEL FOR LIQUID-LIQUID EXTRACTION OF PROTACTINIUM BY 2,6-DIMETHYL-4-HEPTANOL

This chapter was accepted for publication 26 September 2015 and published in a special issue of *Nukleonika* highlighting the Safety of Actinide Separation Processes (SACSESS) conference in Warsaw, Poland. This chapter is reprinted with permission. Please refer to Knight, A. W., Eitrheim, E. S., Nelson, A. W., Schultz, M. K. (2015). A calculation model for liquid-liquid extraction of protactinium by 2,6-dimethyl-4-heptanol. *Nukleonika*, 60(4): 837-845.

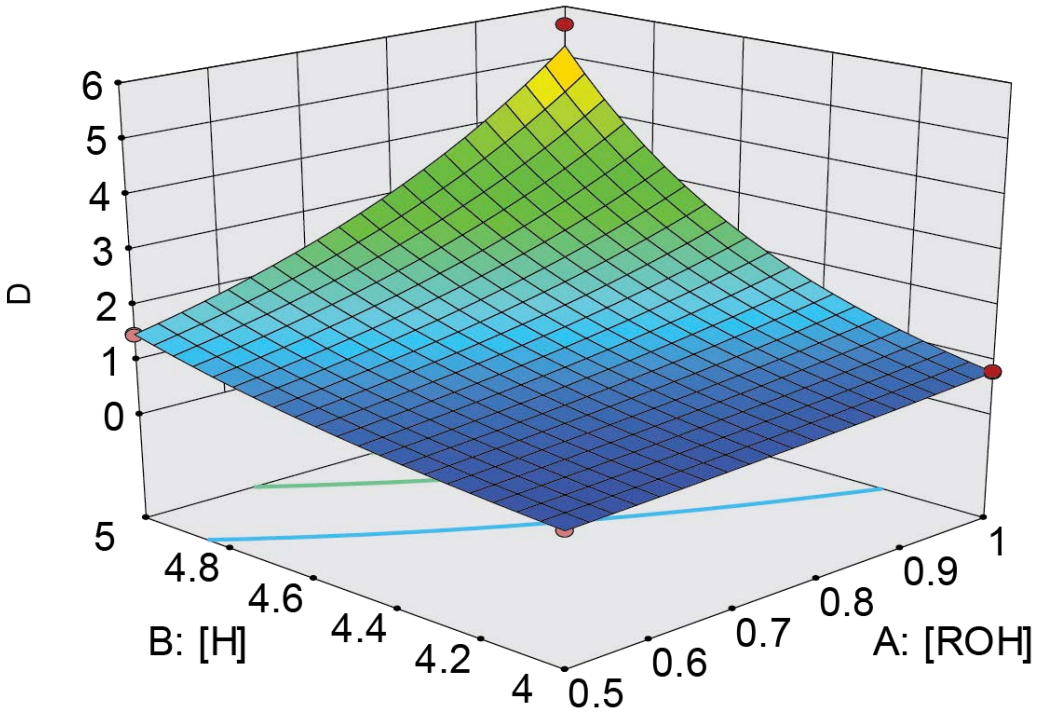

4.1. Abstract

Reprocessing of spent nuclear fuel usually employs the solvent extraction technique to recover fissile material, isolate other valuable radionuclides, recover precious metals, and remove contaminants. Efficient recovery of these species from highly radioactive solutions requires a detailed understanding of reaction conditions and metal speciation that leads to their isolation in pure forms. Due to the complex nature of these systems, identification of ideal reaction conditions for the efficient extraction of specific metals can be challenging. Thus, the developments of experimental approaches that have the potential to reduce the number of experiments required to identify ideal conditions are desirable. In this study, a full-factorial experimental design was used to identify the main effects and variable interactions of three chemical parameters on the extraction of protactinium (Pa). Specifically we investigated the main effects of the anion concentration (NO_3^-, Cl^-) extractant concentration, and solution acidity on the overall extraction of protactinium by 2,6-dimethyl-4-heptanol (diisobutylcarbinol; DIBC) from both HCl and HNO_3 solutions. Our results indicate that in HCl, the extraction of protactinium was dominated by the solution acidity, while in nitric acid the extraction was strongly affected by the [DIBC]. Based on our results, a mathematical model was derived, that describes the relationship between concentrations of anions, extractant, and solution acidity and the expected values of Pa distribution coefficients in both HCl and HNO_3. This study demonstrates the potential to predict the distribution coefficient values, based upon a mathematical model generated by a full-factorial experimental design.

Keywords: design of experiments, protactinium, solvent extraction

4.2. Introduction

Separation and isolation of long-lived radionuclides from aqueous solutions is critical to efficient high-level nuclear-waste management.[90] Due to the nature of nuclear-fission energy production, waste products contain a wide range of radionuclides including: fission products,

actinides, and their radioactive decay products.[90, 91] Separation and isolation of various elements from the nuclear waste are performed to improve the long-term stability of the waste;[91] recycle unused fuel, and recover precious metals contained in the waste stream.[22, 23] Since this process is performed on an industrial scale – and the material is highly radioactive – radionuclide separations that are reproducible, predictable, simple and amendable to safe operations are desirable.[22, 91]

One of the most common techniques employed for this application is liquid-liquid extraction. Liquid-liquid extraction utilizes a biphasic reaction system comprising an aqueous phase (acidic or basic, to insure the metal solubility), and an immiscible organic phase containing an organic-soluble extractant, which displays affinity toward the specific metal or radiometal of interest.[5, 92, 93] Final isolation of radionuclides and non-radioactive metals may also involve a 'back extraction' (stripping) from the initial organic phase to an aqueous phase by use of a water-soluble extractant.[93] Thus, by utilizing rules of solubility and chemical speciation, solvent extraction parameters can be adjusted to extract particular metals and radiometals from the bulk liquid-waste.[23] To the first approximation, the most important parameters for an efficient separation and isolation of a desired radionuclide or stable metal are the pH, the concentration and properties of the counter-ion (i.e. Cl^-, NO_3^-), and the identity of the extractant (i.e. 2,6-dimethyl-4-heptanol).[94]

One element of particular interest to the nuclear fuel cycle is protactinium (Pa).[13, 95] Although the molar concentration of Pa in nuclear fuel is generally low, two isotopes have sufficiently long half-lives to be present in appreciable quantities (in terms of radioactivity) in nuclear materials: ^{231}Pa ($t_{1/2}$ = 3.28 × 10^4 years) and ^{233}Pa ($t_{1/2}$ = 26.98 days)[16] For example, in the production of conventional ^{235}U fuel, uranium ore (0.7% ^{235}U, 99.3% ^{238}U) is isotopically enriched in ^{235}U up to 5%.[91] Because ^{231}Pa is the direct (and longest lived) decay product of ^{235}U, the enrichment process can result in enhanced ^{231}Pa radioactivity in waste streams as a result of chemical preconcentration, and its decrease in the ^{235}U fuel, followed by a slow ingrowth of the radioactivity over a long periods of time.[12] While ^{231}Pa is not likely to exist in significant mass quantities in the nuclear fuel, ^{231}Pa plays unique roles in the nuclear fuel cycle. Due to its relatively high neutron cross section, ^{231}Pa can generate fissile isotopes ^{232}U and ^{233}U, which can improve core performance

and longevity.[96-98] Also, in considering long-term geological repository for spent nuclear fuel, ^{231}Pa and its shorter-lived daughters (i.e. ^{227}Ac) will be major contributors to the total radioactivity after 105 years.[1, 99] Likewise, the shorter-lived isotope, ^{233}Pa, will be present in the nuclear fuel cycle as an immediate decay product of neptunium-237 (^{237}Np), which can originate from several neutron capture and radioactive decay pathways.[100] Furthermore, ^{233}Pa has a unique role in alternative fuels cycles, specifically the thorium (Th) fuel cycle.[13, 74] In the Th fuel cycle, natural, fertile ^{232}Th is neutron-irradiated to form the fissile ^{233}U fuel. In this process ^{233}Pa is an intermediate, formed by neutron capture, ^{232}Th(n,γ)^{233}Th, and subsequent β^- decay of ^{233}Th. The isolation of ^{233}Pa from other products formed during the irradiation of ^{232}Th, could provide near isotopically pure ^{233}U.[13, 74]

While these examples demonstrate the need for an understanding of Pa extraction from spent nuclear fuel, relatively little is known about the chemistry of Pa, and hence its neglect in most (if not all) industrial separation schemes.[94] Research to understand the chemistry of Pa has traditionally been limited due to challenges in obtaining sufficient quantities of Pa to perform spectroscopy. However, much can be learned about the chemical behavior of Pa through observation of its behavior in chemical extraction systems at trace levels.[5, 13, 66, 101] Previous research has suggested that aliphatic alcohols can effectively extract and separate Pa from the other actinides and fission products.[5, 101] Interestingly, an aliphatic alcohol (octanol) is used as a diluent in some separation and extraction systems, suggesting that Pa might be unintentionally extracted at various separation steps.[25]

Whether research is occurring in industry, academia, or government, the experimental efficiency and careful planning are essential to ensure safe operations, while meeting financial and extraction objectives. Thus, identifying the ideal parameter settings for a given radiometal extraction in a minimum number of experimental runs is desirable. One approach to experimental design that is used often to improve the efficiency in data collection and interpretation is referred to as the full-factorial design. Full-factorial experimental designs can be developed to maximize experimental information obtained, while minimizing the number of experimental runs required to obtain that information.[102, 103] In addition to identifying the main effects of changes in important

experimental parameters, the approach also allows for the identification of effects of two-way and three-way interactions between the reactants. This study aims to apply a full-factorial design to broaden the understanding of the behavior of Pa in a liquid-liquid extraction system with 2,6-dimethyl-4-heptanol (diisobutylcarbinol; DIBC) (**Figure 18**) as the extractant in both hydrochloric (HCl) and nitric acid (HNO_3) systems. To achieve this aim, we investigated this system based upon three extraction parameters: [H^+], [DIBC], and [anion (A^-); Cl^- or NO_3^-]. We further aimed to develop the understanding of the effect of two-way and three-way interactions between [DIBC], [H^+], and [A^-] on the extraction of Pa into the organic phase. In addition, our studies were conducted to use the statistical data generated from these experiments to create a mathematical model for the extraction system that can be used to predict Pa extraction using the DIBC/acid liquid-liquid extraction system.

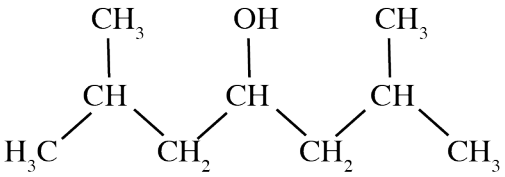

Figure 18. Structure of 2,6-dimethyl-4-heptanol, common name diisobutylcarbinol or DIBC.

4.3. Experimental

4.3.1. General

All chemical regents were ACS Reagent grade (Fisher Scientific, Pittsburg, PA) or higher. These reagents included HCl, HNO_3, sodium chloride (NaCl), and sodium nitrate ($NaNO_3$). The organic solvents, dodecane and DIBC, were Sigma Aldrich (St. Louis, MO). Radioactivity standards of ^{233}Pa were prepared using ultrapure HCl (Fisher Scientific) and diluted using ultra-pure distilled deionized water (Baseline®, Seastar Chemicals, British Columbia, Canada), both were certified to parts-per-trillion metals content. Half-lives and gamma-ray energies values were obtained from the

Evaluated Nuclear Structure Data File (ENSDF) through the United States National Nuclear Data Center (NNDC, Brookhaven National Laboratory, US Department of Energy).[16] All statistical information was generated by Design-Expert® software (Stat-Ease, Inc., Minneapolis, MN). Stated uncertainties are "standard uncertainties", corresponding to a coverage factor k = 1 (unless explicitly stated otherwise) and are estimated based on methodologies adherent to national and international standards bodies.[58]

4.3.2. Safety Considerations

Radioactive materials are potentially hazardous. Appropriate ALARA principles should be considered prior to conducting experiments with radioactive materials. ^{233}Pa and ^{237}Np are radioactive and should only be used in facilities designed to handle radioactivity.

4.3.3 Protactinium-233 Standard Source

Since ^{233}Pa has a relatively short $t_{1/2}$, activity standards must be prepared from a ^{237}Np standard solution via ingrowth of ^{233}Pa.[11, 60, 101] A nominal standard solution of containing 37 kBq of ^{237}Np (Lot #1760-91) used for this study was purchased from the Eckert and Ziegler Radioisotopes (Atlanta, GA, USA) and diluted to working solutions as described by us previously.[8, 101]

For these studies, ^{233}Pa was extracted from the working solution of ^{237}Np using a method described by us previously, which employs an extraction chromatographic resin (Amberchrom CG-71ms, 50–100 μm) impregnated with of 1-octanol.[101] Briefly, a slurry was prepared of the 1-octanol resin beads (0.66 g/5 mL H_2O), then a column was prepared by transferring the resin slurry (5 mL) to an empty plastic column (0.8 cm inner diameter). Prior to isolation of ^{233}Pa from ^{237}Np, the column was preconditioned (6 M HCl) with several column volumes. Following the column preparation, the ^{237}Np solution (15 mL; containing ^{233}Pa) was added to the column, and the eluent containing ^{237}Np was collected for future use. Additional rinses (2x15 mL 6 M HCl) were also collected and combined for future use of the ^{237}Np. ^{233}Pa was next eluted from the column (15 mL of 1 M HCl) and collected in a separate Teflon beaker. The final activity of the ^{233}Pa solution was ~0.75 kBq/mL–1.

4.3.4. Experimental Engineering and Solvent Extraction

The design of experiments was based upon the mathematical principle for maximizing information while minimizing the number of individual experiments by a full factorial design.[102, 103] The computer software Design-Expert® was used to design experiments and the range of experimental parameters were based upon a linear approximation in design space of the extraction of Pa by DIBC at a range of concentrations.[5, 104] The goal was to determine the main effects of changes in $[H^+]$, $[A^-$, Cl^- or $NO_3^-]$, and [DIBC], as well as the effect of two-way and three-way interactions between the reactants on extraction of Pa into the organic phase, and finally, develop a predictive mathematical model of the extraction of Pa. The resulting full factorial design provides an estimation of these effects on the distribution coefficient (D) of Pa (**Equation 13**). Each parameter was assigned a low setting (–), a high setting (+), and a midpoint that exists between the – and + to account for curvature in response. The settings chosen for each parameter were determined based upon previous experiments.[5, 13] Based upon these results, a linear approximation was applied, in which the region of interest selected represented the section of the extraction line where the slope was considered steep, linear and where the end points represented the change from poor to satisfactory extraction of Pa into the organic phase. In HCl, the parameters were $[H^+]$ 4–5 M, $[Cl^-]$ 5–5.5 M, [DIBC] 0.5–1 M. In HNO_3, $[H^+]$ 1–3 M, $[NO_3^-]$ 3–4 M, and [DIBC] 0.5–1 M (**Figure 19**).

Each solvent extraction system consisted of 5 mL aqueous phase and 5 mL organic phase in a 15 mL plastic conical centrifuge tube. The aqueous phase consisted of the appropriate $[H^+]$ from acid (HCl or HNO_3) and $[A^-]$ by the addition of NaCl or $NaNO_3$. The organic phase contained the appropriate [DIBC] in a dodecane diluent. To the system, 100 μL of ^{233}Pa standard solution (~75 Bq) was added, and the contents were mixed for 1 hour and allowed to stand for 10 minutes or until the phases separated. Once biphasic conditions were reached, 4 mL of the organic phase and 4 mL of the aqueous phase were carefully withdrawn and transferred to separate vials and analyzed by gamma spectroscopy for the activity in the organic and aqueous phases, respectively. The D

values were calculated (**Equation 13**) and served as response inputs to the Design-Expert 9 software for further statistical analysis and model generation.

$$D = \frac{Radioactivity\ Pa_{organic\ phase}}{Radioactivity\ Pa_{aqueous\ phase}} \qquad eq.13$$

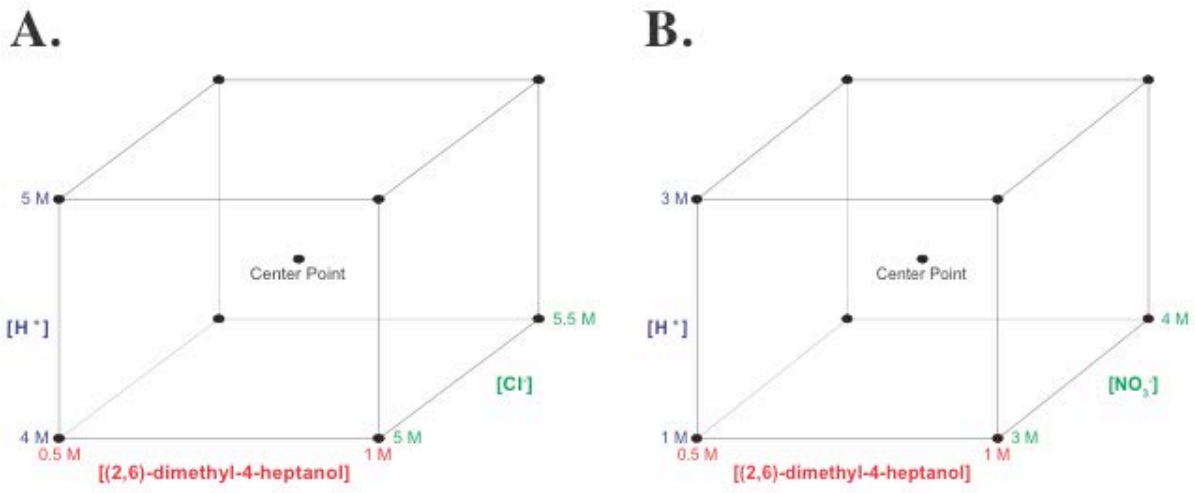

Figure 19. (A). shows a graphical representation of the full factorial experimental design measuring the distribution coefficient, D, as a function of $[H^+]$,[DIBC], and $[Cl^-]$. And (B). Shows the NO_3^- extraction. Each solid black dot represents an experimental data point performed in duplicate; were each vertices was measured as well as a center point to gain information regarding the curvature of the model.

4.3.5. Gamma Spectrometry

The organic and aqueous phases were analyzed separately by gamma-ray spectrometry with a well-type sodium iodide (NaI) detector and spectra were obtained using the gamma spectrometry multi-channel analysis software Maestro (ORTEC, Oak Ridge, TN). Each sample was counted (500 seconds) and normalized with a match-count-time background spectrum. The count-rate of the sample was calculated by dividing the background-corrected total counts by the dead-

time adjusted count-time (500 seconds). The region of interest for the ^{233}Pa activity was centered around the 311 keV gamma emission.[16] Activity balance verification was performed with a vial containing the ^{233}Pa standard (100 μL in 4 mL) of an aqueous phase and an organic phase. The geometry of each sample remained identical; resulting in identical detector efficiency for all samples to determine D values. For each sample, both phases were counted sequentially to minimize the effect of radioactive decay of ^{233}Pa. In the time required to count both phases, only 0.04% of ^{233}Pa would have decayed. Thus, decay during counting corrections is considered negligible and were not applied.

4.4. Results and Discussion

4.4.1. General

Extraction of ^{233}Pa by DIBC in both HCl and HNO_3 was performed based on a full-factorial design to generate a model that describes the effect of changes in $[H^+]$, [DIBC], and $[A^-]$ on the extraction of Pa (**Figure 19, Table 4**). Previous studies have summarized the extraction of Pa by DIBC by sweeping the [HCl] and $[HNO_3]$ to gain an applied understanding of the behavior of Pa in extraction systems,[5, 13] this study aims to understand the effects of the experimental parameters and the development of a mathematical model.

Results of the experiments were recorded by the coded independent variable identity (+ or –) and the response (D value). With three independent variables, there were 9 experimental runs (23 + 1 = 9 combinations including the midpoint). Each set of experiments was performed in duplicate to obtain an experimental estimate of the reproducibility of the experiments and increase the power of the model. The results of each of the experimental scenario are summarized in **Table 4**, where the coded setting (– or +) is shown with the experimental concentration values and the response D values. The midpoint values were included as well to identify curvature that exists with the D values and each of the independent parameters, as described previously.[103]

Table 4. Tabular representation of the full factorial design used to evaluate the distribution coefficient of Pa by DIBC in HCl and HNO_3. The ID represent the low value (-) and high value (+) for each experimental parameter; [DIBC], $[H^+]$, and $[A^-; Cl^-$ or $NO_3^-]$.

ID	- --	- - +	- + -	+ - -	+ - +	mid	- + +	+ + -	+ + +
[DIBC]	0.5	0.5	0.5	1	1	0.75	0.5	1	1
$[H^+]$	4	4	5	4	4	4.5	5	5	5
$[Cl^-]$	5	5.5	5	5	5.5	5.25	5.5	5	5.5
D	**0.18 ± 0.01**	**0.40 ±0.01**	**0.62 ± 0.01**	**0.64 ± 0.03**	**0.79 ± 0.03**	**0.98 ± 0.09**	**1.49 ±0.01**	**2.34 ±0.16**	**5.21 ± 0.62**

ID	**- - -**	**- + -**	**- - +**	**mid**	**- + +**	**+ - -**	**+ - +**	**+ + -**	**+ + +**
[DIBC]	0.5	0.5	0.5	0.75	0.5	1	1	1	1
$[H^+]$	1	3	1	2	3	1	1	3	3
$[NO_3^-]$	3	3	4	3.5	4	3	4	3	4
D	**0.12 ± 0.00**	**0.18 ± 0.01**	**0.19 ± 0.00**	**0.32 ± 0.01**	**0.39 ± 0.03**	**0.45 ± 0.03**	**0.57 ± 0.01**	**0.79 ± 0.08**	**1.20 ± 0.04**

4.4.2. Distribution Coefficients

The D values were determined at each point of the experimental cube (**Table 4**), where the ID represents the experimental concentrations of each parameter. In the chloride scenario, D increases as the parameters shift from low to high concentrations settings, where the average D values range from 0.18 ± 0.01 at (– – –) to 5.21 ± 0.62 at (+ + +). In the nitrate scenario, D generally

increases as the experimental parameters shift from low to high concentrations, but the effects are not as dramatic as those in the chloride system. The D values range from 0.12 ± 0.00 at (– – –) to 1.20 ± 0.04 at (+ + +) experimental conditions. While the extraction of Pa into the organic phase (D > 1) in HNO3 occurs from less concentrated solutions (~2–3 M HNO_3) than HCl (~4–5 M HCl), the extent of the extraction in HCl results in much larger D, which corresponds to the stronger complexing tendency with chloride than with nitrate with respect to Pa.[5] Furthermore, while the extracted species of Pa are not fully agreed upon, research suggests that under the conditions explored here, the Pa-chloro complexes extracted into the organic phase have been identified as cations; PaO^{3+},[89] $Pa(OH)_2^{3+}$,[89] $Pa(OH)Cl_3^{+}$,[105] neutral complexes; $Pa(OH)Cl_4$,[105] $Pa(OH)_2Cl_3$,[105] or anions; $PaOCl_4^{-}$,[89, 106] $Pa(OH)_2Cl_4^{-}$.[89] And in nitrate media, neutral complex; $Pa(OH)_2(NO_3)_3$,[107] or anion; $(Pa(OH)_2(NO_3)_4^{-}$.[13, 107, 108] Future work in our laboratory aims to identify the extracted species of Pa by aliphatic alcohols extractants in both HCl and HNO_3.

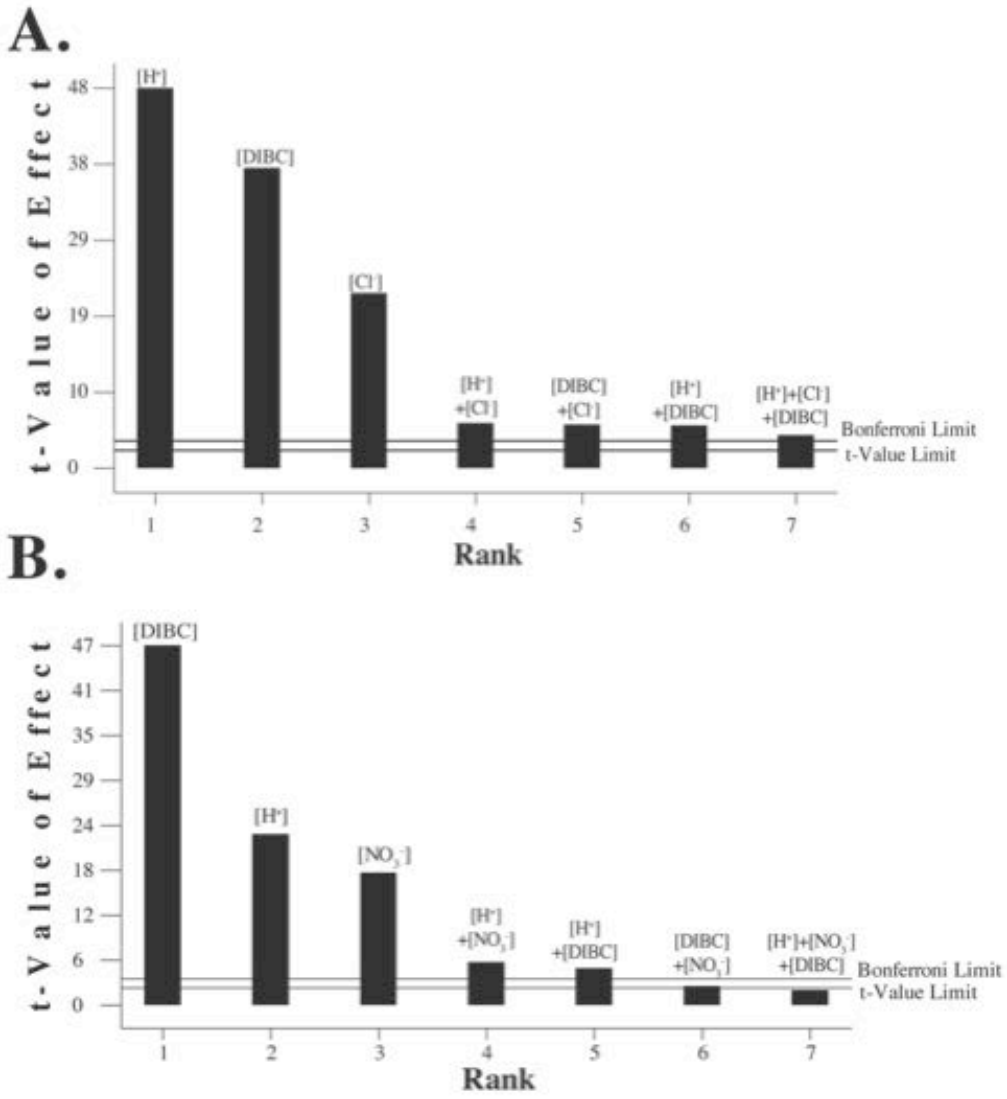

Figure 20. (A). shows the Pereto chart demonstrating the main effects on the Pa extraction by DIBC in Cl^- form. In the Cl^- form all three main effects, all three 2-factor interactions, and the 3-factor interaction were greater than the Bonferroni Limit and t-Value Limit. (B). Shows the Pereto chart demonstrating the main effects on the Pa extraction by DIBC in NO_3^- form. In NO_3^- the three main effects, and two 2-factor interactions were greater than the Bonferroni Limit and t-Value Limit.

4.4.3. Data Transformation and Main Effects

For further statistical analysis to be performed by the software engine, a $\log_{10}$ transformation was necessary because the max/min ≥10 of D responses. The Pereto chart (**Figure 20**) summarizes the main effects that each independent variable has on D.

Interestingly, in chloride medium, in addition to the main effect of each experimental parameter, there were variable-interaction effects (three two-variable and a three-variable interaction), which were statistically significant (Bonferroni limit and t-value significance levels were 3.46 and 2.26, respectively). Note, for this experiment, interactions were considered significant when the t-value effect was larger than the Bonferroni limit.[109] The largest effect on D resulted from the $[H^+]$ followed by [DIBC] and $[Cl^-]$. This suggests that the formation dominant extracted species of Pa was most strongly dependent on the acidity of the solution and not the counterion concentration. These findings correspond with previous investigations, in which it was demonstrated that the extracted species, $PaOCl_4^-$ by DIBC becomes the dominant species as [HCl] is increased from 3 to 6 M,[106] however it was unclear from this study if the formation of $PaOCl_4^-$ was more strongly dependent on $[Cl^-]$ or $[H^+]$. Interestingly, our findings would suggest that the formation of the extractable species of Pa can be controlled, given sufficient $[Cl^-]$ and [DIBC], by solution acidity. Furthermore, the small, but statistically significant, effects of the 2- and 3-variable terms appear to contribute synergistic (or anti-synergistic) effects between the DIBC, Cl^-, and H^+; all having a fairly equal contribution to D. The Pereto chart of the model suggests that the effect of a small change in one experimental parameter cannot be fully predicted without propagating that change through the combination effects.

In the nitrate, the main effects on D were caused by the [DIBC] followed by the $[H^+]$ then $[NO_3^-]$. The 2- and 3-variable interactions were much weaker than in the chloride system, and only two 2-variable interaction were statistically significant, $[H^+]+[NO_3^-]$ and $[H^+]+$[DIBC]. The remaining 2-variable interaction and 3-variable interaction effects were below the Bonferroni limit and the t-value limit of 3.46 and 2.26, respectively; meaning their effect on the system was not statistically significant. Unlike chloride, in which the main effect on D was most significantly determined by

[H^+], in the nitrate scenario, the main effect was determined by [DIBC]. Therefore, we believe that under the conditions evaluated, the extractable species of Pa was already the dominant species and D was largely enhanced by the additional of more DIBC to coordinate with the Pa species.[13, 107] This assertion is supported by previous studies, in which it was demonstrated that the extractable species $Pa(OH)_2(NO_3)_4$ – formed as the dominant species when the [HNO_3] > 1 M.[110] These results point to future studies to develop a more detailed understanding of the dominant extractable species of Pa and conditions under which these species were formed.

4.4.4. Statistical Quality of the Model

The data was fit to an unadjusted model (includes the midpoint) to develop the model coefficients. The statistics of the model (**Table 5**) in chloride (model F value = 540.5, $p < 0.0001$) and in nitrate (model F value = 195.2, $p < 0.0001$) show the overall F value for the models were statistically significant. With these model F values, there is <0.01% chance that this could have resulted due to background variation; therefore, the effect that the variables had on D, and the ability of the model to represent the experiment al D are likely to be true, and not variations in the signal to noise.

The quality of the model was quantified with a lack of fit F value (F*), which provides the statistical power to reject the null hypothesis for an alternative one. In chloride system, the model fit the data well (F* = 2.43, p = 0.153), as F* was not significant. This implies that the uncertainty associated with the model fit was not significant relative to the pure uncertainty, and there is a 15.3% chance that F* could be produced by variation in the background measurements. Therefore, H_0 can be rejected and the model can be used to evaluate D of Pa by DIBC in HCl. While the F* value is not significant in chloride system, in the nitrate one (F* = 9.64, p = 0.0036) F* was statistically significant. Where the p value implies that there is only a 0.36% chance that this F* could be due to variations in the noise or background of the measurement, which means that the model could fail to successfully represent D based upon input parameters. However, F* values presented here are calculated directly by the software, which does not take into account the experimental uncertainty.

With the experimental uncertainty taken into account, the F* would likely decrease. Additionally, the range of D in nitrate system was smaller than in chloride, the system as a whole is less dynamic; therefore equal deviations about the linear regression due to experimental uncertainty will have a much larger effect in nitrate than chloride.

Table 5. Summary of the statistical values describing the quality of the model to reflect the experimental data of the extraction of Pa by DIBC in both HCl and HNO_3.

Statistical Value	HCl	HNO_3
Model F- Value	540.53	195.23
Lack of Fit F-Value	2.43	9.64
R^2	0.9974	0.9910
Adjusted R^2	0.9955	0.9828
Predicted R^2	0.9923	0.9873

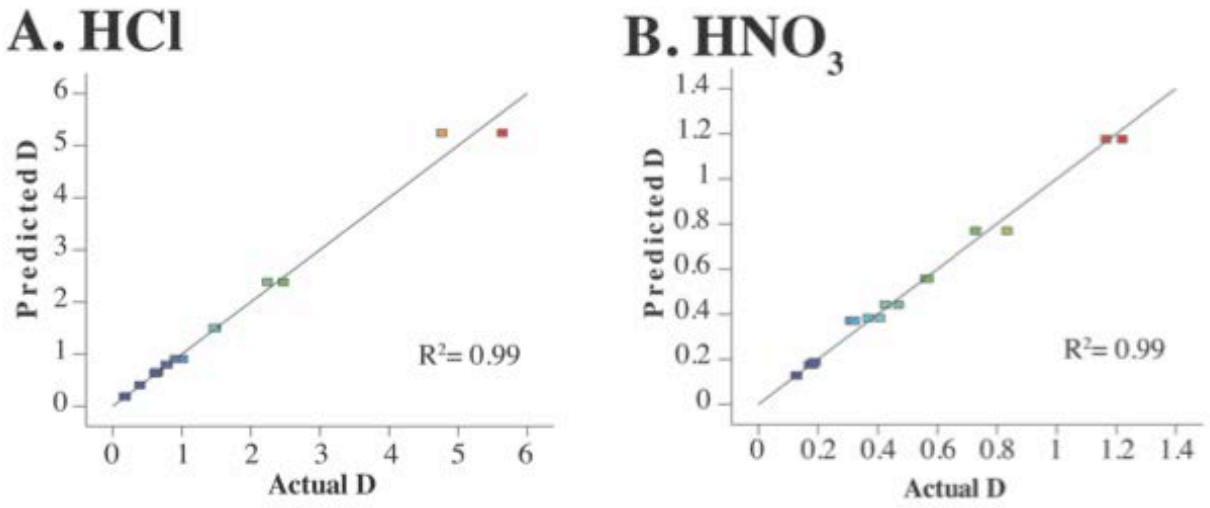

Figure 21. Plot of the of predicted distribution coefficient based upon the model versus the actual distribution of Pa by DIBC. Plot (A). is in HCl and (B). is in HNO_3^-. In both cases there is a strong correlation ($R^2 = 0.99$) between predicted values and the actual values.

4.4.5. Data Correlation and Predictability

The overall goodness of fit of the model to represent the data can be summed up in the R^2 values. The values predicted by the model strongly correlate with those in the chloride (R^2 = 0.9974) and nitrate systems (R^2 = 0.9910). A plot (**Figure 21**) demonstrating the correlation between the models and experiments in which predicted D (calculated from the model) are plotted vs. the experimental D. Because R^2 is close to 1, we can be confident in the ability of the model to be effectively used to understand the extraction of Pa from DIBC within the range of experimental concentrations studied. However, due to the nature of the mathematical determination of R^2, as the number of data points increases, R^2 may erroneously increase by chance alone, therefore we need to further assess the quality R^2.[111]

To better understand how the model fits the experimental results as additional data points are added, the adjusted-R^2 (R^2_{adj}) can be evaluated.[111, 112] The R^2_{adj} values are calculated from the R^2 but also include terms of sample size (n = 18 data points; degrees of freedom = 17) and number of regressors (p = 3 independent variables), therefore R^2_{adj} only increases if the new observations improve R^2 more than would be expected by chance.[111] After the adjustment, the correlation in chloride (R^2_{adj} = 0.9955) and nitrate (R^2_{adj} = 0.9847) changed very little, which strongly suggest that the quality of the correlation did not increase from additional data points alone, suggesting that there is a true correlation between predicted and experimental data points within the modeled region.

An important property of models is the ability to predict future results. While R^2 and R^2_{adj} measure correlation, a predicted- R^2 (R^2_{pred}) quantifies the models ability to predict.[113] To calculate a R^2_{pred}, the individual data points are systematically removed, and the regression line is re-determined to assess how well the model fit the removed data point.[113] In the current study, the R^2_{pred} values for the chloride (R^2_{pred} = 0.9923) and nitrate (R^2_{pred} = 0.9973) are in agreement with the other calculated correlation coefficients (R^2 and R^2_{adj}) and the R^2_{adj} is in reasonable agreement ($|R^2_{adj} - R^2_{pred}| < 0.2$). Thus, it is reasonable to conclude that the model sufficiently predicts extraction of Pa by DIBC in HCl and HNO_3 systems when the experimental concentrations of each parameter are within the range of the model.

4.4.6. Mathematical Equation of the Model

The model for the extraction of Pa as a function of the experimental [DIBC], $[H^+]$, and $[A^-]$ is represented with respect to $\log_{10}D$ (**Equations 14; Equation 15**).

$$\log_{10}D = -16.182 + 23.041\,[DIBC] + 2.255\,[H^+] + 2.578\,[Cl^-] - 4.237\,[DIBC][H^+] - 4.440\,[DIBC][Cl^-] - 0.351\,[H^+][Cl^-] + 0.860\,[DIBC][H^+][Cl^-] \quad \text{eq. 14}$$

$$\log_{10}D = -2.487 + 0.968\,[DIBC] + 2.277\,[H^+] + 0.306\,[NO_3^-] - 0.056\,[DIBC][H^+] - 0.054\,[H^+][NO_3^-] \quad \text{eq. 15}$$

A graphical representation of these equations (**Figure 22**) shows the D values plotted as a function of the true concentrations, [DIBC] and $[H^+]$, at different $[A^-]$. This representation demonstrates the effect of increasing the $[A^-]$.

While the values of the coefficient cannot be directly correlated to the extracted species stoichiometric relationship to Pa, they can provide an estimation of a quantitative effect of a change to the extraction system. To compare, the coefficients in the chloride are an order of magnitude larger than those in the NO_3^-, reflecting the range of D in chloride being larger than D in NO_3^-. Additionally, with regards to the y-intercepts; these values represent a control experiment for the extraction of Pa when [DIBC], $[H^+]$, and $[A^-]$ are all approximately 0. In this case, the extraction system contains 5 mL H_2O (1×10^{-7} M of H^+) and 5 mL dodecane. Experimentally, Pa remains fully in the aqueous phase, $D < 0.0005$. We would expect that the y-intercept values be near 0, because the equation is represented in a $\log_{10}$ transformation, the y-intercept values for chloride (6.58×10^{-17}) and NO_3^- (3.26×10^{-3}). In the chloride the y-intercept can be considered 0 and therefore the extraction model agrees with the experimental data. In the NO_3^-, the y-intercept calculated from the model is an order of magnitude larger than the experimentally determined value. While the calculated initial D is near 0, the model does not appear to fit the data perfect, as we described earlier from a statistically significant F*.

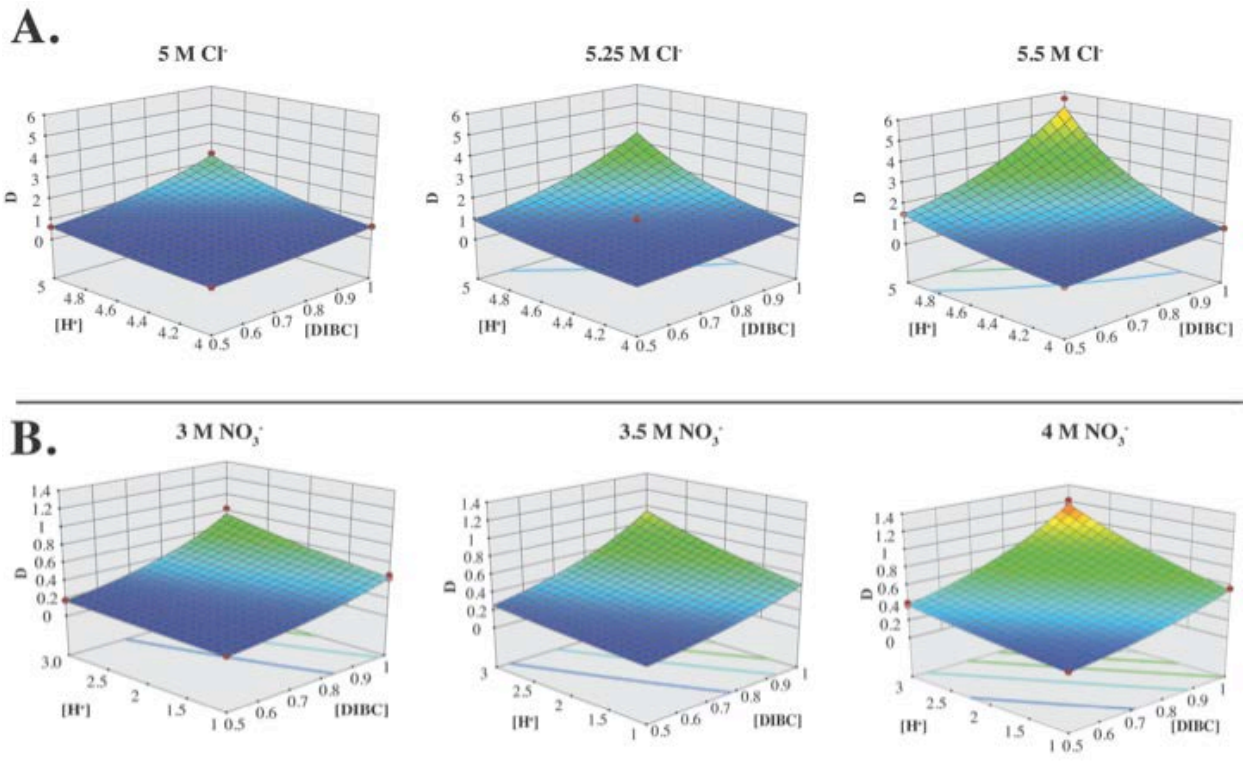

Figure 22. (A). 3D surface plot showing the interaction of $[H^+]$ and [DIBC] as a function of $[Cl^-]$ and Pa distribution coefficient. (B). shows the 3D surface plot for the interaction of $[H^+]$ and [DIBC] as a function of $[NO_3^-]$ and the Pa distribution coefficient.

4.5. Conclusions and Future Experiments

A full-factorial experimental design has been conducted to model the extraction of Pa by DIBC from HCl and HNO_3. The resulting model predicts D of Pa extraction from these solutions within the range of parameters examined. Using this model, we gain an understanding of how changes in the [DIBC], $[H^+]$, and $[A^-]$ effect extraction of Pa individually, and gain insight on the effect of two-way and three-way variable-interactions. Statistical analysis of the model, suggests that the model may be used to predict future experimental observations that occur within the experimental variable range **(Figure 18)**. This approach is considered a first step towards a better model of Pa extraction systems. Future experiments will investigate the identity of the species of Pa extracted by DIBC to gain a more detailed understanding of the chemistry of this extraction system.

Based on experimental results presented here, the most effective extraction of Pa by DIBC can be achieved using the following settings: in HCl (1 M DIBC, 5 M H^+, 5.5 M Cl^-; D = 5.21 ± 0.62); and in HNO_3 (1 M DIBC, 3 M H^+, and 4 M NO_3^-; D = 1.20 ± 0.04) occur at the high values of each parameter (+ + +). These results provide a baseline of experimental conditions, which can be used to guide a further optimization of the extraction of Pa from DIBC in HCl and HNO_3. Important parameters that are expected to be included in this future work include reaction time, analyte concentration, radiolytic effects, effect of hydrolysis and others.

4.6. Associated Content

Notes: The authors declare no competing financial interest.

Acknowledgements: The authors would like to thank Stéphane Bourg and the safety of actinide separation community for the opportunity to share this work. Also the authors would like to thank Nik Barkve for his consultation and expertise in statistical analysis. This work is funded by the United States Nuclear Regulatory Commission under grants NRC-HQ-84-14-FOA-0003 and NRC-HQ-12-G-38-0041 and the Department of Homeland Security DHS-DNDO 2012-DN-130-NF0001-02. This material is based upon work supported by the U.S. Department of Homeland Security under Grant Award Number, 2012-DN-130-NF0001-02. The views and conclusions contained in this document are those of the authors and should not be interpreted as representing the official policies, either expressed or implied, of the U.S. Department of Homeland Security.

CHAPTER V: TRACE-LEVEL EXTRACTION BEHAVIOR OF ACTINIDE ELEMENTS BY ALIPHATIC ALCOHOL EXTRACTANTS IN MINERAL ACIDS: INSIGHTS INTO THE TRACE SOLUTION CHEMISTRY OF PROTACTINIUM

This chapter was accepted for publication 12 May, 2016. This chapter is reprinted with permission. Please refer to Knight, A. W., Eitrheim, E. S., Nelson, A. W., Peterson, M., McAlister, D., Forbes, T. Z., Schultz, M. K. (2016). Trace-level Extraction Behavior of Actinide Elements by Aliphatic Alcohol Extractants in Mineral Acids: Insights into the Trace Solution Chemistry of Protactinium. *Solvent Extraction and Ion Exchange,* **34**(6): 509-521

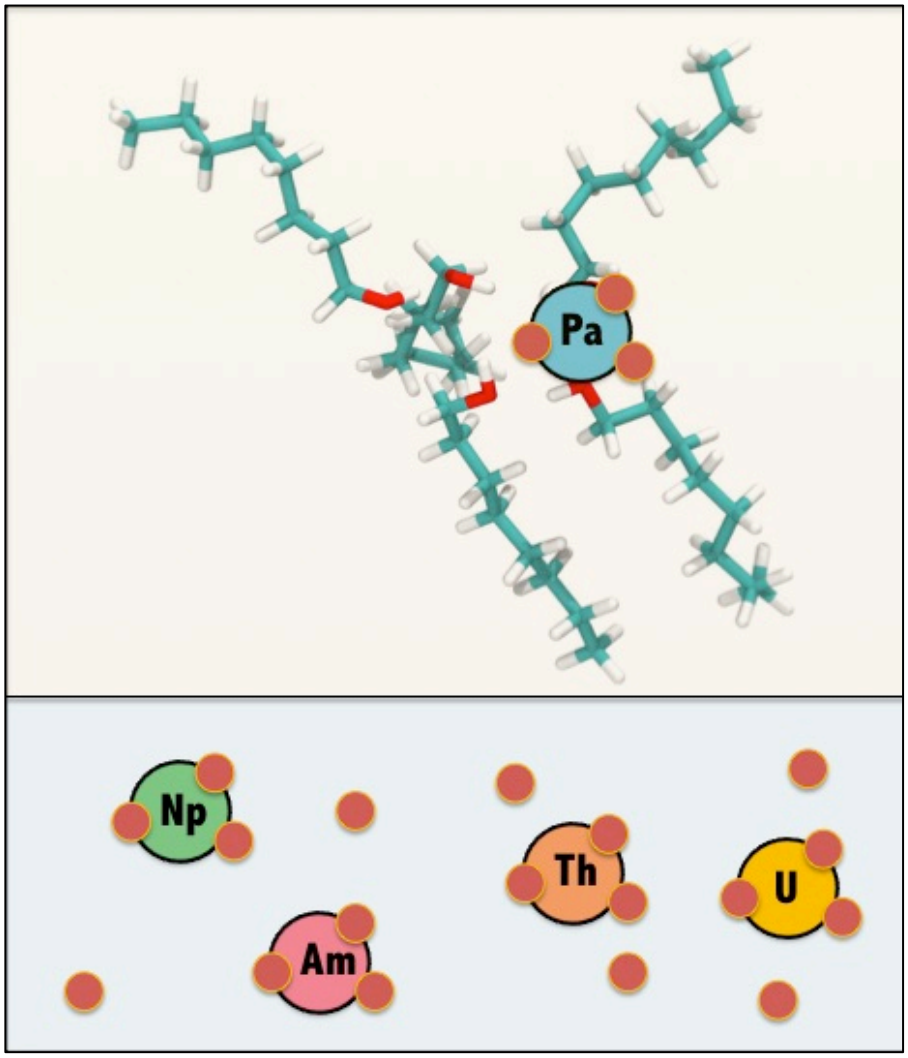

5.1. Abstract

The extraction of actinide elements thorium, protactinium, uranium, neptunium, and americium by aliphatic alcohols (1-octanol, 2-ethyl-hexanol, and 2,6-dimethyl-4-heptanol) were investigated with solvent extraction and extraction chromatographic techniques from hydrochloric and nitric acid solutions. These systems provide the potential for low-cost, high quality methods for the isolation of Pa from complex matrices. Acid dependency experiments demonstrate the selective extraction of protactinium from hydrochloric and nitric acids, relative to the other actinides explored. Experiments were conducted to elucidate the equilibrium chemical stoichiometry of the protactinium complex that underlies this unique extraction behavior. Slope analysis with respect to the alcohol concentration infers a stoichiometric relationship of 2:1 for the alcohol extractant to the protactinium ion. Slope analysis with respect to the chloride ion (when $[H^+]$= 0.1, 1 and 4 M) suggests that the stoichiometric identity of the protactinium chloro-complexes depends on the $[H^+]$ (0.1 M to 4 M). Extraction of Pa increases as the Pa:Cl ratio increases from 1:2, at low acid concentration, to 1:6 at high acid concentration. With respect to the nitrate ion (when $[H^+]$ = 1 and 4 M), the stoichiometric relationship was determined to be 2:1 nitrate to protactinium throughout the range investigated. The sum of these findings and observations contribute to a deeper understanding of the unique chemistry of protactinium compared to the other members of the actinide group.

Keywords: protactinium, aliphatic alcohols, solvent extraction, extraction chromatography

5.2. Introduction

Protactinium (Pa) is a naturally-occurring element, whose unique chemical behavior has been referred to as “peculiar”; “mysterious”; “puzzling”; and “witchcraft”.[3-5, 46] Reflecting these enigmatic properties, it has been recently noted that “Pa might be the only natural-chemical species whose aquo-ions have not really been experimentally identified”.[3] Similarly, it has recently been observed that Pa-aquo-chemistry shares little chemical similarity to other actinide group elements

(An) (even in the same oxidation state).[2-5] Thus, the use of An as Pa analogues to better understand the chemistry of Pa is considered questionable.[2-5]

The analytical need for determining the radioactivity concentration of Pa in materials arises from several important applications. In general, these applications require quantitative determination of Pa at very low concentrations ($<10^{-8}$ M) and separation of Pa from key isobaric and radiometric impurities. For example, quantitative evaluation of Pa in marine and terrestrial samples is critical for dating quaternary age materials by the $^{231}Pa/^{235}U$ radioactivity ratio.[7, 9, 11, 114] Analytical methods employed in this application must effectively recover ^{231}Pa (and ^{233}Pa tracer) in high yield, while separating it from interfering impurities for mass spectrometric or radiometric analysis. Similar analytical requirements (although often at higher concentrations of Pa) exist for the age determination of illicit nuclear material for nuclear forensics applications.[12, 14] Another key application, in which Pa chemistry is important, is in the development of alternative fuel cycles (*i.e.* thorium reactors). In this case, natural ^{232}Th is irradiated to form the fissile ^{233}U fuel. In this process ^{233}Pa is formed as an intermediate, thus requiring the knowledge of Pa chemistry for removal and processing of the fuel.[13 74] The analytical isolation of Pa is complicated by sample matrices that often include much larger quantities of other actinides, lanthanides, transition metals, and other interfering complexants and chemical constituents.

Uncertainties in the understanding of Pa chemistry can be attributed to its low-natural elemental abundance; challenges associated with obtaining sufficient quantities for spectroscopy; and high specific radioactivity of isotopes isolated for analysis.[2, 4, 115] For example, there are only two naturally-occurring isotopes (^{231}Pa; $t_{1/2}$ = 32,760 years, and $^{234}Pa/^{234m}Pa$; $t_{1/2}$ = 6.7 hours/1.17 min),[2, 7] which combine for a terrestrial-elemental abundance of less than 300 fg/g of material in typical soils – making Pa one of the rarest naturally-occurring elements.[11] Thus, with a few exceptions (*i.e.* Argonne National Laboratory, US Department of Energy),[115] mass quantities necessary to perform spectroscopic analysis of aqueous speciation of Pa are not available, representing a significant challenge to advancing the understanding of this enigmatic element.

To improve upon these analytical procedures to isolate Pa from complex matrices, it is essential to improve upon our understanding of Pa chemistry. For example, most analytical procedures designed to isolate Pa from complex matrices rely on the strong complex formation of Pa with the fluoride ion (F^-). The strongly-associated Pa-flouro complex was first identified by aqueous-phase precipitation reactions involving K_2PaF_7, which is sparingly soluble.[2] More recent investigations have revealed numerous solid and aqueous phase Pa-fluoro complexes analyzed by crystallography and Raman spectroscopy.[74]

In solvent extraction and radioanalytical chemistry, the aqueous Pa-fluoro complex ion PaF_7^{2-} is reported to be poorly extracted into organic phases.[2] Numerous examples exist in the literature in which Pa is either extracted into the organic phase in liquid-liquid extraction methods; or retained in the stationary phase in extraction chromatography – and then subsequently back-extracted by use of dilute hydrofluoric acid (HF) or oxalic acid into an aqueous phase.[5, 8, 11, 63] While HF and oxalic acid are effective complexing agents for Pa back extraction, there are significant limitations. For example, the presence of dilute HF can prevent Pa from being extracted in subsequent separation steps,[11] and can also complicate source preparation for alpha- or mass-spectrometry analysis.[11, 14] Recent studies have aimed to understand the weight distribution ratios of Pa on common extraction chromatographic resins (TEVA, TRU, UTEVA) and anion exchange columns (AG1-X8), and the results illuminated numerous possibilities for the separation of Pa from other actinides and interfering metals in the absence of complexing agents.[70] Nevertheless, separation challenges are generally experienced due to adsorption behavior of the other actinides on these materials as well.

The low natural abundance and lack of technologically-produced Pa limits the potential for direct-spectroscopic determinations of Pa aqueous speciation for most researchers. However, significant information concerning the chemical species of Pa can be obtained by carefully-designed analytical experiments. Classical approaches, such as slope analysis, are used to derive physical meaning from analytical extraction experiments; and the results can provide supporting information regarding the physico-chemical forms of the dominant extracted species.[13, 116, 117] Our

aim is to use slope analysis of log-log plots to relate the distribution coefficient (D) to the extractant concentration. In this way, slope analysis provides a qualitative estimation of the equilibrium stoichiometric relationship of analytes.[116]

Here, we present the results of a series of solid-liquid and liquid-liquid extraction experiments that provide insights into the differences between Pa chemistry and other elements in the actinide group and suggest likely chemical species of Pa present under specific chemical conditions. This study examines the extraction of Pa by aliphatic alcohols within the context of using its distribution behavior in different acidic environments as a tool for developing a more detailed understanding of the speciation of Pa at trace concentrations. We determined the D_{Pa} from liquid-liquid extractions from three different aliphatic alcohols; 1-octanol, (2,6)-dimethyl-4-heptanol, and 2-ethyl-hexanol in both hydrochloric (HCl) and nitric (HNO_3) acid environments. Approximation of the chemical speciation and average stoichiometric relationships are determined based upon the understanding of extraction equilibrium constant ($K_{extraction}$). Lastly, experiments were performed to observe and compare the extraction behavior of Pa on the liquid-solid interface by use of extraction chromatography, when these aliphatic alcohols were coordinated to an inert solid substrate.

5.3. Experimental Section

5.3.1. General

Acids and salts used in extraction experiments were ACS reagent grade purity or higher (Fischer Scientific, Pittsburg, PA), including; HNO_3, HCl, sodium chloride (NaCl), sodium nitrate ($NaNO_3$). All radioactive standards were prepared with Ultra Pure acids (HCl, HNO_3; Fisher Scientific) and diluted to working solutions with ultra-pure distilled deionized water (Baseline®, Seastar Chemicals, British Columbia, Cananda). Organic reagents were reagent grade (99% or greater) for 1-octanol, 2-ethyl-1-hexanol, dodecane and 80% or greater for 2,6-dimethyl-4-heptanol and were purchased from Sigma Aldrich (St. Louis, MO). Half-life information and radioactive emission (alpha particle, beta particle, and gamma ray) energies originated from the Evaluated

Nuclear Structure Data File (ENSDF) and from the United States National Nuclear Data Center (NNDC, Brookhaven National Laboratory, US Department of Energy).

5.3.2. Preparation of Th, Pa, U, Np, and Am Standards

The isotopes used for this study were ^{237}Np ($t_{1/2}$ = 2.144x10^6 years), ^{233}Pa ($t_{1/2}$= 26.967 days), ^{232}U ($t_{1/2}$= 68.81 years), ^{228}Th ($t_{1/2}$= 1.9 years), and ^{241}Am (432.6 years). These isotopes were obtained from standard reference solutions (^{232}U; SRS 92403, certified in secular equilibrium with ^{228}Th) and nominal liquid sources (^{241}Am; Lot # 1701-72 and ^{237}Np; Lot #1760-91) were purchased from Eckert and Ziegler. Protactinum-233 ingrowth was monitored in the ^{237}Np source and reached secular equilibrium after 7 months as modeled by standard ingrowth equations. Standard and nominal solutions were diluted to working solutions using Ultra pure 0.1 M HNO_3 (^{232}U, ^{241}Am) and Ultra pure 6 M HCl (^{237}Np), which were prepared by serial dilutions and analyzed volumetrically with gravimetric and radiometric confirmations. Dilution factors were determined by gravimetrically and radiometrically *via* liquid scintillation counting and were confirmed within 2%.

Isolation of decay product standards (^{228}Th and ^{233}Pa) were obtained by routine extraction chromatographic procedures developed in our laboratory.[8, 101] Briefly, ^{228}Th and ^{232}U were separated and purified by TEVA resin (Eichrom Technologies, LLC, Lisle, IL), where ^{228}Th can be eluted in 4 M HCl, while ^{232}U is retained and subsequently eluted with 0.1 M HCl. Separation and purification of ^{233}Pa and ^{237}Np was performed using a resin form of 1-octanol, where ^{237}Np can be eluted and collected in 9 M HCl, whereas ^{233}Pa is strongly retained and subsequently eluted with 1 M HCl.

5.3.3. Extraction Methods

Chemical partitioning and $D_{actinide}$ values were evaluated by liquid-liquid extractions and column chromatography. For liquid-liquid extractions, all experiments were performed in a 15 mL conical centrifuge tube with a phase ratio of 1:1 in 5 mL phase fractions. The aqueous phases were prepared with the corresponding concentration of anion (A^-) and acidity (H^+) by the addition of HCl/NaCl or HNO_3/$NaNO_3$, where the concentration of A^- and H^+ ranged 1 M to 9 M. The organic

phases were prepared by diluting the aliphatic alcohol extractants (1-octanol, 2-ethylhexanol, or 2,6-dimethyl-4-heptanol) to concentrations ranging from 0.2 M to 2.5 M in dodecane. Finally, following pre-equilibration with unspiked aqueous phases, the conical tubes were spiked with 50 Bq or greater of the radionuclide of interest (^{228}Th, ^{233}Pa, ^{232}U, ^{237}Np, or ^{241}Am). Once the system was prepared, the conical tubes were capped and vortexed for 1 min at 1000 rpm, and then thoroughly mixed for 1 hour using a rotator. Following 1 hour of mixing, the solutions were set aside until the phases were completely separated (samples were allowed to separate naturally without centrifugation). Following complete phase separation, 4 mL aliquots of each phase were transferred to separate 20 mL glass scintillation vial to be counted via sodium iodide (NaI) gamma spectrometry (^{233}Pa, ^{237}Np, ^{241}Am) or liquid scintillation (LS) counting (^{228}Th, ^{232}U). A volume correction was performed during the sample analysis to account for only 4/5 of the solution being measured, as described previously.[118]

In acid and salt dependency experiments, the solution activities (a) were used to better reflect the effective concentrations in solution, which can deviate significantly from molar concentrations (M) especially in high concentrations of HCl. The molar activity coefficients were obtained from tabulated values.[119]

5.3.3.1. Acid Dependency On Distribution Ratios

Experiments were performed to evaluate the effect of solution acidity on the extraction of ^{228}Th, ^{233}Pa, ^{232}U, ^{237}Np, and ^{241}Am. In both HNO_3 and HCl, a series of experiments were performed in triplicate in which extractions systems were prepared with an extractant concentration of 2.5 M (2,6-dimethyl-4-heptanol, 1-octanol, or 2-ethyl-hexanol) and the acid concentration (HNO_3 or HCl) was adjusted from 1 M to 9 M (a_{HCl} = 0.81 – 124.2; a_{HNO3}= 0.73- 20.7) To quantify the effect of solution acidity to the extraction of each metal, D was calculated (**Equation 16**).

$$D = \frac{Radioactivity_{organic}}{Radioactivity_{aqueous}} \quad eq.16$$

5.3.3.2. Effect of Anion and Extractant

Further experiments (n=3) were performed with ^{233}Pa to understand the role of A^- (*i.e.* Cl^- or NO_3^-) and extractant (2,6-dimethyl-4-heptanol) on distribution ratio of Pa. To assess the anion contribution, aqueous-phase solutions were prepared at three acidities ($[H^+]$= 0.1 M, 1 M, and 4 M) by the addition of HNO_3 or HCl and the anion (A^-) concentration was adjusted from ($[NO_3^-]$ =1 – 7 M; $[Cl^-]$ = 1 – 6 M) by the addition of the sodium salt ($NaNO_3$ or NaCl). The mixed electrolyte activities were calculated using activity coefficients from literature tabulated values.[119, 120] In all experiments the organic phase was held at a constant [2,6-dimethyl-4-heptanol] = 2.5 M. To evaluate the effect of the anion, the distribution coefficient of Pa was calculated from **Equation 16**. To assess the role of the extractant concentration on the distribution of Pa into the organic phase, a series of experiments (triplicate), were conducted with a constant acid concentration (6 M; HNO_3 or HCl) and the concentration of 2,6-dimethyl-4-heptanol was adjusted from 0.3 M to 1 M. In each experimental system, the distribution coefficient of Pa used to evaluate the extraction and was calculated using **Equation 16**.

5.3.3.3. Extraction Chromatography

Extraction chromatographic resins containing each alcohol (1-octanol, 2-ethylhexanol, or 2,6-dimethyl-4-heptanol) were made as described previously.[81] Briefly, each extractant alcohol (10 g) was dissolved in methanol (100 mL) and added to the resin support (15 g; Amberchrom CG71, 25-50 µm, Rohm and Haas, Philadelphia, PA USA). The mixture was stirred on a rotary evaporator (1 h) and the methanol was slowly removed under reduced pressure (20-25 mmHg) at 50 °C. The resulting material consists of 40% (w:w) of the extractant alcohol, which was verified by thermogravimetric analysis.

To assess the uptake for metals with extraction chromatography, the weight distribution coefficient (D_w) was measured. To determine D_w, between 20-35 mg of resin was weighed out into a

15 mL conical centrifuge tube (n=2). Then 2 mL of acid (range 1-9 M HCl and HNO_3) and a known radioactivity of each radiometal (^{228}Th, ^{233}Pa, ^{232}U, ^{237}Np, ^{241}Am) were added. The conical tubes were vortexed for 1 min, mixed on a rotator for 1 hour, and allowed to settle for about 5 min. Next, the contents were transferred to a 10 mL syringe capped with a 0.45 µm polyether-sulphone filter (PES), and the aqueous phase was collected into a tarred 20 mL liquid scintillation vial. Control experiments verified quantitative recoveries, confirming no adsorption onto the PES filter. Each vial was weighed after the aqueous phase was transferred to correct for the recovery of the aqueous phase. The subsequent aqueous phase was counted via NaI gamma spectrometry (^{233}Pa, ^{237}Np, ^{241}Am) or LS counting (^{228}Th, ^{232}U). To calculate D_w the following equation was used (**Equation 17**):

$$D_w = \frac{\frac{A_o - A_A}{w}}{\frac{A_A}{V}} \qquad eq.17$$

where, A_0 is the original radioactivity added and A_A is the amount of radioactivity recovered in the aqueous phase, w is the mass of the resin in grams, and V is the volume of acid in mL. For a better representation of metal separation and extraction on a column apparatus, the capacity factor (k') was calculated as shown previously.[81] To calculate k' additional physical properties were assessed (**Table 8**) using **Equation 18.**[81] A detailed description of the calculation of D_w to k' is provided in the supplementary material.

$$k' = \frac{D_w * (d_{extractant} * v_s)}{0.4 * v_m} \qquad eq.18$$

The k' value is proportional to the number of free column volumes added to the column to reach the elution peak maximum of a given radionuclide in milliliters.

5.3.4. Source Counting

Gamma-spectroscopy and LS counting were utilized to determine the radioactivities of each radionuclide in the aqueous and organic phases to calculate $D_{actinide}$ values. Gamma-spectroscopy was carried out with a well-type NaI solid scintillating detector equipped with a Digibase™ (ORTEC,

Oak Ridge, TN) and Maestro Software (ORTEC). All measurements were made using the manufacturer recommended voltage (800 V). Energies were calibrated with a two-point calibration (^{137}Cs 661 keV, ^{152}Eu 344 keV) from known sources. Analyses of gamma emitting radionuclides (^{233}Pa, ^{237}Np, ^{241}Am) were performed by integrating the number of counts in each region of interest (ROI). Each sample phase was counted individually for 300 seconds and the counts in each ROI were determined from subtracting a matched count time blank spectra. Corrections were applied to account for phase recovery based upon density of phase withdrawn and counted. LS counting was performed on a Packard (1600 CA Tri-Carb) LS counter using Ecolite LS cocktail in glass LS vials with approximately 10% water fraction. Each vial was counted (60 min) using a standard protocol, and background subtracted using a blank of similar matrix.

5.4. Results and Discussion

5.4.1. Solvent Extraction Behavior

The results summarizing the liquid-liquid extraction of Pa with three aliphatic alcohols (1-octanol, 2-ethylhexanol, and 2,6-dimethyl-4-heptanol) as a function of the chemical activities of HCl and HNO_3 are summarized in **Figure 23**. In both mineral acid forms, we observed no significant difference in the extraction of Pa as a function of alcohol chain length or position of the OH group. Notably, our results suggest that extraction of Pa by alcohols is consistent so long as the alcohol is immiscible in water. Because the observed extraction of Pa among each alcohol investigated was identical, the subsequent of the experiments were performed with 2,6-dimethyl-4-heptanol.

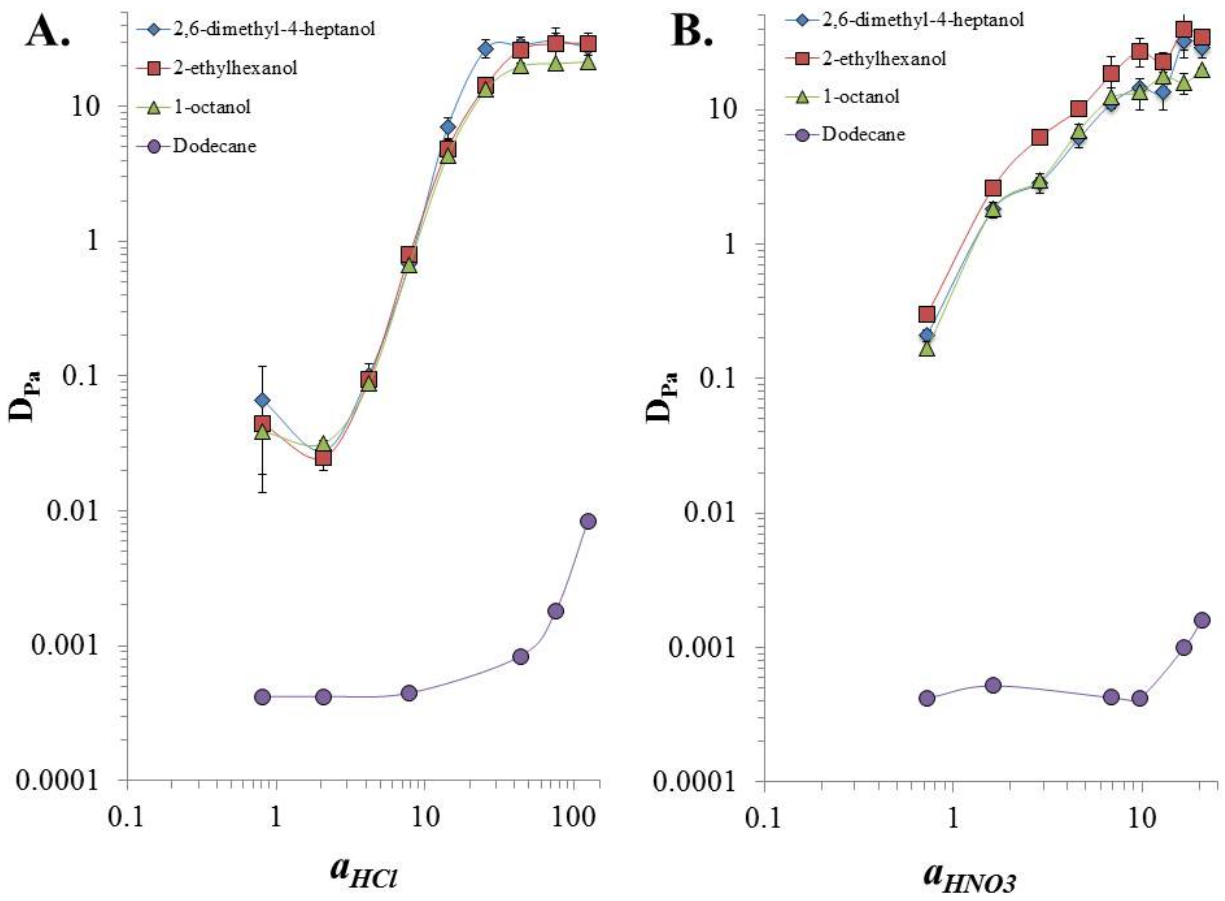

Figure 23. Extraction of ^{233}Pa by three aliphatic alcohols 2,6-dimethyl-4-heptanol, 2-ethy-hexanol, and 1-octanol versus the activities of HCl (A) and HNO_3 (B).

In HCl, the extraction trend of Pa by the 2,6-dimethyl-4-heptanol fits a sigmoidal relationship, in which poor extraction occurred in dilute concentrations ([HCl] < 4 M (a_{HCl} = 7.8)), followed by a short, steep, linear region (4 M (a_{HCl} = 7.8) < [HCl] > 6 M (a_{HCl} = 25.8)), and finally complete extraction ([HCl] > 6 M (a_{HCl} = 25.8)). This behavior is consistent with previous investigations into the solvent extraction behavior of Pa by oxygen containing functional groups (*i.e.* alcohols and ketones).[5, 13] And suggests that in dilute [HCl] the extractable complex ion of Pa in the organic phase is not the prevailing complex, but with increasing acidity and chloride, the extracted form of Pa becomes the dominant solution phase species when [HCl] exceeds 4 M (a_{HCl} =7.8). Pa

extraction from HNO_3 by aliphatic alcohols behaved uniformly, but slightly different than in HCl, observed by moderate extraction occurring when [HNO_3] < 2 M (a_{HNO3} = 1.6), and followed by a gradual, linear region when 2 M (a_{HNO3} =1.6) < [HNO_3] > 6 M (a_{HNO3} =9.6), and finally complete extraction when [HNO_3] > 6 M (a_{HNO3} = 9.6).

To ensure that the extraction of Pa requires the presence of aliphatic alcohols, a control experiment was performed to analyze the extraction of Pa by neat dodecane. The results (**Figure 23**) indicate very poor extraction of Pa in the absence of an immiscible alcohol extractant in the organic phase, thus suggesting the extraction of Pa occurs from interactions of a complex-Pa-ion with the hydroxyl group of the alcohol. Future experiments aim to investigate organic phase for the interactions between Pa and the alcohols as well as the macro-structural ordering of the alcohols (*i.e.* aggregation).

The extraction behavior of Pa was compared with actinide elements (Am (III), Th (IV), Np (V), and U (VI)) (no oxidation/reduction adjustments were made). Minimal extraction of the other actinides by 2,6-dimethyl-4-heptanol is observed as a function of the activities of HCl or HNO_3 (**Figure 24**). In high activities of HNO_3, we did observe an increase in D_{Np} values of about 0.24 when a_{HNO3} = 20.7, however this is significantly lower than D_{Pa} of 28.84 in the same conditions. Generally, actinides in the same oxidation state are often considered chemical analogues.[3] While pentavalent oxidation states of Np and Pa are known to exist,[1] their aqueous-phase chemistries are not analogous. While the chemistry of Pa differs significantly from that of Np, some detailed studies have noted similarities between chemistry of Pa with transition metals niobium (Nb) and tantalum (Ta).[5, 13] To further investigate the potential chemical species that underlie the observed differences in chemistry between Pa(V) and Np(V), we investigated the effects of anion and extractant concentrations to elucidate the identity of the dominant extracted species.

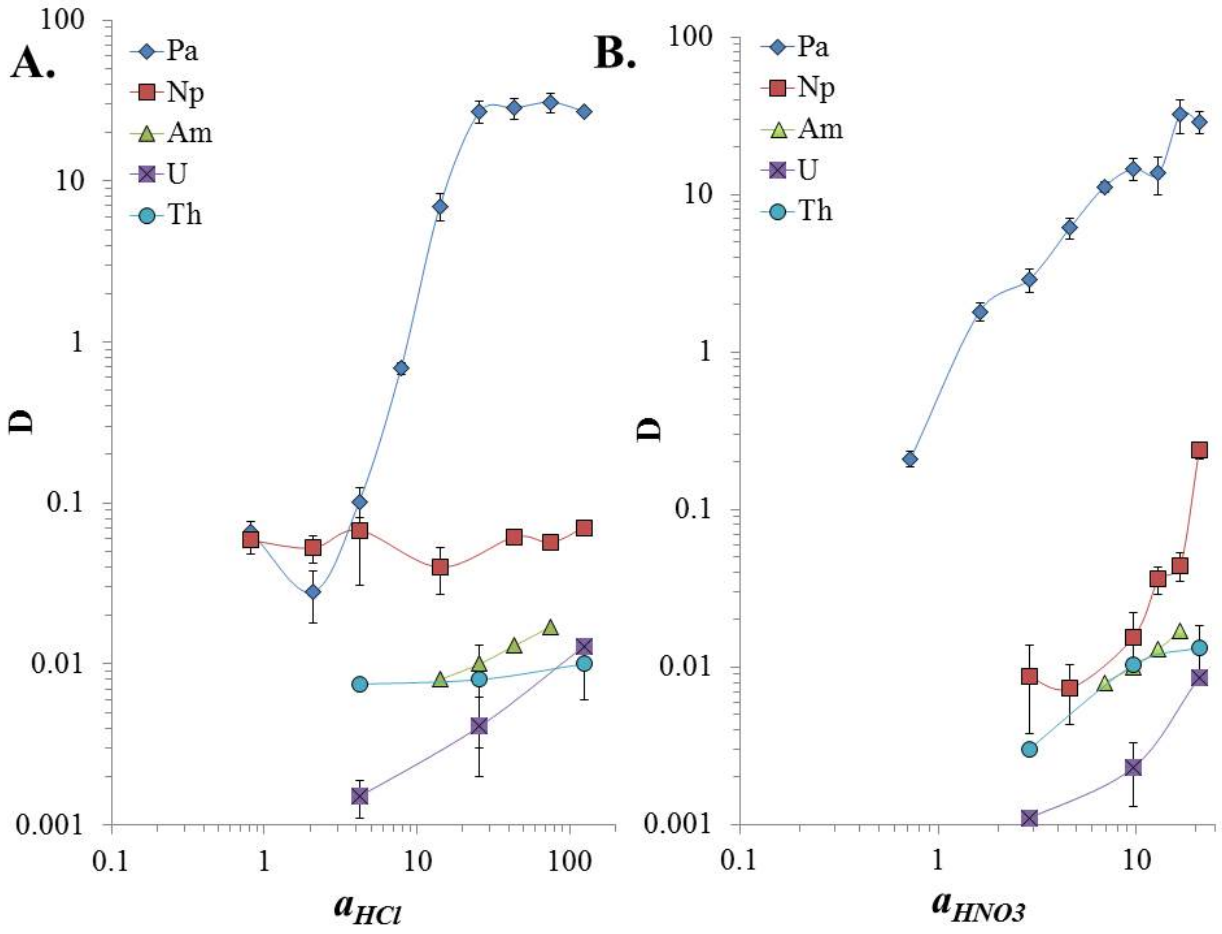

Figure 24. Extraction of early actinides Th, Pa, U, Np, and Am by 2,6-dimethyl-4-heptanol as a function of the activities of HCl (A) and HNO_3 (B).

5.4.1.1. Approximation of Equilibrium Protactinium Species at Trace Concentrations

While it is understood that the metal concentration in extraction processes plays a role in the complex formation and the extraction efficiency, in these experiments, analysis were limited to trace concentration of Pa relevant to radioanalytical chemistry. In doing so, we aimed to establish a qualitative approximation to the average equilibrium stoichiometric relationship between Pa and 2,6-dimethyl-4-heptanol– and to the anion (Cl^- or NO_3^-). The average stoichiometric relationship of extractant and anion to central Pa metal is based upon a *simplified* modeled-relationship of the extraction system (**Equation 19; Equation 20; Equation 21; Equation 22; Equation 23;**

Equation 24). The proton has been omitted from this simplified expression due to the challenges associated with determining the empirical speciation of potential Pa-H^+ at the concentrations available for our solvent extraction studies. The PaO^{3+} species is considered generic to the existing species. The results demonstrating the relationships between change in [2,6-dimethyl-4-heptanol] and a_{anion} with the D are summarized in log-log plots (**Figures 25; Figure 26**).

$$PaO^{3+}_{(aq)} + mA^{-}_{(aq)} + n\overline{ROH} \xrightarrow{K_{ex}} \overline{PaOA_mROH_n^{3-m}} \qquad eq.19$$

$$K_{ex} = \frac{\overline{[PaOA_mROH_n^{3-m}]}}{[PaO^{3+}]_{aq} * [A^-]^m_{aq} * \overline{[ROH]^n}} \qquad eq.20$$

$$D_{Pa} = \frac{\overline{[PaOA_mROH_n^{3-m}]}}{PaO^{3+}_{(aq)}} \qquad eq.21$$

$$K_{ex} = \frac{D_{Pa}}{[A^-]^m_{aq} * \overline{[ROH]^n}} \qquad eq.22$$

$$D_{Pa} = K_{ex} * [A^-]^m_{aq} * \overline{[ROH]^n} \qquad eq.23$$

$$\log D_{Pa} = \log K_{ex} + m \log[A^-]_{aq} + n \log\overline{[ROH]} \qquad eq.24$$

When a log-log plot of D_{Pa} versus [2,6-dimethyl-4-heptanol] was generated from solvent extraction experiments at constant acid (a_{HCl} = 25.8 or a_{HNO3} = 9.6), we observed a linear relationship in which the slope of the line is approximately 2 for both acid systems (HCl and HNO_3) (**Figure 25**). In HNO_3, it can be demonstrated that under these conditions the Pa extraction into the organic phase occurs via a 2:1 interaction with the extractant. This conclusion is supported by Kumari *et. al.* (2012) who observed a similar relationship and concluded that the organic phase nitrato-species is likely the $[Pa(OH)_2(NO_3)_4]^-$ anion with a protonated $[H(ROH)_{1\text{-}2}]^+$, thus suggesting an electrostatic interaction.[13] In HCl, we also observed a 2:1 stoichiometric relationship that can be attributed to a 2,6-dimethyl-4-heptanol complex with the Pa-chloro species. Yet, from these experiments the interaction between Pa and the alcohol is not definitively determined. Within this context, if the interaction with the Pa complex anion is driven by an electrostatic interaction with a

protonated alcohol cation, we would expect other actinides (*i.e.* U) to be extracted when the acid concentration is sufficiently high to form an actinyl nitrato or chloro (*i.e.* uranyl nitrato or chloro) anion. For the experiments in the present study, the goal was to establish a qualitative approximation to the average equilibrium stoichiometry of extractant to Pa at trace concentrations; results suggest a 2:1 relationship in both HNO_3 and HCl. Future studies will seek to further probe into the coordination of the ligands around Pa by increasing concentrations of Pa to approach the limiting organic concentration to further probe into the coordination of the ligands around Pa.

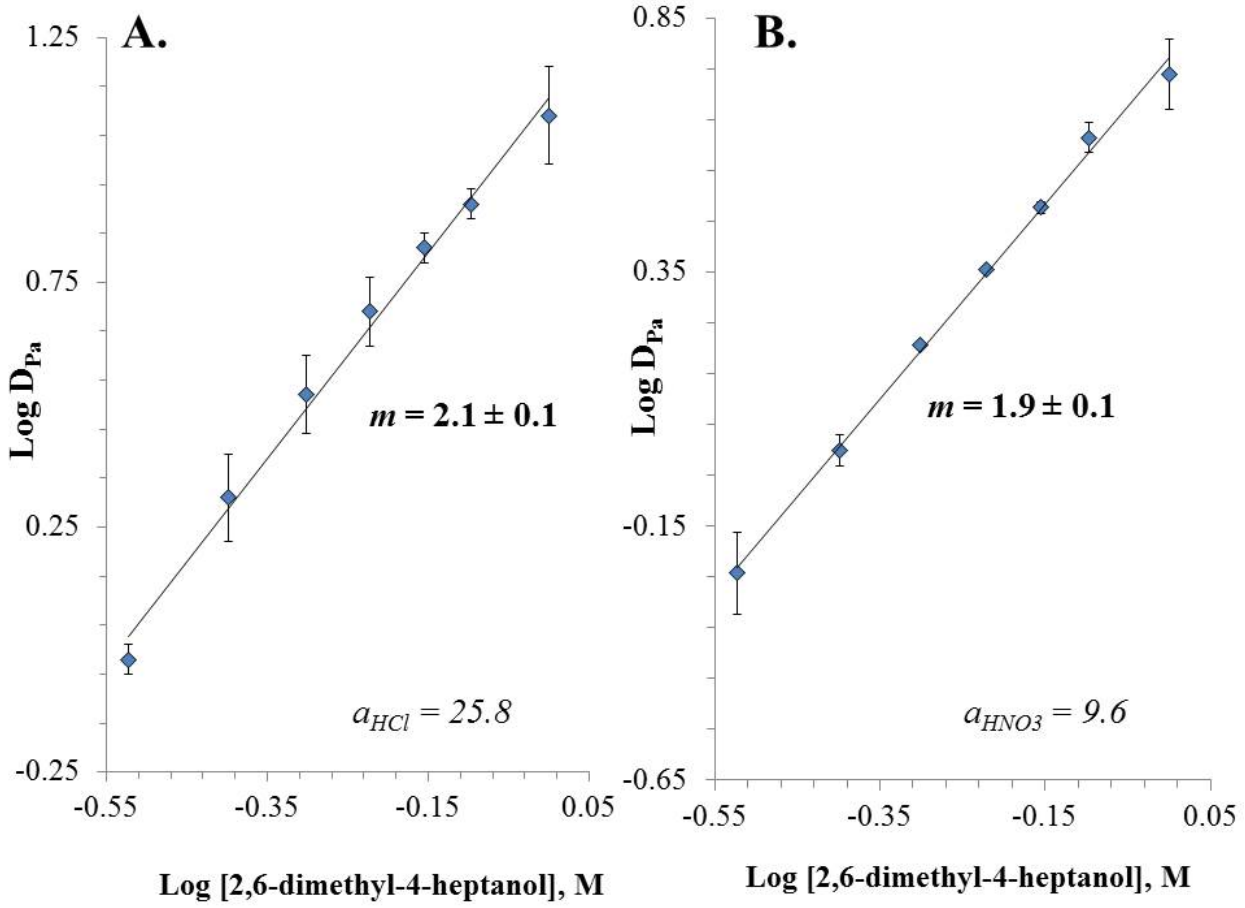

Figure 25. Log-Log plots of D versus the concentration of 2,6-dimethyl-4-heptanol. (A). The relationship between the distribution of Pa and the concentration of the extractant in HCl. Pa. (B). The relationship between 2,6-dimethyl-4-heptanol and Pa in HNO_3.

We investigated the relationship between Pa and the A^- (Cl^- and NO_3^-) at different concentrations of H^+ – while maintaining a constant concentration of 2,6-dimethyl-4-heptanol (2.5 M) in dodecane. The results from these experiments are summarized in **Figure 26** where $Log(D_{Pa})$ is plotted versus Log a_{anion}. In chloride form (**Figure 26a**), extractions were performed at $[H^+]$ = 0.1, 1 and 4 M. When $[H^+]$ = 0.1 M, Pa extraction was poor, yet a linear relationship was observed, where the slope represents an approximation to the average stoichiometry of Cl^- to Pa (m = 3.5 ± 0.5). As the solution acidity increases, both the extraction of Pa into the aqueous phase and the stoichiometric relationship of Cl^- increases from nearly 4 when $[H^+]$ = 0.1 M to nearly 6 when $[H^+]$ = 1 and 4. From this plot, it can be observed that Pa extraction at 4 M Cl^- forms a hexacoordinate Pa-chloro species and is readily extracted, however, in 1 M Cl^- a similar species is observed but extraction is poor. This suggests that the solution acidity plays a major role in the extraction of Pa from chloride solutions. We can postulate further regarding the Pa-chloro species based upon the understanding that extracted metals (*i.e.* gold) by alcohols and ketone are generally in the form of a single charged anion charge balanced by a solvated proton through a hydrate solvate mechanism.[121] Therefore, a hexa-coordinated Pa-chloro species is not likely to exist as $PaOCl_6^{3-}$, but rather, the O^{2-} is more labile than that of common actinyl cations, and forms a $PaCl_6^-$ complex anion charge balanced with a solvated proton. The strength of the Pa-O bond in the PaO^{3+}, has been shown to be labile in the presence of halide ions (*i.e.* F^-, Cl^-).[74, 122]

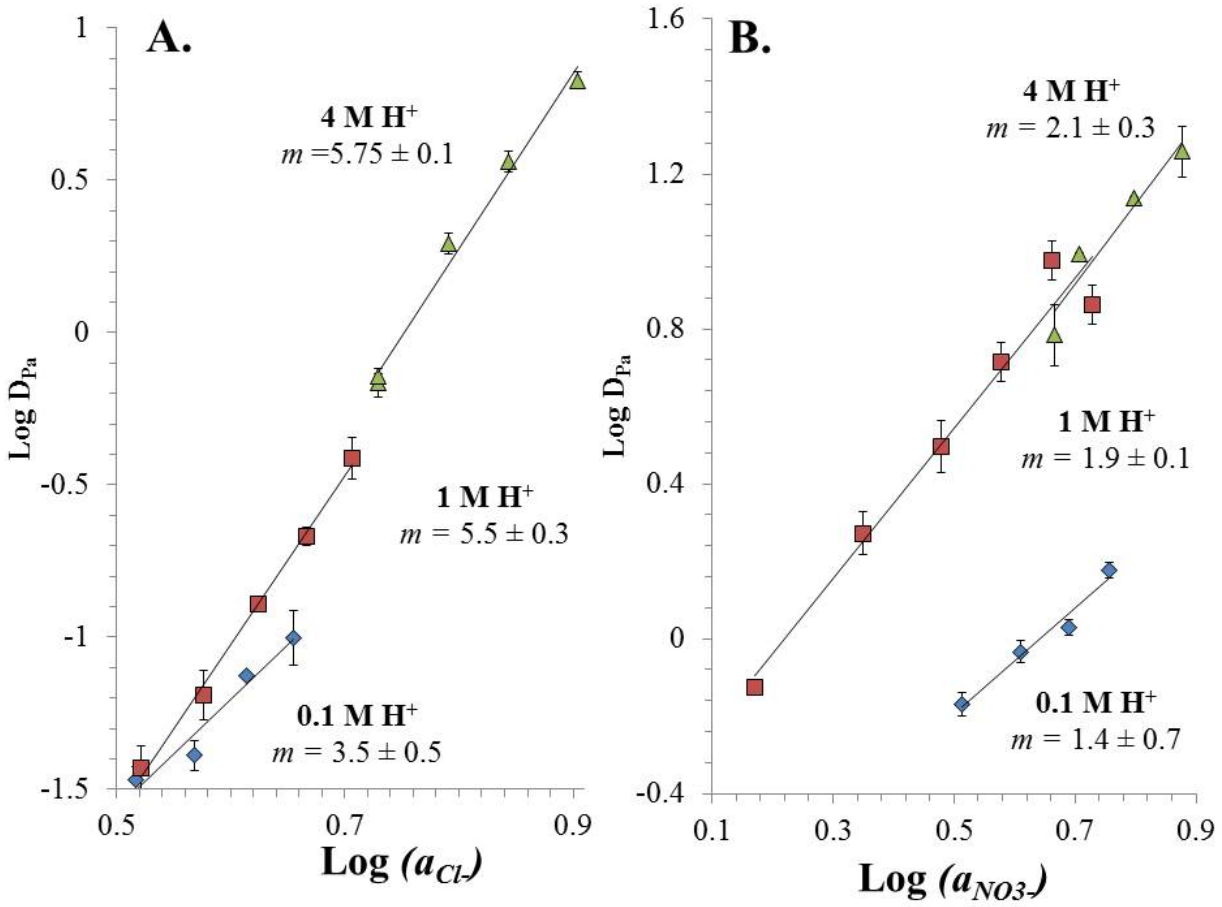

Figure 26. Log-Log plots of D versus the anion activity when the [2,6-dimethyl-4-heptanol] = 2.5 M. (A). The relationship between the distribution of Pa and the a_{Cl^-}. (B). A plot of Log D_{Pa} versus Log a_{NO3^-}.The $[H^+]$ was determined from adding HCl or HNO_3 and the adjustment of the anion activity was made through the addition of NaCl or $NaNO_3$.

In nitrate form, the same solvent extraction experiments at $[H^+]$ = 0.1, 1 and 4 M. At low acidity $[H^+]$= 0.1 M the extraction of Pa was relatively ineffective, but a linear relationship was established and the stoichiometry appears to be on average 1.35 nitrate anions per Pa cation. As the acidity increases to 1 M and 4 M H^+, the extraction of Pa improves, which is reflected in an increase in the Log D_{Pa}. Likewise, as the $[NO_3^-]$ increases, the D_{Pa} increases. It is interesting to note, that the linear relationship between Log D_{Pa} and Log a_{HNO3} remains relatively constant with an average of 2 from $[H^+]$ = 1 - 4 M. Literature suggests that Pa-nitrato species are mainly present as hydroxy-

nitrato complexes and take on the general form of $Pa(OH)_x(NO_3)_y^{5-x-y}$, where $x + y \leq 8$, the coordination capacity of Pa.[2] From these experiments it is unknown whether or not NO_3^- coordinates to the central Pa metal in a monodentate or bidentate fashion. Future experiments aim to establish an understanding of the Pa coordination chemistry in the organic phase of solvent extraction systems.

Table 6. Average stoichiometric coefficients of the extractant (DIBC) and anions (Cl^- and NO_3^-) obtained from the slope of the log-log plots

Form	Extractant	Anion (0.1 M H^+)	Anion (1 M H^+)	Anion (4 M H^+)
HCl	2.1 ± 0.1	3.5 ± 0.5	5.5 ± 0.3	5.75 ± 0.1
HNO_3	1.9 ± 0.1	1.4 ± 0.7	1.9 ± 0.1	2.1 ± 0.3

From these experiments, we have established an average stoichiometric approximation to better understand the interaction between Pa with 2,6-dimethyl-4-heptanol and A^- (Cl^- or NO_3^-) (**Table 6**). This information provides a deeper understanding of the extraction process but this methodology does not allow us to identify the speciation of the O-containing ligands (*i.e.* O^{2-}, OH^-, OH_2) or the coordination mode of the alcohol. Although speciation and coordination of oxygen species can be identified via spectroscopy, the concentration of Pa must be dramatically increased to levels that are unattainable to most academic research groups. Herein we have provided a framework for future studies to further our understanding of Pa complex formation and speciation.

5.4.2. Extraction Chromatography with Alcohol Containing Resins

The acid dependency information for each extraction chromatographic resin containing 1-octanol, 2-ethyl-hexanol, or 2,6-dimethyl-4-heptanol was performed to determine the k' values of Pa and the other actinides. This information can assist development of rapid methods for the extraction and purification of Pa from complex matrices for environmental analysis or nuclear

forensics. The results from our experiments are shown with respect to a_{HCl} and a_{HNO3} (**Figure 27; Figure 28; Equation 33; Equation 34**). The k' profile of Pa adsorption onto the resins versus acid concentration of a_{HCl} and a_{HNO3} shares the same trend among all the resins in both HCl and HNO_3 (**Figure 27**). These observed variations in the k' values generally reflect the differences in the alcohol densities, which are used to convert D to k'. Similar to the previously described solvent extraction experiments, these results suggest that the chain length and alcohol substitution does not affect the adsorption of Pa. Unexpectedly, we observe a decrease in k' in 9 M HCl for 1-octanol, which we attribute to the extraction reagent (1-octanol) eluting from the column or competition between extraction of the metal anion with the acid, thus decreasing the capacity of the adsorption.[25, 121]

All other actinide elements (Th, U, Pa, Np, Am) were analyzed for their acid dependencies with a resin form of 2,6-dimethyl-4-heptanol in trace level experiments. The analysis of the adsorption behavior of the other actinide elements onto the 2,6-dimethyl-4-heptanol resin resulted in poor adsorption. This conclusion was reflected in low k' values in both HCl and HNO_3 forms (**Figure 28**). These actinides elements generally follow demonstrate a slight increase in adsorption in higher acid activities . Despite this slight increase in adsorption, Pa can be easily separated from actinides (Th, U, Np, Am) in higher acidities due to exceptionally high k' values. Consistent with this observation, we have previously reported Pa and Np can be separated with a high level of radiochemical purity using a 1-octanol based resin,[101] and now **Figure 28** provides the information needed to sequester Pa from matrices containing actinide interferences from Th, U, Np, or Am.

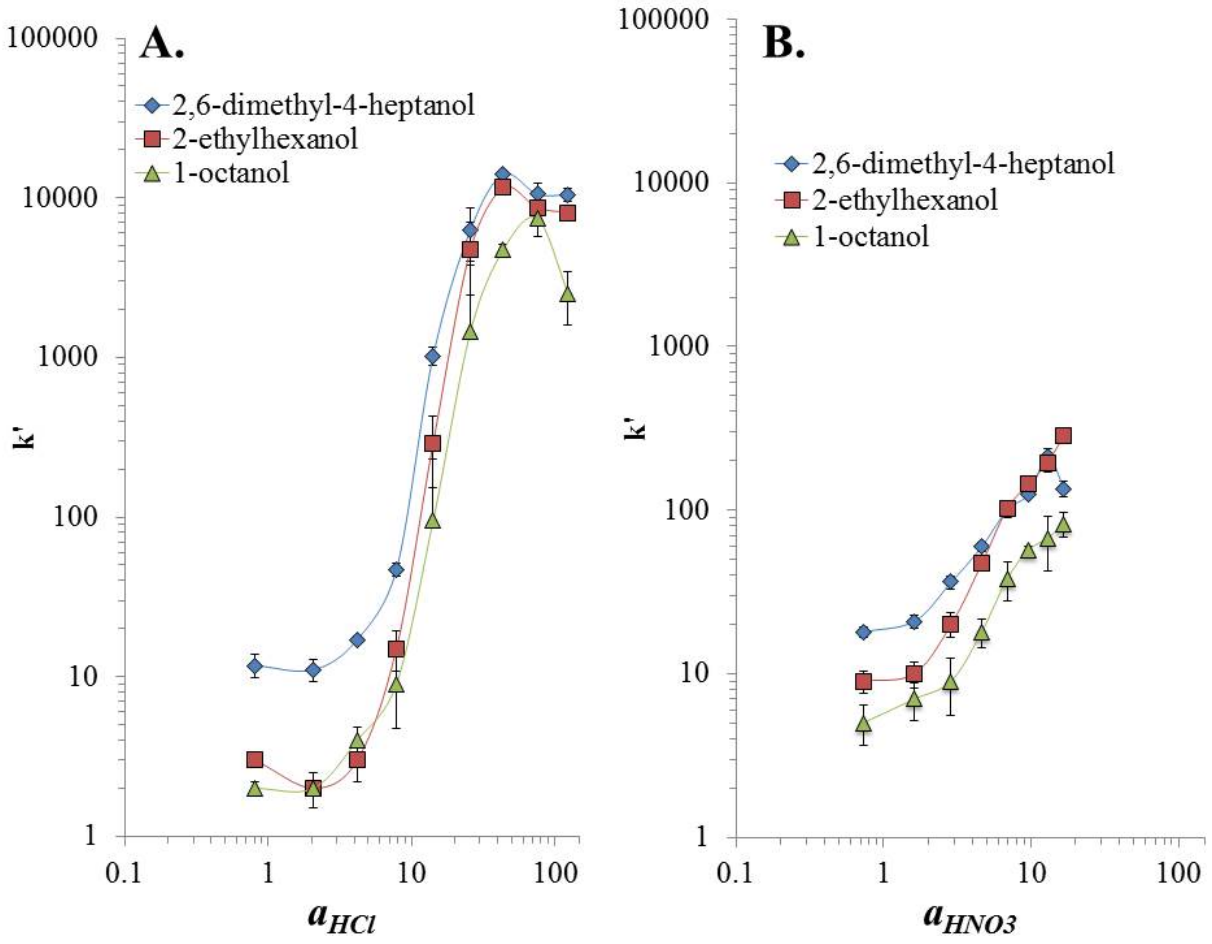

Figure 27. The k' values of Pa by 2,6-dimethyl-4-heptanol, 2-ethylhexanol, and 1-octanol extraction chromatographic resins as function of the activity of HCl (A) and HNO_3 (B).

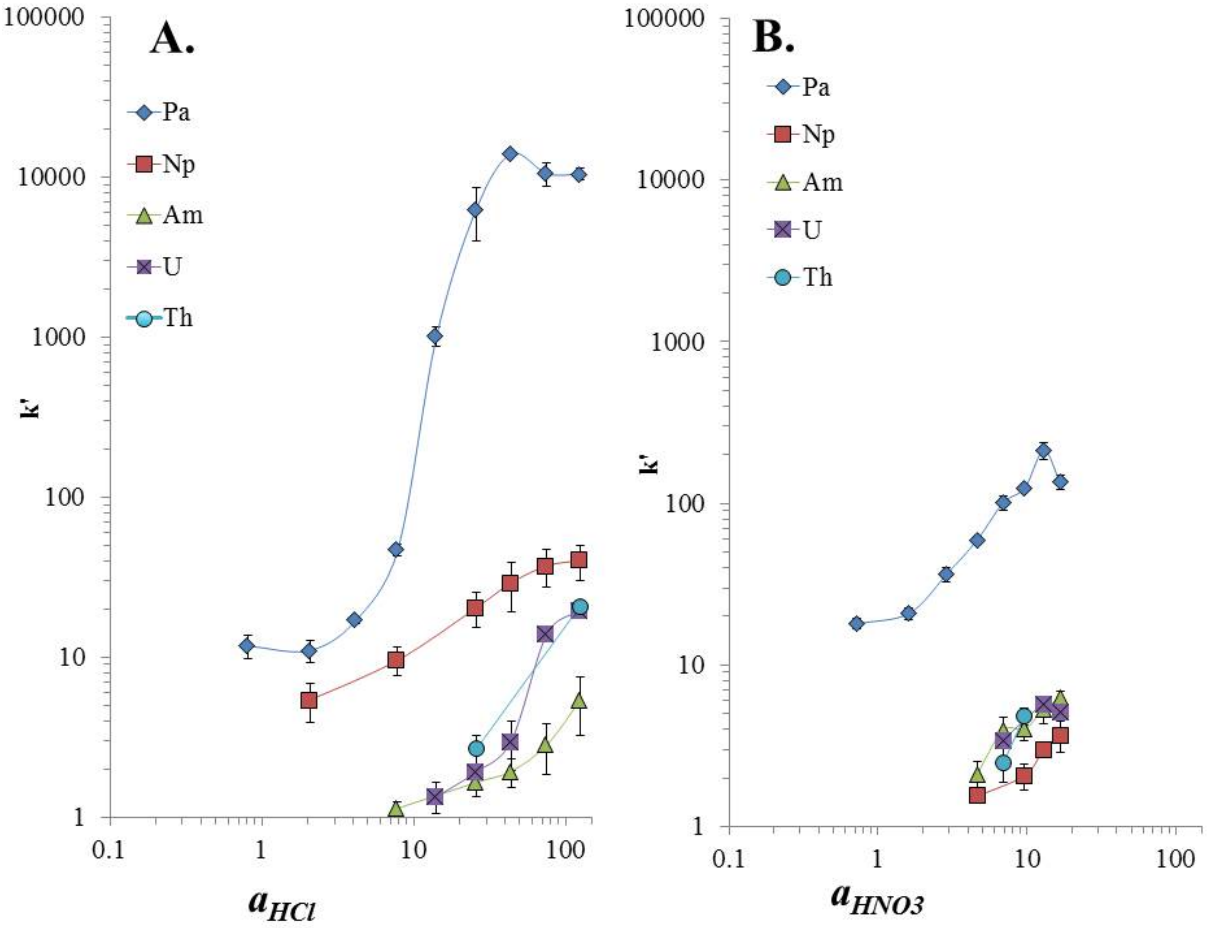

Figure 28. The k' values of the early actinides Th, Pa, U, Np, and Am by 2,6-dimethyl-4-heptanol in the solid resin form as function of the activity of HCl (A) and HNO_3 (B).

5.5. Conclusion

In this study, we have presented the extraction behavior of the actinide elements (Th, Pa, U, Np, Am) by aliphatic alcohols (1-octanol, 2-ethyl-hexanol, and 2,6-dimethyl-4-heptanol) under acidic conditions (HNO_3 and HCl). Our findings highlight the unique chemistry of Pa with respect to the other actinides. For example, we find that Pa is the only extractable actinide under highly acidic conditions in the HNO_3 and HCl systems. Thus, our results reveal numerous potential separation and purification avenues for isolating Pa from complex matrices in HNO_3 and HCl media. We further used the extraction results to estimate stoichiometric relationships of Pa with respect to the

alcohol and the anion. These interpretations (in HCl and HNO_3), suggest that the alcohol forms a 2:1 complex with Pa, which is likely charge balanced by a solvated proton. The extractable 2:1 nitrate:Pa complex was found to form when the $[H^+] \geq 1$ M. On the other hand, in the chloride form, our results suggest that the Cl:Pa complex exists in a 6:1 extractable chloro-species ($[H^+] \geq 1$ M).

These results of these experiments further our understanding of the chemistry of Pa at trace levels. In addition, our results suggest several new separation and purification pathways (via acid dependency charts for liquid-liquid and extraction chromatographic systems) that can be used for Pa analysis for nuclear forensics, geochronology, or other Pa analysis challenges.

5.6. Associated Content

Notes: The authors declare no conflict of interest.

Acknowledgments: The authors extend sincere thanks to Eichrom Technologies, Inc. for kindly supplying resin materials. This manuscript is based upon work supported by the U.S. Department of Homeland Security under Grant Award Number, 2012-DN-130-NF0001-02. The views and conclusions contained in this document are those of the authors and should not be interpreted as necessarily representing the official policies, either expressed or implied, of the U.S. Department of Homeland Security. Further support was provided by the US Nuclear Regulatory Commission, US NRC-HQ-12-G-38-0041.

CHAPTER VI: DO ALIPHATIC ALCOHOLS BEHAVE AS SURFACTANTS IN DODECANE-WATER SYSTEMS?

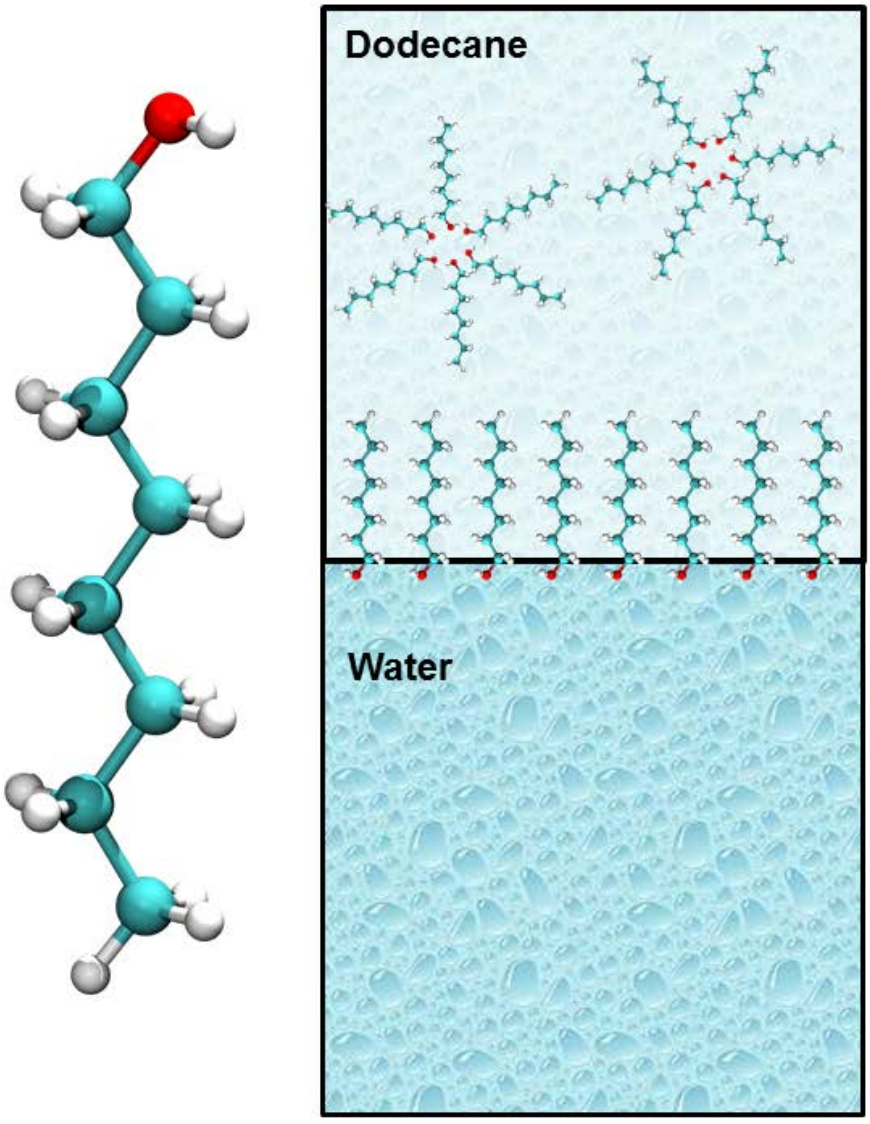

6.1. Abstract

Recently reported nano-domains in "surfactant-free" octanol-ethanol-water mixtures – where octanol is considered an oil – have challenged traditional microemulsion definitions. Here we examine the interfacial and self-assembling properties of 1-octanol and structural isomer, 2-ethyl-hexanol, in a biphasic dodecane-water system, through converging atomistic molecular dynamic simulations with synchrotron X-ray scattering and physical measurements. Organic phase aggregates emerge in dodecane at elevated alcohol concentrations, which coincides with the rapid uptake of water. The observed aggregate structure is dependent on the alcohol tail-group geometry -- consistent with surfactant packing parameter. Furthermore, physical properties such as decreasing surface tension in a surfactant-like manner, although lacking a pronounced critical micelle point, necessitate a new look at the solution energetics that lead to the formation of these aggregates. We propose a new chemical equilibrium for the formation of these aggregates in alcohol-bearing solutions of dodecane and water, which may help explain the occurrence of the nano-structural domains. Our results show that, in biphasic dodecane-water systems, aliphatic alcohols share many characteristics with lipophilic surfactants, blurring the definitions of 'polar oil' and 'surfactant amphiphile'.

Keywords: Surfactant, Reverse-Micelles, SAXS, Molecular Dynamics, 1-octanol, 2-ethyl-hexanol

6.2. Introduction

Structured fluids, consisting of large polyatomic structures, are a broad class of liquids that exhibit a variety of mechanical responses and self-organization.[123] While these solutions range in physical properties (*i.e.* viscosity), advanced spectroscopic methods have provided insight into their complex micro and nano-scopic behavior and ordering. A major class of structured fluids is called surfactants, or substances, when present at low concentration in a system, have the ability of adsorbing onto the surface or interface of a system to minimizing surface or interfacial free energies and contain two components; a hydrophilic headgroup and hydrophobic tail group. [123, 124]

Surfactants are unqiue because of their ability to minimize the energy in solution by forming micelles, or a molecular configuration in which the immiscible compents cluster together and are sheilding by the immiscible component so to create distinct hydrophobic and hydrophilic nanoscale domains.[123] The formation of micelles in solution is a thermodynamically driven process, which aims to minimize the overall energy of the system at equilibiurm. Because of this distintive property, the oil-water interface is an favorable environement for surfactants to exists. As a result, surfactant molecules will arrange along the interface and decrease the overal surface or interfacial tension to the point at which a microemulsion forms.[123]

Microemulsions are thermodynamically stable nanoscale domains of oil and water that coexist and traditionally require a surfactant to minimize the interfacial energy.[123, 125] Applications of microemulsions are abundant and span from uses in food additives to nanoparticle synthesis, and recently advanced spectroscopy has led for a better understanding of their micro and nano-scopic ordering.[125-127] However, recent reports of microemulsions forming in the absence of conventional surfactants have challenged this notion, where unprecedented large lipophilic-hydrophilic nano-domains have been observed in octanol-water-ethanol mixtures.[128-130] These mixtures are sometimes referred to as "surfactant-free microemulsions" and have spawned several impactful papers concerned with understanding the energetics of nano-domain formation in such systems.[128-130]

Octanol (and other lipophilic alcohols) are amphiphilic molecules; however, these molecules are not considered to be conventional surfactants in aqueous solutions.[130] This is because lipophilic alcohols do not fulfill the requirements of a micelle forming surfactant as it is suggested that a single hydroxyl headgroup is not sufficiently polar.[130] As a result lipophilic alcohols are considered to be hydrotropes or co-surfactants in aqueous solutions and generally aid in the solubilization of surfactants.[130, 131] While the role of these alcohols as hydrotropes is unequivocal,[131] their surfactant-like behavior is unsettled.[128-130] It has been observed on a molecular level, in solutions consisting of 1-octanol and water, 1-octanol arranges into living polymers in a 3D mesh,[132, 133] and upon the addition of ethanol, the 1-octanol molecules form unique nano-domains

described as being "loose agglomeration of more than one aggregate".[129] It has also been concluded that these large, diffuse agglomerations of aggregates are dynamic, relatively short lived, and comprised on numerous smaller, stable aggregates.[129] Further, these authors observed an influence of the packing parameter on the morphology, similar to the behavior of classical surfactants, producing aggregates that diverge from perfectly spherical governed by the tail-group geometry.[129]

In organic solutions, vibrational spectroscopic studies of octanol-solvent systems have found significant degrees of self-association from dimers to more complex structures.[134] Such structures form through hydrogen bonding interactions, evidenced by monitoring the OH-stretching frequencies.[134, 135] In solutions of decane, 1-octanol molecules are arranged into cyclic-tetramer aggregates strongly associated through hydrogen bonding.[135] Hydrogen bonding interactions are understood to underpin the assembly of surfactants into micelles to form microemulsions in water/oil systems, as stated in foundational studies.[136, 137] Therefore, we aimed to probe the interface of solutions containing dodecane, water and alcohols (1-octanol and 2-ethyl-hexanol) to establish a better understanding of the driving forces that result in these large, distinct hydrophilic and hydrophobic regions. Additionally, we sought to develop an understanding of the molecular organization of the alcohols that drives the formation of a thermodynamically stable microemulsion.

In this study, we investigated 1-octanol and 2-ethyl-hexanol in biphasic systems consisting of a lipophilic oil (dodecane) and water. The interfacial and bulk properties of these systems were investigated using a combination of physical measurements, synchrotron small angle X-ray scattering (SAXS), and atomistic molecular dynamic (MD) simulations.[138, 139] The results presented in this manuscript supplement recent reports and provide a detailed account of the occurrence of nano-scale domains formed in the organic phase of oil/water systems containing an alcohol. We also provide further discussion of the chemical equilibration necessary for understanding the energetics of aggregate formation involving alcohols 1-octanol and 2-ethyl-hexanol in solutions of water and dodecane.[129]

6.3. Experimental Section

6.3.1. Biphasic Systems

The organic solutions used in these studies consisted of 1-octanol and 2-ethyl-hexanol at a range of concentration (0.1 mM to pure alcohol) dissolved in dodecane. The organic reagents, dodecane, 1-octanol and 2-ethyl-hexanol were purchased from Sigma Aldrich (St. Louis, MO). The organic solutions were mixed *via* shaker table with distilled deionized water, in equal 0.5 mL volumes, for 15 minutes. Following the mixing stage, the aqueous and organic phases were separated via centrifugation and subsequently removed and stored in a separate glass vials. Each solution was analyzed by Karl Fisher titration, tensiometry, and corroborated with SAXS and atomistic MD simulations.

6.3.2. Titrations

The Karl Fischer titration method was used to determine the concentration of water transferred into the organic phase after mixing and equilibration.[140] The apparatus used in these experiments was an 831 KF Coulometer (Metrohm AG, Switzerland). To measure the equilibrium concentration of water in the organic phase, a known mass of the organic solution (following contact with water) was injected into the Karl Fisher apparatus and titration was initiated at the time of injection. This method provides a concentration of water in parts-per-million (ppm). To determine the water concentration in molarity, the equilibrium organic phase densities were measured, and used to convert ppm to molarity.

6.3.3. Small Angle X-Ray Scattering (SAXS)

Following mixing, equilibration, and phase separation, the organic solutions were transferred to the Advanced Photon Source (Argonne National Laboratory) at the beamline 12-ID-C to be analyzed by SAXS. Data were obtained by injecting the organic phases through a flow cell at a fixed distance from the detector. Sample-to-detector distance was adjusted to provide a detecting range for momentum transfer of $0.04 < q(Å^{-1}) < 2.41$. The scattering vector, q, was calibrated using

a silver behenate standard and incident photon energy 19.0 keV, providing sufficient X-ray transmittance for the data acquisition. Scattering profiles were obtained via 0.5 second exposure times with a MAR 165 CCD detector (Norderstedt, Germany), with a 165 mm diameter active area and resolution of 2048 x 2048 pixels. The 2D scattering images were corrected for spatial distortion and detector sensitivity, then radially averaged to produce plots of scattered intensity, I(q) versus q. The I(q) data were normalized on an absolute scale (cm^{-1}) by calibration with deionized water, and after a thorough background subtraction consisting of just the diluent, dodecane. SAXS data were collected at various concentrations of alcohol (1-octanol and 2-ethyl-hexanol) in dodecane ranging from 0.1 mM to 2 M, with the assumption that the signal recorded at 0.1 mM corresponds to the monomers contribution. Background subtracted and normalized SAXS data were interpreted using the Percus-Yevick interacting sphere model. [141]

6.3.4. Interfacial Tension Measurements

To measure the interfacial tension between the organic and aqueous phases, a Drop Shape Analyzer DSA 100 Krüs tensiometer coupled with a high-speed ½'' CCD sensor camera and DSA4 software. Following the contact with water, organic solutions were loaded into a 5 mL deposable syringe equipped with a reverse pendant drop hook. The syringe was placed onto a mechanical arm with an injection pump and slowly immersed into a cuvette containing water to create the organic/aqueous phase interface, which was centered in the sight of the camera. The camera was focused and magnification scale was determined, then a drop was partially dispensed from the syringe. The software extracted the bubble outline and the drop was equilibrated for 30 minutes. The shape and volume of the drop was analyzed with the DSA4 software and the mass (m) was determined using the known density of the organic solution.[142] From this experiment interfacial tension was calculated *via* **Equation 25**:

$$\gamma = \frac{m * g}{2\pi * r} \qquad eq.25$$

where γ is the interfacial tension, *m* is the mass of the drop, *g* is gravity, and *r* is the radius of the tip of the syringe hook.

6.3.5. Molecular Dynamics

Classical MD simulations were performed at the all-atoms resolutions by means of the package GROMACS 4.5.5.[143] The CHARMM General Force Field (CGenFF 3.0.1) was utilized along with the recommended TIP3P water model.[144, 145] For aggregation behavior in organic solution, two alcohol systems were investigated composed of either 1-octanol or 2-ethyl-hexanol. For each system, the alcohol concentrations were simulated at 0.5 M and 2 M and the concentration of water molecules was set to mimic the experimental values from Karl Fischer titration. See **Table 10**; **Table 11** in the **Appendix B** for the detailed concentrations and number of components.

The initial structures of the simulations were built using the package Packmol,[146] where all the molecules are randomly distributed (**Figure 32**). These structures were subjected to energy minimizations and annealing simulations to speed up the aggregation behavior.[137, 139, 142, 147] In the annealing simulation, the system temperature increased from 298 K to 360 K in the duration of 0.1 ns, maintained at 360 K for 0.8 ns, and then was cooled down to 298 K within 0.1 ns. The temperature was maintained at 298 K for another 2 ns. The annealing simulation was repeated four times for each system. During the annealing simulations, the system density, the potential energy, and the radial distribution function (RDF) between the alcohol oxygen atoms was calculated to justify the convergence of the aggregation behavior (**Figure 32**).

In the production simulations, the isothermal-isobaric ensemble (constant number of particles, temperature, and pressure) was employed. The reference temperature of 298 K was employed using the Nosé-Hoover algorithm[148] with the relaxation time of 0.5 ps. The system pressure was coupled to 1 bar using the Parrinollo-Rahman algorithm[149] with the compressibility of 44.6×10^{6} bar^{-1} and the relaxation time of 4 ps. The three-dimensional periodic boundary conditions were employed and the short-range Coulomb and van der Waals interactions were both calculated up to 1.2 nm. Long-range Coulomb interactions were included using the smooth Particle Mesh

Ewald method,[150, 151] in addition to the long-range dispersion correction for energy and pressure. All valent bonds were constrained by means of LINCS algorithm, which supported the stable simulations with an integration time of 2 femtoseconds.[152, 153] Each simulation was performed for 50 ns, with a saving frequency of 10 ps per frame to collect the simulation trajectory.

6.4. Results

6.4.1. Extraction of H_2O into Dodecane

In these ternary, biphasic solutions containing structural isomers 1-octanol or 2-ethyl-hexanol in dodecane contacted with water, we observe a rapid increase in the concentration of water into the organic phase as the alcohol concentration is increased **(Figure 29).** As a general trend when the alcohol concentration is less than 1 M, relatively little water is extracted into dodecane. For instance, the equilibrium $[H_2O]_{org.}$ = 0.02 ± 0.02 M when [1-octanol or 2-ethyl-hexanol] = 0.5 M. However, when the concentration of alcohol is increased above 1 M, there is an exponential increase in the extraction of water as evidenced by log-log plot (**Figure 29 inset**). At equilibrium, 1-octanol extracts nearly twice amount of water as 2-ethyl-hexano1 does ($[H_2O]_{org.}$= 1.62 ± 0.04 M and 0.92 ± 0.06 M for 1-octanol and 2-ethyl-hexanol, respectively when [alcohol] = 5 M). The extraction of water into an organic phase can be an indication that nano-structural polar domains exist in the organic phase through the formation of reverse micelles. Conventional surfactant molecules aggregate to form micelles, which generally solvate pools of water in the otherwise immiscible organic phase. [154]

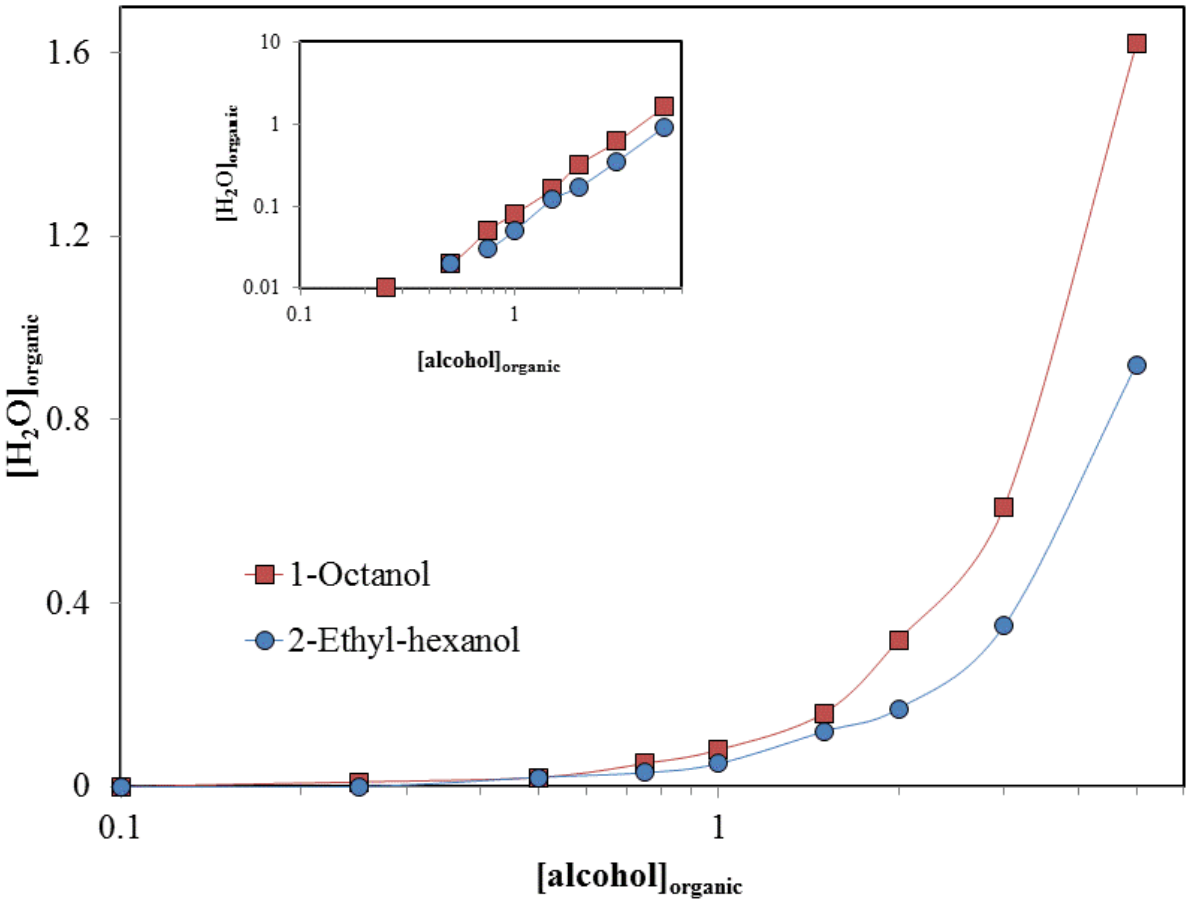

Figure 29. Equilibrium concentration (M) of H_2O extracted into the organic phase as a function of the initial alcohol concentration (M). Inset shows the data plotted on a log scale to verify the exponential increase of water.

6.4.2. Small Angle X-ray Scattering

SAXS data obtained from the organic phases of each biphasic system demonstrate the formation of aggregates at concentrations consistent with the observed increase in water extracted into the organic phases. Samples with a range of concentrations (0.1 mM, 0.1 M, 0.5 M and 2 M) of 1-octanol and 2-ethyl-hexanol were analyzed. However, only measured samples containing 0.5 and 2 M alcohol generated a scattering pattern that suggested aggregation. Experimental data show the presence of a scattering peak in the high *q*-region at approximately 1.4 $Å^{-1}$ **(Figure 30)**, which is identified as a correlation peak between hydrocarbon atoms.[139, 142] Long-range correlation peaks in

the low *q*-region were observed in systems containing 0.5 M and 2 M alcohol -- though very weak signals in 0.5 M systems in this region. While both 1-octanol and 2-ethyl-hexanol produced aggregates in these systems, the aggregates formed differed as indicated by their scattering pattern in the low *q*-region. In the 2-ethyl-hexanol systems, a correlation peak is observed at around 0.5 $Å^{-1}$, while in 1-octanol a small broad peak is observed around 0.4 $Å^{-1}$.

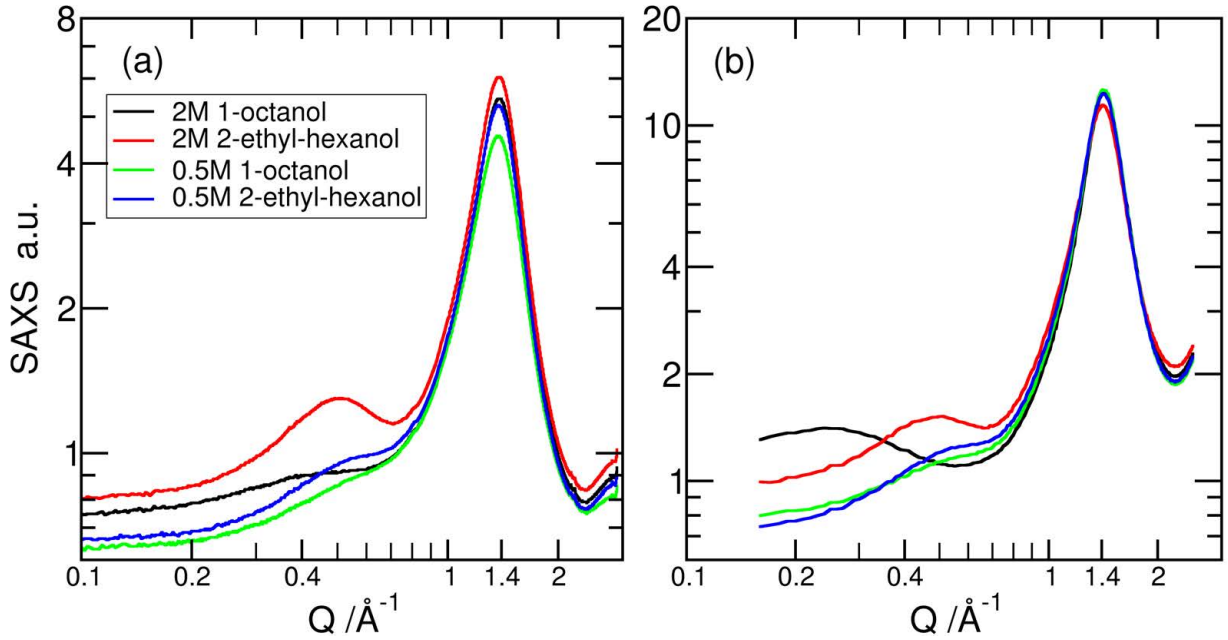

Figure 30. (A) Experimental and (B) simulated SAXS data of the four systems. A solvent peak is observed in the high *q*-region at approximately 1.4 Å^{-1}, identified as a correlation peak between hydrocarbon atoms.[139, 142] Long-range correlation peaks in the low *q*-region were observed in systems containing 0.5 M and 2 M alcohol. In the 2-ethyl-hexanol systems, (blue and red lines) a correlation peak is observed at around 0.5 Å^{-1}, while in 1-octanol (green and black lines) a small broad peak is observed around 0.4 Å^{-1} when the [1-octanol] = 2.

Table 7. Fitting Parameters of the Percus-Yevick Fit of the SAXS Data at 2 M Alcohol.

Fitting Parameter	**1-octanol**	**2-ethyl-hexanol**
Sphere Radius	5.5 ± 0.3 Å	4.16 ± 0.04 Å
Interaction Radius	6.4 ± 0.1 Å	5.58 ± 0.02 Å
Volume Fraction	0.11 ± 0.01	0.204 ± 0.003
[a]Reduced χ^2	0.122	0.351

[a] Generally it is considered that reduced χ^2 values significantly less than 1 are a result of overfitting data. In this case, we observe small χ^2 values largely as result of a small signal to noise ratio in the high-*q* region ($Q/(A^{-1}) > 0.55$), from background subtracting hydrocarbon interactions. The observed noise is small variations in the scattering of hydrocarbons among different measurements. Conclusions regarding aggregations are made from observation in the low *q*-region.

The Percus-Yevick interaction sphere model was used to evaluate the SAXS data (**Figure 31)**.[141] For this analysis, a robust background subtraction was performed so that only scattering from the oxygen atoms (alcohol and water) were fit to the model. Consequently, only samples with a concentration of 2 M produced a signal strong enough to show the presence of aggregates following the robust background subtraction. The Percus-Yevick fitting parameters include scale factor, sphere radius, interaction radius, volume fraction, and reduced χ^2 **(Table 7, Figure 41)**. These parameters help describe the form factor and structure factor of the aggregates in solutions. The sphere radius quantifies the average size of an individual aggregate core, and was determined to be 5.5 ± 0.3 Å for 1-octanol and 4.17 ± 0.04 Å for 2-ethyl-hexanol. The interaction radius quantifies the core-to-core distances of the aggregates, and was determined to be 6.4 ± 0.1 Å and 5.58 ± 0.02 Å for 1-octanol and 2-ethyl-hexanol, respectively. The difference between the sphere radius and interaction radius values signifies the minimum distance the aggregates can exist (**Equation 26**).

$$Distance\ between\ adjacent\ clusters = interaction\ radius - \ sphere\ radius \quad eq. 26$$

The widths of these non-contact regions are approximately 0.9 Å and 1.42 Å, for 1-octanol and 2-ethyl-hexanol, respectively. The total volume fraction of the aggregates (including water but

not including the monomers) is the scattering volume headgroup that is taken up by all of the aggregates, was determined to be 0.11 ± 0.01 and 0.204 ± 0.003 for 1-octanol and 2-ethyl-hexanol, respectively. The monomer concentration is excluded simply because monomers do not participate in aggregation. Instead, the monomers will contribute to the flat background scattering intensity. The SAXS region intensity is dominated by the aggregate particles because they have the nanometer sized cross sections necessary to produce a signal in these regions. Therefore, the model only includes the molecules that are involved in the aggregate and not those that are not (*i.e.* monomers). It is important to note that the Percus-Yevick interaction sphere model does not require the spherical aggregates, non-spherical cylindrical have been sufficiently described by this model previously.[155]

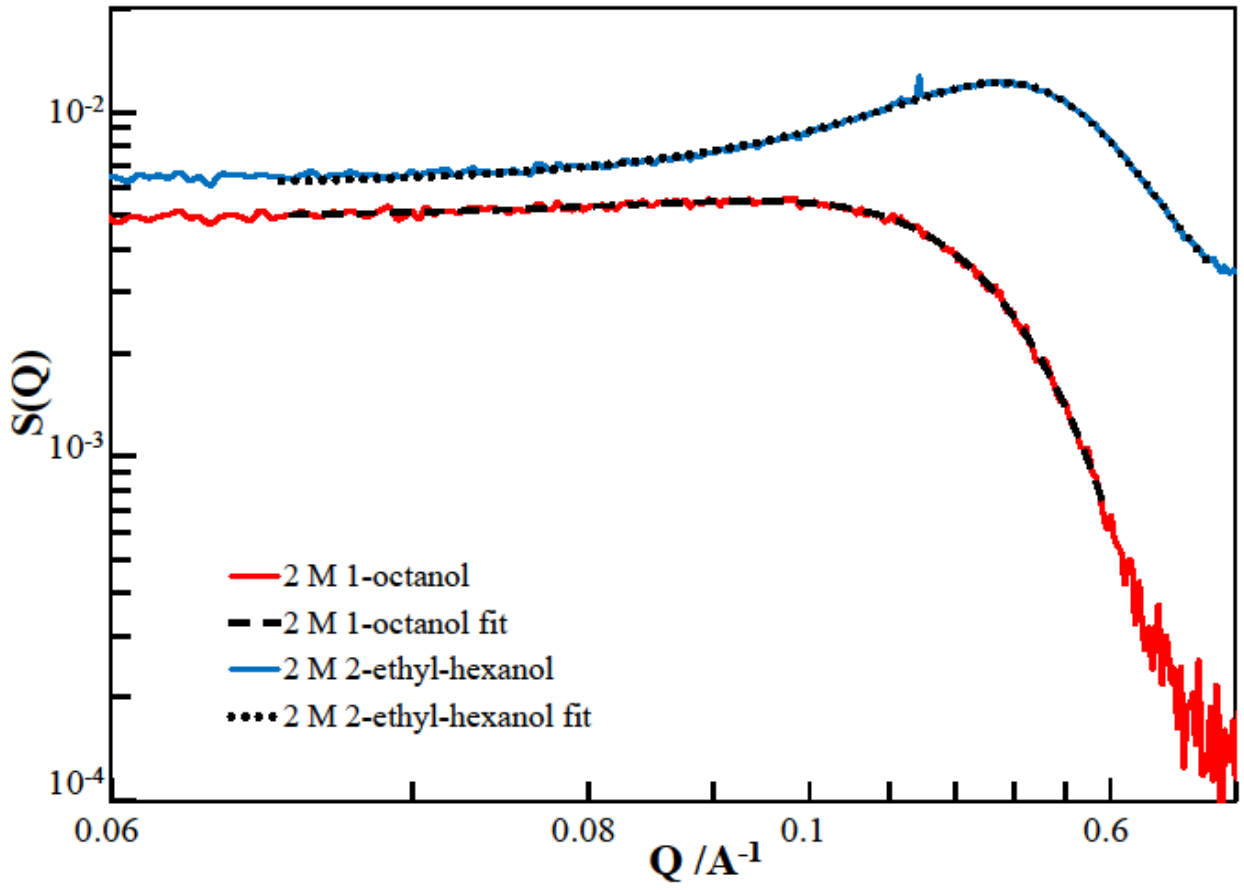

Figure 31. SAXS spectra of the organic phases consisting of 2 M 2-Ethyl-hexanol (blue line) and 2 M 1-Octanol (red line). The background scattering are subtracted from air, the sample holder, and the solvent of dodecane. The dashed and dotted lines represent a spectra fitting based upon Percus-Yevick model.

6.4.3. Tensiometry

The behavior of 1-octanol and 2-ethyl-hexanol at the water-dodecane interface was investigated *via* tensiometry. It was determined that the interfacial tension (σ) at the water-dodecane interface decreased as a function of the increased concentration of the alcohols (1-octanol or 2-ethyl-hexanol) (**Figure 32)**. The interfacial tension in 1-octanol decreased from 24.3 ± 2.1 mN/m (0.5 mM) to 7.7 ± 0.4 mN/m (pure 1-octanol). The interfacial tension in 2-ethyl-hexanol decreased from 25.3 ± 1.2 (0.5 mM) to 13.1 ± 0.5 mN/m (pure 2-ethyl-hexanol). A plot of σ versus the ln[alcohol] of 1-octanol and 2-ethyl-hexanol was fit to the equations y = - 1.99x + 12.50 and y = - 1.54x + 1.37, respectively.

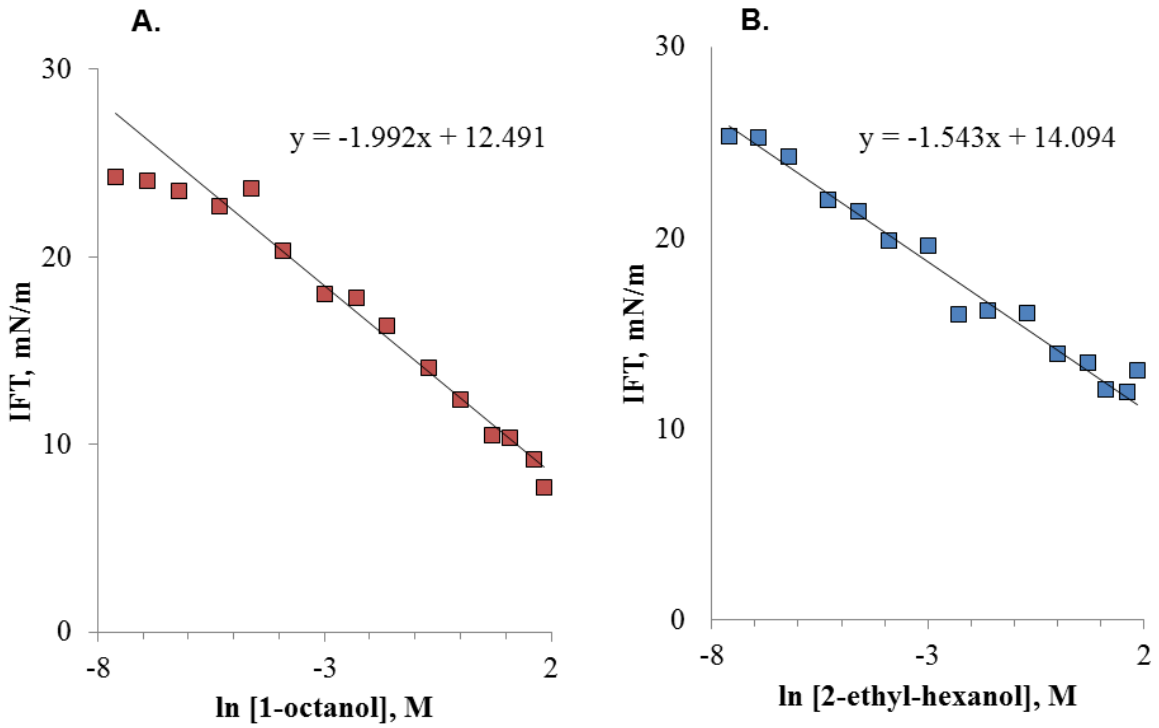

Figure 32. Interfacial tension as a function of (A.) [1-octanol] and (B.) [2-ethyl-hexanol] following equilibration with H_2O.

6.4.5. Simulated Small Angle X-Ray Scattering

Atomistic MD simulations were performed to replicate the scenarios of 0.5 M and 2 M alcohol in dodecane contacted with water. The simulated SAXS data were calculated by means of nMoldyn.[156] Note that nMoldyn actually calculates the atomic number weighted structure factor for SAXS.[157, 158] The atomic form factor $f(q)$ is related to the atomic number (Z) *via* **Equation 27**;

$$f_i(q)|_{q\to 0} = Z_i, \qquad \text{eq. 27}$$

for atom *i*, where q is the wave vector.[159] Simulated data show the presence of a high q-peak at approximately 1.4 Å^{-1} **(Figure 30b)**. Long-range correlation peaks were also observed with intensities dependent on the alcohol concentration. In the 2 M 2-ethyl-hexanol system, a correlation peak is observed at around 0.5 Å^{-1}, while in 2 M 1-octanol a broad peak is observed at 0.25 Å^{-1}. Consistent with the corresponding experimental SAXS, the 2-ethyl-hexanol peak is narrower than that in the 1-octanol system, suggesting a stronger correlation at a smaller, fixed distance.

From the simulations, the average aggregation number and morphology were also obtained. In 2 M 1-octanol and 2-ethyl-hexanol solutions, the average aggregation number was 5.3 ± 0.3 and 4.6 ± 0.2, respectively. In 0.5 M solutions the corresponding average aggregation number was 5.2 ± 0.5 and 4.1 ± 0.3. Moreover, a histogram of alcohol cluster sizes shows that clusters reached up to 40 alcohol molecules for 1-octanol and 25 for 2-ethyl-hexanol (**Figure 33; Figure 34**). The MD simulations describe the morphology and demonstrate the association of alcohol molecules through H-bond and suggest that the morphology of 1-octanol favors the elongated, non-spherical aggregates, while 2-ethyl-hexanol prefers curved and spherical aggregates (**Figure 30b; Figure 35**).

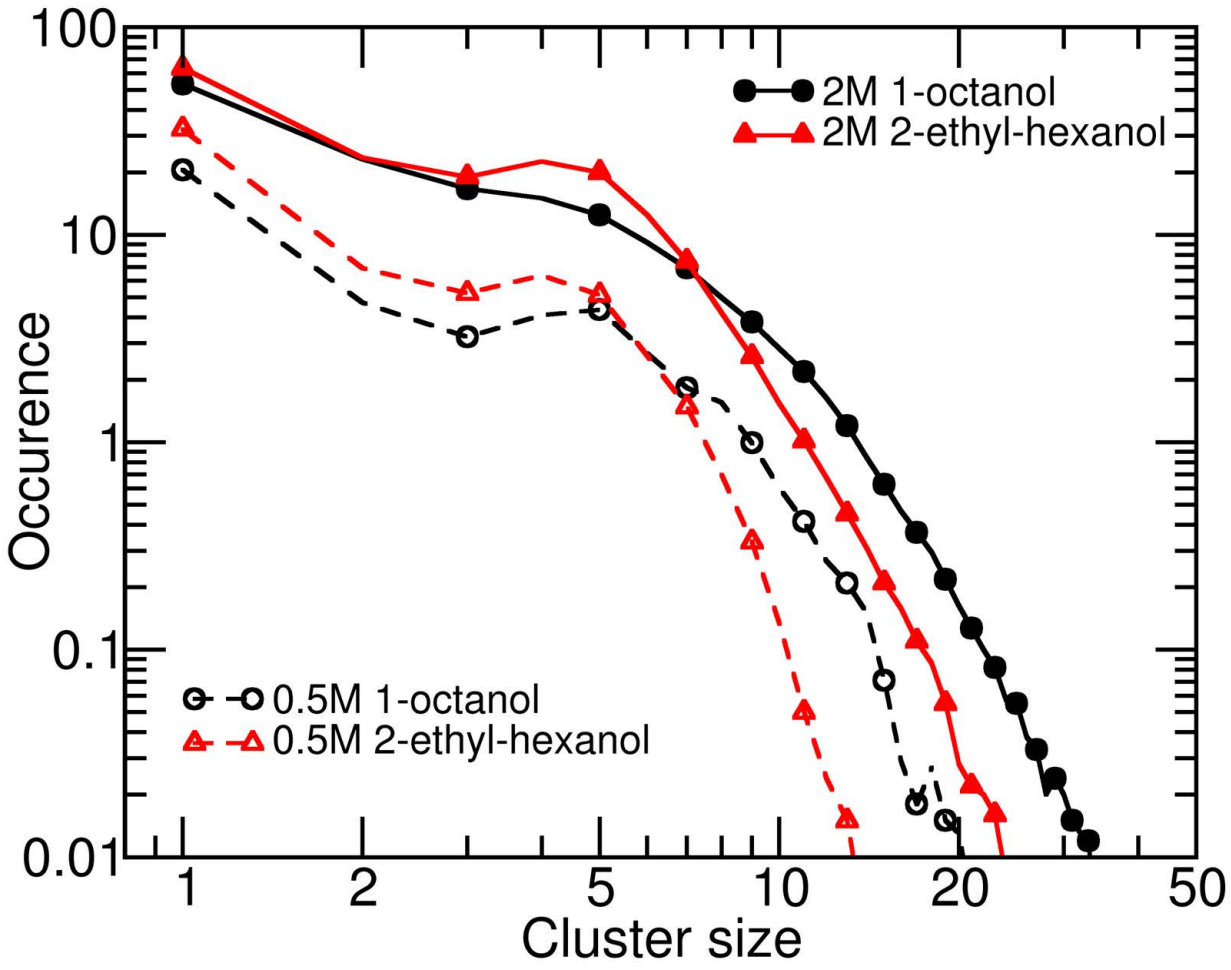

Figure 33. Histogram distribution of the clusters composed of alcohol oxygen atoms. Occurrence stands for the number of clusters with certain amount (i.e., cluster size) of alcohol oxygen atoms in the simulation box, which are averaged over the production simulations. The cutoff distance of 0.35 nm was employed for the definition of clusters based on the corresponding RDF between alcohol oxygen atoms.

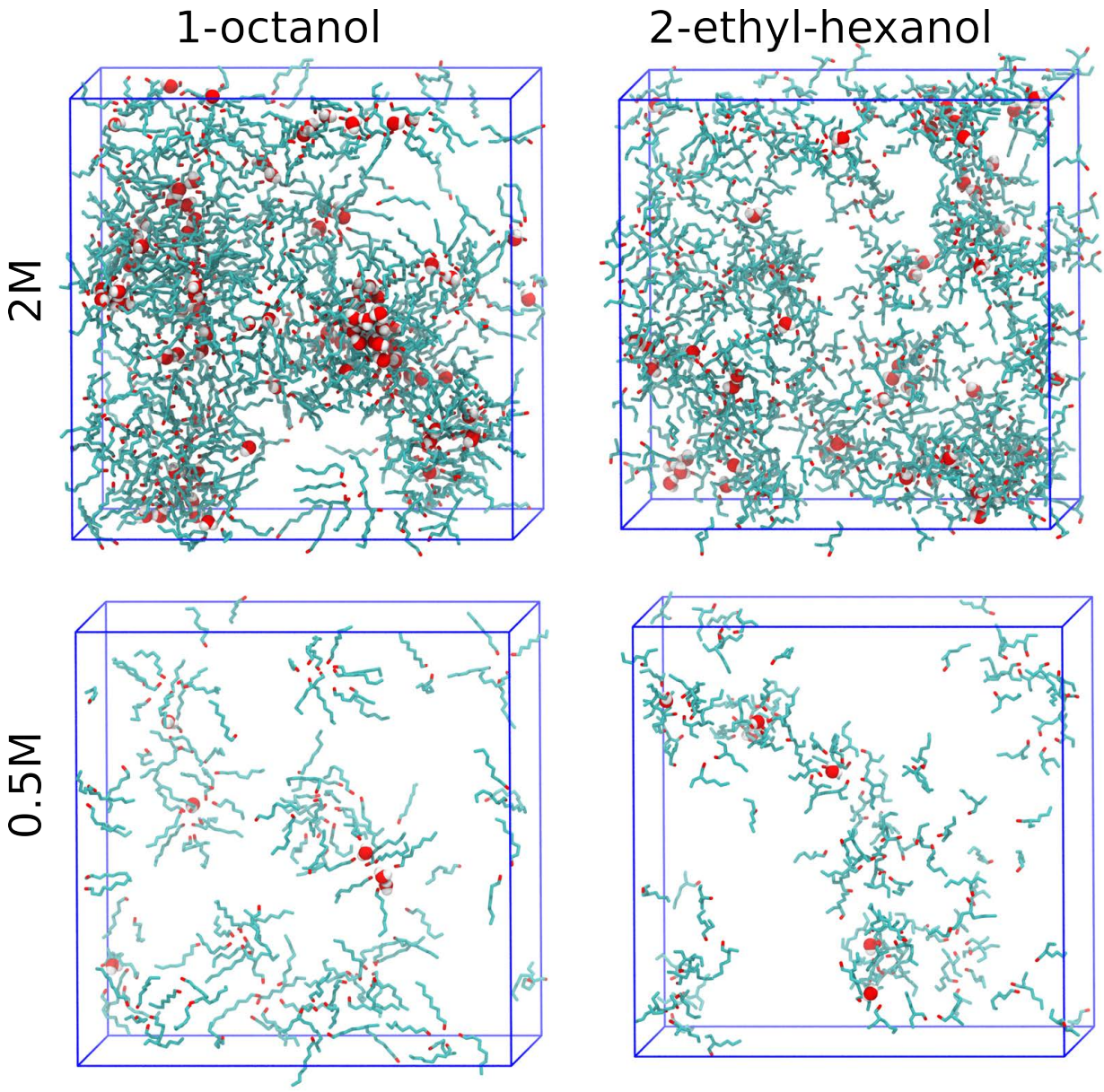

Figure 34. Snapshots of the last frame for each atomistic simulation. All alcohols are presented as stick models in which the hydrocarbon chains (CH_x) are green and the hydroxyl group is red (O) and white (H). Water molecules are presented as ball models with red (O) and white (H). The solvent of dodecane molecules are omitted for the display.

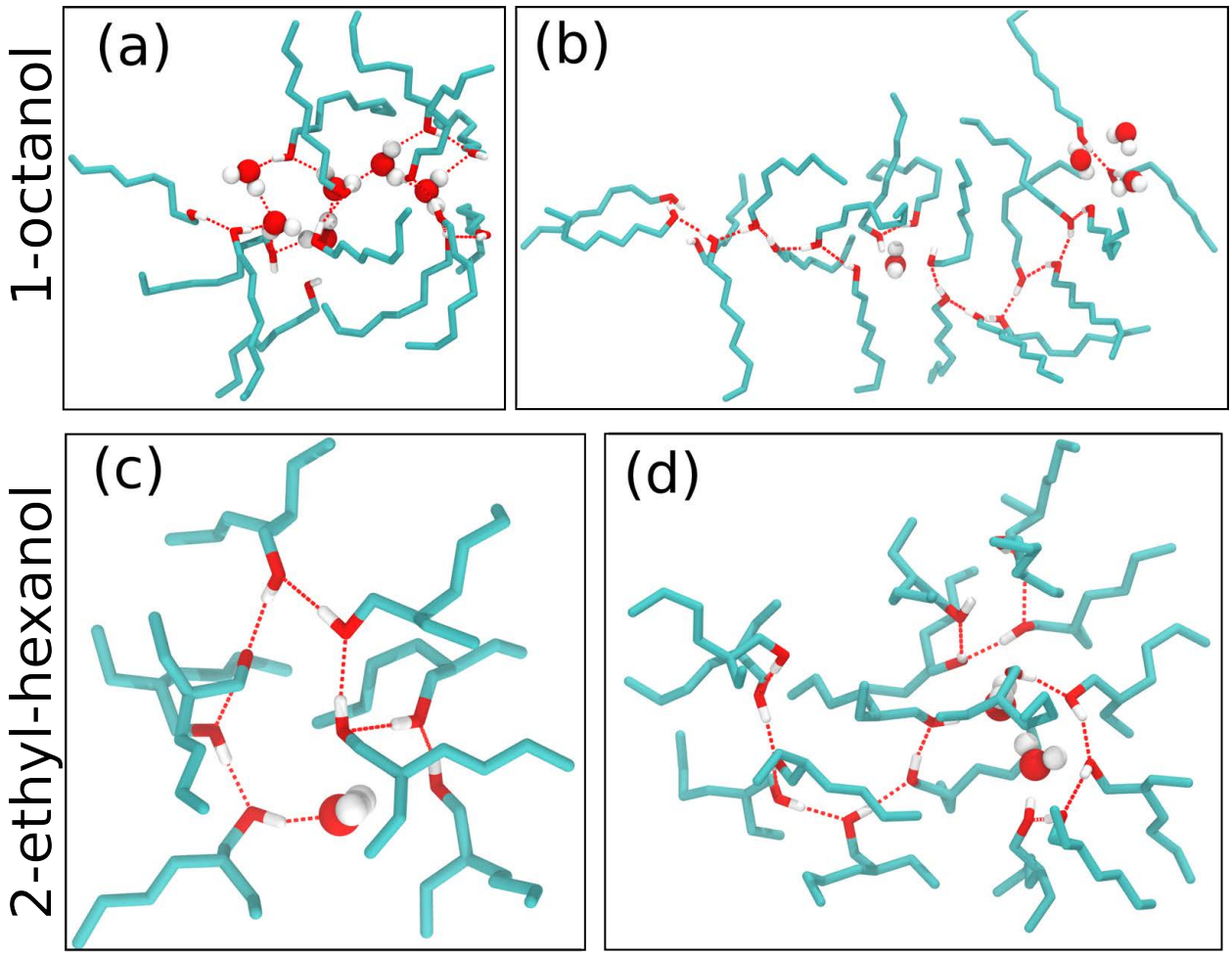

Figure 35. Simulation snapshots of some typical aggregates in octanol and 2-ethylhexanol system, both at 2 M. The rotation movies of structures (B) and (D) are also provided in the SI. The hydrocarbon chains (CH_x) are green and the hydroxyl group is red (O) and white (H) and the red dotted lines denotes the H-bonds.

6.5. Discussion

Collectively, from the results, corroborating physical measurements with experimental SAXS data and atomistic molecular dynamic simulations, we observe that neither 1-octanol nor 2-ethyl-hexanol behave as classical surfactants. However, they do present themselves with many surfactant-like properties. This discussion aims to highlight the extent of which 1-octanol and 2-ethyl-hexanol behave as surfactants in systems containing dodecane and water.

The primary result suggesting that the behavior of 1-octanol and 2-ethyl-hexanol is atypical to conventional surfactants is the absence of a critical micelle concentration (CMC). Conventional surfactants have the remarkable ability of readily assembling at the hydrophilic/hydrophobic interface thus decreasing the interfacial tension.[123, 160] Once the surfactant concentration is high enough to saturate the interface at the CMC,[160] micellization and aggregation begin in the bulk. Any additional surfactant molecules dissolved in solution will be in dynamic equilibrium between monomers and micelles.[130, 161] A high CMC (> 0.1 M) indicates a weak surfactant, while a low CMC (< 0.1 M) indicates a strong surfactant and a greater propensity to target the interface and subsequently form aggregates and micelles.[160] This behavior and understanding of surfactants demonstrate that these solutions are complex, structured fluids rather than uniform molecular solutions.[123, 160, 162]

The interfacial behavior of 1-octanol and 2-ethyl-hexanol in dodecane-water biphasic solutions were analyzed *via* inverted drop tensiometry. The tensiometry data (**Figure 32)** demonstrates that, as the concentration of 1-octanol and 2-ethyl-hexanol increases, the interfacial tension decreases. The resulting trend is linear for the $\sigma - \ln(c)$ plot, typical of a conventional surfactant.[160, 163] However, unlike conventional surfactants, in which a slope-break exists (around the CMC), the interfacial tension of these alcohols-bearing dodecane-water biphasic solutions continues to decrease -- steadily approaching the interfacial tension in alcohol-water biphasic systems (this study: 7.7 ± 0.4 mN/m; literature 8.71 ± 0.2 mN/m for 1-octanol in water).[164] While additional physical information can be extrapolated from the slope analysis of the $\sigma - \ln(c)$ plot regarding the surface excess and head group area derived from the Gibbs adsorption equations.[165-167] These calculations require the existence of a CMC to represent physical

meaning. Therefore, we cannot determine the surface excess or the average head group area from the tensiometry data. However from the absence of a CMC, we can conclude that the dodecane-water interface is not saturated with alcohol molecules, yet SAXS data confirms the formation of aggregates in the organic phase and their dependence on the alcohol concentration. This observation leads to the hypothesis that the tendency to form aggregates for alcohol derives from a different origin than in conventional surfactants. Instead, a balance between the alcohol distributions at the interface and in the organic bulk phase exists before the interface is saturated.

The formations of aggregates in alcohol-bearing solutions of dodecane and water appear to suggest a different equilibrium than the formation of aggregates by classical surfactants. A diagram demonstrating the proposed aggregation equilibrium and compared to the equilibrium for conventional surfactants is shown in **Figure 36**. In solutions containing conventional surfactants, there exists a stepwise process of saturating the surface prior to aggregating the bulk.[160] In the case of aliphatic alcohols, the formation of aggregates and the interfacial species exist in a dynamic equilibrium with monomers in the bulk. This results in poorer efficiency (than conventional surfactants) to reduce the interfacial tension as a function of alcohol concentration as well as the occurrence of aggregates without saturating the interface. Instead of a stepwise model, as for conventional surfactants, where surfactant molecules first saturate the interface prior to developing achieving equilibrium with monomers in the bulk and aggregated species, we observe simultaneous equilibrium between interfacial species with monomers along with aggregated species in the bulk with monomers.

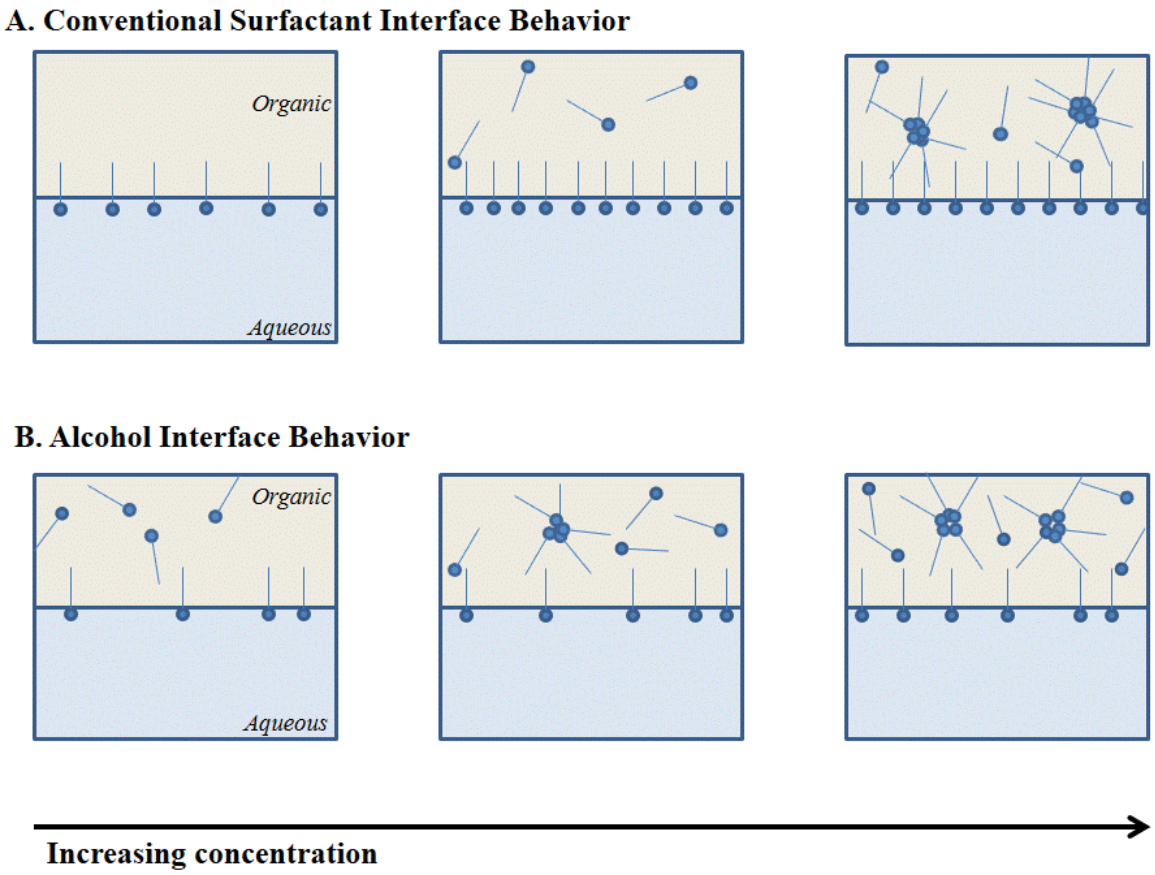

Figure 36. Simplified equilibrium of micellization for a typical surfactant **(A)**. And **(B)**, proposed equilibrium occurring for systems containing 1-octanol and 2-ethyl-hexanol.

6.5.1. Tail Group Effects Leading to Different Aggregates

The formation of aggregates is observed in biphasic solutions containing 1-octanol as well as 2-ethyl-hexanol at 0.5 and 2 M, yet there are distinct differences in the organic phase ordering and physical properties that are a result of tail group differences. These differences observed from solutions of isomers are consistent to the behavior of conventional surfactants,[168] as tail group differences in surfactant isomers have been reported to drive the variations in the aggregate structures.[169] Our findings coincide with the literature that the tail group plays a significant role in physical properties, aggregation, and micellization.[160, 170, 171] These differences can be observed in the physical measurements (tensiometry and water extraction) as well as in experimental and simulated SAXS data.

Physical measurements suggest that 1-octanol is a slightly stronger surfactant than 2-ethyl-hexanol. A stronger surfactant has a greater ability to decrease the interfacial tension between two phases.[123, 124] As indicated by the tensiometry experiments, the 1-octanol is more surface active, and lowering the interfacial tension more efficiently (**Figure 32**), where the slope of the regression line for the $\sigma - \ln(c)$ plot for 1-octanol has a larger negative slope, m = -1.922, versus m = -1.543 for 2-ethyl-hexanol. The final interfacial tension between pure 1-octanol and water is also lower than that of the solutions of pure 2-ethyl-hexanol and water. Lower interfacial tension will consequently facilitate the transport of water from the aqueous phase to the organic phase because less energy is required to overcome the phase boundary (**Table 10**). Beyond more effectively decreasing the interfacial tension between organic and aqueous phases, 1-octanol also extracts more water into the organic phase than 2-ethyl-hexanol. The strength of the association between water and 1-octanol is stronger which leads to a smaller amount of energy required to transport a water molecule across the dodecane-water interface.

Beyond differences observed in the physical properties of these solutions, the size and distribution of the aggregates as seen in SAXS data also demonstrate variations between these two systems. The Percus-Yevick model demonstrates that the average aggregates radius in solutions of 2 M 1-octanol solution (5.5 ± 0.3 Å) is found to be around 1.3 Å larger than that in the 2 M 2-ethyl-

hexanol solution (4.17 ± 0.04 Å). Simulations also revealed that solutions containing 1-octanol formed aggregates with a higher aggregation number (*i.e.* number of monomers per aggregate) than 2-ethyl-hexanol for both 0.5 M and 2 M: the average cluster size is 5.3 ± 0.3 (2 M 1-octanol) versus 4.6 ± 0.2 (2 M 2-ethyl-hexanol), and 5.2 ± 0.5 (0.5 M 1-octanol) versus 4.1 ± 0.3 (0.5 M 2-ethyl-hexanol). These data agree on that on average the 1-octanol systems favor the formation of larger aggregates. Furthermore, the differences in the equilibrium water concentrations in the organic phases are related to the aggregate size as solutions of 2 M 1-octanol extract nearly twice as much water ($[H_2O]_{org.}$ = 0.32 M) as 2 M 2-ethyl-hexanol ($[H_2O]_{org.}$ = 0.17 M) **(Figure 29)**. Consequently, a higher concentration of (polar) water molecules in the organic phase favors the larger aggregates which could be a result of swelling of the aggregates.[21]

The volume fraction parameter from the Percus-Yevick model indicates that 2-ethyl-hexanol demonstrates a greater propensity to form aggregates; however, the aggregates in the 2-ethyl-hexanol systems are smaller. The volume fraction for 2-ethyl-hexanol (0.204 ± 0.003) accounts for nearly twice as much as that of solutions of 1-octanol (0.11 ± 0.01) suggesting that there are more detectable (i.e. greater number) aggregates by X-rays in solutions containing 2-ethyl-hexanol. SAXS data shows that solutions of 2-ethyl-hexanol show a stronger correlation peak at a relatively higher q suggesting that the hydroxyl groups of 2-ethyl-hexanol are generally more associated at a fixed, closer distance than those of 1-octanol **(Figure 30; Figure 31)**. The Percus-Yevick model provides an evaluation of the interaction radius between aggregates. The interaction radius for 1-octanol (6.4 ± 0.1 Å) is nearly 1 Å larger than 2-ethyl-hexanol (5.58 ± 0.02 Å) at 2 M. The larger interaction radius suggest that 1-octanol aggregates participate in limited inter-aggregate interactions, while 2-ethyl-hexanol aggregates, at a higher concentration as seen by the volume fraction, have a significant correlation peak. This peak suggests increased inter-aggregate interactions **(Figure 31)**. Using this information, along with the sphere radii, can be used to describe the regions between clusters, where the widths of the non-zero regions are smaller for 1-octanol (~0.9 Å) than 2-ethyl-hexanol (~1.42 Å) as calculated by **Equation 26**. Further, since these values are much less than the length of the fully extended –octyl (~14 Å) or -hexyl (~10 Å) groups,

this data suggests significant inter-digitating among tail groups of adjacent clusters. Systems containing the 1-octanol system is more inter-digitated than 2-ethyl-hexanol, by about 0.54 Å.

6.5.2. Aggregate Description

By corroborating the physical measurements with X-ray absorption techniques and simulated data we can speculate a description of these aggregates. We evaluated the aggregates to determine the average aggregation number for alcohol molecules per aggregate as well as average number of water molecules per aggregates from two independent calculations. The first calculation uses SAXS data and the second calculation utilizes simulation data both aided by geometric approximations.

The SAXS data can be used to provide a physical description of the aggregates formed in solutions of 1-octanol in dodecane and water. Using the sphere radius from **Table 7** we obtain the volume of the aggregate:

$$sphere\ volume\ (V_s) = \frac{4}{3}\pi r^3 \quad eq.28$$

Where r is the sphere radius in nm, for 1-octanol, V_s = 0.696 nm^3. This can be used in the equation for the volume fraction (V_f), relating the total number of aggregates (N_{agg}) and V_s to V_T.

$$V_f = \frac{N_{agg} * V_s}{V_T} \quad eq.29$$

Which can be rearranged to give the effective volume (V_{eff}) of an aggregate or the average volume an aggregate and its surroundings take up.

$$V_{eff} = \frac{V_s}{V_f} = \frac{V_T}{N_{agg}} \quad eq.30$$

For 1-octanol, V_{eff} = 6.336 nm^3/aggregate. The product of V_{eff} and the molar organic phase concentration water can lead us to the average number of water molecules per aggregate (N_{water}).

$$\bar{n}_{water} = \left(\frac{[H_2O]_{org} * N_A * V_{eff}}{1x10^{24} \frac{nm^3}{L}} \right) \quad eq.31$$

For 1-octanol, the $\bar{n}_{\text{water}}$ = 1.22 molecules per aggregate. Assume all the water is associated with an aggregate of alcohols, the organic phase ratio of 1-octanol:water should be maintained at 6.25, therefore $\bar{n}_{\text{alcohol}}$ = 7.63 molecules of 1-octanol per aggregate.

We can compare this observation with an independent calculation using the simulated data. From simulations, the radius of the aggregate and the core were estimated to be, $r_{core} \approx 0.3$ nm and $r_{agg} \approx 1.14$ nm. Assuming the aggregates and cores are spherical, the corresponding volumes were determined to be V_{core} = 0.113 nm^3, and V_{agg} = 6.205 nm^3/aggregate. Simulations determined the $\bar{n}_{\text{alcohol}}$ = 5.3 ± 0.3 molecules/aggregate for 1-octanol. By maintaining the 1-octanol:water ratio, and assuming that all water is limited to the core of the aggregate, we observe:

$$\bar{n}_{water} = \frac{\bar{n}_{\text{alcohol}} * [water]_{org}}{[alochol]_{eq}} \quad eq\ 32$$

For 1-octanol, the $\bar{n}_{\text{water}}$ = 0.848 molecules/aggregate (**Figure 37**).

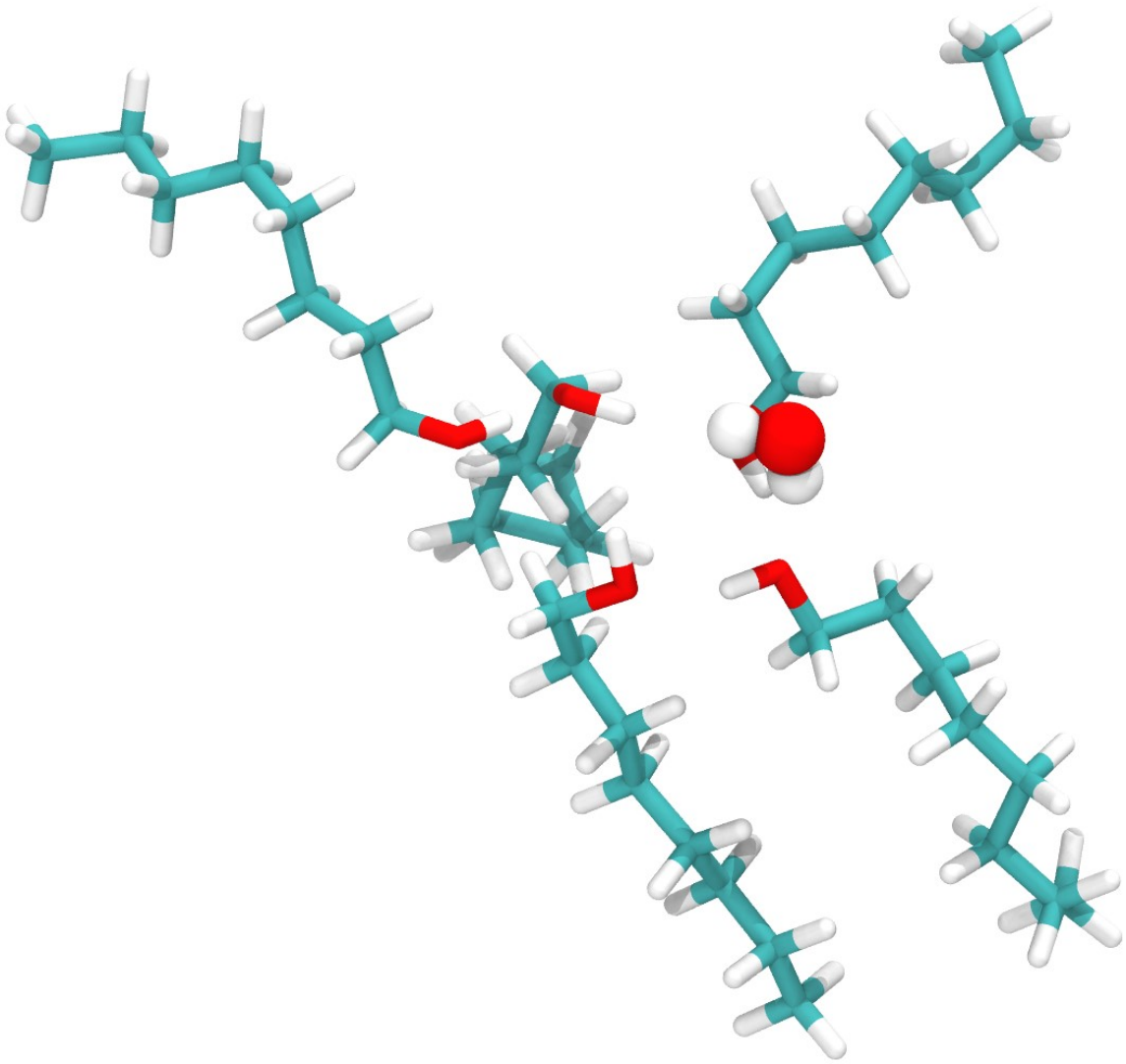

Figure 37. A simulated example of an aggregate consisting of 5 molecules of 1-octanol and 1 water molecules arranged through hydrogen bonding interactions.

From these two independent methods, we obtain aggregation numbers for 1-octanol and water to be in relative agreement. We observe, on average, that around 1 water molecules exist in the center of the aggregates in the organic phase, which concludes that 1-octanol forms reverse micelles. When we apply the same models to determine a physical description of the aggregates that form in 2-ethyl-hexanol, we observe that the aggregates are not of sufficient size for water to exist predominantly on the inside. Likewise we observed considerably less water extracted by 2-ethyl-hexanol than 1-octanol. From these results it is difficult to conclude if the extraction of water is excluded because the aggregates formed are not large enough for water fit, or because very little water is extracted the aggregates remain small and primarily interaction exclusively with alcohol hydroxyl groups.

6.5.3. Hydrogen Bonding Interactions

As stated in previous studies, H-bonding interactions play a significant role in the aggregation of amphiphiles in organic solutions.[136, 137] With respect to the analysis of 1-octanol and 2-ethyl-hexanol, we can evaluate the hydrogen bonding interactions through an understanding of their aggregated structures. As suggested by tensiometry data and the extraction of water, we hypothesize that the H-bonding interactions between 1-octanol and water are stronger than those between 2-ethyl-hexnaol and water. From the tensiometry data we see that the slope of the regression line is steeper with respect to the concentration of 1-octanol than with respect to 2-ethyl-hexanol. While the difference is minor, we believe these observed differences are due to an increased affinity for 1-octanol to target the interface, thus decreasing the interfacial tension, and interact more readily with water molecules. Likewise, we see a greater amount of water in the organic phase in solutions of 1-octanol than solutions of 2-ethyl-hexanol, and on average a molecule of water is associated with the aggregates of 1-octanol, while water appears to be excluded in the aggregates consisting of 2-ethyl-hexanol.

These observations lead to hypothesis regarding how the presence of a single ethyl-group near the hydroxyl head group can drastically changes the surfactant behavior and organic phase

ordering. While we do not have a definitive reason to explain these differences, we approach this conversation from two perspectives: (*i*) electrostatic and hydrogen bonding properties and (*ii*) physical and steric properties.

As stated previously, we believe that 1-octanol participates in stronger H-bonding interactions with water and as a result the interfacial tension decreases, water extraction increases, and solution forms large aggregates, this discussion attempts to explain why these H-bonding interactions may be stronger. On a molecular level, the only difference between 1-octanol and 2-ethyl-hexanol is the location of an ethyl group. In 1-octanol, the ethyl group is a part of the linear alkyl chain, whereas in 2-ethyl-hexanol the ethyl group is branched from the second carbon. The dipole moments of 1-octanol and 2-ethyl-hexanol are 1.76 and 1.74 D, respectively, and water is 1.85 D.[172] While the dipole moment for 1-octanol is slightly stronger, it would not be expected that a 0.02 D change to the dipole would be the sole factor that would result in the observed differences in aggregation. Another factor that could play a role in these ordered structures is the differences in basicity and other intermolecular forces (*i.e.* Van der Waals) between 1-octanol and 2-ethyl-hexanol. Previous studies have identified that more basic extractants form aggregates more readily because there is a greater electron density involved in the hydrogen bonding.[168] In a study looking at third phase formation of solvent extraction systems consisting of difference organophosphorus reagents, they observed an increased extraction of HCl in the organophosphorus reagent with the octyl tail versus the reagent with an ethyl-hexyl tail group.[168] While these systems are very different from the ones being analyzed in our studies, the results suggest a similar dependence on the tail group for the extraction of aqueous speciation as well as aggregation.

Additional chemical properties to discuss include boiling point and water solubility differences, which could provide insight into differences in the intermolecular forces between 1-octanol and 2-ethyl-hexanol that lead to these differences in the organic phase ordering. The boiling point of 1-octanol is 194.7 ˚C and 2-ethyl-hexanol is 184.34˚C.[172] This difference in boiling points demonstrates that 1-octanol has greater intermolecular forces, which include but not limited to H-bonding interactions, which may suggest greater basicity for 1-octanol. We can also consider the

solubility of these alcohols, in which the solubility of 1-octanol is 540 mg/L[173] and 2-ethyl-hexanol is 880 mg/L[174] in water. The greater solubility of 2-ethyl-hexanol in water may suggest that upon mixing, more 2-ethyl-hexanol may distribute between the organic and aqueous phases, which the lower solubility of 1-octanol may keep it in the organic phase. Therefore instead of water being extracted from the aqueous phase to the organic phase and associated with aggregates of 1-octanol, molecules of 2-ethyl-hexanol may transfer to the aqueous phase more readily; decreasing the extraction of water into the organic phase.

Another approach to postulate the enhanced surfactant properties of 1-octanol relative to 2-ethyl-hexanol is an evaluation of the in H-bonding interaction probabilities between the hydroxyl group and water from the perspective of steric interactions. For 2-ethyl-hexanol, the lone pairs on the H-bond accepting hydroxyl O are partially obscured by the ethyl group. The proximity of the hydrophobic ethyl to the headgroup acts as a lipophilic 'shield' against the approach of water to the hydroxyl lone pairs; thus limiting the angle at which H-bonding interactions can occur. As such, simulated SAXS data demonstrate that these aggregates form spherical aggregates that are dependent on the approach angle of the H-bonding donor to H-bonding acceptor (**Figure 35)**. In contrast, the hydroxyl lone pairs on the linear 1-octanol are more exposed, allowing a wider range of angles from which water can approach and increasing the likelihood of forming alcohol-water H-bonds. As a result, the aggregates that form in these systems are elongated. This results are in consistent with studies of 1-octanol in ethanol and water, in which dynamic organization was observed, and the influence of the octyl tail prevents the aggregates from forming a perfect sphere at high aggregation numbers,[128, 129] and preferentially forms elongated aggregates (**Figure 35**).

While it is challenging to definitively discuss the extend of which these factors influence the formation of aggregates, the fact that these systems exist at a interstitial transition state allows for small energetic differences to have a significant effect on system. The chemistries of 1-octanol and 2-ethyl-hexanol are very similar however in these highly polarizing environments consisting of solutions of water and dodecane, these chemical nuances become highlighted in efforts to minimize the free energy of the system at equilibrium.

6.6. Conclusions

With recent enthusiasm regarding "surfactant free micro-emulsions" and the existence of microemulsions in ternary systems without conventional surfactants,[128-130] we investigated the occurrence and morphology of the aggregation of structural isomers 1-octanol and 2-ethyl-hexanol in a water-dodecane system. Our findings suggest that a different equilibrium expression must be proposed to properly understanding these systems. We propose that systems containing 1-octanol and 2-ethyl-hexanol undergo a simultaneous equilibrium between interfacial species with monomers and between monomers and aggregated species. The hypothesized equilibrium obviates the need for a CMC and interfacial (or surface) saturation to occur prior to aggregation to occur. Further discussion regarding the tail group effects on the formation of aggregates deepens our understanding of alcohol molecules in ternary solutions. While 1-octanol and 2-ethyl-hexanol are not conventional surfactants, the proposed equilibrium may help explain why we observe the presence of nano-structural domains and a reduction of interfacial tension between immiscible phases in the presence of an aliphatic alcohol. Future research aims to expose the electrostatic and physical properties that govern the formation of aggregates and the parameters that influence the occurrence and morphology of the aggregates. These studies will develop a better understanding of the equilibrium expression for the organic phase ordering of aliphatic alcohol systems.

6.7. Associated Content

Supporting Information: The supporting information can be found in **Appendix B** and includes a cartoon showing the physical relevance of the Percus-Yevick fitting parameters, a detailed description of the atomistic molecular dynamic simulations, and movies of the simulations.

Notes: The authors declare no conflict of interest.

Acknowledgements: This work and the use of the Advanced Photon Source are supported by the U.S. Department of Energy, Office of Basic Energy Science, Division of Chemical Sciences, Biosciences and Geosciences, under contract No. DE-AC02- 06CH11357 and with support from the U.S. Department of Energy, Office of Science, Office of Workforce Development for Teachers and

Scientists, Office of Science Graduate Student Research (SCGSR) program. The SCGSR program is administered by the Oak Ridge Institute for Science and Education for the DOE under contract number DE-AC05-06OR23100.

CHAPTER VII: SUMMARY, IMPACTS, AND FUTURE WORK

7.1. Global Conclusions

This thesis aims to develop a greater understanding of the chemistry of protactinium at trace levels with in the context of nuclear energy, nuclear forensics, and the environment. Each chapter has a different focus and method to advance our understanding of protactinium. Furthermore, additional information is learned regarding the chemistry of other actinide elements (Th, U, Np, and Am) as well as a broader understanding of solvent extractions systems – with significant advanced in our understanding of organic phase ordering (**Chapter VI**). Developments in this thesis include (1) a new rapid method for the separation of Pa from complex samples, (2) the production of a convenient radiotracer, ^{233}Pa, from a ^{237}Np standard source using a novel extraction chromatographic resin, (3) a mathematical model describing the extraction of Pa from 2,6-dimethyl-4-heptanol in acidic conditions to allow for predictive D values to be viable with regards to this system, (4) an in-depth understanding of the chemistry of Pa with respect to extraction by aliphatic alcohols and how these equilibrium studies can lead to a better understanding of Pa and the other actinide elements, and (5) insights into the organic phase ordering with solutions containing 1-octanol or 2-ethyl-hexanol and a better understanding of how these aggregates form in the absence of a critical micelle concentration.

7.1. Chapter II Summary and Impacts

In chapter II, we introduce a new rapid method to separate U, Th, and Pa from complex matrices for application in geochronology and to be adapted for a nuclear forensic analysis. We analyzed carbonate samples from Paleolithic Lake Bonneville to provide (^{231}Pa/^{235}U) and (^{230}Th/^{234,238}U) ages to corroborate with previously determined ^{14}C ages (from Brigham Young University) that provide ages of about 35-40 ka. [9, 57] The ages of these samples represent a geologic time at which Lake Bonneville underwent a catastrophic draining event, as reflected by Th, Pa, U isotopic information as well as ^{14}C. [57] Providing U-series ages to support ^{14}C ages is a critical need within the geoscience community. While ^{14}C ages are a mainstay of dating samples (up to about 50

ka), the liberation of ^{14}C from fossil fuel emission and nuclear fallout has complicated the measurement because ^{14}C concentrations can fluctuate. Corroborating ^{14}C with U-series ages will help to calibrate the ^{14}C measurements as well as decrease uncertainties in older samples.

With respect to nuclear forensics, there is a critical need to develop rapid method for the age dating of illicit material that can lead to a legally defensible argument to aid in the determination of the last legal owner of that material. Because nuclear material is enriched in ^{235}U (up to 5% for fuels and up to 95% for weapons), the ($^{231}Pa/^{235}U$) measurement is invaluable to determining the age of these materials. [12] These studies aim in this goal by providing a method that can reproducibly determine ages of samples rapidly.

7.3. Chapter III Summary and Impacts

In chapter III, we develop a new, convenient method to produce a radiotracer for Pa for isotope dilution analysis. This objective directly addresses the work of Claude Sill, where he mentioned that the development of a convenient radiotracer for Pa would greatly facilitate our understanding of Pa chemistry. [46] We developed a rapid separation of ^{233}Pa from ^{237}Np to isolate ^{233}Pa a radiotracer for ^{231}Pa for isotope dilution studies. This method utilizes a novel extraction chromatographic resin consisting of 1-octanol adsorbed onto an AmberChrom resin bead (produced by Eichrom, similar to their other commercially available resins [61]). The advances in this method dramatically reduced the hands-on time required to perform this separation as well as minimizes aqueous and organic waste and eliminates the need to complexing agents (*i.e.* H_2SO_4, HF).

This work has also spawned a relationship between the University of Iowa and commercial partner TrisKem International (Bruz, France). The novel extraction chromatographic resin developed from these studies is now a commercially available product marketed by TrisKem.

7.4. Chapter IV Summary and Impacts

In chapter IV, we development a mathematical model to represent the extraction of Pa from biphasic systems containing 2,6-dimethyl-4-heptanol in dodecane contacted with aqueous phases

in the nitrate or chloride forms. The mathematical model was developed using DesignEase software and a full factorial experimental design. [103] From these studies we were able to quantify the main effects describing the extraction dependence of Pa with respect to [2,6-dimethyl-4-heptanol], [anion: Cl^-or NO_3^-], and [H^+], as well as develop a model that allows for the prediction of distribution ratios with respect to the extraction of Pa.

The impact of this work is that this is the first work to use experimental engineering to quantify main effects and predict chemical behavior in solvent extraction systems. Also, using the mathematical equation provided in these studies, future investigators will be able to fully understand the extraction of Pa by 2,6-dimethyl-4-heptanol in chloride and nitrate forms. Furthermore, this work lays the foundation for future investigations looking into additional parameters that impact the extraction behavior of metals in solvent extraction. A few examples of these include contact time, diluent effects, radiolysis, and metal concentration.

7.5. Chapter V Summary and Impacts

In chapter V, we investigate the extraction behavior of Pa and other actinide elements (Th, U, Np, and Am) in systems containing aliphatic alcohol extractants (1-octanol, 2-ethyl-hexanol, and 2,6-dimethyl-4-heptanol) and mineral acids (HNO_3 and HCl) in both solvent extraction and extraction chromatographic resin systems. These studies highlight the trace level chemistry and demonstrate the Pa is unique among the actinide elements, likely attributed to the degeneracy of the 5*f* and 6*d* electron orbitals. [3] In this study we determine the acid dependencies of Th, Pa, U, Np, and Am with each of the studied alcohols in both solvent extraction and extraction chromatographic resin forms. From these studies we have develop numerous ways to separate Pa from the other actinide elements from complex matrices or mixed actinide systems. Further, through a detailed understanding of the extraction equilibrium for Pa, we have performed extractant dependency and ligand dependency (Cl^- and NO_3^- at 0.1, 1 and 4 M H^+) to approximate the average stoichiometric equivalent of required for the extraction to occur. It was determine, in chloride that the extracted species is a hexachloro-Pa anion extracted by two alcohols.

Corroborating this information with historically proposed species, we believe that the complex formed is $PaCl_6^-$ and is solvated with a H^+ in the organic phase. In the nitrate system, the extracted species is a dinitrate-Pa complex extracted by two alcohol molecules. Because we are not able to probe the speciation of Pa spectroscopically we are unable to determine the additional ligand coordinated to the central Pa metal. Yet, from these results we highlight the chemical complexities of Pa and demonstrate its unique chemistry within the actinide group elements.

These investigations appeal to researchers interested in trace level actinide extraction behavior. More specifically the novelty of these studies is found in the analytical experiments performed focused on advancing our understanding of the trace level chemistry of Pa. Additionally, the investigations in this chapter lay the foundation for further studies using higher levels of Pa to compare the trace level speciation to the speciation at higher concentrations.

7.6. Chapter VI Summary and Impacts

In chapter VI, we investigated the organic phase of the solvent extraction systems consisting of an aliphatic alcohol (1-octanol or 2-ethyl-hexanol) in dodecane contacted with water to observe the organic phase ordering. The organic phases were investigated in the absence of metal, to better understand the organic phase order at equilibrium of biphasic systems following chemical mixing. Samples were analyzed at concentrations of alcohol ranging from 1 mM to 2 M by experimental SAXS and compared with molecular dynamic simulated SAXS data. Additional physical properties, including tensiometry and equilibrium extracted organic phase water, were measured to corroborate the spectroscopic and simulated data to gain a better understanding the molecular scale ordering in the organic phase. We observed the presence of aggregates in systems containing either alcohol, as verified by SAXS and simulations, however these alcohols do not have behavior consistent with surfactant molecules. A significant divergent observation is the formation of organic phase aggregates however the absence of a critical micelle concentration (CMC). This led up to propose a new equilibrium expression to describe the formation of aggregates in solutions containing aliphatic alcohols.

This work was motivated by investigations into ternary systems consisting of water-ethanol-octanol in which nanoscale domains form in the absence of a "conventional surfactant" and thus has challenged current definitions in soft matter science. [128, 175, 176] Our work looks at the organic phase of these solutions consisting of water-dodecane-aliphatic alcohol, and continues to challenge our current understanding and definitions in soft matter chemistry. The heart of these findings challenge the understanding of what exactly constitutes as a surfactant, and what drives a surfactant to form micelles or reverse micelles. Since these aliphatic alcohols existing in as a transitional state, the subtleties that drive these nano-domains emerges and improves our overall understanding of structured fluids and, within the context of solvent extraction, how the organic phases exists at equilibrium.

7.7. Future Work

7.7.1. Future Work Regarding Coordination Chemistry of Protactinium

Future investigations regarding the chemistry and radiochemistry of Pa and how it applies to nuclear forensics, nuclear fuel cycle, and the environment will involve developing deeper understanding of the coordination chemistry of Pa. Within the context of solvent extraction, availability to increased concentrations of Pa, relevant to spectroscopic techniques (*i.e.* > 50 mM for EXAFS and > 200 mM for HEXS), will result in a more complete understanding of the coordination environment of Pa. We would be able to examine how the ligands coordinate (inner vs. outer sphere complexation), the extractant interactions, as well as directly probe at the oxygen species. The oxygen species will help verify the present of a mono-oxo PaO^{3+} cation versus mixed oxo/hydroxyl present in solution as well as verify the coordination of HNO_3 acting as a bidente or monodente ligand. Furthermore, future investigations into organic phase ordering *via* SAXS could potentially expose the impact that aggregation may have on selective extractions. Recent studies have demonstrated a strong correlation between the interaction energy between adjacent aggregates and the separation factor in the lanthanide series. [177] This work is very fascinating and

has the potential to bring a paradigm shift with regards to how scientist view solvent extraction--beyond a metal-centric approach to a solvent-centric approach.

7.7.2. Future Work Regarding Applications and Methods Involving Protactinium

With developing a greater understanding of the chemistry of Pa, more applications will reveal themselves to make a Pa analysis more relevant. Currently the more important application involving Pa is regarding chronometric studies to age date geologic quaternary age samples or for nuclear forensics. Currently there is a critical need to develop a rapid method for the determination of $^{231}Pa/^{235}U$ age information from special nuclear material with results that are defensible in front of a global judiciary council. While a few methods exist to analyze special nuclear material by alpha spectrometry [14], and by mass spectrometry [12], however significant challenges still remain.

Protactinium isotope exists as important intermediates for alterative fuel cycles and development in targeted alpha-therapy for certain cancers. In alternative fuel cycles, natural, fertile ^{232}Th is irradiated to form the fissile fuel ^{233}U through the pathway shown in **Figure 37** in which ^{233}Pa is the longest-lived intermediate. Because ^{233}Pa is an intermediate, methods to control Pa in extraction processes is critical to the development of these technologies. [13] Likewise, preliminary research has investigated the use of ^{226}Th for targeted alpha therapy by way of a generator system with a ^{230}U parent. The production pathways for ^{230}U are shown in **Figure 38**, and **Figure 39** in which both pathways involve a Pa intermediate. [178] Each of these methods rely on an understanding of the chemistry of Pa. Therefore there is a need to further develop methods for the extraction and separation of Pa isotopes from complex matrices as well as improve our understanding of the chemical behavior of Pa.

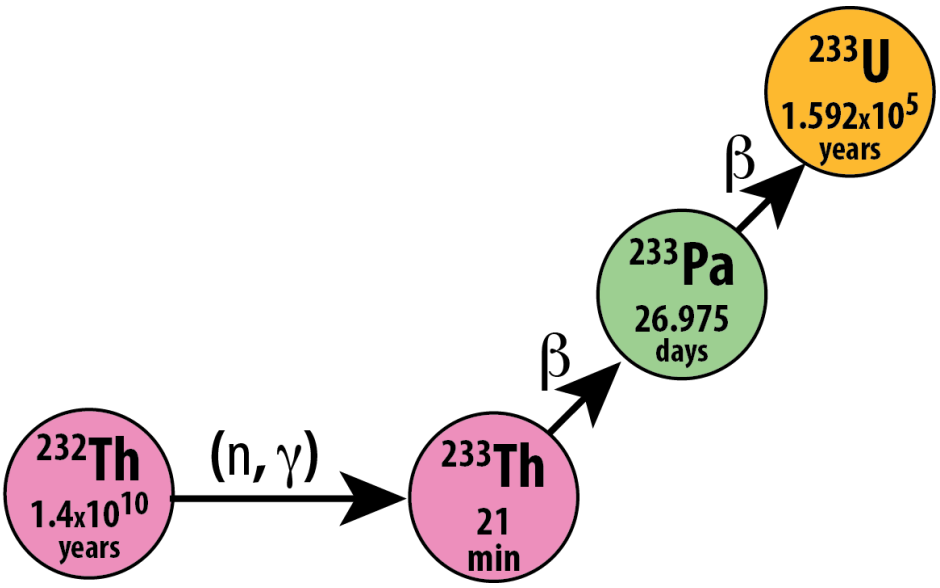

Figure 38. Pathway for the production of ^{233}U fuel from natural ^{232}Th through ^{233}Pa intermediate.

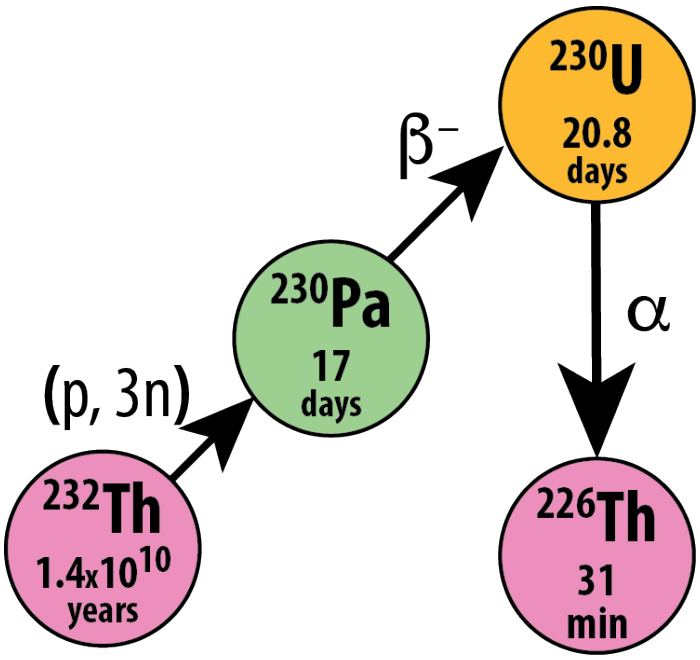

Figure 39. Pathway I for the production of ^{226}Th targeted alpha therapy isotope from natural ^{232}Th through ^{230}Pa intermediate.

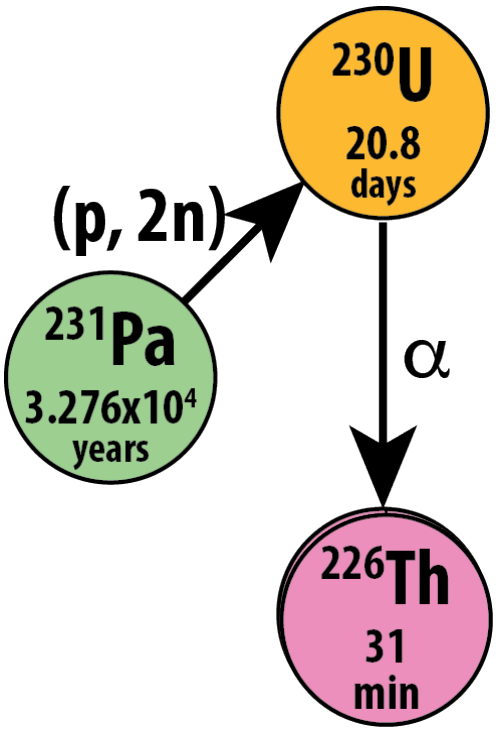

Figure 40. Pathway II for the production of ^{226}Th targeted alpha therapy isotope from natural ^{231}Pa.

APPENDIX A: SUPPLEMENTAL INFORMATION FOR CHAPTER V

AA.1 Conversion of Weight Distribution values to k' values

To convert D_w to k′, the D_w must first be converted to a volume distribution coefficient (D_v), using that values from table S1 and equation S1:

$$D_v = \frac{D_w * d_{extractant}}{0.4} \qquad eq.33$$

Where $d_{extractant}$ is the density of the pure extractant (1-octanol; 0.824 g/cm^3, 2-ethylhexanol; 0.833 g/cm^3, and DICB; 0.809 g/cm^3) and 0.4 is the extractant mass per gram of resin [81]. Next, D_v can be converted to k' from determining the *resin* density (g/cm^3), *bed* density (g/cm^3) and the stationary (extractant) and mobile phase volumes, v_s and v_m respectively. The *bed* density was determined by transferring the dry resin to a tarred graduated cylinder; weighing the resin and dividing by the volume in the cylinder determined the mass per cm^3. Then, v_s is calculated by multiplying the *bed* density by 0.4 (or the 40% w:w). The *resin* density was determined by achieving neutral buoyancy in solutions of known densities (dilute HNO_3). Lastly, the v_m was determined by subtracting the *resin* density by the *bed* density.

$$k' = D_v * \frac{v_s}{v_m} \qquad eq.34$$

All half-life data and primary gamma emission energies for radionuclides in this study are summarized in **Table 9**.

Table AA-1. Extraction chromatographic resin physical parameters and conversion factors

Resin	**(2,6)-dimethyl-4-heptanol**	**2-ethylhexanol**	**1-octanol**
Extractant Density (g/mL)	0.801	0.833	0.824
Bed Density (g/mL)	0.35	0.34	0.34
Resin Density (g/mL)	1.069	1.123	1.194
v_s	0.141	0.136	0.135
v_m	0.716	0.782	0.853
v_s/v_m	0.197	0.173	0.158
Dv conversion factor	2.00	2.00	2.00
K’ conversion factor	0.39	0.35	0.31

Table AA-2. Radionuclide used in these experiments shown with their half-lives and primary gamma energy emission.

Radionuclide	**Half Life**	**Major Gamma Energy Peak (keV)**
^{233}Pa	26.9 days	311.9 (38.5 %)
^{237}Np	2.14x10^{6} years	86.5 (12.4 %)
^{241}Am	432.6 years	59.5 (35.9%)
^{228}Th	1.91 years	N/A
^{232}U	68.9 years	N/A

APPENDIX B: SUPPLEMENTAL INFORMATION FOR CHAPTER VI

AB.1. Description of Percus-Yevick Fitting Parameters

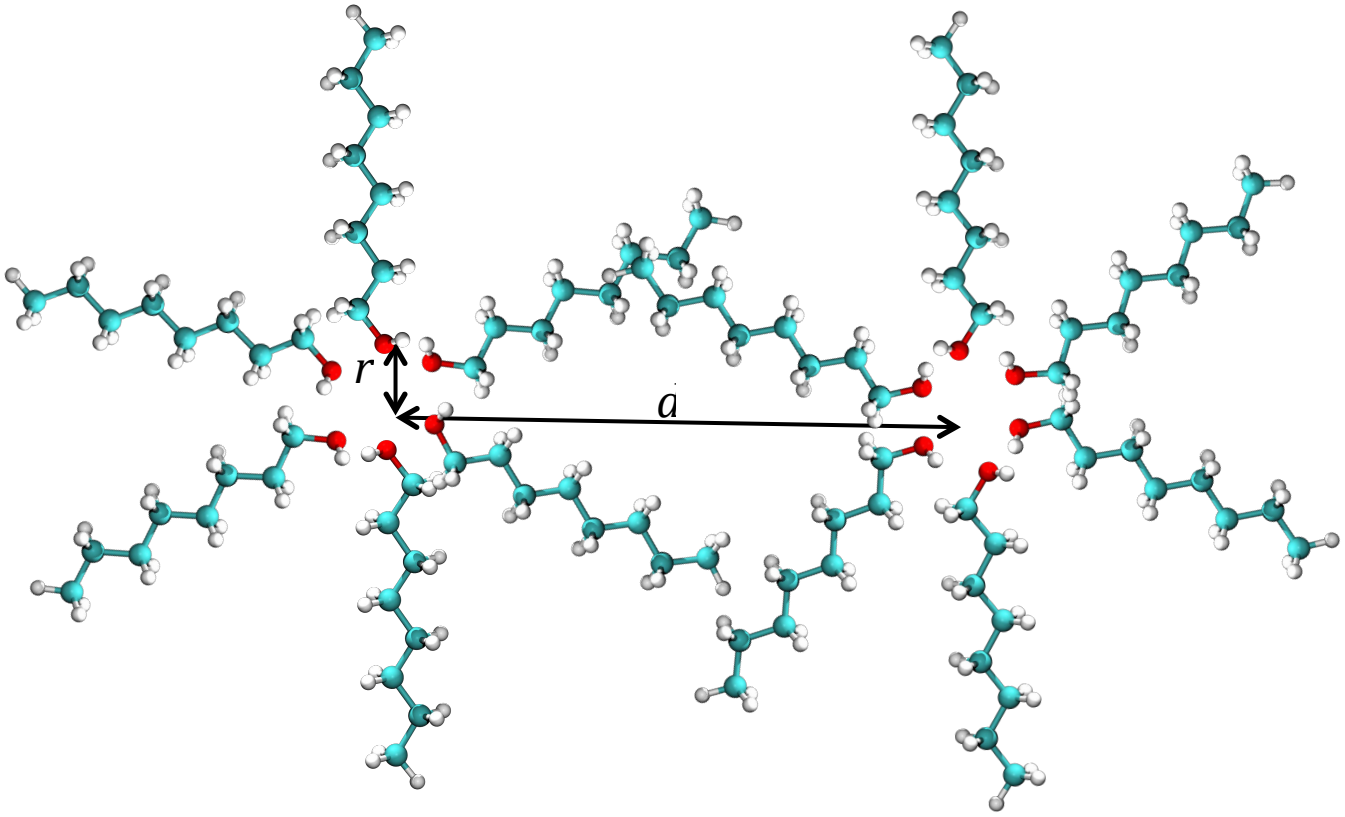

Figure AB-1. A cartoon summarizing the inter- and intra-aggregate Percus-Yevick fitting parameters, where *r* is the sphere radius and *d* is the interaction radius.

AB.2. Description of Simulation Methods

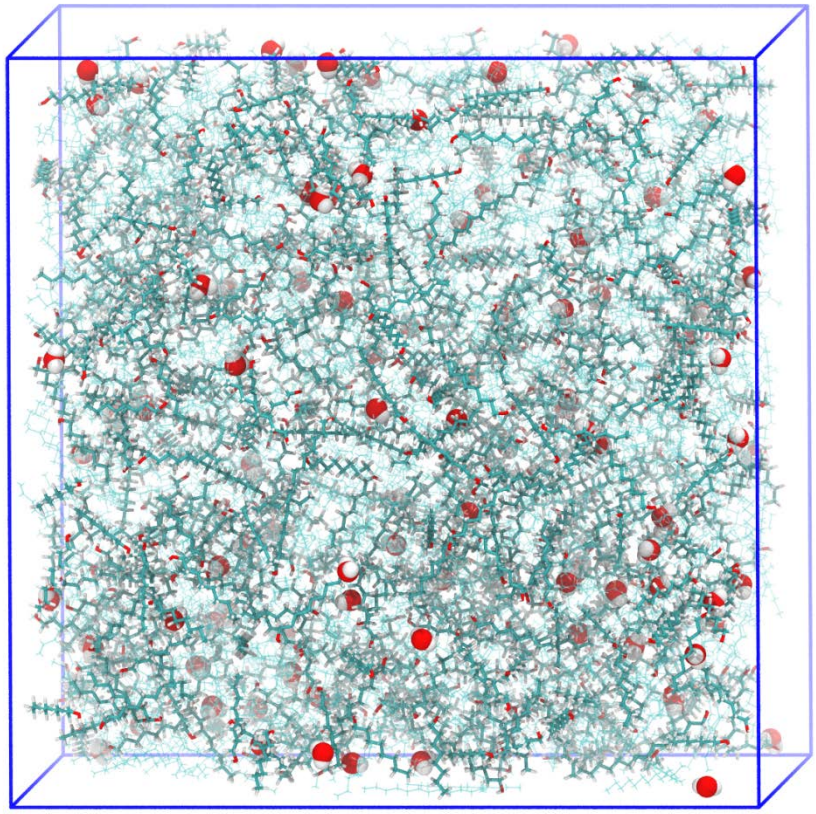

Figure AB-2. Initial structure of the atomistic simulation on the system with 2 M 1-octanol dissolved in bulk dodecane solution. All the molecules are randomly distributed using Packmol. The solute molecules (i.e., water and octanol) are highlighted for the display using VMD (via the VDW and Licorice drawing method, respectively).

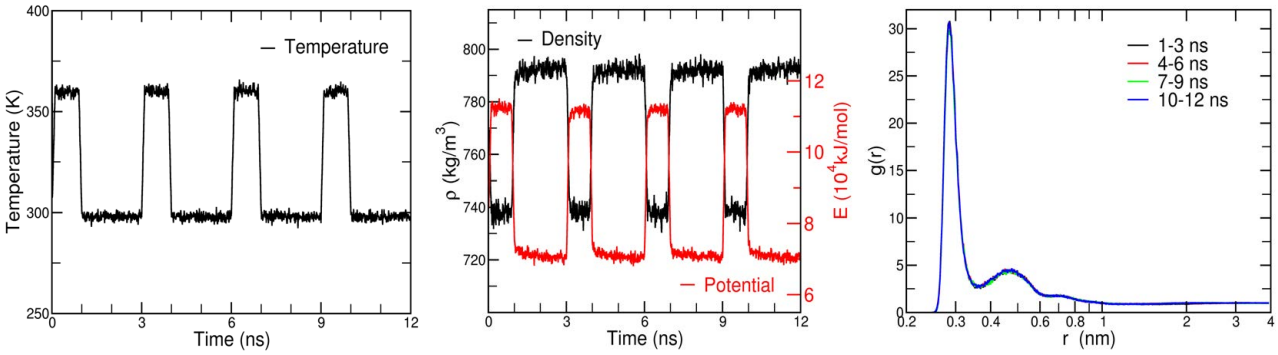

Figure AB-3. Equilibration of the annealing simulation on the system of 2 M 1-octanol dissolved in bulk dodecane solution. (a) Temperature; (b) density and potential energy; (d) RDF between octanol oxygen atoms at 298 K.

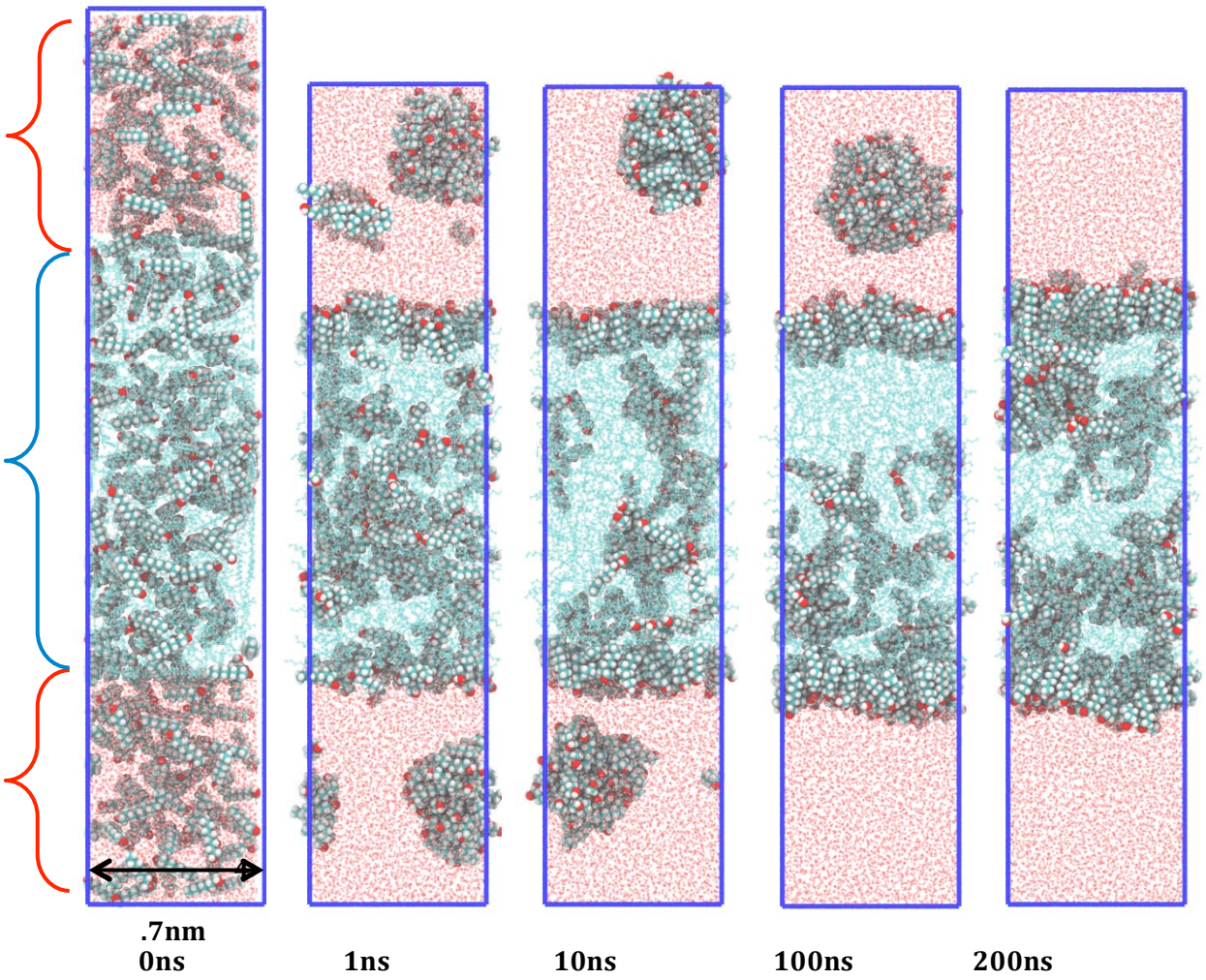

Figure AB-4. Snapshots of the atomistic simulations on the water/dodecane biphasic system with 2 M 1-octanol. The 1-octanol molecules (highlighted) are initially distributed in both the water phase and the organic phase. The solid blue lines denote the boundary of the simulation box under 3D periodic boundary conditions.

Table AB-1. Concentrations of Solutes (M) in the Atomistic Simulations on Bulk Dodecane Systems [a]

System	1-octanol	2-ethyl-hexanol	water
2 M 1-octanol	2	-	0.32
2 M 2-ethyl-hexanol	-	2	0.17
0.5 M 1-octanol	0.5	-	0.02
0.5 M 2-ethyl-hexanol	-	0.5	0.02

[a] These concentrations are obtained from the corresponding experiments.

Table AB-2. Number of Components in the Atomistic Simulations on Bulk Dodecane Systems [a,b]

System	1-octanol	2-ethyl-hexanol	water	dodecane	Time /ns [b]
2 M 1-octanol	600	-	96	920	12/50
2 M 2-ethyl-hexanol	-	600	51	920	12/50
0.5 M 1-octanol	150	-	6	1250	12/50
0.5 M 2-ethyl-hexanol	-	150	6	1250	12/50

[a] The equilibrium simulation box length is around 8 nm in each dimension.

[b] Annealing/production simulation time.

Table AB-3. Properties Calculated From the Atomistic Simulations on Bulk Dodecane Systems

System	Density /kg×m^{-3}	Cluster size
2M 1-octanol	792±2	5.3±0.3
2M 2-ethyl-hexanol	791±2	4.6±0.2
0.5M 1-octanol	771±2	5.2±0.5
0.5M 2-ethyl-hexanol	770±2	4.1±0.3

APPENDIX C: ADDITIONAL METHODS AND MESOPOROUS CARBON

AC.1. Motivation to develop organic-inorganic hybrid materials to protect extraction reagents from radiation induced damage

In metal sequestration processes involving highly radioactive material, radiolysis is a common event that has plagued aqueous separation for decades. These highly oxidizing environments, such as nuclear fuel reprocessing, produce electrophilic free radicals promoted through the deposition of the energy of radioactive decay on matter. As most extractants are large Lewis bases, the formation of free radicals is inevitable when exposed to high levels of radioactivity. This will invariably result in the formation of radiolytically induced degradation byproducts of the extraction reagents.

The development of organic-inorganic hybrid materials, consisting of an extraction reagent hosted by a mesoporous carbon nanostructure, has suggested that radiolytical "shielding" properties may exist thus preventing radiolysis from occurring. Therefore, these investigations evaluate this potential and assess the ability of organic-inorganic hybrid materials ability to prevent radiolytic degradation (**Figure AC-1; Figure AC-2**). In these studies, the extraction behavior of Eu^{3+} and Am^{3+} are evaluated with a di(2-ethylhexyl)-phosphoric acid (HDEHP) extractant in nitric acid media as well as extraction of Pa with aliphatic alcohol extractants.

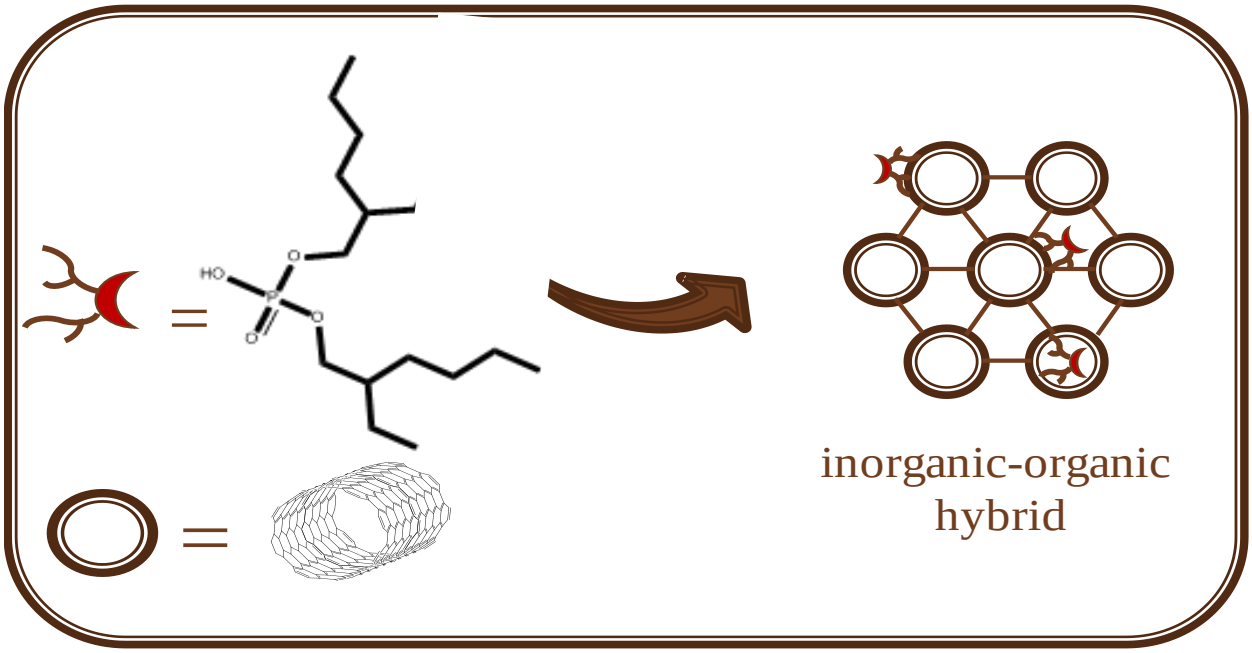

Figure AC-1. Schematic showing the CMK:HDEHP hybrid system. Figure provided by Peter Zalupski (INL).

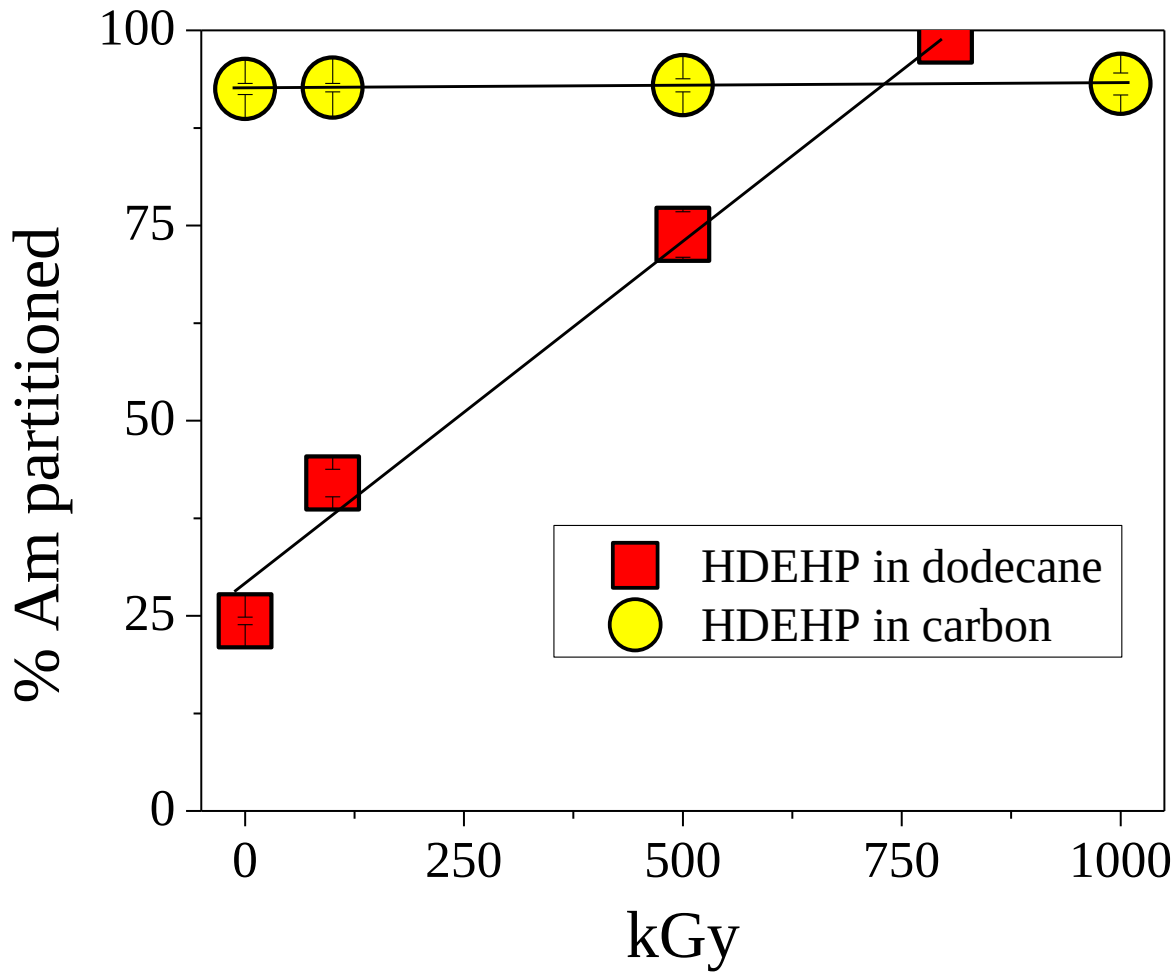

Figure AC-2. Percent Am extracted by HDEHP in solvent extraction and hybrid systems as a function of received dose. Figure provided by Peter Zalupski (INL).

AC.2. Methods

AC.2.1. Method for Preparing CMK-3 Hybrid Materials

For the preparation of the CMK/HDEHP hybrid at 40% w/w HDEHP:CMK. A suspension of 0.20 g of neat HDEHP (Aldrich, 97%) in 10 mL of 3 M HNO_3 was sonicated for 3 minutes to disperse the extractant into microdroplets. To this milky emulsion 0.20 g of CMK-3 (ACS Material, www.acsmaterial.com) was added. The suspension was vortexed for 1 hour. The extractant adheres to CMK quantitatively. The suspension is then isolated by filtration, washed with 3 M HDEHP, and deionized water. The collected solid is dried in the oven at 50° C, or on the bench overnight. The mass of the collected hybrid should additively illustrate that all HDEHP was immobilized on CMK (*i.e.* 0.40 g should be isolated). Once dry, the hybrid preparation is complete.

To prepare hybrid materials with aliphatic alcohols, the method is the same as described above but instead the 0.20 g of neat alcohol (*i.e.* 1-decanol) is added. Below shows the functionalization efficiency.

Table AC-1. The percent functionalization of extraction reagents.

Extraction Reagent	% Functionalized
HDEHP	39.5
1-decanol	39.3
1-octanol	1.2
2-ethyl-hexanol	0.5
2,6-dimethyl-4-heptanol	2.5

AC.2.2. Method to Evaluate Weight Distributions

To measure weight distribution values (D_w), 10 mg of CMK:hybrid material is weight out into a 15 mL centrifuge tube (n=3). The aqueous feed (containing acid, salt, and metal) is added to each tube (1 mL). The solutions are counted prior to phase separation to give the initial radioactivity added (A_o). The solutions are then vortexed for 1 hour and then the suspensions are filtered *via* 10 mL syringe fit with a PVDF filer disc at the end. The aqueous phases are collected from each solution (and filter properly discarded) into a liquid scintillation vial. Next a 0.5 mL aliquot is sampled and counted to determine the amount of metal adsorbed onto the mesoporous carbon hybrid (A_f). To calculate D_w, **Equation AC-1** is used:

$$D_w = \frac{A_o - A_f}{A_f} * \frac{v}{m} \qquad eq\ AC-1$$

where *v* is the volume of the aqueous feed solution and *m* is the mass of CMK:hybrid.

AC.2.3. Sample Irradiation

To observe the shielding capabilities of the CMK:hybrid, solutions were irradiated and subsequently analyzed by thermogravimetric analysis and solid state NMR to observe the presence of degradation byproducts. The samples were irradiated using a ^{137}Cs source with a flux of 24.8 Gy/minute. Samples were irradiated up to 500 kGy. Only solid, dry CMK:hybrid systems were irradiated in glass, no biphasic systems. Following irradiations the samples were kept in a deep freezer until analyses to assess the radiolytic degradation were performed.

AC.2.4. Thermogravimetric Analysis and Solid State NMR

Following irradiation samples were weighed and transferred for a thermogravimetric analysis (TGA). The TGA was purged with N_2 until all the O_2 has been purged from the sample cell. Once purged about 25 mg of CMK:hybrid material was place on the TGA pan and set on the sample

tray. The analysis protocol was set up with a ramp rate of 2 °C / min from 25 °C to 250 °C. This analysis provides a weight loss as a function of temperature profile.

The rationale for this approach to assess the radiolytic degradation of extraction reagents is, if the degradation products form, the temperature at which they are removed from the CMK framework would likely be different. Therefore the temperature profile of an irradiated sample would have a stepwise or broad trend versus a single weigh loss event in the sample that has not been irradiated.

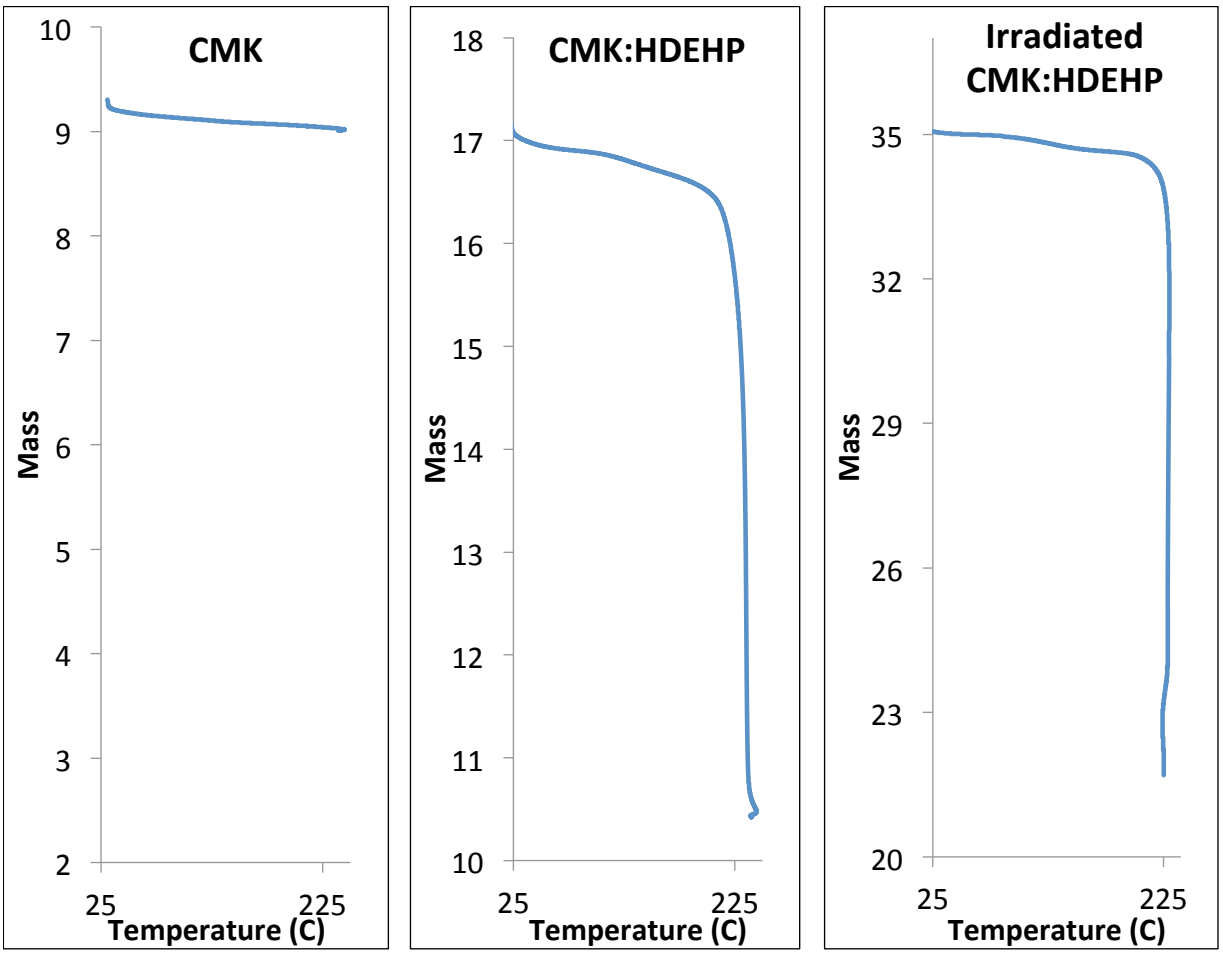

Figure AC-3. Thermogravimetric analysis of CMK material, CMK:HDEHP, and irradiate CMK:HDEHP.

From **Figure AC-3**, it is observed that the weight loss profile is not dependent on the irradiation of the CMK:HDEHP sample. This result would suggest that the CMK framework is preventing radiolysis from occurring.

Solid state NMR (^{13}C, ^{1}H, ^{31}P) was also used to assess the radiolytic degradation of extraction reagents in hybrid systems containing CMK:HDEHP. Following irradiation, samples were loaded into NMR tubes and transferred to the NMR facility with Fu Chen. The NMR was then tuned to probe the element of interest. The rationale for this analysis is, should radioytic degradation products form, the carbon, hydrogen, and phosphorous environments would be distinct and result in a noticeable shift in the NMR spectra.

Proton and carbon NMR provided very little helpful information. The ^{1}H spectrum was flooded with H environments as a result of a heterogeneous surface in the CMK material itself. The carbon environment produced indistinguishable carbon shifts. Upon looking into the degradation products of HDEHP (*i.e.* 2-ethyl-hexanol, mono-ethylhexyl-phosphoric acid, and phosphoric acid), it is realistic to conclude, even if radiolysis had occur, ^{13}C NMR would not distinguish these byproducts.

Based on the proposed radiolysis products, ^{31}P is a viable option to assess their formation as a function of dose. The results of the ^{31}P NMR experiments show different P environments following irradiation (>100 kGy) (**Figure AC-4**). This results suggests that radiolysis is occur in CMK:hybrid extraction materials. One possible explanation for the discrepancy between the NMR data and the distribution data (**Figure AC-2** is that the radiolysis products are no sufficiently hydrophobic to remain associated with the CMK material. This claim is supported by **Table AC-1**, in which the percent functionalization for all alcohols (except for 1-decanol) is extremely poor (<5% of the expected 40%). To add, one of those radiolytic degradation products is 2-ethyl-hexanol, which according to **Table AC-1**, resulted in a functionalization percent of 0.5%. Likewise, the degradation product phosphoric acid would not be expected to remain associated with the CMK material. Therefore when irradiated samples of CMK:HDHEP hybrids are used in extraction process, the radiolytic degradation products are simply expelled to the aqueous phase. The impact of this

process is much smaller than the incorporation of heterogeneous extraction reagent on the CMK framework.

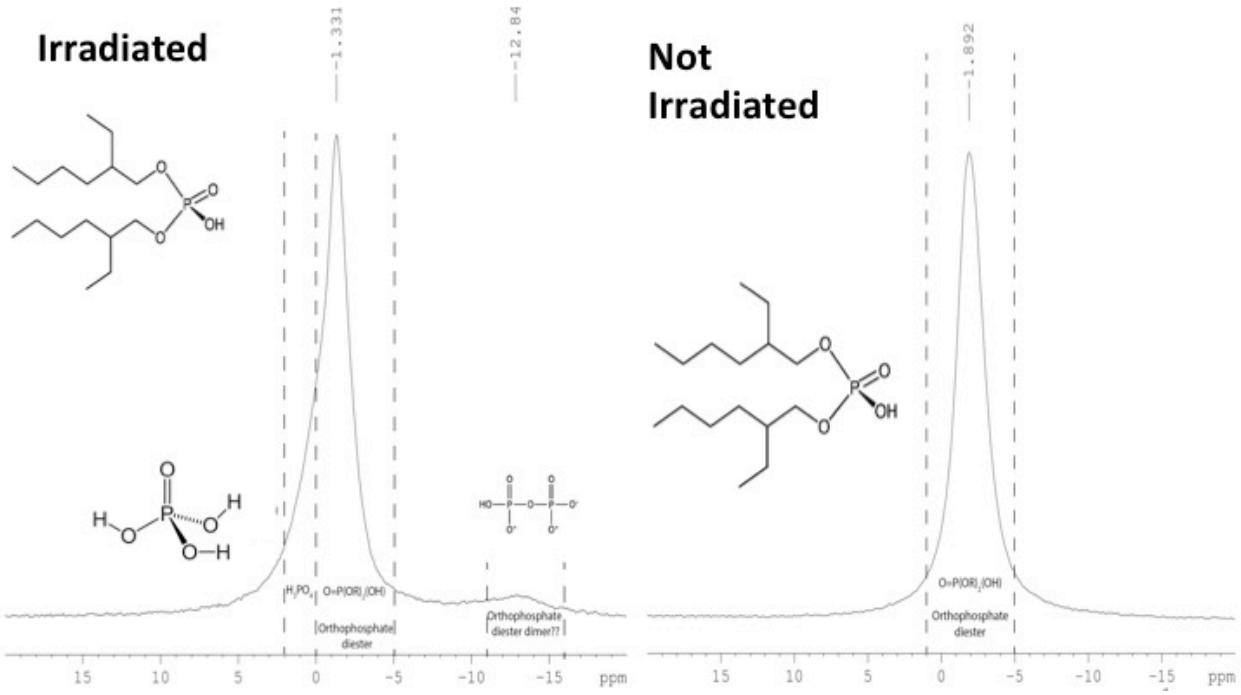

Figure AC-4. ^{31}P solid state NMR of irradiated and not irradiated CMK:HDEHP hybrid materials.

REFERENCES

1. *The Chemistry of the Actinide and Transactinide Elements*. Springer: Dordretch, Netherlands, 2010; Vol. 1.
2. Pal'shin, E. S., Myasoedov, B. F., Davydov, A. V, *Analytical Chemistry of Protactinium*. Ann Arbor-Humphrey Science Publishers, Inc: Ann Arbor, Michigan, 1970.
3. Siboulet, B.; Marsden, C. J.; Vitorge, P., What Can Quantum Chemistry Tell Us About Pa(v) Hydration and Hydrolysis? *New J. Chem.* **2008,** 32, (12), 2080-2094.
4. Wilson, R. E., Peculiar Protactinium. *Nat. Chem.* **2012,** 4, (7), 586-586.
5. Kirby, H. W., The Radiochemistry of Protactinium. *National Academy of Sciences National Research Council* **1959,** Nuclear Series, (NAS-NS 3016).
6. G. Choppin, J. R., *Radiochemistry and Nuclear Chemistry* Butterworth-Heinemann: Woburn, Ma, 2002.
7. Bourdon, B., Turner, S., Henderson, G. M., Lundstrom, C. C., Introduction to U-series Geochemistry. *Rev. Mineral. Geochem.* **2003,** 52, 1-21.
8. Knight, A. W.; Eitrheim, E. S.; Nelson, A. W.; Nelson, S.; Schultz, M. K., A Simple-Rapid Method to Separate Uranium, Thorium, and Protactinium for U-series Age-Dating of Materials. *J. Environ. Radioact.* **2014,** 134, (0), 66-74.
9. Peate, D. W.; Hawkesworth, C. J., U-Series Disequilibria: Insights into Mantle Melting and the Timescales of Magma Differentiation. *Rev. Geophys.* **2005,** 43, (1), 1-43.
10. Pickett, D. A.; Murrell, M. T.; Williams, R. W., Determination of Femtogram Quantities of Protoactinium in Geologic Samples by Thermal Ionization Mass-Spectrometry. *Anal. Chem.* **1994,** 66, (7), 1044-1049.
11. Regelous, M.; Turner, S. P.; Elliott, T. R.; Rostami, K.; Hawkesworth, C. J., Measurement of Femtogram Quantities of Protactinium in Silicate Rock Samples by Multicollector Inductively Coupled Plasma Mass Spectrometry. *Anal. Chem.* **2004,** 76, (13), 3584-3589.
12. Eppich, G. R., Williams, R. W., Gaffney, A. M., Schorzman, K. C., U-235/Pa-231 Age Dating of Uranium Materials for Nuclear Forensic Investigations. *J. Anal. Atom. Spectrom.* **2013,** 28, (5), 666-674.
13. Kumari, N.; Pathak, P. N.; Prabhu, D. R.; Manchanda, V. K., Solvent Extraction Studies of Protactinium for its Recovery from Short-Cooled Spent Fuel and High-Level Waste Solutions in Thorium Fuel Cycle Using Diisobutylcarbinol (DIBC) as Extractant. *Desalin. Water Treat.* **2012,** 38, (1-3), 46-51.
14. Morgenstern, A.; Apostolidis, C.; Mayer, K., Age Determination of Highly Enriched Uranium: Separation and Analysis of 231Pa. *Anal. Chem.* **2002,** 74, (21), 5513-5516.
15. Patterson, C., Age of Meteorites and the Earth. *Geochim. Cosmochim. Ac.* **1956,** 10, (4), 230-237.
16. National Nuclear Science Data Center. (Infomation Extracted from the NuDat 2 Data Base).
17. Nelson, A. W.; Knight, A. W.; May, D.; Eitrheim, E. S.; Schultz, M. K., Naturally-Occurring Radioactive Materials (NORM) Associated with Unconventional Drilling for Shale Gas. In *Hydraulic Fracturing: Environmental Issues*, American Chemical Society: 2015; Vol. 1216, pp 89-128.
18. Choppin, G. R.; Liljenzin, J.-O.; Rydberg, J., *Radiochemistry and Nuclear Chemistry*. 3rd ed.; Butterworth-Heinemann: Woburn, MA, 2002.
19. Kenton J. Moody, P. M. G., Ian D. Hutcheon, *Nuclear Forensic Analysis*. 2nd ed.; CRC Press: Boca Raton, Florida, 2014.
20. Chiarizia, R.; Jensen, M.; Borkowski, M.; Nash, K. L., New interpretation of third phase formation in the solvent extraction of actinides by TBP. *Abstr Pap Am Chem S* **2004,** 227, U1251-U1252.

21. Chiarizia, R.; Rickert, P. G.; Stepinski, D.; Thiyagarajan, P.; Littrell, K. C., SANS study of third phase formation in the HCl-TBP-n-octane system. *Solvent Extr. Ion Exch.* **2006,** 24, (2), 125-148.
22. In *Use of Reprocessed Uranium* Technical Committee Meeting, Vienna, Austria August 2007, 2007; International Atomic Energy Agency: Vienna, Austria 2007.
23. Simpson, M. F.; Law, J. D. *Nuclear Fuel Reprocessing*; Idaho National Laboratory Idaho Falls, Idaho, 2010.
24. Chiarizia, R.; Gatrone, R. C.; Horwitz, E. P., Am(Iii) and Eu(Iii) Extraction by Aliquat-Center-Dot-336 and Benzyl Substituted Quaternary Ammonium-Salts from Nitrate and Thiocyanate Solutions. *Solvent Extr. Ion Exch.* **1995,** 13, (4), 615-645.
25. *Ion Exchange and Solvent Extraction: A Series of Advances*. Taylor & Francis Group, LLC: Boca Raton, FL, 2010; Vol. 19.
26. Chiarizia, R., Gatrone, R. C., Horwitz, E. P., Am(III) and Eu(III) Extraction by Aliquat-336 and Benzyl Substituted Quaternary Ammonium Salts from Nitrate and Thiocyanate Solutions *Solvent Extr. Ion Exch.* **1995,** 13, (4), 615-645.
27. Hallerod, J.; Ekberg, C.; Foreman, M.; Engdahl, E. L.; Aneheim, E., Stability of phenyl trifluoromethyl sulfone as diluent in a grouped actinide extraction process. *J Radioanal Nucl Ch* **2015,** 304, (1), 287-291.
28. Losh, L., Fuel Qualification Plan. In Energy, D. o., Ed. 2001; Vol. 2.
29. Nash, K. L.; Rickert, P. G.; Horwitz, E. P., Degradation of Truex-Dodecane Process Solvent. *Solvent Extr. Ion Exch.* **1989,** 7, (4), 655-675.
30. Horwitz, E. P.; Dietz, M. L.; Chiarizia, R.; Diamond, H.; Maxwell, S. L.; Nelson, M. R., Separation and Preconcentration of Actinides by Extraction Chromatography Using a Supported Liquid Anion-Exchanger - Application to the Characterization of High-Level Nuclear Waste Solutions. *Anal Chim Acta* **1995,** 310, (1), 63-78.
31. Landgren, A.; Liljenzin, J. O., Extraction behaviour of technetium and actinides in the Aliquat-336/nitric acid system. *Solvent Extr. Ion Exch.* **1999,** 17, (6), 1387-1401.
32. Horwitz, E. P. Extraction Chromatography of actinides and Selected Fission Products: Principles and Achievement of Selectivity. http://www.eichrom.com/eichrom/products/extraction.aspx (30 June 2016),
33. Maxwell, S. L.; Culligan, B. K.; Hutchison, J. B.; Spencer, R. B., Rapid Fusion Method for Determination of Actinides in Fecal Samples. *J. Radioanal. Nucl. Chem* **2013,** 298, (3), 1533-1542.
34. Kressin, I. K., Electrodeposition of Plutonium and Americium for High-Resolution Alpha Spectrometry. *Anal. Chem.* **1977,** 49, (6), 842-846.
35. Garcia-Torano, E., Current status of alpha-particle spectrometry. *Appl Radiat Isotopes* **2006,** 64, (10-11), 1273-1280.
36. Pomme, S., Typical uncertainties in alpha-particle spectrometry. *Metrologia* **2015,** 52, (3), S146-S155.
37. Emsley, J., Protactinium In *Nature's Building Blocks: An A to Z Guide to the Elements* Oxford University Press: Oxford, England, UK, 2003.
38. Rosman, K. J. R.; Taylor, P. D. P., Isotopic Compositions of the Elements 1997. *Journal of Physical and Chemical Reference Data* **1998,** 27, (6), 1275-1287.
39. Yokoyama, Y.; Falgueres, C.; deLumley, M. A., Direct dating of a Qafzeh Proto-Cro-Magnon skull by non destructive gamma-ray spectrometry. *Cr Acad Sci Ii A* **1997,** 324, (9), 773-779.
40. Schwarcz, H. P.; Simpson, J. J.; Stringer, C. B., Neanderthal skeleton from Tabun: U-series date by gamma-ray spectrometry. *J Hum Evol* **1998,** 34, (3), A18-A19.
41. Koornneef, J. M.; Stracke, A.; Aciego, S.; Reubi, O.; Bourdon, B., A New Method for U-Th-Pa-Ra Separation and Accurate Measurement of U-234, Th-230, Pa-231, Ra-226 Disequilibria in Volcanic Rocks by MC-ICP-MS. *Chem. Geol.* **2010,** 277, (1-2), 30-41.
42. Richards, D. A.; Dorale, J. A., Uranium-Series Chronology and Environmental Applications of Speleothems. *Uranium-Series Geochemistry* **2003,** 52, 407-460.

43. Sims, K. W. W.; Pichat, S.; Reagan, M. K.; Kyle, P. R.; Dulaiova, H.; Dunbar, N. W.; Prytulak, J.; Sawyer, G.; Layne, G. D.; Blichert-Toft, J.; Gauthier, P. J.; Charette, M. A.; Elliott, T. R., On the Time Scales of Magma Genesis, Melt Evolution, Crystal Growth Rates and Magma Degassing in the Erebus Volcano Magmatic System Using the U-238, U-235 and Th-232 Decay Series. *J. Petrol.* **2013,** 54, (2), 235-271.
44. Kaltsoyannis, N., Covalency Hinders AnO2(H2O)+ → AnO(OH)2+ Isomerisation (An = Pa-Pu). *Dalton Trans.* **2016,** 45, (7), 3158-3162.
45. Toraishi, T.; Tsuneda, T.; Tanaka, S., Theoretical Study on Molecular Property of Protactinium(V) and Uranium(VI) Oxocations: Why Does Protactinium(V) Form Mono-oxo Cations in Aqueous Solution? *J. Phys. Chem. A* **2006,** 110, (49), 13303-13309.
46. Sill, C. W., Preparation of Protactinium-233 Tracer. *Anal. Chem.* **1966,** 38, (11), 1458.
47. Orlandini, K. A.; Wahlgren, M. A.; Barclay, J., Solvent extraction studies with a hydrochloric acid-2-ethylhexanol system. *Anal. Chem.* **1965,** 37, (9), 1148-51.
48. Robert C. Aller, J. K. C., Th-234/U-238 Disequilibrium in Near-Shore Sediment: Particle Reworking and Diamagnetic Time Scales. *Earth Planet. Sci. Lett.* **1976,** 29, 37-50.
49. Chabaux, F., Blaes, E., Stille, P., Roupert, R. D., Pelt, E., Dosseto, A., Ma, L., Buss, H. L., Brantley, S. L., Regolith Formation Rate from U-series Nuclides: Implications from the Study of a Spheroidal Weathering Profile in the Rio Icacos Watershed (Puerto Rico). *Geochim. Cosmochim. Ac.* **2013,** 100, 73-95.
50. Ivanovich, M.; Latham, A. G.; Ku, T.-L., Uranium-Series Disequilibrium: Applications to Earth, Marine, and Enviromental Problems. **1992**, 62-94.
51. Martínez-Aguirre, A., Alcaraz Pelegrina, J.M., U/Th Dating of Carbonate Deposites from Chafarinas Islands, Spain. . *J. Radioanal. Nucl. Chem* **2013,** 298, (2), 1005-1016.
52. Mola, M., Nieto, A., Peñalver, A., Borrull, F., Aguilar, C.,, Uranium and Throium Sequential Separation from NORM Samples by Using an SIA System. *Journal of Enviornmental Radioactivity* **2014,** 127, 82-87.
53. El-Sweify, F. H.; Abdel Fattah, A. A.; Ali, S. M., Comparative Studies on the Extraction of Protactinium Using Different Kinds of Organic Extractants. *Separ. Sci. Technol.* **2009,** 44, (3), 753-772.
54. Negre, C.; Thomas, A. L.; Mas, J. L.; Garcia-Orellana, J.; Henderson, G. M.; Masque, P.; Zahn, R., Separation and Measurement of Pa, Th, and U Isotopes in Marine Sediments by Microwave-Assisted Digestion and Multiple Collector Inductively Coupled Plasma Mass Spectrometry. *Anal. Chem.* **2009,** 81, (5), 1914-1919.
55. Jeandel, C.; Venchiarutti, C.; Bourquin, M.; Pradoux, C.; Lacan, F.; van Beek, P.; Riotte, J., Single Column Sequential Extraction of Ra, Nd, Th, Pa and U from a Natural Sample. *Geostand. Geoanal. Res.* **2011,** 35, (4), 449-459.
56. Makarova, T. P.; Preobrazhenskaya, L. D.; Lovtsyus, A. V.; Fridkin, A. M.; Stepanov, A. V.; Lipovskii, A. A.; Belyaev, B. N., Application of Isotope-Dilution Method for Mass-Spectrometric and Alpha-Spectrometric Determination of Burn-up and Uranium, Plutonium and Transplutonium Element Content in Vver-440 Spent Fuel. *J. Radioanal. Chem.* **1983,** 80, (1-2), 173-182.
57. Oviatt, C. G., Lake Bonneville Fluctuations and Global Climate Change. *Geology* **1997,** 25, (2), 155-158.
58. Currie, L. A., Limits For Qualitative Detection and Quantitative Determination. *Anal. Chem.* **1968,** 40, (3), 586-593.
59. McCabe, W. J.; Ditchburn, R. G.; Whitehead, N. E., Method for Separation of Polonium, Thorium, Protactinium, and Uranium in High Yields from Various Matrixes. *J. Radioanal. Nucl. Chem* **1992,** 159, (2), 267-79.
60. Burnett, W. C., Yeh, C. C., Separation of Protactinium From Geochemical Materials via Extraction Chromatography. *Radioactivity and Radiochemistry* **1995,** 6, (4), 22-32.
61. Horwitz, E. P.; Dietz, M. L.; Chiarizia, R.; Diamond, H.; Maxwell, S. L.; Nelson, M. R., Separation and Preconcentration of Actinides by Extraction Chromatography Using a Supported Liquid Anion exchanger: Application to the Characterization of High-Level Nuclear Waste Solutions. *Anal. Chim. Acta.* **1995,** 310, 63-78.

62. Inn, K. G. W., Hall, E., Woodward IV, J. T., Stewart, R., Pollanen, L. Selvig, S. Turner, I. Outola, S. Nour, H. Kurosaki, J. LaRosa, M. Schultz, Z. Lin, Z. Yu, McMahon, C., Use of Thin Collodion Films to Prevent Recoil-Ion Contamination of Alpha Spectrometry Detectors *J. Radioanal. Nucl. Chem* **2008,** 276, (2), 385-390.
63. Hull, C. D., Burnett, B., Cable, P. Yeh, C. C., U- Series Dating Using Extraction Chromatography. *38th Annual Conference on Bioassy, Analytical and Environmental Radiochemistry* **1992**.
64. Tiessen, H.; Roberts, T. L.; Stewart, J. W. B., Carbonate Analysis in Soils and Minerals by Acid Digestion and 2-Endpoint Titration. *Commun. Soil Sci. Plan.* **1983,** 14, (2), 161-166.
65. Sill, C. W.; Puphal, K. W.; Hindman, F. D., Simultaneous Determination of Alpha-Emitting Nuclides of Radium through Californium in Soil. *Anal. Chem.* **1974,** 46, (12), 1725-1737.
66. Eskandari Nasab, M., Solvent Extraction Separation of Uranium (VI) and Thorium (IV) with Neutral Organophosphorus and Amine Ligands *Fuel* **2014,** 116, 595-600.
67. Vandenhove, H. H., C.; Payne, T. , *Radionuclides In the Environment* John Wiley and Sons Ltd: West Sussex, 2010.
68. Cotton, F. A., *Advanced Inorganic Chemistry* Wiley: New York, 1999.
69. Katz, J. J., *The Chemistry of the Actinide and Transactinide Elements*. Springer: Dordretch, 2006.
70. Mendes, M.; Aupiais, J.; Jutier, C.; Pointurier, F., Determination of Weight Distribution Ratios of Pa(V) and Np(V) with Some Extraction Chromatography Resins and the AG1-X8 Resin. *Anal. Chim. Acta.* **2013,** 780, 110-116.
71. Sill, C. W.; Hindman, F. D.; Anderson, J. I., Simultaneous Determination of Alpha-Emitting Nuclides of Radium Through Californium in Large Environmental and Biological Samples. *Anal. Chem.* **1979,** 51, (8), 1307-1314.
72. Gabriels, R., A General Method for Calculating Detection Limit in Chemical Analysis. *Anal. Chem.* **1970,** 42, (12), 1439.
73. Keegan, R. P.; Gehrke, R. J., A Method to Determine the Time Since Last Purification of Weapons Grade Plutonium. *Appl. Radiat. Isot.* **2003,** 59, (2–3), 137-143.
74. De Sio, S. M., Wilson, R. E., Structural and Spectroscopic Studies of Fluoroprotactinates. *Inorg. Chem.* **2014,** 53, (3), 1750-1755.
75. Uhlir, J., Fluoride Technologies Applications Within Molten-Salt Reactors Fuel Cycle. In *Fluorinated Materials For Energy Conversion*, Nakajima, T.; Groult, H., Eds. Elsevier Amsterdam, The Netherlands 2005.
76. Turner, D. R.; Pabalan, R. T.; Bertetti, F. P., Neptunium(V) Sorption on Montmorillonite: An Experimental and Surface Complexation Modeling Study. *Clay Clay Miner.* **1998,** 46, (3), 256-269.
77. Zhao, P.; Tinnacher, R. M.; Zavarin, M.; Kersting, A. B., Analysis of Trace Neptunium in the Vicinity of Underground Nuclear Tests at the Nevada National Security Site. *J. Environ. Radioact.* **2014,** 137, (0), 163-172.
78. Nakata, K.; Fukuda, T.; Nagasaki, S.; Tanaka, S.; Suzuki, A.; Tanaka, T.; Muraoka, S., Sorption of Neptunium on Iron-Containing Minerals. *Czech. J. Phys.* **1999,** 49, 159-166.
79. Bubernak, J., Lew, M. S., Matlack, George M., Ion Exchange, Extraction, Separation, and Radiochemical Determination of Neptunium-237 in Plutonium-238. *Anal. Chim. Acta.* **1969,** 48, (2), 233-41.
80. Carolyn A. Tylenda, D. J., Lisa Ingerman, Gloria Sage, Lara Chappell, Toxicological Profile for Fluorides, Hydrogen Fluoride, and Fluorine. In Registry, A. f. T. S. a. D., Ed. Atlanta, GA, 2001.
81. Horwitz, E. P.; McAlister, D. R.; Dietz, M. L., Extraction Chromatography Versus Solvent Extraction: How Similar are They? *Separ. Sci. Technol.* **2006,** 41, (10), 2163-2182.

82. Nelson, A. W.; May, D.; Knight, A. W.; Eitrheim, E. S.; Mehrhoff, M.; Shannon, R.; Litman, R.; Schultz, M. K., Matrix Complications in the Determination of Radium Levels in Hydraulic Fracturing Flowback Water from Marcellus Shale. *Environ. Sci. Technol. Lett.* **2014,** 1, (3), 204-208.
83. Le Naour, C.; Trubert, D.; Di Giandomenico, M. V.; Fillaux, C.; Den Auwer, C.; Moisy, P.; Hennig, C., First Structural Characterization of a Protactinium(V) Single Oxo Bond in Aqueous Media. *Inorg. Chem.* **2005,** 44, (25), 9542-9546.
84. Tananaev, I. G.; Dzyubenko, V. I., Reaction of Neptunium (V) with Hydrogen Peroxide in Nitric Acid Solutions. *Soviet Radiochemistry (English Translation)* **1989,** 30, (6), 797-800.
85. Burney, G. A., Harbour, R. M., The Radiochemistry of Neptunium. *National Academy of Sciences National Research Council* **1974,** Nuclear Series.
86. Johnsen, A. M. Neptunium Dioxide Precipitation Kinetics in Aqueous Systems University of California- Berkeley, Berkeley, California 2008.
87. Mendes, M.; Leguay, S.; Le Naour, C.; Hamadi, S.; Roques, J.; Moisy, P.; Guillaumont, D.; Topin, S.; Aupiais, J.; Den Auwer, C.; Hennig, C., Thermodynamic Study of the Complexation of Protactinium(V) with Diethylenetriaminepentaacetic Acid. *Inorg. Chem.* **2013,** 52, (13), 7497-7507.
88. Guillaumont, R.; Bouissie, G.; Muxart, R., Protactinium Chemistry: 1. Aqueous Solutions of Penta- and Tetravalent Protactinium. *Actin. Rev.* **1968,** 1, (2), 135.
89. Scherff, H. L.; Herrmann, G., Ionic Species of Pentavalent Protactinium in Hydrochloric Acid Solutions. *Radiochim. Acta* **1966,** 6, (2), 53-&.
90. King, J. C., *Separation & Purification: Critical Needs and Opportunities* National Academy Press: Washington, D. C., 1987.
91. *Spent Nuclear Fuel Assay Data for Isotopic Validation*; 2011.
92. Rydberg, J., Musikas, C., Choppin, G. R., Cox, M, *Solvent Extraction Principles and Practices* 2nd ed.; Marcel Dekker: New York, 2004.
93. MARLAP, 14.4 Solvent Extraction. In *Multi-Agency Radiological Laboratory Analytical Protocols Manual (MARLAP)*, Environmental Protection Agency: 2004.
94. Energy, U. S. D. o. *Nuclear Separations Technologies Workshop Report: Getting From Where We Are to Where We Want to be in Nuclear Separations Technologies*; Bethesda, Maryland, 2011.
95. Rampolla, D. S. Method of Increasing the Deterrent to Proliferation of Nuclear Fuels. 1982.
96. Trianti, N.; Su'ud, Z.; Riyana, E. S., Design Study of Thorium-232 and Protactinium-231 Based Fuel for Long Life BWR. *Aip. Conf. Proc.* **2012,** 1448, 96-100.
97. Imamura, T.; Saito, M.; Yoshida, T.; Artisyuk, V., Production of Pa–U Fuel with Proliferation Resistance by 14 MeV Neutron for Long-life Core. *J. Nucl. Sci. Technol.* **2004,** 40, (6), 655-664.
98. Tsvetkov, P. V.; Kryuchkov, E. F.; Shmelev, A. N.; Apse, V. A.; Kulikov, G. G.; Masterov, S. V.; Kulikov, E. G.; Glebov, V. B., Isotopic Uranium and Plutonium Denaturing as an Effective Method for Nuclear Fuel Proliferation Protection in Open and Closed Fuel Cycles. In 2011.
99. Berry, J. A., Hobley, J., Lane, S. A., Littleboy, A. K., Nash, M. J., Oliver, P., Smith-Briggs, J. L., Williams, S. J., Solubility and Sorption of Protactinium in Near-field and Far-field Environments of a Radioactive Waste Repository *Analyst* **1989,** 114, 339-347.
100. Forbes, T. Z.; Burns, P. C.; Soderholm, L.; Skanthakumar, S., Hydrothermal Synthesis and Structure of Neptunium(V) Oxide. *Mater. Res. Soc. Symp. P.* **2007,** 985, 401-406.
101. Knight, A. W. N., A. W.; Eitrheim, E. S.; Forbes, T. Z. .; Schultz, M. K., A Chromatographic Separation of Neptunium and Protactinium Using 1-octanol Impregnated onto a Solid Phase Support. *J. Radioanal. Nucl. Chem* **2015,** DOI 10.1007/s10967-015-4124-3.
102. Box, G. E. P., Hunter, W. G., Hunter, J. S. , *Statistics for Experimenters: An Introduction to Design Analysis and Model Building*. John Wiley and Sons New York, NY, 1978.

103. Schultz, M. K.; Inn, K. G. W.; Lin, Z. C.; Burnett, W. C.; Smith, G.; Biegalski, S. R.; Filliben, J., Identification of Radionuclide Partitioning in Soils and Dediments: Determination of Optimum Conditions for the Exchangeable Fraction of the NIST Standard Sequential Extraction Protocol. *Appl. Radiat. Isot.* **1998,** 49, (9–11), 1289-1293.
104. Silva, A.; Delerue-Matos, C.; Fiuza, A., Use of Solvent Extraction to Remediate Soils Contaminated with Hydrocarbons. *J. Hazard. Mater.* **2005,** 124, (1-3), 224-229.
105. Casey, A. T., Maddock, A. G., The Chemistry of Protactinium: 4. Some Spectrophotometric Observations. *J. Inorg. Nucl. Chem.* **1959,** 10, (1-2), 58-68.
106. Guillaumont, R.; Muxart, R.; Bouissieres, G.; Haissinsky, M., Spectres Dabsorption Du Protactinium En Solution Aqueuse. *J. Chim. Phys. Pcb.* **1960,** 57, (11-2), 1019-1028.
107. Hardy, C. J.; Scargill, D.; Fletcher, J. M., Studies on Protactinium(V) in Nitric Acid Solutions. *J. Inorg. Nucl. Chem.* **1958,** 7, (3), 257-275.
108. Spitsyn, V. I.; Dyachkov.Ra, Concentrating 231Pa from Uranium Production Waste. *J. Nucl. Energy. Ab.* **1964,** 18, (12PA), 731.
109. Hochberg, Y.; Tamhane, A. C., *Multiple Comparison Procedures*. Wiley: New York, 1987.
110. Spitsyn, V. I.; D'Yachkova, R. A.; Khlebnikov, V. P., State of Protactinium in Nitrate Solutions. *Dokl. Akad. Nauk SSSR* **1964,** 157, (1), 135-8.
111. Theil, H., *Principles of Econometrics*. John Wiley & Sons: New York, 1971.
112. Theil, H., *Economic Forecasts and Policy*. 2nd Edition ed.; North Holland, Amsterdam, 1961.
113. Anderson, M. J., Whitcomb, P. J., *DOE Simplified: Practical Tools for Effective Experimentation*. Productivity New York, NY, 2007.
114. Edwards, R. L., Gallup, C. D., Cheng, H. , Uranium-series Dating of Marine and Lacustrine Carbonates. *Rev. Mineral. Geochem.* **2003,** 52, 363-405.
115. Wilson, R., Retrieval and Purification of an Aged 231Pa Source from its Decay Daughters. *Radiochim. Acta* **2014** 102, (6), 505-511.
116. Danesi, P. R., Chiarizia, Renato, Scibona, Giancarlo, The Meaning of Slope Analysis in Solvent Extraction Chemistry. *J. Inorg. Nucl. Chem.* **1970,** 32, (7), 2349-2355.
117. Moyer, B. A.; McDowell, W. J.; Baes, C. F.; Case, G. N.; Case, F. I., Liquid-Liquid Equilibrium Analysis in Perspective: Part 1. Slope Analysis of the Extraction of Uranyl Nitrate from Nitric Acid by Di-2-ethyl-hexylsulfoxide. *Solvent Extr. Ion Exch.* **1991,** 9, (5), 833-864.
118. Andrew W. Knight, E. S. E., Andrew W. Nelson, Michael K. Schultz, A Calculation Model for Liquid-liquid Extraction of Protactinium by 2,6-dimethyl-4-heptanol. *Nukleonika* **2015,** 60, (4), 837–845.
119. Robinson, R. A.; Stokes, R. H., *Electrolyte Solutions*. 2nd ed.; Dover Publications Mineola, New York, 2002.
120. Jr., W. D.; Bruin, H. J. D., New Activity Coefficients of 0-100 per cent aqueous nitric acid *J. Inorg. Nucl. Chem.* **1964,** 26, (6), 1069-1093.
121. Petrova, A. M.; Nikolaev, A. E.; Kasikov, A. G., Extraction of Gold(III) from Hydrochloric Acid Solutions with High-Molecular Aliphatic Alcohols. *Russian Journal of Applied Chemistry* **2014,** 87, (2), 234-240.
122. De Sio, S. M., Wilson, Richard E., EXAFS Study of the Speciation of Protactinium(V) in Aqueous Hydrofluoric Acid Solutions. *Inorg. Chem.* **2014,** 53, (23), 12643-12649.
123. Witten, T. A., Structured Fluids. *Phys Today* **1990,** 43, (7), 21-28.
124. Rosen, M. J.; Kunjappu, J. T., *Surfactants and Interfacial Phenomena*. 4th ed.; Wiley New Jersey, 2012.
125. Danielsson, I.; Lindman, B., The Definition of Microemulsion. *Colloids Surf., A* **1981,** 3, (4), 391-392.
126. Malik, M. A.; Wani, M. Y.; Hashim, M. A., Microemulsion method: A novel route to synthesize organic and inorganic nanomaterials: 1st Nano Update. *Arabian J. Chem.* **2012,** 5, (4), 397-417.

127. Flanagan, J.; Singh, H., Microemulsions: A Potential Delivery System for Bioactives in Food. *Crit. Rev. Food. Sci.* **2006,** 46, (3), 221-237.
128. Schottl, S.; Marcus, J.; Diat, O.; Touraud, D.; Kunz, W.; Zemb, T.; Horinek, D., Emergence of Surfactant-Free Micelles from Ternary Solutions. *Chem. Sci.* **2014,** 5, (8), 2949-2954.
129. Schottl, S.; Touraud, D.; Kunz, W.; Zemb, T.; Horinek, D., Consistent definitions of "the interface" in surfactant-free micellar aggregates. *Colloid Surf., A* **2015,** 480, 222-227.
130. Zemb, T.; Klossek, M.; Lopian, T.; Marcus, J.; Schottl, S.; Horinek, D.; Prevost, S.; Touraud, D.; Diat, O.; Marcelja, S.; Kunz, W., How to explain microemulsions formed by solvent mixtures without conventional surfactants. *Proc. Natl. Acad. Sci.* **2016**.
131. Bauduin, P.; Testard, F.; Zemb, T., Solubilization in Alkanes by Alcohols as Reverse Hydrotropes or "Lipotropes". *J. Phys. Chem. B* **2008,** 112, (39), 12354-12360.
132. Tomšič, M.; Jamnik, A.; Fritz-Popovski, G.; Glatter, O.; Vlček, L., Structural Properties of Pure Simple Alcohols from Ethanol, Propanol, Butanol, Pentanol, to Hexanol: Comparing Monte Carlo Simulations with Experimental SAXS Data. *J. Phys. Chem. B* **2007,** 111, (7), 1738-1751.
133. Dixit, S.; Crain, J.; Poon, W. C. K.; Finney, J. L.; Soper, A. K., Molecular segregation observed in a concentrated alcohol-water solution. *Nature* **2002,** 416, (6883), 829-832.
134. Sassi, P.; Morresi, A.; Paolantoni, M.; Cataliotti, R. S., Structural and dynamical investigations of 1-octanol: A spectroscopic study. *J. Mol. Liq.* **2002,** 96-7, 363-377.
135. Iwahashi, M.; Hayashi, Y.; Hachiya, N.; Matsuzawa, H.; Kobayashi, H., Self-Association of Octan-1-Ol in the Pure Liquid-State and in Decane Solutions as Observed by Viscosity, Self-Diffusion, Nuclear-Magnetic-Resonance and near-Infrared Spectroscopy Measurements. *J. Chem. Soc., Faraday Trans.* **1993,** 89, (4), 707-712.
136. Eicke, H. F., Aggregation in Surfactant Solutions - Formation and Properties of Micelles and Micro-Emulsions. *Pure Appl. Chem.* **1980,** 52, (5), 1349-1357.
137. Qiao, B.; Demars, T.; de la Cruz, M. O.; Ellis, R. J., How Hydrogen Bonds Affect the Growth of Reverse Micelles around Coordinating Metal Ions. *J. Phys. Chem. Lett.* **2014,** 5, (8), 1440-1444.
138. Ferru, G.; Gomes Rodrigues, D.; Berthon, L.; Diat, O.; Bauduin, P.; Guilbaud, P., Elucidation of the Structure of Organic Solutions in Solvent Extraction by Combining Molecular Dynamics and X-ray Scattering. *Angew. Chem. Int. Ed.* **2014,** 53, (21), 5346-5350.
139. Ferru, G.; Reinhart, B.; Bera, M. K.; Olvera de la Cruz, M.; Qiao, B.; Ellis, R. J., The Lanthanide Contraction beyond Coordination Chemistry. *Chem. Eur. J.* **2016,** 22, (20), 6899-6904.
140. Scholz, E., *Karl Fischer Titration: Determination of Water*. Springer: Berlin 1984.
141. Percus, J. K.; Yevick, G. J., Analysis of Classical Statistical Mechanics by Means of Collective Coordinates. *Phys. Rev.* **1958,** 110, (1), 1-13.
142. Qiao, B.; Ferru, G.; Olvera de la Cruz, M.; Ellis, R. J., Molecular Origins of Mesoscale Ordering in a Metalloamphiphile Phase. *ACS Cent. Sci.* **2015,** 1, (9), 493-503.
143. Hess, B.; Kutzner, C.; van der Spoel, D.; Lindahl, E., GROMACS 4: Algorithms for Highly Efficient, Load-Balanced, and Scalable Molecular Simulation. *J. Chem. Theory Comput.* **2008,** 4, (3), 435-447.
144. Vanommeslaeghe, K.; Hatcher, E.; Acharya, C.; Kundu, S.; Zhong, S.; Shim, J.; Darian, E.; Guvench, O.; Lopes, P.; Vorobyov, I.; Mackerell, A. D., CHARMM general force field: A force field for drug-like molecules compatible with the CHARMM all-atom additive biological force fields. *J. Comput. Chem.* **2010,** 31, (4), 671-690.
145. Bjelkmar, P.; Larsson, P.; Cuendet, M. A.; Hess, B.; Lindahl, E., Implementation of the CHARMM Force Field in GROMACS: Analysis of Protein Stability Effects from Correction Maps, Virtual Interaction Sites, and Water Models. *Journal of Chemical Theory and Computation* **2010,** 6, (2), 459-466.

146. Martínez, L.; Andrade, R.; Birgin, E. G.; Martínez, J. M., PACKMOL: A Package for Building Initial Configurations for Molecular Dynamics Simulations. *J. Comput. Chem.* **2009,** 30, (13), 2157-2164.
147. Vo, Q. N.; Hawkins, C. A.; Dang, L. X.; Nilsson, M.; Nguyen, H. D., Computational Study of Molecular Structure and Self-Association of Tri-n-butyl Phosphates in n-Dodecane. *J. Phys. Chem. B* **2015,** 119, (4), 1588-1597.
148. Cheng, A.; Merz, K. M., Application of the Nosé−Hoover Chain Algorithm to the Study of Protein Dynamics. *J. Phys. Chem.* **1996,** 100, (5), 1927-1937.
149. Parrinello, M.; Rahman, A., Polymorphic transitions in single crystals: A new molecular dynamics method. *J. Appl. Phys.* **1981,** 52, (12), 7182-7190.
150. Darden, T.; York, D.; Pedersen, L., Particle mesh Ewald: an N·log(N) method for Ewald sums in large systems. *J. Chem. Phys.* **1993,** 98, 10089-92.
151. Essmann, U.; Perera, L.; Berkowitz, M. L.; Darden, T.; Lee, H.; Pedersen, L., A Smooth Particle Mesh Ewald Method. *J. Chem. Phys.* **1995,** 103, 8577-93.
152. Hess, B., P-LINCS: A Parallel Linear Constraint Solver for Molecular Simulation. *J. Chem. Theory Comput.* **2008,** 4, (1), 116-122.
153. Hess, B.; Bekker, H.; Berendsen, H. J. C.; Fraaije, J. G. E. M., LINCS: A Linear Constraint Solver for Molecular Simulations. *J. Comput. Chem.* **1997,** 18, (12), 1463-1472.
154. Despa, F., Water confined in reverse micelles-probe tool in biomedical informatics. *Phys. Chem. Chem. Phys.* **2008,** 10, (32), 4740-4747.
155. Shrestha, L. K.; Sato, T.; Dulle, M.; Glatter, O.; Aramaki, K., Effect of Lipophilic Tail Architecture and Solvent Engineering on the Structure of Trehalose-Based Nonionic Surfactant Reverse Micelles. *The Journal of Physical Chemistry B* **2010,** 114, (37), 12008-12017.
156. Róg, T.; Murzyn, K.; Hinsen, K.; Kneller, G. R., nMoldyn: A program package for a neutron scattering oriented analysis of molecular dynamics simulations. *J. Comput. Chem.* **2003,** 24, (5), 657-667.
157. Schoettl, S.; Marcus, J.; Diat, O.; Touraud, D.; Kunz, W.; Zemb, T.; Horinek, D., Emergence of surfactant-free micelles from ternary solutions. *Chem. Sci.* **2014,** 5, 2949-2954.
158. Ferru, G.; Gomes Rodrigues, D.; Berthon, L.; Diat, O.; Bauduin, P.; Guilbaud, P., Elucidation of the Structure of Organic Solutions in Solvent Extraction by Combining Molecular Dynamics and X-ray Scattering. *Angew. Chem., Int. Ed.* **2014,** 53, 5346-5350.
159. Cromer, D. T.; Mann, J. B., X-ray scattering factors computed from numerical Hartree-Fock wave functions. *Acta Cryst.* **1968,** 24, (2), 321-324.
160. Testard, F.; Zemb, T.; Bauduin, P.; Berthon, L., Third Phase Formation in Liquid/Liquid Extraction: A Colloidal Approach In *Ion Exchange and Solvent Extraction: A Series of Advances*, Moyer, B., Ed. Taylor and Francis Group: Boca Raton, FL, 2010; Vol. 19.
161. IUPAC, *Compendium of Chemical Terminology*. 2nd ed.; Blackwell Scientific Publications: Oxford, 1997.
162. Osseo-Asare, K., Aggregation, reversed micelles, and microemulsions in liquid-liquid extraction: the tri-n-butyl phosphatediluent-water-electrolyte system. *Adv. Colloid Interface Sci.* **1991,** 37, (1), 123-173.
163. Friberg, S., Microemulsions, hydrotropic solutions and emulsions, a question of phase equilibria. *J. Am. Oil Chem. Soc.* 48, (10), 578-581.
164. Rashidnia, N.; Balasubramaniam, R.; Delsignore, D., Interfacial-Tension Measurement of Immiscible Liquids Using a Capillary-Tube. *Aiche J* **1992,** 38, (4), 615-618.
165. Lin, S. Y.; Wang, W. J.; Hsu, C. T., Adsorption kinetics of 1-octanol at the air-water interface. *Langmuir* **1997,** 13, (23), 6211-6218.
166. Hans-Jurgen Butt, K. G., Michael Kappl, Themodynamics of Interfaces. In *Physics and Chemistry of Interfaces*, John Wiley and Sons: 2006; p 14.

167. He, Y. F.; Shang, Y. Z.; Liu, H. L.; Dominique, L.; Anniina, S., Surfactant Adsorption onto Interfaces: Measuring the Surface Excess in Time. *Langmuir* **2012,** 28, (6), 3146-3151.
168. Chiarizia, R.; Stepinski, D.; Antonio, M. R., SANS Study of HCl Extraction by Selected Neutral Organophosphorus Compounds in n-Octane. *Separation Science and Technology* **2010,** 45, (12-13), 1668-1678.
169. Nagarajan, R., Molecular Packing Parameter and Surfactant Self-Assembly: The Neglected Role of the Surfactant Tail. *Langmuir* **2002,** 18, (1), 31-38.
170. Vidyalakshmi, V.; Subramanian, M. S.; Srinivasan, T. G.; Rao, P. R. V., Effect of extractant structure on third phase formation in the extraction of uranium and nitric acid by N,N-dialkyl amides. *Solvent Extr. Ion Exch.* **2001,** 19, (1), 37-49.
171. Smit, B.; Schlijper, A. G.; Rupert, L. A. M.; Vanos, N. M., Effects of Chain-Length of Surfactants on the Interfacial-Tension - Molecular-Dynamics Simulations and Experiments. *J Phys Chem-Us* **1990,** 94, (18), 6933-6935.
172. *Handbook of Chemistry and Physics* 97 ed.; CRC Press: Boca Raton, FL, 2016.
173. Yaws, C. L.; Hopper, J. R.; Sheth, S. D.; Han, M.; Pike, R. W., Solubility and Henry's Law Constant for Alcohols in Water. *Waste Manage.* **1998,** 17, (8), 541-547.
174. Amidon, G. L., Yalkowsky, S. H., Leung, S., Solubility of Nonelectrolytes in Polar Solvents II: Solubility of Aliphatic Alcohols in Water. *J. Pharm. Sci.* **1974,** 63, (12), 1858-1866.
175. Zemb, T. N.; Klossek, M.; Lopian, T.; Marcus, J.; Schöettl, S.; Horinek, D.; Prevost, S. F.; Touraud, D.; Diat, O.; Marčelja, S.; Kunz, W., How to Explain Microemulsions Formed by Solvent Mixtures Without Conventional Surfactants. *Proc. Natl. Acad. Sci.* **2016,** 113, (16), 4260-4265.
176. Schöttl, S.; Touraud, D.; Kunz, W.; Zemb, T.; Horinek, D., Consistent Definitions of "The Interface" in Surfactant-Free Micellar Aggregates. *Colloids Surf., A* **2015,** 480, 222-227.
177. Ferru, G.; Reinhart, B.; Bera, M. K.; Olvera de la Cruz, M.; Qiao, B.; Ellis, R. J., The Lanthanide Contraction beyond Coordination Chemistry. *Chem. Eur. J.* **2016,** 22, (20), 6899-6904.
178. Morgenstern, A.; Lebeda, O.; Stursa, J.; Bruchertseifer, F.; Capote, R.; McGinley, J.; Rasmussen, G.; Sin, M.; Zielinska, B.; Apostolidis, C., Production of U-230/Th-226 for Targeted Alpha Therapy via Proton Irradiation of Pa-231. *Anal. Chem.* **2008,** 80, (22), 8763-8770.